architecture of biofilms and resistance to disinfection : contribution of multimodal fluorescence imaging

Arnaud Bridier

Doctorat ParisTech

T H È S E

pour obtenir le grade de docteur délivré par

L'Institut des Sciences et Industries du Vivant et de l'Environnement

(AgroParisTech)

Spécialité : Microbiologie

présentée et soutenue publiquement par

Arnaud Bridier

le 9 juin 2011

Architecture des biofilms et résistance à la désinfection : apport de l'imagerie de fluorescence multimodale

Directeurs de thèse : **Florence Dubois-Brissonnet**
Romain Briandet

Devant le Jury composé de:

Mr. Jean-Claude Block, Professeur, Nancy-université — Rapporteur
Mr. Jean Guzzo, Professeur, Université de Bourgogne — Rapporteur
Mme. Simone Séror, Directeur de recherche, Université Paris-sud
Mr. Armel Guyonvarch, Professeur, Université Paris-sud
Mme. Florence Dubois-Brissonnet, Maitre de conférences, AgroParisTech
Mr. Romain Briandet, Chargé de recherche, INRA

Institut MICALIS UMR1319 INRA-AgroParisTech
Equipe Bioadhésion, Biofilms et Hygiène des Matériaux
25 avenue de la république F-91300 Massy

REMERCIEMENTS

Cette thèse a été financée par le pôle de compétitivité MEDICEN Paris-région dans le cadre du programme GLOBAL DECONTA (PGD) et réalisée au sein de l'institut MICALIS, UMR 1319 INRA-AgroParisTech, équipe Bioadhésion, Biofilm et hygiène des matériaux à Massy.

Je tiens à remercier Jean-Claude Block, Jean Guzzo, Simone Séror et Armel Guyonvarch de m'avoir fait l'honneur de faire partie de mon jury de thèse.

J'exprime ma vive reconnaissance à Florence Dubois-Brissonnet et Romain Briandet pour m'avoir encadré et soutenu durant ces trois années, pour leur grande disponibilité et leur enthousiasme.

Un grand merci à tous les membres de l'équipe pour ces trois ans à vos cotés. Merci de m'avoir permis de réaliser cette thèse dans les meilleures conditions et dans la bonne humeur.

Merci à Vincent Thomas, coordinateur du projet PGD, pour notre collaboration et nos discussions toujours très enrichissantes.

Je remercie chaleureusement Dominique Le Coq et Stéphane Aymerich pour notre collaboration sur les biofilms et la génétique de Bacillus subtilis et pour mon « stage » de biologie moléculaire à Grignon.

Merci également à Marie-Pierre Fontaine-Aupart, Karine Steenkeste et, Samia Daddi-Oubekka de l'Institut des Sciences Moléculaires d'Orsay et François Waharte de l'institut Curie.

Merci à mes parents, à ma famille, à mes amis pour leur soutien affectueux.

Et enfin merci à Milie…

SOMMAIRE

INTRODUCTION GENERALE

Les implications en termes de santé publique d'une non maîtrise de la contamination environnementale par des agents infectieux sont considérables. Malgré les progrès réalisés dans ce domaine ces dernières années en France, 33404 cas d'intoxications alimentaires d'origine microbiologique ont été déclarés entre 2006 et 2008 (Delmas *et al.*, 2010) et les infections nosocomiales concernaient encore 1 patient hospitalisé sur 20 en 2006 d'après l'Institut National de Veille Sanitaire (InVS). De plus, la médiatisation des crises ainsi que l'utilisation de plus en plus large du principe de précaution ont considérablement augmenté les niveaux d'exigences des populations vis-à-vis des pouvoirs publics et de tous les acteurs de la chaîne industrielle. La contamination des surfaces constitue un maillon important de la transmission d'agents pathogènes à l'homme et le développement de traitements de décontamination efficaces demeure une problématique majeure que ce soit à l'hôpital ou dans diverses activités industrielles (agroalimentaire, pharmacie, biotechnologies, ...). Dans ce contexte, le programme GLOBAL DECONTA financé par le pôle de compétitivité MEDICEN-Paris région (http://www.medicen.org/) et coordonné par Vincent Thomas (STERIS SA) a eu pour ambition la mise au point et la validation de traitements de décontamination de surface innovants permettant de prendre en compte une large gamme d'agents infectieux, conventionnels (bactéries, virus) et non conventionnels (prions, ADN plasmidique). Pour cela, le projet a fédéré des acteurs industriels directement concernés par cette problématique en temps qu'utilisateurs ou formulateurs de solutions de décontamination et des laboratoires publics de recherche pour leur expertise dans ce domaine. Dans le cadre de ce travail de thèse, financé par ce projet et réalisé au sein de l'équipe Bioadhésion, Biofilm et Hygiène des Matériaux de l'Institut MICALIS (UMR1319 INRA-AgroParisTech), nous avons eu en charge l'axe « bactériologie-biofilm » dont la problématique générale était une meilleure compréhension des phénomènes limitant l'efficacité d'agents désinfectants sur les bactéries en prenant en compte l'état « biofilm ».

En effet, même si les bactéries sont encore souvent étudiées sous forme planctonique en culture liquide, il est bien admis que la majorité d'entre elles sont présentes dans l'environnement en étant adhérées aux surfaces au sein de communautés complexes appelées biofilms (Costerton *et al.*, 1978). Ces biofilms sont des associations denses et structurées de cellules englobées dans une matrice extracellulaire hydratée qui paraît être majoritairement constituée de polysaccharides, de protéines, d'acides nucléiques et de lipides (Flemming & Wingender, 2010) bien que sa composition et ses propriétés physiques varient selon les espèces présentes et les conditions environnementales. La présence de germes pathogènes

dans ces structures peut avoir une incidence particulièrement importante sur le plan de la santé publique. Les biofilms seraient impliqués dans plus de 65% des infections nosocomiales du fait de leur développement sur les implants cardiaques, les prothèses, les cathéters, les endoscopes et autres matériels et équipements médicaux (Mack *et al.*, 2006, Shirtliff & Leid, 2009). Le développement d'un grand nombre d'infections chroniques est directement lié à la formation de biofilms par différents pathogènes tels que *Pseudomonas aeruginosa* dans des infections pulmonaires chez les patients atteints de mucoviscicode, *Haemophilus influenzae* et *Streptococcus pneumoniae* dans l'otite moyenne chronique, *Staphylococcus aureus* dans la rhinosinusite chronique et *Escherichia coli* dans les infections récurrentes des voies urinaires (Hall-Stoodley & Stoodley, 2009, Burmolle *et al.*, 2010). Dans le secteur agroalimentaire, la présence en biofilms de pathogènes tels que *Listeria monocytogenes* ou *Salmonella enterica* sur la chaine alimentaire peut également conduire à la contamination des denrées engendrant des problèmes sanitaires très importants (Brooks & Flint, 2008, Carpentier & Cerf, 1993). La contamination des équipements seraient responsables de 40% des intoxications d'origine alimentaire en France (Haeghebaert *et al.*, 2001). Ces problèmes sont liés au fait que la formation d'un biofilm constitue une stratégie de survie étonnement efficace conférant aux microorganismes la capacité de résister à différents stress environnementaux tels que les traitements de nettoyage et de désinfection (Prakash *et al.*, 2003, Kim *et al.*, 2007, Cloete, 2003, Nett *et al.*, 2008). Ces propriétés de résistance permettent aux bactéries de persister dans l'environnement malgré les traitements curatifs, les biofilms constituant ainsi des réservoirs de germes potentiellement pathogènes. Une des problématiques actuelles est que les tests utilisés dans les normes d'évaluation de l'activité bactéricide des désinfectants sont encore aujourd'hui basés sur l'utilisation de cellules en suspension ou déposées et séchées, conditions très éloignées du mode de vie en biofilm et conduisent donc à la surestimation de l'efficacité des biocides. Dans le but de garantir l'hygiène des surfaces, la prise en compte de l'état « biofilm » est donc nécessaire et cela passe par une meilleure compréhension de l'implication de ces structures dans les phénomènes de résistance aux traitements de désinfection.

Les travaux scientifiques sur le sujet montrent **un lien étroit, qu'il soit direct ou indirect, entre l'architecture de l'édifice biologique et sa résistance**. En effet, la multiplication des cellules adhérées et la production d'une matrice mucoïde extracellulaire conduisent au développement d'une structure tridimensionnelle complexe dans laquelle les biocides peuvent rencontrer des problèmes de diffusion/réaction limitant leur efficacité

(Stewart *et al.*, 2001, Jang *et al.*, 2006). De plus, la structure tridimensionnelle gouverne la mise en place de gradients en nutriments, en oxygène et en produits métabolites qui résultent en l'apparition d'une hétérogénéité chimique dans le biofilm (Stewart & Franklin, 2008). En réponse à leur microenvironnement local, les cellules peuvent alors évoluer vers des phénotypes de résistance par des modifications physiologiques et/ou l'expression de gènes spécifiques. La résistance globale de la communauté bactérienne apparaît donc être un processus multifactoriel structure-dépendant qui implique des phénomènes locaux. Les informations sur la réactivité spatiotemporelle des biocides au sein de ces structures hétérogènes pourraient donc aider à mieux comprendre les mécanismes impliqués dans leur résistance. Ces dernières années, les développements les plus récents en termes d'imagerie non-invasive ont permis l'émergence de nouveaux outils de microscopie permettant d'explorer la structure et la dynamique des systèmes biologiques à l'échelle de la cellule unique (Neu *et al.*, 2010).

Dans ce contexte, le travail présenté dans ce mémoire a eu pour objectif général *i)* de développer des approches s'appuyant sur des techniques d'imagerie non-invasive de fluorescence permettant l'analyse fine de la structure tridimensionnelle et de la réactivité des biofilms, *ii)* d'appliquer ces méthodes à l'étude et à la compréhension des mécanismes limitant l'efficacité de désinfectants dans les biofilms dans le but d'apporter des éléments utiles à l'amélioration de l'efficacité des traitements de désinfection de surface.

Le présent rapport est composé de **trois parties** :

- **La première partie** constitue une étude bibliographique qui ne prétend pas faire une synthèse exhaustive de la littérature sur le sujet mais s'attache à présenter les deux axes majeurs de ce travail, c'est à dire i) l'utilisation de l'imagerie de fluorescence dans l'étude structurale et réactionnelle des biofilms et ii) les mécanismes pouvant jouer un rôle dans leur résistance aux agents désinfectants. Cette étude est présentée sous la forme de deux articles de synthèse.

- **La deuxième partie** est consacrée à l'exposé des résultats obtenus au cours de cette thèse, les travaux étant regroupés en deux chapitres. Le premier chapitre présente le développement d'une méthode d'investigation structurale à haut-débit par microscopie confocale et son application à l'étude de la diversité architecturale des biofilms bactériens. Le deuxième chapitre repose sur l'étude des mécanismes de résistance aux désinfectants des

bactéries en biofilm. Les dynamiques d'action spatiotemporelles des désinfectants au sein de ces structures biologiques ont été analysées par des approches de microscopie confocale de fluorescence en temps réel.

- **La troisième partie** conclut ce mémoire par une synthèse générale avec mise en perspective des résultats obtenus.

ETUDE BIBLIOGRAPHIQUE

A. Article 1 :

“Deciphering biofilm structure and reactivity by multiscale time-resolved fluorescence analysis.”

A. Bridier, E. Tischenko, F. Dubois-Brissonnet, J.-M. Herry, V. Thomas, S. Daddi-Oubekka, F. Waharte, K. Steenkeste, M.-P. Fontaine-Aupart and R. Briandet.

Advances in experimental medicine and biology,

Chapter 21
Deciphering Biofilm Structure and Reactivity by Multiscale Time-Resolved Fluorescence Analysis

Arnaud Bridier, Ekaterina Tischenko, Florence Dubois-Brissonnet, Jean-Marie Herry, Vincent Thomas, Samia Daddi-Oubekka, François Waharte, Karine Steenkeste, Marie-Pierre Fontaine-Aupart, and Romain Briandet

Abstract In natural, industrial and medical environments, microorganisms mainly live as structured and organised matrix-encased communities known as biofilms. In these communities, microorganisms demonstrate coordinated behaviour and are able to perform specific functions such as dramatic resistance to antimicrobials, which potentially lead to major public health and industrial problems. It is now recognised that the appearance of such specific biofilm functions is intimately related to the three-dimensional organisation of the biological edifice, and results from multifactorial processes. During the last decade, the emergence of innovative optical microscopy techniques such as confocal laser scanning microscopy in combination with fluorescent labelling has radically transformed imaging in biofilm research, giving the possibility to investigate non-invasively the dynamic mechanisms of formation and reactivity of these biostructures. In this chapter, we discuss the contribution of fluorescence analysis and imaging to the study at different timescales of various processes: biofilm development (hours to days), antimicrobial reactivity within the three-dimensional structure (minutes to hours) or molecular diffusion/reaction phenomena (pico- to milliseconds).

21.1 Microbial Biofilms in Our Environment

Biofilms have a considerable impact on human existence and well-being because of their involvment in various beneficial ecological phenomena (Singh et al., 2006). Moreover, the ability of microbes to perform specific chemical reactions in surface associated consortia can be used to produce energy (Yadvika et al., 2004; Cournet et al., 2010). Nevertheless, bacterial communities are involved in a large number of detrimental processes such as biofouling or biocorrosion (Beech et al., 2005), and

R. Briandet (✉)
INRA, UMR 1319 MICALIS, Massy, France
e-mail: romain.briandet@jouy.inra.fr

D. Linke, A. Goldman (eds.), *Bacterial Adhesion*, Advances in Experimental Medicine and Biology 715, DOI 10.1007/978-94-007-0940-9_21,

in infectious diseases such as periodontitis, endocarditis, cystic fibrosis pneumonia and most hospital-acquired infections (Costerton et al., 1999). This phenomenon can be explained by the high resistance of biofilm-dwelling cells to antimicrobial agents (Mah and O'Toole, 2001), which enables pathogens to persist on medical devices or industrial equipment, leading thus to critical problems in terms of public health. Although the precise mechanisms of resistance remain unclear, it appears to be a multifactorial process directly or indirectly related to the architectural features of multicellular bacterial edifices. The depletion of active antimicrobial agents in the bulk of biofilm due to diffusion and/or reaction limitations (Huang et al., 1995; Campanac et al., 2002) illustrates the vital role of the shape of the matrix in the resistance of such communities. The biofilm matrix is also known to play a key role in protection against the human innate immune system by decreasing phagocytosis, for example (Vuong et al., 2004). In addition, the development of a complex three-dimensional (3D) biofilm architecture results in the appearance of nutrient and oxygen gradients. These lead to differential gene expression and specific physiological activities throughout the biofilm in response to local microenvironmental conditions (Stewart, 2003; Rani et al., 2007). Consequently, the emergence of phenotypic variants in biofilm subpopulations contributes to the expression of novel community functions such as tolerance to antimicrobial stress, which can increase population fitness (Lewis, 2005; Stewart and Franklin, 2008).

Until now, biofilm imaging has concentrated on identifying and understanding the sequence of events leading to biofilm formation and its structure (Lakins et al., 2009). Specifically, it is now appreciated that biofilm formation can be defined as a process that consists of defined stages including: reversible and irreversible attachment; surface motility and initiation of the formation of microcolonies or other arrangements; maturation, ageing and differentiation of microcolonies; and finally, biofilm dissolution and generation of specialised dispersal cells (Kjelleberg et al., 2007). Numerous studies have shown that this biological process involves a coordinated spatio-temporal expression of adhesion, motility, matrix or cell death genes in response to micro-environmental conditions and signalling molecules (Rieu et al., 2007; Vlamakis et al., 2008). The regulated death of bacterial cells in biofilms constitutes an important component of multicellular development and a telling example of temporal and spatial regulation (Bayles, 2007). In *B. subtilis* biofilms for example, Lopez et al. (2009) showed that matrix-producing cells exhibit cannibalistic behaviour by producing toxins that lyse a part of the population. The nutrients released are preferentially consumed by the surviving matrix-producing subpopulation as they are the only cells expressing resistance to toxins. This phenomenon leads to increase of matrix production and thus favours biofilm formation. The authors showed that this coordinated mechanism may constitute a defense mechanism of *B. subtilis* in adverse conditions. In *Pseudomonas aeruginosa*, some cells in the centre of the microcolonies undergo prophage-mediated autolysis, providing nutrients to the remaining cells that can disseminate and colonise novel ecological niches (Webb et al., 2003; Rice et al., 2009). Moreover, most dispersed cells exhibit specific phenotypes that are associated with increased resistance to environmental stress and higher virulence (Hall-Stoodley and Stoodley, 2005). Both these

competitive or altruistic behaviours are deleterious at the single-cell level, but benefit the global community fitness, demonstrating that biofilm typically results from a balance between these two social behaviours (Dunny et al., 2008; Nadell et al., 2009). It is important to consider that, even if most experimental studies are performed on single species models, biofilms usually contain multiple bacterial species, fungi, viruses and protozoa. This diversity increases the complexity of the relationships between dwelling organisms and can lead to the emergence of specific traits (Hansen et al., 2007).

The functional properties of biofilms therefore result from the complex spatial and temporal differentiation of cells in the dynamic three-dimensional structure in response to environmental signals and cell-cell interactions. The development of tools enabling in-situ observation of dynamic processes within biofilms is required to improve our understanding of biofilm traits and to develop advanced control strategies. Recent developments in confocal laser scanning microscopy (CLSM), and new fluorescent molecules and protein reporters allowing the labelling of specific matrix components or cell states, have deepened our knowledge of biofilms. These new tools allow researchers to explore non-invasively the dynamic architectural and physiological evolution in the three-dimensional structure of biofilms (Palmer and Sternberg, 1999). In this chapter, we review the use of fluorescence imaging for the study of biofilm structure and reactivity at different timescales. We first present the contribution of the method to analyse the 3D architecture and development of the biofilm (hours to days). We then discuss the use of fluorescence in monitoring biocide activity in biofilms by 4D imaging (minutes to hours). Finally, we describe the use of FRAP (Fluorescence Recovery After Photobleaching), FCS (Fluorescence Correlation Spectroscopy) and FLIM (Fluorescence Lifetime Imaging) in insitu molecular diffusion/reaction studies in biofilms (picoseconds to minutes).

21.2 From Free Cells to 3D Organised Multicellular Architecture

21.2.1 Laboratory Biofilms Assays

In laboratories, different devices are used to produce biofilms: we only present here the most commonly used systems in live-cell imaging studies. Two types of systems, “dynamic” or “static”, can be distinguished.

In “dynamic” systems such as flow-cells, biofilms are formed under the flow of medium, which enables continuous renewal of nutrients. This kind of device enables the elimination of planktonic cells by the flow and is particularly well adapted to the monitoring of biofilm development in “real time” using fluorescent strains and CLSM (Pamp et al., 2009). Different flow-cell designs exist, varying according to the number and the dimension of channels, as well as the nature of the base. One major drawback of these systems is the cumbersome and expensive nature of the growth protocol, which does not allow the screening of many samples. Furthermore, the difficulty of standardising biofilm growth in flow-cells and the weak control of

hydrodynamic parameters can limit the repeatability between different experiments or laboratories.

In “static” systems, biofilms are produced without any flow and thus result from the multiplication of attached cells on the surface and also partially from the sedimentation of the planktonic fraction. Static systems also suffer from a lack of standardisation, in particular in the key step of rinsing that can severely affect the biofilm 3D structure.

Using microtiter plates, many high-throughput static assays have been developed to quantify biofilm formation in a large number of strains (Peeters et al., 2008). These methods are very useful for screening mutants and identifying the genes involved in biofilm formation and maintenance, but they do not provide structural information. Recently, a method based on a microtiter plate compatible with high resolution imaging by CLSM was proposed to overcome this limitation (Bridier et al., 2010). The ability of some species to form a floating pellicle at the air-liquid interface or complex macrocolonies on agar can also be exploited to identify developmental steps and genes required in biofilm formation (Branda et al., 2005; Enos-Berlage et al., 2005).

The choice of growth protocol is a critical step in biofilm study because it greatly influences biofilm formation and architecture: this has been clearly illustrated by Yarwood et al. (2004), who demonstrated that mutating a gene involved in *Staphylococcus aureus* biofilm formation had opposing effects depending on the system (microtiter plate, rotating disk reactor or flow-cell).

21.2.2 CLSM for Multi-dimensional Biofilm Fluorescence Imaging

As mentioned previously, most of what makes microbial cells in a biofilm different from their planktonic counterparts is their multicellular spatial organization. The analysis of such structure/function relationships has considerably evolved during the last decade, in line with technical advances in microscopy. To gain access to in situ observations, much effort has been directed toward photonic microscopy associated with the fluorescent labelling of biofilm elements. Hence, in conventional widefield fluorescence microscopy, the biofilm is illuminated by a cone of light, thus obtaining almost uniform sample excitation and fast image acquisition. The drawback is poor depth resolution due to the collection of light coming from regions of the sample located at different depths. Practically, it means that only very thin biofilms (close to a monolayer in structure) can be adequately observed. Deconvolution can in some cases allow 3D imaging enhancement in such systems (Conchello and Lichtman, 2005).

The emergence of CLSM has radically transformed biofilm optical imaging, and in particular allows the analysis of thick biofilms. Due to the introduction of a “pinhole” in the path of the fluorescence light emitted by the sample, only the fluorescence coming from the focal plane reaches the detector and the contribution

of out-of-focus light is eliminated. This optical sectioning ensures a submicron resolution compatible with observation of a single bacterium within the biofilm. It is also now possible to add two other dimensions to these image stacks: time (t) for 2D or 3D dynamics analysis, and wavelength (λ) for spectral imaging, for example to unmix multi-fluorescent labels or subtract interference from a fluorescent background. Therefore, the introduction of CLSM has led to considerable progress in studying the architecture, physiology and molecular interactions within the biofilm without prior chemical fixation (in situ observations in aqueous medium).

The widespread use of lasers has led to the emergence of new methods, including approaches based on nonlinear optics. Hence, the limited depth penetration of CLSM can be overcome by employing two-photon laser scanning microscopy (2PLSM). Experimentally, two-photon excitation of the fluorescent molecule is obtained by the quasi-simultaneous absorption of two photons of half the energy of the photons used in CLSM (Vroom et al., 1999), typically using near-infrared lasers (Neu et al., 2010; Lakins et al., 2009).

These laser microscopy methods are constantly evolving to improve both image acquisition rate (fast confocal spinning-disk microscopes, multiphoton multifocal microscopy; Deniset-Besseau et al., 2007) and spatial resolution, for instance: structured illumination, total internal reflection fluorescence microscopy (TIRF), stimulated emission depletion microscopy (STED), photoactivation localisation microscopy (PALM), stochastic optical reconstruction microscopy (STORM) and 4pi microscopy. Researchers involved in the study of biofilms may benefit from these new developments in fluorescence microscopy.

The extensive use of CLSM in biofilm research is also intrinsically related to the development of dedicated specific fluorophores. Available fluorophores allow visualisation of different components of the biofilms, of individual cells and their local physiology or patterns of gene expression, or of the organic matrix and the existence of heterogeneous microdomains.

The analysed fluorescence can come either from fluorescent labels incorporated into the biofilm or from the microorganism. The main requirement is that it is a good fluorophore: i.e. that it has high brightness (product of fluorescence quantum yield and molar extinction coefficient ε) and suitable photostability.

The most widespread methods of fluorescent labelling of biofilm components are:

- Indicators of microbial membrane integrity, e.g. Live/dead stain (Pamp et al., 2008).
- Indicators of metabolic activity markers, e.g. Calcein AM (Takenaka et al., 2008).
- Fluorescent lectins to label extracellular polysaccharides, e.g. concanavalin A (Neu et al., 2001).
- Fluorescent in situ hybridisation (FISH) for identification of community members within complex biofilms (Amann et al., 1990).
- Expression of fluorescent proteins from the microbial genome: green fluorescent protein (GFP) has proven to be a powerful method to study in vivo gene expression in a broad range of hosts (Veening et al., 2004).

21.2.3 Time-Course Structural Analysis of Events Leading to Biofilm Formation

Tracking of the time-course of biofilm construction was pioneered in the last decade by the Tolken-Nielsen group on *P. aeruginosa* biofilms grown in flow-cells (Tolker-Nielsen et al., 2000; Klausen et al., 2006). The ideal situation for non-destructive time-course biofilm imaging is to grow bacterial cells expressing fluorescent reporter protein(s) for the biofilm assay on a transparent substratum compatible with in situ CLSM observation (i.e. flowcells or dedicated microtiter plates). In this configuration, it is possible to record 4D image series (3D images as a function of time) of the same microscopic field and to trace in "real time" the multicellular assemblage as a movie. This approach was used to identify the molecular determinants involved in biofilm construction. The experimental method compares the sequence of events involved in the formation of a wild type biofilm

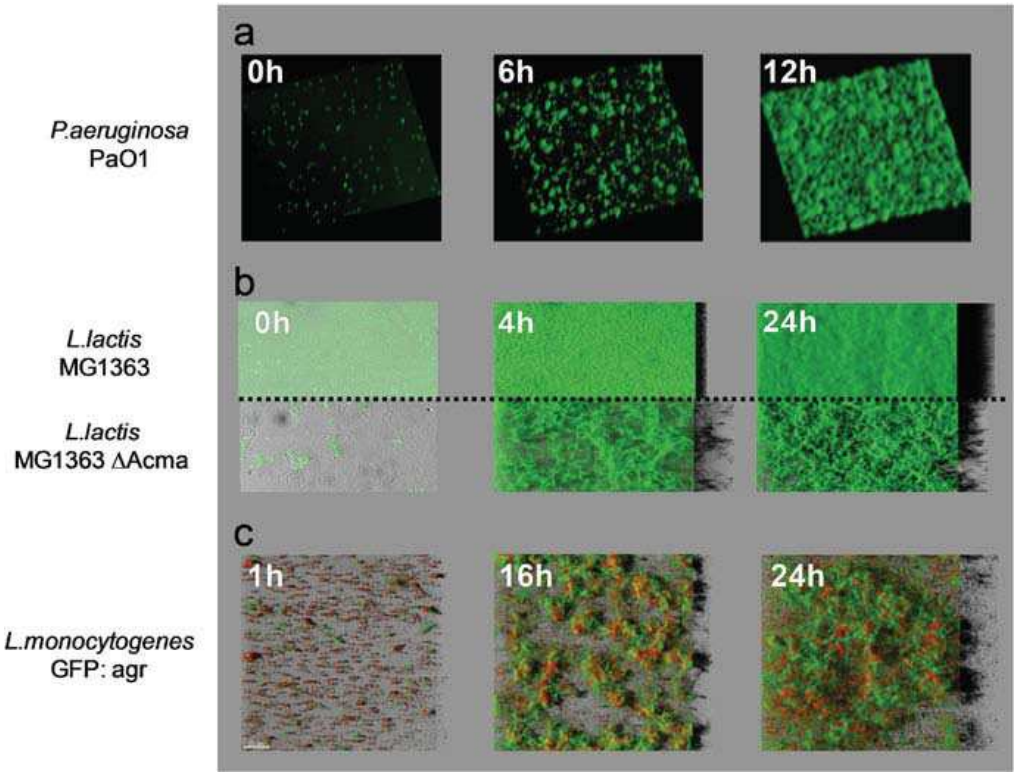

Fig. 21.1 3D reconstruction of biofilm development under flowing conditions from confocal image series. (**a**) Structural development of GFP-tagged *Pseudomonas aeruginosa* PaO1 biofilm using time-lapse CLSM. (**b**) Time-course CLSM of GFP-tagged WT *Lactococcus lactis* MG1363 (*top*) and its cell wall mutant, ΔacmA (inactivation of N-acetyl glucosaminidase) (*bottom*). The mutation leads to the development of cell chains forming a biofilm with different architectural properties than wild-type. Adapted from Habimana et al. (2009). (**c**) Sequence illustrating the spatiotemporal regulation of *agr* expression during biofilm formation by *Listeria monocytogenes*. *Green* indicates cells expressing GFP from the reporter plasmid pGID128, which contain a fusion of the *agr* promoter region with *gfp*. The red cells are stained with the nucleic acid SYTO61 dye (cells in red lacks *agr* activity). Adapted from Rieu et al. (2008)

with the sequence of events in a series of mutants. Using this scheme, it has been possible for example to identify the involvement of F plasmid, pilus and putative membrane proteins in *E. coli* biofilms (Beloin et al., 2004; May and Okabe, 2008), and the involvement of exopolysaccharide synthesis in *Lactococcus lactis* biofilms (Habimana et al., 2009).

As the understanding of biofilm complexity increases, "simple" descriptive architectural studies are being replaced by those in which the three-dimensional organization of the biofilm is related to other information, such as species composition, relationship with substrate or physiology (Palmer and Sternberg, 1999). Indeed, most studies of gene expression by bacteria in biofilms described levels that reflect the average gene expression over the entire population (Lenz et al., 2008). CLSM associated with fluorescent reporter fusions has recently been used to trace the spatio-temporal expression of specific genes at the single cell level in the overall biofilm structure. The approach has shown than some genes are specifically expressed on the interfacial layers of the biofilm (Lenz et al., 2008; Ito et al., 2009; Rieu et al., 2008), while others are expressed in more specific patterns, such as the *agr* system implicated in quorum sensing regulation in *Staphylococcus aureus* biofilms, which is expressed in patches within cell clusters and where the expression oscillates with time (Yarwood et al., 2004). Some examples of biofilm structural dynamics are presented in Fig. 21.1.

21.3 Real Time 3D Visualization of Biofilm Inactivation by Antimicrobials

The latest surge of interest in biofilms was triggered by the observation of their unprecedented microbial tolerance to antimicrobial agents e.g. antibiotics or biocides. Previous studies suggested that biofilm resistance is clearly multifactorial, and only a combination of different mechanisms could account for the observed resistance levels in biofilm communities (Anderson and O'Toole, 2008). Exopolymeric matrix can serve as a protective environment. For example, the activity of an antibiotic on mucoid *P. aeruginosa* biofilms can be significantly enhanced by addition of alginate lyase and DNAase, suggesting that alginate and extracellular DNA function as antibiotic barriers (Alipour et al., 2010; Harmsen et al., 2010). The heterogeneity of cell physiology within the biofilm matrix due to oxygen and nutrient gradients can also constitute a protective phenotype (Xu et al., 1998; Stewart and Franklin, 2008). In addition, regulated cell differentiation, collective coordinated behaviour and inter-cellular genetic exchange can contribute to the resistance of biofilm cells to antimicrobial stress. As a result, there is particular interest in developing biocides able to overcome such tolerance.

Conventional methods to study biofilm inactivation, such as bacterial enumeration on agar plates, are time-consuming, static and incompatible with structural observations. Therefore, the development of fast (minutes to hours), dynamic and non-destructive methods is required. Non-invasive direct time-lapse microscopic observation of biofilm viability was pioneered by Hope and Wilson (2004). Cells

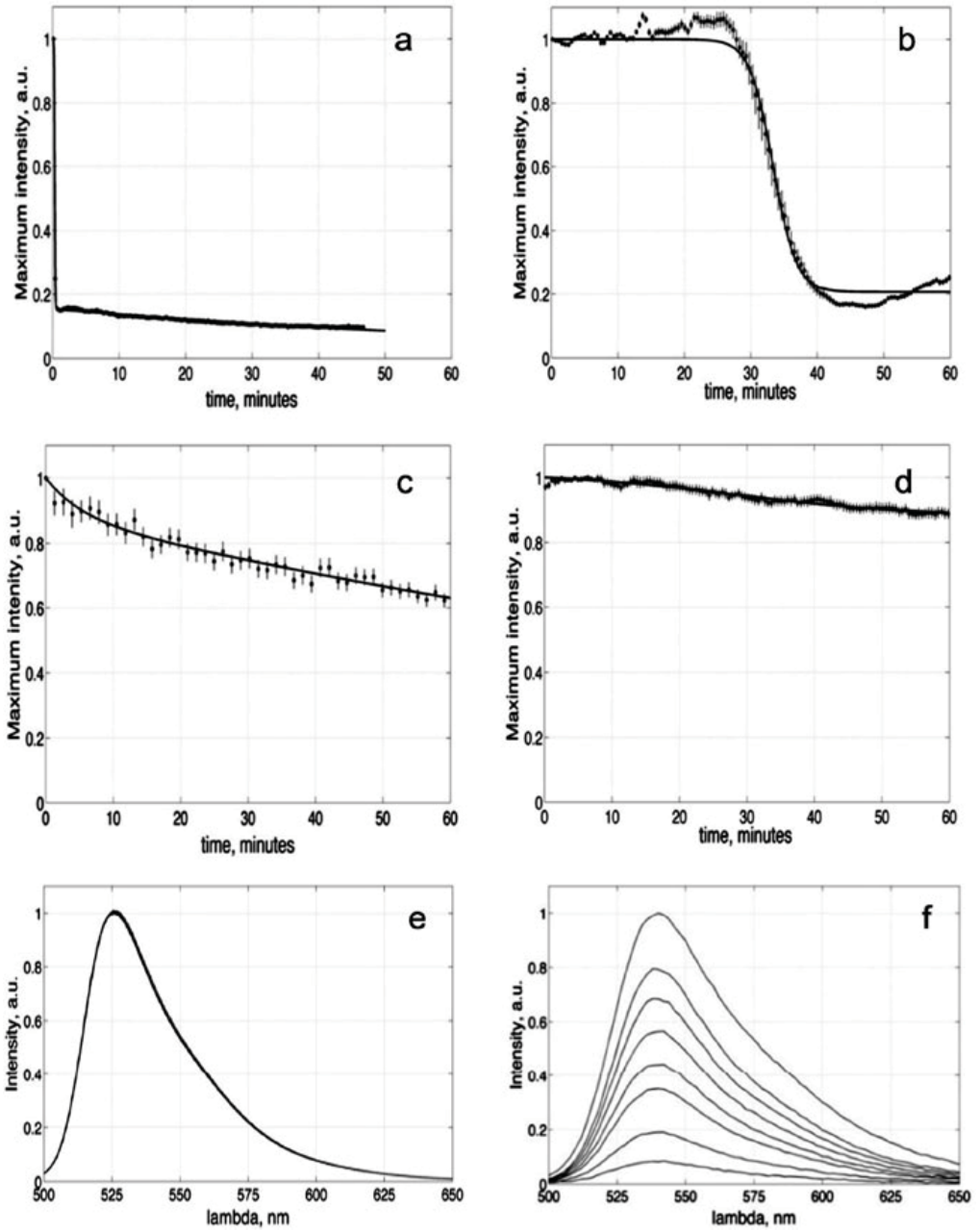

Fig. 21.2 Dynamics of *Staphylococcus aureus* biofilm inactivation by (**a**) 0.3% Peracetic Acid; (**b**) 0.05% C14-benzalkonium chloride; (**c**) 0.03% O-phthaldialdehyde and (**d**) saline solution. Fluorescent intensity of ChemChrome V6 is integrated over the image and normalized to the maximal value. Each *curve* represents the evolution of the mean fluorescent intensity of biofilm during biocide treatments. Dynamic profiles obtained illustrate the different modes of action of the three biocides tested. Fluorescent spectra ChemChrome V6 during: (**e**) C14-benzalkonium chloride and (**f**) 0.3% Peracetic acid action. Time between subsequent measurements (*curves*) is 5 min. Results show the loss of fluorescence intensity of the marker in presence of PAA showing an interaction between the two molecules. There was no interaction between ChemChrome V6 and the other biocides tested, as shown for C14-benzalkonium chloride as example

were visualised with the commercial BacLight Live/Dead kit (Invitrogen) composed of DNA-intercalating dyes, which is widely used for the time-independent measurements of bacterial membrane integrity. Later, the Stewart group (Takenaka et al., 2008) further improved the method by using the esterase activity marker Calcein-AM, which meets the basic requirements for cell viability tagging, i.e. it is stable and it efficiently tags the intracellular space in live cells without any changes in morphology or physiology of the cells and bacterial community structure. There is another essential requirement for "direct time-lapse microscopic observation": either the marker should not interact at all with the biocide, or the biocide-marker interactions should be fully understood and subtracted from the observed effect. Focusing on chemical biocides, there is evidence that such strongly reactive molecules and fluorescent dye or its target can interact (Phe et al., 2007). In this case, intracellular fluorescent reporters such as metabolic activity fluorophores are the most relevant. Their foremost advantage is that the marker is already inside cells, and is only affected by biocide after the biocide penetrates the cell or after the marker leaks out.

As an illustration, we measured the time and spatial inactivation of *Staphylococcus aureus* biofilms by three biocides used for disinfection of medical equipment and food processing areas (Fig. 21.2). In the absence of antimicrobials, the cell viability reporter used (esterasic marker V6 ChemChrome, AES Chemunex) stays inside the cell without any noticeable influence on the cell. When the plasma membrane is damaged during disinfection, the fluorophore leaks out of the cell, which allows direct visualization of biocide action within the 3D structure. The profiles of inactivation dynamics obtained underlined the specific mode of action of each biocide tested and enabled a deeper understanding of the treatment limitations. We could determine how well the dynamics of marker fluorescence intensity and biofilm cell inactivation correlate using model systems. For instance, using fluorescent spectroscopy in an in vitro system containing DNA and esterase enzyme to mimic the intracellular environment, we detected a strong biocide-marker interaction only with peracetic acid (PAA) (Fig. 21.2e–f). Consequently, the evolution of the intracellular marker fluorescent intensity under PAA action in biofilm tells us that the contact between marker and antimicrobial agent took place, and thus that the antimicrobial agent at least penetrated the cell. Moreover, the classical cell enumeration on agar was in good agreement with the fluorescent kinetics for the three biocides, including PAA.

CLSM 4D time-lapse experiments allow direct in situ visualization of antimicrobial action throughout the biofilm and the standardization of tools for the selection of active molecules in order to achieve efficient biofilm treatments.

21.4 Understanding the Process of Diffusion-Reaction Within Biofilms

Both the physiological properties of microorganisms and the structure of the extracellular polymeric substances play a crucial role in the reactivity of biofilms towards scattering entities. To analyse the molecular interactions within biofilms, it is

necessary to have non-invasive efficient methods of investigation in terms of spatial resolution, sensitivity and acquisition speed. Besides fluorescence intensity imaging techniques, more advanced fluorescence-based approaches can be implemented for in situ molecular diffusion/reaction studies within "live" biofilms, including FRAP (Fluorescence Recovery After Photobleaching), FCS (Fluorescence Correlation Spectroscopy) and FLIM (Fluorescence Lifetime IMaging).

21.4.1 Fluorescence Recovery After Photobleaching (FRAP)

As described previously, time-lapse imaging in CLSM allows following the diffusion of fluorescent molecules in such spatially organised biofilms (Rani et al., 2005; Takenaka et al., 2009). However, this method only allows estimating average and global diffusion coefficients over the macrostructure and ignores its heterogeneity (e.g. water channel, mushroom-like structures).

To measure local diffusion/reaction through a 3D biological structure, FRAP is a simple method that is now routinely implemented on commercial CLSMs (Waharte et al., 2010). FRAP is based on a brief excitation of fluorescent molecules by a very intense light source in the volume defined by the confocal microscope objective (for single spot FRAP) or in a user-defined region to quench their fluorescence (photobleaching) irreversibly (Fig. 21.3a,b). Fluorescence redistribution is then observed if the fluorophores are allowed to move in the sample. The analysis of the time course of fluorescence intensity recovery with proper mathematical models thus gives access to the quantitative mobility of the fluorescent molecules (determination of diffusion coefficient and/or rate of molecular association) (Fig. 21.3a).

FRAP typically requires micromolar concentrations of fluorescent tracers, and consequently gives access only to average diffusion coefficients unlike FCS (see below), potentially masking the effects of local heterogeneity. FRAP is not sensitive enough to detect the motion of a single molecule. Furthermore, the quantification of FRAP measurements requires mathematical models adapted to the experimental conditions and the geometrical/structural configuration of the sample; these difficulties explain why most FRAP studies are essentially based on a qualitative and relative analysis. Recently, an image-based FRAP protocol and its corresponding analysis that can be readily applied by anyone familiar with a CLSM has been published; it improves the accuracy and accessibility of FRAP measurements of molecular diffusion inside bacterial biofilms (Fig. 21.3d,e). The method was supported by an original representation that allows checking the presence of bacterial movement during image acquisition that would alter the measurements (Fig. 21.3c) (Waharte et al., 2010).

21.4.2 Fluorescence Correlation Spectroscopy (FCS)

FCS, on the other hand, is the most appropriate technique to analyse diffusion/reaction processes within biological entities with single molecule

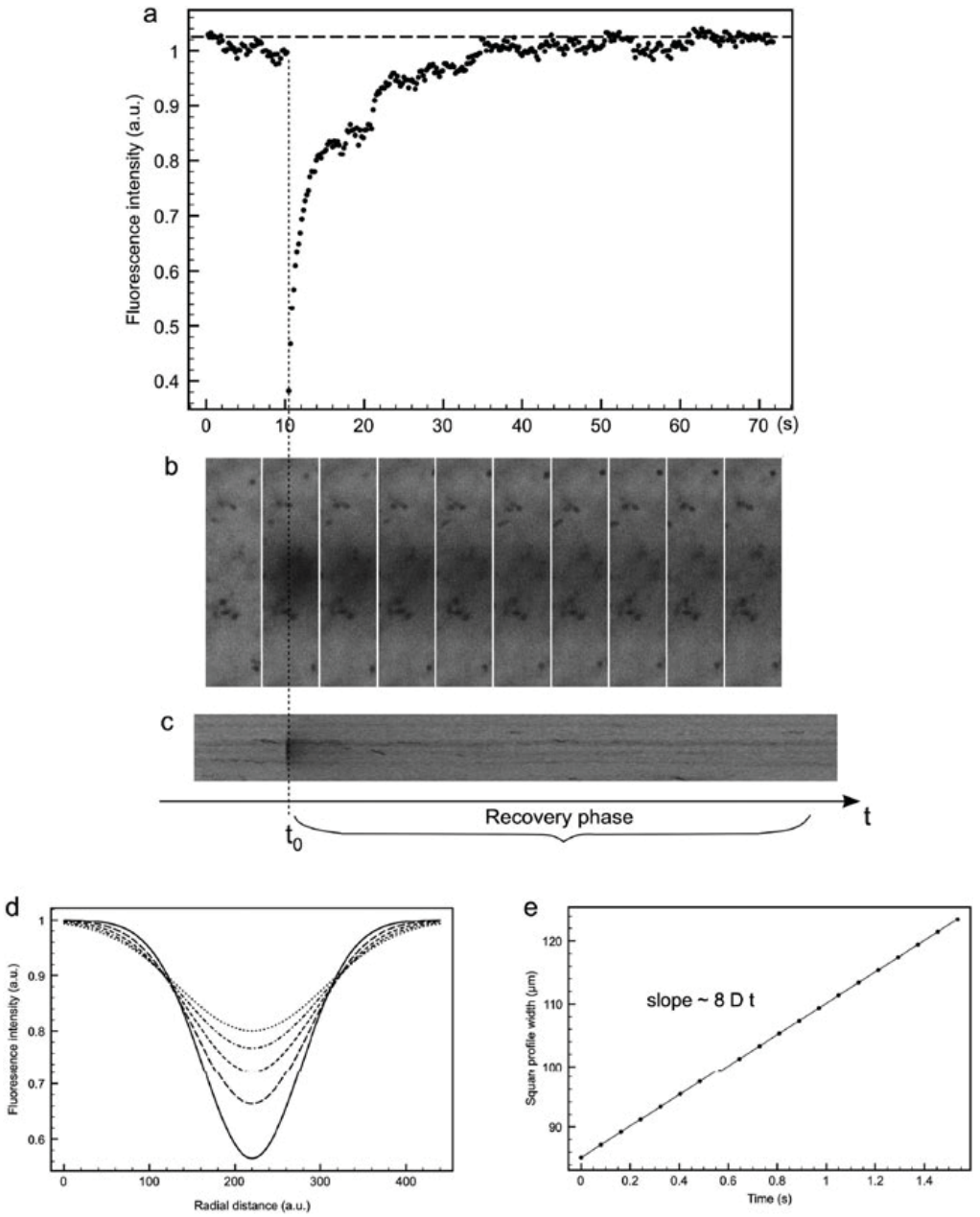

Fig. 21.3 Principle of molecular diffusion measurements in biofilms by FRAP (**a**) Example of fluorescence recovery curve. The *vertical points* show the start of the recovery phase just after photobleaching. The *horizontal dashed line* shows the initial level of fluorescence to estimate the mobile fraction (100% here). (**b**) Image sequence taken during the FRAP experiment on a *Stenotrophomonas maltophilia* biofilm loaded with FITC-dextran. The *dark area* in the centre of the images is the photobleached area. (**c**) Kymogram representation (intensity along a *vertical centered line* crossing the image for each time point) giving a graphical representation of spatial position over time. (**d**) Illustration of the evolution of the intensity spatial profile overtime (*dark line* is the initial profile after photobleaching and successive profiles in *dashed lines* with decreasing amplitudes with time). (**e**) Evolution of the squared intensity profile width with time showing the proportionality of the slope of the graph with the diffusion coefficient (profile analysis)

resolution. FCS is based on monitoring the emission intensity fluctuations due to a small number of molecules passing through the confocal excitation volume. These fluctuations can be quantified in their amplitude and duration by temporally autocorrelating the recorded intensity signal.

The experimental conditions required for this technique (a small number of fluorophores, characterization and control of the excitation volume) explain why FCS was mainly developed after the advent of confocal and two-photon microscopy (excitation volume < 1 fL) and of ultrasensitive new systems for detecting fluorescence photons (photomultipliers, avalanche photodiodes) allowing the use of low fluorophore concentrations (Guiot et al., 2000). Fluorescence intensity fluctuations reflect not only the diffusion of fluorescent molecules through the 3D structure of the biofilm, but also the photophysical and photochemical reactions that quench the fluorescence (charge transfer transition to the triplet state of the molecule), or conformational changes of molecules (molecular complexation, aggregate formation). Thus the FCS signal analysis quantifies a range of reaction parameters on a large time scale from microseconds to several seconds.

In practice, although this method is highly sensitive, has high resolution and is and non-invasive, it remains difficult to use and imposes some constraints. In particular, the fluorophores must have high fluorescence quantum yields and low photo-destruction yields. Furthermore, because of the small number of molecules involved, it is often necessary to temporally accumulate the fluorescence signal to obtain a representative statistic of fluctuation correlations with a satisfactory signal to noise ratio. This condition can be greatly improved by the use of two-photon excitation (TPE). The probability of fluorophore excitation by quasi-simultaneous ($<10^{-16}$ s delay) absorption of two photons is very low, thus significant TPE only occurs at the objective focal volume where the concentration of photons (also temporally concentrated by the use of femtosecond pulsed lasers) is very high. These properties give TPE microscopy several advantages over one photon excitation microscopy, in particular in a classical confocal setup: (i) intrinsic localisation of the excitation allows fluorescence detection with extremely low background noise and thus easier detection of single molecules, (ii) use of an infrared excitation wavelength (e.g. from a Titanium-sapphire laser) results in greater penetration of biological samples, (iii) photodamage is limited and restricted to the excitation volume and (iv) the excitation volume can easily be characterised and mathematically modelled.

FCS was first explored using homemade equipment and the associated specific know-how. The method has now been adapted to commercial CLSM and TPE setups. Whatever the setup used, FCS has allowed the following of the penetration, diffusion and reaction capabilities of fluorescent probes (latex beads and fluorescein isothiocyanate–dextran) of different sizes and electrical charge (Guiot et al., 2002), of fluorescently stained bacteriophages (Briandet et al., 2008), and of antimicrobial agents in models of static and dynamic biofilms with different EPS density. Steric hindrance and even total inhibition of diffusion have been observed, particularly in areas with a high cotent of extracellular polymeric substances. Alternative explanations for this were attractive electrostatic interactions between cationic particles and negatively charged bacteria, specific interactions between the diffusing fluorophore

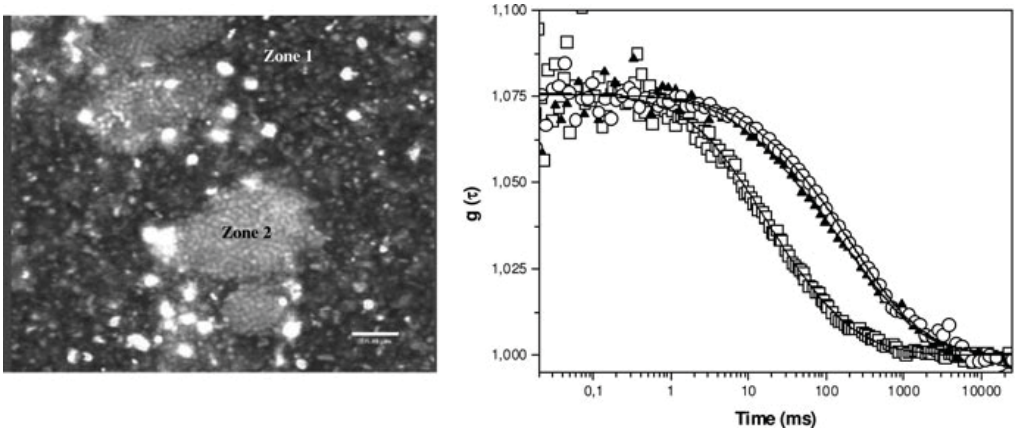

Fig. 21.4 (**a**) CLSM image of *S. maltophilia* biofilms near the substratum. Zone 1 and zone 2 correspond to homogeneous and heterogeneous parts of the biofilm respectively. Cells were stained with SYTO nucleic acid stain (scale bar = 20 μm). (**b**) Fluorescence correlation curves (g(τ)) corresponding to c2 bacteriophages stained with sytox green in solution (□), in zone 1 (▲) and zone 2 (◯) of *S. maltophilia* biofilms. The curve fits (*straight lines*) were obtained using a two diffusional component equation

and elements in the biofilm (e.g. sugar-matrix interaction, cell envelope and phage) (Fig. 21.4) or antibiotics. Such studies have given a better understanding of the role of the exopolymer matrix as a molecular "reservoir" and of its ability to modulate the transport and interaction of entities within the biofilm.

21.4.3 Fluorescence Lifetime Imaging (FLIM)

FLIM is well-suited for characterising such molecular interaction processes as fluorescence lifetime is an intrinsic property of a fluorophore, independent of its concentration. The fluorescence lifetime of a molecule varies locally depending on its reactivity with the biological environment. It is hence possible to build fluorescence lifetime images that allow assessment of the reactivity of a fluorophore at the molecular level throughout a 3D biological structure such as a biofilm. FLIM was used in biofilm studies to characterise the interaction between sugars in the exopolymeric matrix (Guiot et al., 2002), to probe the local pH (Vromm et al., 1999) and more recently to measure the differentiation of active and inactive bacteria by the estimation of the intracellular RNA:DNA ratio (Walcysko et al., 2008).

21.5 Conclusion

Recent advances in photonic microscopy, fluorophore design and molecular tools have dramatically transformed biofilm experimental analysis by making it possible to explore the dynamic structure and reactivity of these biological edifices non-invasively. The current development of high content screening automated systems

(Bridier et al., 2010), alternative label-free imaging methods such as scanning transmission X-ray microscopy (STXM) and magnetic resonance imaging (MRI) (Neu et al., 2010), and the development of correlative microscopy (Schaudinn et al., 2009) will dramatically improve our understanding of biofilm structure/function relationships, offering new perspectives in the field of biofilm research.

Acknowledgements Funding for our work from the French "Pole de Compétitivité Ile-de-France MEDICEN" is greatly appreciated. AES-Chemunex is warmly acknowledged for providing ChemChrom V6 fluorophore. We thank the "department of Essonne" for financial support of the confocal microscope (ASTRE n°A02137) and the INRA MIMA2 microscopic facilities for CLSM imaging. O. Habimana, P. Latour-Lambert and P. Piveteau are acknowledged for their contribution to image acquisition.

References

Alipour M, Suntres ZE, Lafrenie RM, Omri A (2010) Attenuation of *Pseudomonas aeruginosa* virulence factor and biofilms by co-encapsulation of bismuth-ethanedithiol with tobramycin in liposomes. J Antimicrob Chemother 65:684–693

Amann RI, Binder BJ, Chisholm SW, Devereux R, Stahl DA (1990) Combination of 16S rRNA-targeted oligonucleotide probes with flow cytometry for analyzing mixed microbial population. Appl Environ Microbiol 56:1919–1925

Anderson GG, O'Tolle GA (2008) Innate and Induced resistance mechanisms of bacterial biofilms. Curr Top Microbiol Immunol 322:85–105

Bayles KW (2007) The biological role of death and lysis in biofilm development. Nat Rev Microbiol 5:721–726

Beech IB, Sunner JA, Hiraoka K (2005) Microbe-surface interactions in biofouling and biocorrosion processes. Int Microbiol 8:157–168

Beloin C, Valle J, Latour-Lambert P, Faure P, Kzreminski M, Balestrino D, Haagensen JA, Molin S, Prensier G, Arbeille B, Ghigo JM (2004) Global impact of mature biofilm lifestyle on *Escherichia coli* K-12 gene expression. Mol Microbiol 51:659–674

Branda SS, Vik S, Friedman L, Kolter R (2005) Biofilms: the matrix revisited. Trends Microbiol 13:20–26

Briandet R, Lacroix-Gueu P, Lecart S, Renault M, Meylheuc T, Bidnenko E, Bellon-Fontaine M-N, Fontaine-Aupart M-P (2008) Fluorescence correlation spectroscopy to study diffusion-reaction of bacteriophages inside bacterial biofilms. Appl Environ Microbiol 74:2135–2143

Bridier A, Dubois-Brissonnet F, Boubetra A, Thomas V, Briandet R (2010) The biofilm architecture of sixty opportunistic pathogens deciphered using a high throughput CLSM method. J Microbiol Methods 82:64–70

Campanac C, Pineau L, Payard A, Baziard-Mouysset G, Roques C (2002) Interaction between biocide cationic agents and bacterila biofilms. Antimicrob Agent Chemother 46:1469–1474

Conchello J-A, Litchman J (2005) Optical sectioning microscopy. Nat Methods 2:920–931

Costerton JW, Stewart PS, Greenberg EP (1999) Bacterial biofilms, a common cause of persistent infections. Science 284:1318–1322

Cournet A, Delia M-L, Bergel A, Roques C, Bergé M (2010) Electrochemical reduction of oxygen catalyzed by a wide range of bacteria including Gram-positive. Electrochem Commun 12: 505–508

Deniset-Besseau A, Lévêque-Fort S, Fontaine-Aupart M-P, Roger G, Georges P (2007) Three-dimensional time-resolved imaging by multifocal multiphoton microscopy for a photosensitizer in living cells. Appl Optics 46:8045–8051

Dunny GM, Brickman TJ, Dworkin M (2008) Multicellular behavior in bacteria communication, cooperation, competition and cheating. BioEssays 30:296–298

Enos-Berlage JL, Guvener ZT, Keenan CE, McCarter LL (2005) Genetic determinants of biofilm development of opaque and translucent *Vibrio parahaemolyticus*. Mol Microbiol 55: 1160–1182

Guiot E, Enescu M, Arrio B, Johannin G, Roger G, Tosti S, Tfibel F, Mérola F, Brun A, Georges P, Fontaine-Aupart MP (2000) Molecular dynamics of biological probes by fluorescence correlation microscopy with two-photon excitation. J Fluoresc 10:413–419

Guiot E, Georges P, Brun A, Fontaine-Aupart MP, Bellon-Fontaine MN, Briandet R (2002) Heterogeneity of the diffusion inside microbial biofilms using fluorescence correlation microscopy under two-photon excitation. Photochem Photobiol 75:570–578

Habimana O, Meyrand M, Meylheuc T, Kulakauskas S, Briandet R (2009) Genetic features of resident biofilm determine attachment of *Listeria monocytogenes*. Appl Environ Microbiol 75:7814–7821

Hall-Stoodley L, Stoodley P (2005) Biofilm formation and dispersal and the transmission of human pathogens. Trends Microbiol 13:7–10

Hansen SK, Rainey PB, Haagensen JAJ, Molin S (2007) Evolution of species interactions in a biofilm community. Nature 445:533–536

Harmsen M, Yang L, Pamp SJ, Tolker-Nielsen T (2010) An update on *Pseudomonas aeruginosa* biofilm formation, tolerance, and dispersal. FEMS Immunol Med Microbiol 59:253–268

Hope CK, Wilson M (2004) Analysis of the effects of chlorhexidine on oral biofilm vitality and structure based on viability profiling and an indicator of membrane integrity. Antimicrob Agents Chemother 48:1461–1468

Huang CT, Yu FP, McFeters GA, Stewart PS (1995) Non-uniform spatial patterns of respiratory activity within biofilms during disinfection. Appl Environ Microbiol 61:2252–2256

Ito A, May T, Taniuchi A, Kawata K, Okabe S (2009) Localized expression profiles of rpoS in Escherichia coli biofilms. Biotechnol Bioeng 103:975–983

Kjelleberg S, Marshall KC, Givskov M (2007) The biofilm mode of life. In: Kjelleberg S, Marshall KC, Givskov M (eds) The biofilm mode of life, mechanisms and adaptations. Horizon Bioscience, Wymondham

Klausen M, Gjermansen M, Kreft J-U, Tolker-Nielsen T (2006) Dynamics of development and dispersal in sessile microbial communities: examples from *Pseudomonas aeruginosa* and *Pseudomonas putida* model biofilms. FEMS Microbiol Lett 261:1–11

Lakins MA, Marrison JL, O'Toole PJ, Van der Woude MW (2009) Exploiting advances in imaging technology to study biofilms by applying multiphotons laser scanning microscopy as an imaging and manipulation tool. J Microsc 235:128–137

Lenz AP, Williamson KS, Pitts B, Stewart PS, Franklin MJ (2008) Localized gene expression in *Pseudomonas aeruginosa* biofilms. Appl Environ Microbiol 74:4463–4471

Lewis K (2005) Persister cells and the riddle of biofilm survival. Biochemistry 70:267–274

Lopez D, Vlamakis H, Losick R, Kolter R (2009) Cannibalism enhances biofilm development in *Bacillus subtilis*. Mol Microbiol 74:609–618

Mah T-F C, O'Toole GA (2001) Mechanisms of biofilm resistance to antimicrobial agents. Trends Microbiol 9:34–39

May T, Okabe S (2008) Escherichia coli harboring a natural IncF conjugative F plasmid develops complex mature biofilms by stimulating synthesis of colanic acid and curli. J Bacteriol 190:7479–7490

Nadell CD, Xavier JB, Foster K (2009) The sociobiology of biofilms. FEMS Microbiol Rev 33:206–224

Neu TR, Manz B, Volke F, Dynes JJ, Hitchcock AP, Lawrence JR (2010) Advanced imaging techniques for assessment of structure, composition and function in biofilm systems. FEMS Microbiol Ecol 72:1–21

Neu TR, Swerhone GDW, Lawrence JR (2001) Assessment of lectin binding analysis for *in situ* detection of glycoconjugates in biofilm systems. Microbiology 147:299–313

Palmer RJ, Sternberg C (1999) Modern microscopy in biofilm research: confocal microscopy and other approaches. Curr Opin Biotechnol 10:263–268

Pamp SJ, Gjermansen M, Johansen HK, Tolker-Nielsen T (2008) Tolerance to the antimicrobial peptide colistin in Pseudomonas aeruginosa biofilms is linked to metabolically active cells, and depends on the pmr and mexAB-oprM genes. Mol Microbiol 68:223–240

Pamp SJ, Sternberg C, Tolker-Nielsen T (2009) Insight into the microbial multicellular lifestyle via flow-cell technology and confocal microscopy. Cytometry A 75:90–103

Peeters E, Nelis HJ, Coenye T (2008) Comparison of multiple methods for quantification of microbial biofilms grown in microtiter plates. J Microbiol Methods 72:157–165

Phe MH, Dossot M, Guilloteau H, Block JC (2007) Highly chlorinated *Escherichia coli* cannot be stained by propidium iodide. Can J Microbiol 53:664–670

Rani SA, Pitts B, Beyenal H, Veluchamy RA, Lewandowski Z, Buckingham-Meyer K, Stewart PS (2007) Spatial patterns of DNA replication, protein synthesis and oxygen concentration within bacterial biofilms reveal diverse physiological states. J Bacteriol 189:4223–4233

Rani SA, Pitts B, Stewart PS (2005) Rapid diffusion of fluorescent tracers into *Staphylococcus epidermidis* biofilms visualized by time lapse microscopy. Antimicrob Agents Chemother 49:728–732

Rice SA, Tan CH, Mikkelsen PJ, Kung V, Woo J, Tay M, Hauser A, McDougald D, Webb SA, Kjelleberg S (2009) The biofilm life cycle and virulence of *Pseudomonas aeruginosa* are dependent on a filamentous prophage. ISME J 3:271–282

Rieu A, Briandet R, Habimana O, Garmyn D, Guzzo J, Piveteau P (2008) *Listeria monocytogenes* EGD-e biofilms: no mushrooms but a network of knitted-chains structures. Appl Environ Microbiol 74:4491–4497

Rieu A, Weidmann S, Garmyn D, Piveteau P, Guzzo J (2007) Agr system of *Listeria monocytogenes* EGD-e: role in adherence and differential expression pattern. App Environ Microbiol 73:6125–6133

Schaudinn C, Carr G, Gorur A, Jaramillo D, Costerton JW, Webster P (2009) Imaging of endodontic biofilms by combined microscopy (FISH/cLSM – SEM). J Microsc 235:124–127

Singh R, Debarati P, Rakesh KJ (2006) Biofilms, implications in bioremediation. Trends Microbiol 14:389–397

Stewart PS (2003) Diffusion in biofilms. J Bacteriol 185:1485–1491

Stewart PS, Franklin MJ (2008) Physiological heterogeneity in biofilms. Nat Rev Microbiol 6: 199–210

Takenaka S, Pitts B, Trivedi HM, Stewart PS (2009) Diffusion of macromolecules in model oral biofilms. Appl Environ Microbiol 75:1750–1753

Takenaka S, Trivedi HM, Corbin A, Pitts B, Stewart PS (2008) Direct visualization of spatial and temporal patterns of antimicrobial action within model oral biofilms. Appl Environ Microbiol 74:1869–1875

Tolker-Nielsen T, Brinch UC, Ragas PC, Andersen JB, Jacobsen CS, Molin S (2000) Development and dynamics of *Pseudomonas* sp. Biofilms J Bacteriol 182:6482–6489

Veening JW, Smits WK, Hamoen LW, Jongbloed JD, Kuipers OP (2004) Visualization of differential gene expression by improved cyan fluorescent protein and yellow fluorescent protein production in *Bacillus subtilis*. Appl Environ Microbiol 70:6809–6815

Vlamakis H, Aguilar C, Losick R, Kolter R (2008) Control of cell fate by the formation of an architecturally complex bacterial community. Genes Dev 22:945–953

Vroom JM, De Grauw KJ, Gerritsen HC, Bradshaw DJ, Marsh PD, Watson GK, Birmingham JJ, Allison C (1999) Depth penetration and detection of pH gradients in biofilms by two photon excitation microscopy. Appl Environ Microbiol 65:3502–3511

Vuong C, Kocianova VJM, Yao Y, Fischer ER, DeLeo FR, Otto M (2004) A crucial role for exopolysaccharide modification in bacterial biofilm formation, immune evasion, and virulence. J Biol Chem 279:54881–54886

Waharte F, Steenkeste K, Briandet R, Fontaine-Aupart MP (2010) Local diffusion measurements inside biofilms by FRAP analysis with a commercial confocal laser scanning microscope. Appl Environ Microbiol 76:5860–5869

Walczysko P, Kuhlicke U, Knappe S, Cordes C, Neu TR (2008) *In situ* activity of suspended and immobilized microbial communities as measured by fluorescence lifetime imaging. Appl Environ Microbiol 74:294–299

Webb JS, Thompson LS, James S, Charlton T, Tolker-Nielsen T, Koch B, Givskov M, Kjelleberg S (2003) Cell death in *Pseudomonas aeruginosa* biofilm development. J Bacteriol 185: 4585–4592

Xu KD, Stewart PS, Xia F, Huang C-T, McFeters GA (1998) Spatial physiological heterogeneity in *Pseudomonas aeruginosa* biofilm is determined by oxygen availability. Appl Environ Microbiol 64:4035–4039

Yadvika S, Sreekrishnan TR, Kohli S, Rana V (2004) Enhancement of biogas production from solid substrates using different techniques – a review. Bioresour Technol 95:1–10

Yarwood JM, Bartels DJ, Volper EM, Greenberg EP (2004) Quorum sensing in *Staphylococcus aureus* biofilms. J Bacteriol 186:1838–1850

B. Article 2 :

“Resistance of bacterial biofilms to disinfectants: a review.”

A. Bridier, R. Briandet, V. Thomas, F. Dubois-Brissonnet.

Accepté dans Biofouling (2011).

Resistance of bacterial biofilms to disinfectants: a review

A. Bridier[1, 2], R. Briandet[2,1], V. Thomas[3], F. Dubois-Brissonnet[1,2*]

[1] AgroParisTech, UMR MICALIS, F-91300 Massy, France; [2] INRA, UMR 1319 MICALIS, F-78350 Jouy-en-Josas, France; [3] STERIS SA, CEA, F- 92265 Fontenay-aux-Roses, France.

* Author for correspondance: E-mail: florence.dubois-brissonnet@jouy.inra.fr ; AgroParisTech, UMR Micalis, B2HM, 25 avenue République F-91300 Massy France, Tel: (33) 1 69 53 64 72; Fax: (33) 1 69 93 51 44.

Abstract

A biofilm can be defined as a community of micro-organisms adhering to a surface and surrounded by a complex matrix of extrapolymeric substances. It is now generally accepted that biofilm mode of growth induces microbial resistance to disinfection that can lead to dramatic economic and health concerns. Although the precise origin of such resistance remains unclear, different studies have shown that it is a multifactorial process involving the biofilm spatial organization. This review will discuss the mechanisms identified up to now to play a role in biofilm resistance to disinfectants as well as the novel anti-biofilm strategies recently explored.

Keywords: biofilm, biocide, resistance, tolerance, adaptation, spatial architecture, control

Introduction

Disinfectants are chemical agents used on inanimate objects to inactivate virtually all recognized pathogenic micro-organisms (Centers for Disease Control and Prevention, USA). Unlike antibiotics, which are chemotherapeutic drugs mostly used internally to control infections and which interact with specific structures or metabolic processes in microbial cells, disinfectants act non-specifically against multiple targets (Meyer and Cookson 2010). The mode of action of disinfectants depends on the nature of biocide employed, as has been extensively described in numerous reviews (McDonnell and Russell 1999, Russell 2003). Potential target sites in Gram-positive or Gram-negative bacteria are the cell wall or outer membrane, the cytoplasmic membrane, functional and structural proteins, DNA, RNA and other cytosolic components. Disinfection treatments are used in medical, industrial and domestic environments to control biocontamination of the surfaces. Although these biocide treatments eliminate most surface contamination, some micro-organisms may survive and give rise to dramatic problems in terms of public health. Indeed, numerous reports have highlighted the survival of micro-organisms after cleaning and disinfection in food (Bagge-Ravn et al. 2003, Stocki et al. 2007, Weese and Rousseau 2006), medical (Deva et al. 1998, Martin et al. 2008) and domestic environments (Cooper et al. 2008). Resistance of micro-organisms to disinfection is frequently associated with the presence of biofilms on surfaces (Bressler et al. 2009, Vestby et al. 2009). In most wet environments, micro-organisms are able to adhere to a surface, producing a matrix of extracellular polymeric substances mainly composed of exopolysaccharides, proteins and nucleic acids (Branda et al. 2005, Costerton et al. 1995, Hoiby et al. 2010). Cells embedded in the biofilm matrix are well known to express phenotypes that differ from those of their planktonic counterparts, and to display specific properties including an increased resistance to biocide treatments (Nett et al. 2008, Smith and Hunter 2008, Wong et al. 2010). The definition of "resistance" needs to be clarified as it changes depending on whether planktonic or biofilm cells are considered. In the former case, a bacterial strain is defined as being resistant to a biocide if it is not inactivated by a specific concentration or period of exposure that usually inactivates the majority of other strains(Langsrud et al. 2003). Biofilm cells, conversely, are generally said to be resistant by comparison with their planktonic counterparts. From a mechanistic point of view, bacterial resistance to biocides may be intrinsic, acquired resistance or tolerance (phenotypic adaptation) (Langsrud et al. 2003, Russell 2003). Biofilm insusceptibility is sometimes considered to be a tolerance rather than a real "resistance" since it is mainly induced by a physiological adaptation to the biofilm mode of

life (sessile growth, nutrient stresses, contact with repeated sub-lethal concentrations of disinfectant) and can be lost or highly reduced when biofilm cells revert to the planktonic state (Russell 1999). Nevertheless, stable resistant variants can appear in biofilms (see section A4). Therefore, throughout this review, we will use the general term of "biofilm resistance" to refer to biofilm insusceptibility compared to the planktonic state.

As opposed to planktonic cells for which several well-defined standards have been published (EN 1040, NF T 150), various laboratory methods allow evaluating the susceptibility of biofilm cells to disinfectants. Standard protocols for planktonic cells can be adapted (Meylheuc et al. 2006, Ntsama-Essomba et al. 1997), or specially-designed systems can be used, such as the MBEC assay system (MBEC^{TM} assay system, Biofilm technologies Ltd., Calgary, Alberta) (Ceri et al. 1999)which has been approved as an ASTM standard method (number E2799-11). The resistance of biofilm cells can be evaluated by measuring the ratio of concentrations (Rc) or time (Rt) required to achieve the same reduction in the planktonic or biofilm population, or by comparing the reductions obtained after exposure to the same concentration during the same time. Examples of Rc or Rt values found in the literature for commonly used biocides are shown in Table 1. Depending on the species and the biocide considered, these values can range from 1 to 1000 and from 20 to 2160 for Rc and Rt coefficients respectively, thus highlighting the potentially high level of biofilm resistance to different disinfectants. It should be noted that it is often difficult to compare results between studies due to the lack of standardized protocols for the testing of biocides on biofilms (Buckingham-Meyer et al. 2007).

However, having this global and quantitative information on biofilm resistance is not sufficient to improve the control of surface contamination. A clearer understanding of the mechanisms involved in biofilm resistance to biocides is thus a major concern among microbiologists. While many papers have focused on mechanisms of biofilm resistance to antibiotics (Fux et al. 2005, Hoiby et al. 2010, Stewart 2002, Stewart and Costerton 2001), there are no recent reviews that specifically deal with the mechanisms of biofilm resistance to disinfectants. In this context, this paper first aims to review the different factors related to the physiological and structural characteristics of the biofilm that influence its resistance to disinfectants. It will afterwards focuses on the most recent strategies that have been proposed in the literature to overcome biofilm resistance.

Biocide	Strains	Rc	Rt	References	Biofilm formation method
Benzalkonium chloride	*Escherichia coli* ATCC 10536	1000		(Ntsama-Essomba *et al.*, 1997)	continuous flow conditions in Tygon PVC tubing
	Pseudomonas aeruginosa ATCC 15442	100		(Dubois-Brissonnet *et al.*, 1995)	static conditions on stainless steel coupons
	Pseudomonas aeruginosa ATCC 15442	250		(Ntsama-Essomba *et al.*, 1995)	continuous flow conditions in Tygon PVC tubing
	Pseudomonas aeruginosa ERC1		2160	(Grobe et al., 2002)	alginate gel bead substrate in agitated medium
	Staphylococcus aureus ATCC 6538	50		(Luppens *et al.*, 2002)	continuous flow conditions on glass coupons
	Listeria monocytogenes		>20	(Frank & Koffi, 1990)	static conditions on glass slides
Benzalkonium chloride C12	*Pseudomonas aeruginosa* CIP A22	10		(Campanac et al., 2002)	continuous flow conditions in Tygon PVC tubing
Benzalkonium chloride C14	*Pseudomonas aeruginosa* CIP A22	50		(Campanac et al., 2002)	continuous flow conditions in Tygon PVC tubing
Benzalkonium chloride C16	*Pseudomonas aeruginosa* CIP A22	>50		(Campanac et al., 2002)	continuous flow conditions in Tygon PVC tubing
Benzalkonium chloride C18	*Pseudomonas aeruginosa* CIP A22	>50		(Campanac et al., 2002)	continuous flow conditions in Tygon PVC tubing
Benzalkonium chloride C12	*Staphylococcus aureus* CIP 53 154	>50		(Campanac et al., 2002)	continuous flow conditions in Tygon PVC tubing
Benzalkonium chloride C14	*Staphylococcus aureus* CIP 53 154	>50		(Campanac et al., 2002)	continuous flow conditions in Tygon PVC tubing
Benzalkonium chloride C16	*Staphylococcus aureus* CIP 53 154	>50		(Campanac et al., 2002)	continuous flow conditions in Tygon PVC tubing
Benzalkonium chloride C18	*Staphylococcus aureus* CIP 53 154	>50		(Campanac et al., 2002)	continuous flow conditions in Tygon PVC tubing
cetrimide	*Pseudomonas aeruginosa* ATCC 15442	>400		(Dubois-Brissonnet et al., 1995)	static conditions on stainless steel coupons
	Pseudomonas aeruginosa ATCC 15442	>400		(Ntsama-Essomba et al., 1995)	continuous flow conditions in PVC tubing
Chlorine	*Pseudomonas aeruginosa* ERC1		290	(Grobe et al., 2002)	alginate gel beads in agitated broth medium
sodium hypochlorite	*Pseudomonas aeruginosa* ATCC 15442	20		(Dubois-Brissonnet et al., 1995)	static conditions on stainless steel coupons
Hydrogen peroxide	*Pseudomonas aeruginosa* ATCC 15442	5		(Ntsama-Essomba et al., 1995)	continuous flow conditions in Tygon PVC tubing
	Escherichia coli ATCC 10536	5		(Ntsama-Essomba et al., 1997)	continuous flow conditions in Tygon PVC tubing
	Staphylococcus aureus ATCC 6538	600		(Luppens et al., 2002)	continuous flow conditions on glass coupons
	Mycobacterium fortuitum (clinical isolate)	38		(Bardouniotis *et al.*, 2003)	MBEC™ assay system on rocking platform
	Mycobacterium marinum (clinical isolate)	>2		(Bardouniotis et al., 2003)	MBEC™ assay system on rocking platform
	P.aeruginosa + *K.pneumoniae*		>60	(Stewart et al., 2001)	continuous flow conditions on stainless steel coupons
	Mycobacterium fortuitum (clinical isolate)	1		(Bardouniotis et al., 2003)	MBEC™ assay system on rocking platform
peracetic acid + hydrogen peroxide	*Mycobacterium marinum* (clinical isolate)	1		(Bardouniotis et al., 2003)	MBEC™ assay system on rocking platform
	Pseudomonas aeruginosa ATCC 15442	40		(Dubois-Brissonnet et al., 1995)	static conditions on stainless steel coupons
Chlorosulfamate	*Pseudomonas aeruginosa* ATCC 15442	4		(Ntsama-Essomba et al., 1995)	continuous flow conditions in Tygon PVC tubing
	Escherichia coli ATCC 10536	25		(Ntsama-Essomba et al., 1997)	continuous flow conditions in Tygon PVC tubing
	P.aeruginosa + *K.pneumoniae*		>60	(Stewart et al., 2001)	continuous flow conditions on steel coupons
glutaraldehyde	*Mycobacterium fortuitum* (clinical isolate)	1,15		(Bardouniotis et al., 2003)	MBEC™ assay system on rocking platform
	Mycobacterium marinum (clinical isolate)	2		(Bardouniotis et al., 2003)	MBEC™ assay system on rocking platform
	Pseudomonas aeruginosa ERC1		30	(Grobe & Stewart, 2000)	alginate gel bead supports in agitated medium
	Pseudomonas aeruginosa ERC1		47	(Grobe et al., 2002)	alginate gel bead supports in agitated medium
Chlorhexidine digluconate	*Staphylococcus epidermidis* ATCC 35984	4		(Karpanen *et al.*, 2008)	Static conditions in polystyrene microtitre plate
silver nitrate	*Mycobacterium marinum* (clinical isolate)	4,2		(Bardouniotis et al., 2003)	MBEC™ assay system on rocking platform
	Mycobacterium fortuitum (clinical isolate)	12		(Bardouniotis et al., 2003)	MBEC™ assay system on rocking platform
phénol	*Pseudomonas aeruginosa* ATCC 15442	1		(Dubois-Brissonnet et al., 1995)	static conditions on stainless steel coupons
	Pseudomonas aeruginosa ATCC 15442	1		(Ntsama-Essomba et al., 1995)	continuous flow conditions in Tygon PVC tubing
oregano	*Staphylococcus epidermidis* ATCC 35984	4		(Nostro *et al.*, 2007)	static conditions in polystyrene microtitre plate
carvacrol	*Staphylococcus epidermidis* ATCC 35984	4		(Nostro et al., 2007)	static conditions in polystyrene microtitre plate
thymol	*Staphylococcus epidermidis* ATCC 35984	4		(Nostro et al., 2007)	static conditions in polystyrene microtitre plate
tea tree oil	*Staphylococcus epidermidis* ATCC 35984	0,125		(Karpanen et al., 2008)	static conditions in polystyrene microtitre plate
	Staphylococcus epidermidis ATCC 35984	16		(Karpanen et al., 2008)	static conditions in polystyrene microtitre plate
eucalyptus oil	*Staphylococcus epidermidis* ATCC 35984	4		(Karpanen et al., 2008)	static conditions in polystyrene microtitre plate

Table 1. Resistance coefficients of biofilm cells compared to planktonic cells, obtained from studies involving the use of commonly used disinfectants. $R_C = C_{biofilm}/C_{planktonic}$, where $C_{biofilm}$ corresponds to the biocide concentration required to kill a given level of biofilm cells and $C_{planktonic}$ corresponds to the biocide concentration required to kill the same level of planktonic cells. $R_t = t_{biofilm}/t_{planktonic}$, where $t_{biofilm}$ corresponds to the biocide exposure time at a fixed concentration necessary to kill a given level of biofilm cells and $t_{planktonic}$ corresponds to the biocide exposure time at a fixed concentration necessary to kill the same level of planktonic cells.

A- What do we know about the mechanisms involved in biofilm resistance to disinfectants?

A1-Diffusion/reaction limitations of disinfectants in biofilms

The formation and maintenance of mature biofilms are intimately linked to the production of extracellular matrix (Branda et al. 2005, Ma et al. 2009). The multiple layers of cells and extrapolymeric substances may constitute a complex and compact structure within which biocides find it difficult to penetrate and reach internal layers, thus hampering their efficacy. For example, it was shown that chlorine levels measured within mixed biofilms of *P. aeruginosa* and *K. pneumoniae* using a microelectrode only reached 20% of concentrations measured in the bulk liquid (De Beer et al. 1994). Similarly, a more recent study showed that chlorine at 25 mg l^{-1} did not penetrate beyond a depth of 100 µm into a complex dairy biofilm that was 150-200 µm thick (Jang et al. 2006). The restricted diffusion of molecules within the range 3-900 kDa in biofilms due to size exclusion has already been reported (Thurnheer et al. 2003). However, since biocides are often highly chemically reactive molecules, the presence of organic matter such as proteins, nucleic acids or carbohydrates can profoundly impair their efficacy (Lambert and Johnston 2001) and potential interactions between antimicrobials and biofilm components seemed more likely to explain the limitations of penetration into the biofilm. Indeed, interesting findings were produced when measuring the mean penetration time into a 1mm-thick mixed biofilm of *P.aeruginosa* and *K.pneumoniae*, which was eight times higher for alkaline hypochlorite (48 min) than for chlorosulfamate (6 min), even though the latter has a higher molecular weight (Stewart et al. 2001). The decreased penetration of the alkaline biocide was hypothesized to be related to its greater capacity to react with matrix constituents. It was also reported that the delayed penetration of chlorine, glutaraldehyde and 2, 2-dibromo-3-nitrilopropionamide into an artificial biofilm model (*P.aeruginosa* entrapped in alginate gel beads) was due to interactions between the biocides and constituents of the gel beads (Grobe et al. 2002). Moreover, biocide molecules may simply adsorb to cells and matrix components in biofilms. Using fluorescence spectroscopy correlation (FCS), the diffusion capabilities of fluorescent probes (latex beads and fluorescein isothiocyanate–dextran) of different sizes and electrical charges were measured in biofilms with variable EPS contents (Guiot et al. 2002). These authors demonstrated that in the absence of any electrostatic interactions, the majority of particles tested could penetrate and diffuse into a biofilm, thus suggesting that nothing prevented the diffusion of antimicrobial agents as a function of their size from a steric standpoint. Conversely, the diffusion of positively charged particles within negatively charged biofilms was hindered because of electrostatic

interactions, as has also been proposed for cationic cetylpyridinium chloride (Ganeshnarayan et al. 2009). During the past ten years, the emergence of innovative optical microscopy techniques such as confocal laser scanning microscopy (CLSM), and improvements to fluorescent labeling, have provided an opportunity for the direct investigation of biocide reactivity within the native structure of biofilms (Bridier et al. 2011b). A direct time-lapse confocal microscopic technique was recently developed to enable the real-time visualization of biocide activity within the biofilm (Bridier et al. 2011a, Davison et al. 2010, Hope and Wilson 2004, Stoodley et al. 2001, Takenaka et al. 2008). It can provide information on the dynamics of biocide action in the biofilm and the spatial heterogeneity of bacteria-related susceptibilities that are crucial for a better understanding of biofilm resistance mechanisms. Experimentally, after staining with fluorescent markers to enable the real-time monitoring of cell inactivation, the three-dimensional structure of the biofilm is scanned by CLSM at regular intervals during exposure to the biocide and then spatial and temporal patterns of biocide action are visualized in the structure (Fig. 2).

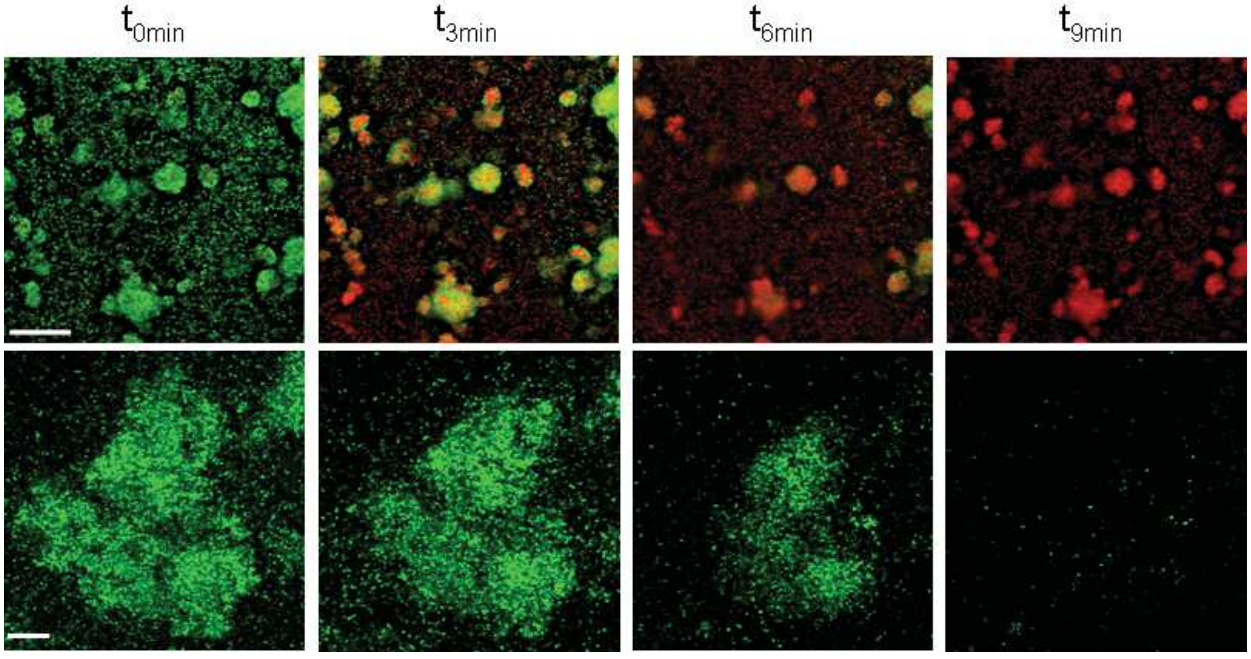

Figure 1. Visualization of cell inactivation in *S. aureus* ATCC 27217 using the BacLight Live/Dead viability kit (Invitrogen) and in a *P. aeruginosa* ATCC 15442 biofilm using the Chemchrome V6 esterasic marker (AES chemunex) during benzalkonium chloride treatments (0.5% w/v), 0, 3, 6 and 9 minutes after biocide application. For *S. aureus*, total cells are stained in green (Syto9) and permeabilized cells are stained in red (propidium iodide). For *P. aeruginosa*, viable (non-permeabilized) cells are stained in green, the loss of fluorescence corresponding to the leakage of fluorophores outside cells permeabilized by biocide activity. Each image corresponds to a horizontal section situated 5-10 µm from the substrate. Scale bar corresponds to 20µm.

This method allowed to demonstrate that the penetration of QAC to the center of a *S. epidermidis* biofilm cluster takes 60 times longer than the time estimated for diffusive access in the absence of sorption (Davison et al. 2010). In *P. aeruginosa* biofilms, different patterns of fluorescence loss were observed depending on the biocide used: peracetic acid caused a uniform and linear loss of cell viability, demonstrating that the greater resistance of biofilm cells could not be due to limitations of penetration (Bridier et al. 2011a). In contrast, the same study showed that benzalkonium chloride first inactivated cells located in peripheral layers of clusters. The positive charge and hydrophobic nature of the biocide could therefore explain the delayed penetration observed. In a *P.aeruginosa* biofilm, the level of bacterial resistance to benzalkonium chloride increased with the C-chain length of the quaternary ammonium compound (QAC from C12 to C18) (Campanac et al. 2002). This increase in the C-chain length, leading to an increase in the hydrophobicity of the molecule, was hypothesized to limit its penetration through the hydrophilic matrix and thus cause a progressive loss of bactericidal efficacy within the biofilm. More recently, the role of C-chain length in the binding of QAC to biofilm components, probably through hydrophobic interactions, has also been proposed (Sandt et al. 2007). In another recent paper, it was reported that bacterial cell wall hydrophobicity could alter the diffusion of nanoparticles within a biofilm (Habimana et al. 2011) suggesting that cell wall interfacial components such as peptidoglycan, fimbriae, capsules and the S-layer could also condition diffusion of the compound within the biofilm. Moreover, other components such as enzymes are present in the extracellular matrix and may play a role in the neutralization of toxic compounds. For example, hydrogen peroxide was shown to be able to penetrate and partially kill cells only in a biofilm formed by catalase-deficient *P. aeruginosa* (Stewart et al. 2000). In a wild-type biofilm, the bacteria were protected from H_2O_2 penetration by catalase-mediated destruction of the biocide.

These studies illustrate that transport limitation may be a mechanism that contributes to the resistance of biofilms to disinfectants. It seems to be related mainly to physicochemical interactions between the biocide and exopolymeric substances or bacterial cells rather than steric hindrance inside the biofilm. Nevertheless, although diffusion/reaction problems can partly explain the resistance of biofilms, some results have shown that despite an effective penetration of a biocide into a biofilm, only a low level of inactivation was achieved (Stewart et al. 2001). Moreover, the resistance of a *S. aureus* biofilm to a QAC could be attributed to a major extent to phenotypic modifications of cells rather than the protective presence of an exopolysaccharide matrix (Campanac et al. 2002). These findings highlight the existence of

additional mechanisms involved in biofilm resistance that will be presented in the next section.

A2-Phenotypic adaptations of biofilm cells to sublethal concentrations of disinfectants

During a disinfection process, the reaction-diffusion limited penetration of biocides into a biofilm may result in only low levels of exposure to the antimicrobial agent in deeper regions of the biofilm. Biofilm cells will therefore develop adaptive responses to sublethal concentrations of the disinfectant. Increased survival following the same QAC shock was reported in adapted *Pseudomonas aeruginosa*, alongside concomitant modifications to membrane composition (Jones et al. 1989, Mechin et al. 1999). Adaptation depends on the type of disinfectant being effective in the presence of QACs contrarily to sodium dichloroisocyanurate or tri-sodium phosphate (Guérin-Méchin et al. 1999). Moreover, cross-resistance to other QACs (Mechin et al. 1999) or to antibiotics (Braoudaki and Hilton 2004) has been reported for adapted cells. Adaptation of biofilm cell populations to disinfectants was first reported in *Salmonella* (Mangalappalli-Illathu et al. 2008): biofilm cells displayed better adaptation to benzalkonium chloride than their planktonic counterparts after continuous exposure. In that case, the up-regulation of specific proteins involved in energy metabolism, protein biosynthesis, adaptation (CspA) and detoxification (Mangalappalli-Illathu and Korber 2006), together with a shift in the fatty acid composition (Mangalappalli-Illathu et al. 2008) suggested that biofilm-specific adaptation conferred better survival on the biofilm-adapted population.

Moreover, the conditions prevailing during the initial adhesion to a substrate may play a key role in biofilm resistance to a disinfectant as it is the initial step in the construction of biofilm architecture (Dynes et al. 2009). Cell morphology, spatial distribution and the relative amounts of exopolymer matrix in *Pseudomonas* biofilms were shown to differ in the presence of sublethal doses of chlorhexidine, benzalkonium chloride or triclosan. Chlorine dioxide at sublethal doses has also been shown to stimulate biofilm formation in *Bacillus subtilis* (Shemesh et al. 2010). During their study, these authors demonstrated that transcription of the major genes responsible for biofilm matrix production was enhanced in the presence of chlorine throughout activation of the membrane-bound kinase KinC. The ability of chlorine to collapse membrane potential has been proposed to provoke activation of this kinase.

A3-Phenotypic adaptations of cells in biofilm environment

From the attachment of cells to the development of a three-dimensional structure, the growth of a biofilm is associated with physiological adaptations of cells that may lead to an increase

in resistance to biocides. These phenotypic adaptations result from the expression of specific genes in response to their direct micro-environmental conditions. Comparisons of gene expression profiles and proteomic analyses of planktonic and biofilm states in different species support this idea (Prigent-Combaret et al. 1999, Sauer 2003, Shemesh et al. 2007, Vilain et al. 2004, Whiteley et al. 2001). For example, some studies have shown that just after a cell reaches a surface, genes coding flagellar proteins are repressed and other genes coding for exopolysaccharides and adhesin proteins such as curli are induced (Davies et al. 1993, Prigent-Combaret et al. 2001, Prigent-Combaret et al. 2000, Sauer and Camper 2001, Vidal et al. 1998). These changes induced by cell adhesion can lead to the appearance of more resistant phenotypes, as suggested by studies reporting the greater resistance of cells that are merely adhered to a surface when compared with their planktonic counterparts (Chavant et al. 2004, Frank and Koffi 1990, Kamgang et al. 2007).

Following the adhesion step, bacteria start to develop into a biofilm with a three-dimensional structure. A direct consequence of the growth of this three-dimensional structure is the emergence of chemical gradients within the biofilm. Cells located at the periphery of the cluster have access to nutrients and oxygen while bacteria in internal biofilm layers experience nutrient-poor microenvironments where the concentrations of metabolic waste products are higher. This chemical heterogeneity governs the onset of physiological heterogeneity (Stewart and Franklin 2008, Xu et al. 1998). Two Green Fluorescent Protein (GFP) gene constructs were used to demonstrate the existence of stratified patterns of growth and protein synthesis in *P. aeruginosa* biofilms (Werner et al. 2004). Protein synthesis and active cell-growth were restricted to the zone where oxygen was available and represented a narrow band in contact with the medium. Cells with distinctive metabolic rates were present throughout the three-dimensional structures, thus constituting a physiologically heterogeneous population. Alterations to growth and activity rates induced modifications of membrane composition and the expression of defense mechanisms that could lead to an increased resistance of bacteria to biocides (Lisle et al. 1998, Sabev et al. 2006, Saby et al. 1999, Stewart and Olson 1992, Taylor et al. 2000). Indeed, it is now widely accepted that the development of a stress response is an important feature of the life cycle of biofilms (Beloin and Ghigo 2005, Coenye 2010). For example, it was reported in *P. aeruginosa* that RpoS, which is the principal regulator of a general stress response, was three times more strongly expressed in 3-day old biofilm cells than in stationary planktonic cells (Xu et al. 2001). Different genes involved in the oxidative stress response have also been shown to be induced

in biofilms of *L. monocytogenes*, *P. aeruginosa, E. coli* or *Tannerella forsythia* (Pham et al. 2010, Ren et al. 2004, Sauer et al. 2002, Tremoulet et al. 2002) and may afford protection for bacteria against the activity of oxidizing agents. Furthermore, the up-regulation or induction of genes coding to multidrug efflux pumps in biofilms may be another possible mechanism to explain bacterial biocide resistance, as already shown for antibiotics (Gillis et al. 2005, Kvist et al. 2008). Efflux pumps are systems that enable cells to rid themselves of toxic molecules and allow bacteria to survive in the presence of such substances. An example of a well-known system specific to biocides is the QAC efflux system of *S. aureus* which is responsible for its high level of resistance to QAC and cationic biocides (Mitchell et al. 1998, Smith et al. 2008). Similar systems have been identified in other species and also for other biocides such as triclosan or chlorhexidine (Poole 2005, Villagra et al. 2008). However, the induction of biocide efflux pumps in biofilms has not yet been clearly demonstrated and further research is necessary to determine whether this phenomenon plays an important role in biofilm resistance.

The appearance of the biofilm-specific phenotype has been shown to be at least partly induced by quorum sensing. Indeed, cell-to-cell communication has been identified as controlling biofilm development in a number of bacterial species (Cvitkovitch et al. 2003, Huber et al. 2001, Labbate et al. 2004, Parsek and Greenberg 2000, Waters et al. 2008). Interestingly, it was observed that a *lasI* signaling *P. aeruginosa* mutant formed a biofilm with a flat architecture when compared to the wild-type, and also displayed evidence of its increased susceptibility to SDS (Davies et al. 1998). Similarly, *lasI* and *rhlI P. aeruginosa* mutants exhibited increased sensitivity to hydrogen peroxide and phenazin methosulfate (Hassett et al. 1999). Moreover, authors demonstrated that the expression of catalase and superoxide dismutase genes coding to protective enzymes against oxidizing stress, was under the control of quorum sensing. Consistent with these findings, regulation of the stress response by quorum sensing has more recently been reported in other species (Joelsson et al. 2007, Lumjiaktase et al. 2006, Pontes et al. 2008).

A final illustration of the adaptation of specific phenotypes that may contribute to the bacterial resistance observed in biofilms is that a small fraction of the population may enter a highly-protected state displaying dramatic resistance and referred to as persisters (Harrison et al. 2005, Lewis 2005). These cells are phenotypic variants but not genetic mutants, and have also been identified in planktonic bacterial populations (Lewis 2001, Shah et al. 2006). One assumption is that persisters develop more frequently in a biofilm than in a planktonic culture,

perhaps induced by the specific environmental conditions prevailing within the structure, and may therefore contribute to better antimicrobial protection in the biofilm (Roberts and Stewart 2005, Stewart 2002).

A4-Gene transfers and mutations

Lateral gene transfer participates in microbial adaptation to the environment through the exchange of genetic sequences including plasmids, transposons or integrons that confer specific phenotypic traits on cells such as their metabolic capabilities, virulence expression and antimicrobial resistance (Hannan et al. 2010, Kelly et al. 2009, Top and Springael 2003). For example, QAC resistance genes carried by transferable genetic elements have been widely identified (Bjorland et al. 2001, Elhanafi et al. 2010, Gillings et al. 2009). Different studies have generated evidence suggesting that biofilms may constitute an optimum environment for the exchange of genetic material (Ando et al. 2009, Hausner and Wuertz 1999, Maeda et al. 2006, Nguyen et al. 2010) leading to dissemination of biocide resistance cassettes within the population. Indeed, high cell density, the presence of a matrix, the release of large quantities of DNA or nutrient conditions within biofilms may promote conjugation and transformation processes. Another consideration is that biofilm growth can lead to the emergence of extensive genetic diversity within a bacterial population. A recent study showed that cells in a *P. aeruginosa* biofilm displayed an increase of up to 105-fold in mutability when compared to a planktonic culture (Driffield et al. 2008). It was observed that *P. aeruginosa* mutations mostly occurred in microcolonies but not elsewhere in a biofilm or in planktonic cultures, showing that these dense areas of biofilm could indeed favor mutations(Conibear et al. 2009). Different studies have reported the appearance of genetic variants in biofilms that display distinctive phenotypic traits (Allegrucci and Sauer 2007, Boles et al. 2004, Kirisits et al. 2005). The production of variants may lead to the appearance of more resistant subpopulations that will enhance the fitness of the entire population under conditions of stress. For example, when *P. aeruginosa* was grown in a biofilm for five days, three different stable colony morphologies called typical (wild-type colony), mini (small variant colony) and wrinkly (rough variant colony) appeared after plating on Petri dishes, whereas the initial inoculum (broth culture) produced only one colony morphology (typical) (Boles et al. 2004). Using CLSM, they demonstrated that the wrinkly variant displayed greater ability to form a biofilm and with larger cells clusters when compared to the wild-type strain. Moreover, the presence of a wrinkly subpopulation was responsible for the better resistance of the biofilm to hydrogen peroxide because this population constituted more than 98% of the biofilm cells

after exposure to the biocide, whereas it had only reached 12% prior to treatment. In addition, these authors also showed that a biofilm composed only of wild-type strains (typical colony) demonstrated a high level of susceptibility to the biocide. These results therefore reveal how genetic mutations induced by biofilm formation can lead to improved resistance to a biocide. However, one issue that remains following these observations concerns the mechanisms involved in the production of genetic variants within a biofilm. Spontaneous mutations related to replication errors are a natural explanation. However, it was found that endogenous oxidative stress provoked double-stranded DNA breaks that caused the emergence of variants when these breaks were repaired by recombinational DNA repair genes (Boles and Singh 2008). In a previous study, Ciofu *et al*. (Ciofu et al. 2005) also reported that the occurrence of hypermutable *P. aeruginosa* was linked to oxidative stress in cystic fibrosis infection. In addition, the endogenous production of reactive oxygen intermediates within biofilm microcolonies has already been reported (Mai-Prochnow et al. 2008). Taken together, these observations suggest that the oxidative stress induced in a biofilm by a harsh microenvironment may cause the emergence of biocide resistant variants through the enhancement of genetic mutations.

A5-Pathogen protection in multispecies biofilms

In their natural environments, it is clear that biofilms are complex mixtures of different species rather than the model single species biostructures studied by the majority of laboratories (Burmolle et al. 2010, Lyautey et al. 2005, Simoes et al. 2008, Zijnge et al. 2010) (Fig. 3). In these complex consortia, species interactions can lead to the emergence of specific biofilm phenotypes. A recent study reported that the food pathogen *E. coli* O157:H7 formed a biofilm with a 400-fold higher biovolume when it was grown in association with *Acinetobacter calcoaceticus*, a meat factory commensal bacterium, rather than in a monoculture (Habimana et al. 2010). It was also shown that four strains isolated from a marine alga interacted synergistically in a biofilm to produce more biomass (Burmolle et al. 2006). Moreover, the mixed four-species biofilm displayed markedly higher resistance to hydrogen peroxide than any of the single-species biofilms. Indeed, numerous studies have demonstrated that multi-species biofilms are generally more resistant to disinfection than mono-species biofilms (Luppens et al. 2008, Simoes et al. 2010, Simoes et al. 2009, Van der Veen and Abee 2010). However, the mechanisms involved remain unclear. The specific nature and composition of a multispecies biofilm matrix is one of the explanations proposed. It has been suggested that chemical interactions between the polymers produced by each

species may lead to a more viscous matrix (Burmolle et al. 2006, von Canstein et al. 2002) and thus reduce the permeation of biocides. Similarly, because a biocide can be inactivated in a biofilm matrix by enzymes, as previously suggested regarding the catalase-mediated inactivation of hydrogen peroxide in a *P. aeruginosa* biofilm (Stewart et al. 2000), the enzymes produced by the different species may act synergistically against toxic compounds so that non-productive species will benefit from the association through enzyme complementation (Shu et al. 2003). Another explanation is that because of the specific spatial arrangement of certain bacterial species within a biofilm, some strains may be protected from a biocide by their aggregation with others within the three-dimensional structure (Fig. 3 B). It was reported for instance that *Staphylococcus sciuri* was protected from chlorine treatment because of the association with microcolonies formed by *Kocuria* sp., a more resistant strain (Leriche et al. 2003). As well as these possible interactions with other bacterial species, bacteria in a biofilm can also be protected by other eukaryotic micro-organisms (Fig. 3 C, D). Many bacterial species have been shown to survive within various amoebal species (for a review see (Thomas et al. 2010). Trophozoites are the actively dividing forms of amoebae; increased resistance to disinfection has been reported for bacteria internalized within trophozoites. The survival and resistance of a range of intracellular bacterial pathogens when challenged with free chlorine were investigated and it was concluded that *Acanthamoeba castellanii* trophozoites played a predominant role in the survival of these pathogens (King et al. 1988). Similar studies have reported *Burkholderia pseudomallei* as being more resistant to monochloramine, chlorine and UV once it is protected in *Acanthamoeba astronyxis* trophozoites (Howard and Inglis 2005). It was reported a decreased efficacy of silver and copper against *Legionella pneumophila* and *Pseudomonas aeruginosa* within *Acanthamoeba polyphaga* trophozoites (Hwang et al. 2006).

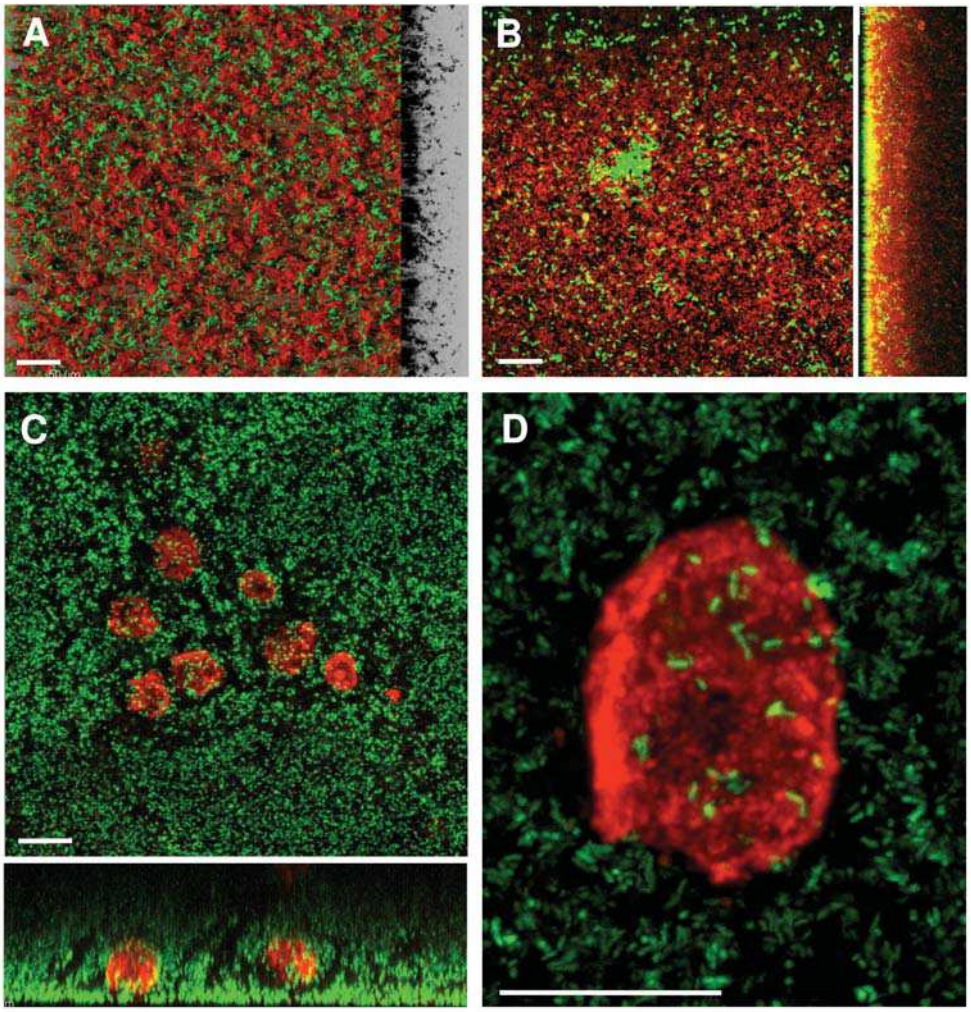

Figure 2. Confocal imaging of mixed biofilms. (A) Three-dimensional projection of a mixed 24h-biofilm of *E. coli* mCherry (red) and *P. aeruginosa* GFP (green). (B) Section of a mixed 24h-biofilm of *S. aureus* mCherry (red) and *P. aeruginosa* GFP (green). (C) Section of a mixed 24h-biofilm of *P. aeruginosa* GFP (green) and the ciliate protozoan *Tetrahymena pyriformis* (red). (D) Higher magnification of the mixed biofilm showing the presence of *P. aeruginosa* (green) in *T. pyriformis* (red). Scale bar corresponds to 20 µm.

Growth in different amoebal hosts may also influence the biocide susceptibility of a particular bacterial strain; this was recently evidenced with *L. pneumophila* replicated from *Hartmannella vermiformis* which displayed greater resistance to chlorine than cells replicated from *A. castellanii* (Chang et al. 2009). Cysts are the dormant stage of amoebae and form in the event of unfavorable conditions such as nutriment depletion and various physical and chemical stresses, including biocidal treatments. The encystment of amoebae is preceded by the expulsion of food vacuoles and vesicles (Schuster 1979). These vesicles may contain bacteria that are protected from the effect of biocides (Berk et al. 1998). The cysts of several

amoebal species (mostly *Acanthamoeba* spp) have been demonstrated to resist extremely high concentrations of biocides used for a variety of applications (Coulon et al. 2010, Thomas et al. 2010). Various bacterial species, including *L. pneumophila* (Kilvington and Price 1990), *Legionella micdadei* (Fallon and Rowbotham 1990), more than 15 mycobacterial species (Adekambi et al. 2006), *Francisella tularensis* (Abd et al. 2003) and *Vibrio cholerae* (Abd et al. 2005, Thom et al. 1992) have been reported to survive within amoebal cysts, thus benefiting from the extremely efficient protection they afford.

B-What are the prospective strategies to eradicate biofilm on industrial and medical devices?

From the studies reviewed in this paper, it is clear that biofilm resistance to disinfectants is a multifactorial process resulting from different mechanisms and causing the inefficiency of antimicrobials even at usable concentrations of commercial solutions (Krolasik et al. 2010). New control strategies are needed to overcome these limitations. Another consideration is that regulation is changing and some of the usual disinfectants will probably be prohibited in the next few years (Reach, EU directive biocide 98/8/EC). It therefore becomes crucial to find alternative "green" molecules or processes that are efficient for eradicating surface contamination. The following part of the review points out some prospective methods that can improve anti-biofilm strategies.

B1-Targeting EPS to denature biofilm spatial organization

The diffusion/reaction limitation within the structure of the biofilm is one of the main mechanisms implicated in the biofilm resistance to disinfectants. Optimizing the removal or the destructuration of the matrix will thus be essential to improve disinfection process. It is well known that mechanical action can be effective for eliminating biofilms (Maukonen et al. 2003), disrupting the extracellular polymeric substances (EPS) of the matrix and making the micro-organisms more accessible. In this context, the use of enzyme-based detergents could be a helpful tool to improve the cleaning process. The elucidation of the exact composition of the biofilm matrix must first be achieved in order to apply adapted enzyme treatments. Biofilm matrix is generally known to be mainly composed of polysaccharides and proteins (Tsuneda et al. 2003) associated with lipids or nucleic acids (Flemming and Wingender 2010), but its composition shows qualitative and quantitative variations depending on the strains and the growth conditions (Branda et al. 2005). For example, cellulose has been shown to be a crucial component of the extracellular matrix of *Salmonella* and *Escherichia coli* (Zogaj et al.

2001) and the poly-N-acetylglucosamine is the major component of staphylococcal biofilms (Jabbouri and Sadovskaya). Mucoid strains of *Pseudomonas aeruginosa* produce mainly alginate while non-mucoid strains produce both distinct carbohydrate-rich polymers (Branda et al. 2005). Depending on the biofilm matrix composition, different enzymes must be preferred like proteases, cellulases, polysaccharide depolymerases, alginate lyase, dispersin B, or DNAse (Jabbouri and Sadovskaya 2010, Orgaz et al. 2007, Xavier et al. 2005). In industrial or medical environments, numerous microbial species grow within the same biofilm increasing the matrix biochemical heterogeneity. Commercial enzyme formulations are composed of mixtures of enzymes with different spectra of substratum. These enzymatic processes have the advantage to disaggregate biofilm clumps rather than just removing them from the surface as mechanical action does.

One prospective way in utilizing enzymatic processes could be to promote natural degradation of biofilm matrix. When nutrients are depleted in the bulk of the biofilm, *P. fluorescens* naturally produces enzymes which degrade its EPS in order to get disseminated in a more favorable environment (Allison et al. 1998). Specific molecules could be developed for interacting with the regulation of genes controlling the biofilm self-destruction pathway.

Besides enzymes, some small molecules can also be efficient helps in dispersing biofilms. Recently, D-amino acids have been shown to prevent and break down *Bacillus subtilis* biofilms by interfering with the integrity of the EPS matrix (Kolodkin-Gal et al. 2010). In addition, biosurfactants, e.g. rhamnolipids, and short-chain fatty acids, e.g. *cis*-2-decenoic acid, can also favor the biofilm disruption (Davies and Marques 2009, Dusane et al. 2010). Combinations of EPS treatments have shown their interest. For example, ultrasonic waves (Oulahal-Lagsir et al. 2003) or surfactant (Parkar et al. 2004) were reported to enhance the efficacy of proteolytic enzymes.

These processes denaturing EPS integrity aim to disperse the bulk of surface contamination but are generally not efficient in killing bacteria. Pathogens can eventually redeposit elsewhere and initiate a new biofilm cycle stressing out the importance of complementary antimicrobial strategies.

B2-Towards natural antimicrobial strategies?

Research on new antimicrobial strategies need to focus on processes that have a high lethal activity against pathogens, are efficient in penetrating biofilm structure, and are easily degraded in the environment. In recent years, there was an emergence of studies dealing with natural antimicrobials as anti-biofilm molecules. Plants are fabulous sources of actives

molecules with antimicrobial properties (Lewis and Ausubel 2006). Some compounds extracted from aromatic plants, natural and ”generally recognized as safe”, have demonstrated their antimicrobial activity on planktonic bacteria. Some are now evaluated for their potential in eradicating biofilms. For example, carvacrol, a natural terpene extracted from thyme or oregano (Knowles et al. 2005), casbane diterpene, isolated from the ethanolic extract of a Brazilian native plant *Croton nepetaefolius* (Carneiro et al. 2011), thymoquinone, an active principle of arabian *Nigella sativa* seed (Chaieb et al. 2011), and a naphthalene derivative isolated from *Trachyspermum ammi* seeds (Khan et al. 2010), limit the biofilm formation of various bacterial species. More interestingly, some of these compounds were tested for their bactericidal activity on established biofilms. The ratio of concentrations (Rc) required to achieve the same reduction in the planktonic or biofilm *Staphylococcus epidermidis* population is about 4 for origan oil, thymol, carvacrol (Nostro et al. 2007) which is fairly competitive with most chemical agents. Eucalyptus oil, tea tree oil or α-terpineol also exhibited a great efficiency in eradicating biofilms (Budzynska et al. 2011, Karpanen et al. 2008). A promising way to apply antibiofilm essential oil is to vaporize the volatile compounds in order to increase their access to the biological targets. For example, vaporization of allyl isothiocyanate, cinnamaldhehyde, and carvacrol have been shown to valuably inactivate lettuce surface-attached *E. coli* O157:H7 (Obaidat and Frank 2009).

A renewed interest appears in controlling biofilms with bacteriophages. Phages are viruses that infect and lyse bacteria. Phages can easily diffuse through EPS (Briandet et al. 2008) and are active on established biofilms (Donlan 2009). For example, it has been shown that the phage φIBB-PF7A was highly efficient in removal of *P. aeruginosa* biofilm within a short time interval (Sillankorva et al. 2008). Moreover, many phages produce depolymerases that hydrolyze biofilm extracellular polymers and trigger the biofilm disruption. Drawbacks of phages are their narrow host range, but phages mixtures or engineered phages could provide interesting solutions. For example, a phage that express a biofilm-degrading enzyme was engineered (Lu and Collins 2007) and showed its efficacy on *E. coli* biofilms giving a reduction of biofilm cell count of 99.997%. Recent works also propose to use phage lysin against *S. aureus* as an alternative agent for skin decontamination (Fischetti 2008). In addition, as cell-to-cell communication is fundamental in biofilm signaling, novel antimicrobials targeting quorum sensing are emerging. Several quorum-sensing inhibitors, such as brominated furanones, succeed in interfering with biofilm formation (Ni et al. 2009, Sintim et al. 2010). Similarly, the cyclic-di-GMP pathway that has been shown to regulate

diverse cellular processes involved in biofilm formation and virulence could be a promising antimicrobial target (Romling and Amikam 2006, Sintim et al. 2010). Other authors propose targeting of the iron uptake pathway to prevent *E. coli* from developing biofilms by addition of competitive Zn^{2+} or Co^{2+} cations (Hancock et al. 2010).

B3- Combining strategies to optimize biofilm control

A strategy to avoid the induction of bacterial adaptation to disinfectant within biofilm structures could be to increase drastically the antimicrobial concentration. However, this approach would not guarantee biofilm eradication while it is costly and unfriendly with the environment. Moreover, microbial communities are constituted of several micro-organisms having distinct mechanisms of resistance. Thus, the eradication of biofilms could rely on the combined use of treatments with different spectra and modes of action. In this regard, synergistic action was reported in numerous papers between two or more processes. Synergy between two processes is generally reported if the observed effect is higher than the one that is predicted by adding the effects created by each single process (Nazer et al. 2005). One method to assess synergistic effect in bactericidal activity can be the calculation of the Fractional Bactericidal Concentration (FBC) (Harrison et al. 2008). Numerous treatments were evaluated associating chemical, natural or physical treatments. For example, combinations of sodium hypochlorite and hydrogen peroxide, Cu^{2+} ions and quaternary ammonium compounds, eucalyptus oil and chlorhexidine, silver and surfactant, or bacteriophage and alkaline cleaner act synergistically to eradicate established biofilms (DeQueiroz and Day 2007, Harrison et al. 2008, Hendry et al. 2009, Rivardo et al. 2010, Sharma et al. 2005). Physical treatments can also be employed in association with chemical disinfectants. For example, the low-intensity ultrasonic or sonic agitation improves the action of chlorhexidine against biofilm bacteria (Shen et al. 2010) and the combination of ultraviolet light with chlorine dioxine was more effective for eradication of drinking water biofilms than each treatment alone (Rand et al. 2007).

Conclusion

Since biofilms constitute a privileged way of life for bacteria, a better understanding of the processes involved in their marked resistance to disinfectants is of crucial importance for their control. From the studies reviewed in this paper, it is now manifest that biofilm resistance to disinfectant is i) intimately related to the three-dimensional structure of the biofilm, ii) heterogeneous within the biostructure and iii) multifactorial, resulting from an accumulation

of different mechanisms. In view of the observed resistance of biofilms to disinfectants, it seems crucial that regulatory standards focused on the assessment of disinfectant efficacy must consider the biofilm "mode of life".

Acknowledgements

This work was funded from the French "Pôle de Compétitivité Ile-de-France MEDICEN". M. Guilbaud is acknowledged for its contribution to image acquisition.

References

Abd H, Johansson T, Golovliov I, Sandstrom G, Forsman M. 2003. Survival and growth of *Francisella tularensis* in *Acanthamoeba castellanii*. Applied and Environmental Microbiology. 69:600-606.

Abd H, Weintraub A, Sandstrom G. 2005. Intracellular survival and replication of *Vibrio cholerae* O139 in aquatic free-living amoebae. Environmental Microbiology. 7:1003-1008.

Adekambi T, Ben Salah S, Khlif M, Raoult D, Drancourt M. 2006. Survival of environmental mycobacteria in *Acanthamoeba polyphaga*. Applied and Environmental Microbiology. 72:5974-5981.

Allegrucci M, Sauer K. 2007. Characterization of colony morphology variants isolated from *Streptococcus pneumoniae* biofilms. Journal of Bacteriology. 189:2030-2038.

Allison DG, Ruiz B, SanJose C, Jaspe A, Gilbert P. 1998. Extracellular products as mediators of the formation and detachment of *Pseudomonas fluorescens* biofilms. Fems Microbiology Letters. 167:179-184.

Ando T, Itakura S, Uchii K, Sobue R, Maeda S. 2009. Horizontal transfer of non-conjugative plasmid in colony biofilm of *Escherichia coli* on food-based media. World Journal of Microbiology & Biotechnology. 25:1865-1869.

Bagge-Ravn D, Ng Y, Hjelm M, Christiansen JN, Johansen C, Gram L. 2003. The microbial ecology of processing equipment in different fish industries - analysis of the microflora during processing and following cleaning and disinfection. International Journal of Food Microbiology. 87:239-250.

Beloin C, Ghigo JM. 2005. Finding gene-expression patterns in bacterial biofilms. Trends in Microbiology. 13:16-19.

Berk SG, Ting RS, Turner GW, Ashburn RJ. 1998. Production of respirable vesicles containing live *Legionella pneumophila* cells by two *Acanthamoeba* spp. Applied and Environmental Microbiology. 64:279-286.

Bjorland J, Sunde M, Waage S. 2001. Plasmid-borne smr gene causes resistance to quaternary ammonium compounds in bovine *Staphylococcus aureus*. Journal of Clinical Microbiology. 39:3999-4004.

Boles BR, Singh PK. 2008. Endogenous oxidative stress produces diversity and adaptability in biofilm communities. Proceedings of the National Academy of Sciences of the United States of America. 105:12503-12508.

Boles BR, Thoendel M, Singh PK. 2004. Self-generated diversity produces "insurance effects" in biofilm communities. Proceedings of the National Academy of Sciences of the United States of America. 101:16630-16635.

Branda SS, Vik A, Friedman L, Kolter R. 2005. Biofilms: the matrix revisited. Trends in Microbiology. 13:20-26.

Braoudaki M, Hilton AC. 2004. Adaptive resistance to biocides in *Salmonella enterica* and *Escherichia coli* O157 and cross-resistance to antimicrobial agents. Journal of Clinical Microbiology. 42:73-78.

Bressler DC, Balzer M, Dannehl A, Flemming HC, Wingender J. 2009. Persistence of *Pseudomonas aeruginosa* in drinking-water biofilms on elastomeric material. Water Science and Technology. 9:81-87.

Briandet R, Lacroix-Gueu P, Renault M, Lecart S, Meylheuc T, Bidnenko E, Steenkeste K, Bellon-Fontaine MN, Fontaine-Aupart MP. 2008. Fluorescence correlation spectroscopy to study diffusion and reaction of bacteriophages inside biofilms. Applied and Environmental Microbiology. 74:2135-2143.

Bridier A, Dubois-Brissonnet F, Greub G, Thomas V, Briandet R. 2011a. Dynamics of biocide action in *Pseudomonas aeruginosa* biofilms. Antimicrobial Agents and Chemotherapy. 55:2648-2654.

Bridier A, Tischenko E, Dubois-Brissonnet F, Herry J-M, Thomas V, Daddi-Oubekka S, Waharte F, Steenkeste K, Fontaine-Aupart M-P, Briandet R. 2011b. Deciphering biofilm structure and reactivity by multiscale time-resolved fluorescence analysis. Advances in Experimental Medecine and Biology Bacterial Adhesion. 715:333-349.

Buckingham-Meyer K, Goeres DM, Hamilton MA. 2007. Comparative evaluation of biofilm disinfectant efficacy tests. Journal of Microbiological Methods. 70:236-244.

Budzynska A, Wieckowska-Szakiel M, Sadowska B, Kalemba D, Rozalska B. 2011. Antibiofilm activity of selected plant essential oils and their major components. Polish Journal of Microbiology. 60:35-41.

Burmolle M, Thomsen TR, Fazli M, Dige I, Christensen L, Homoe P, Tvede M, Nyvad B, Tolker-Nielsen T, Givskov M, et al. 2010. Biofilms in chronic infections - a matter of opportunity - monospecies biofilms in multispecies infections. Fems Immunology and Medical Microbiology. 59:324-336.

Burmolle M, Webb JS, Rao D, Hansen LH, Sorensen SJ, Kjelleberg S. 2006. Enhanced biofilm formation and increased resistance to antimicrobial agents and bacterial invasion are caused by synergistic interactions in multispecies biofilms. Applied and Environmental Microbiology. 72:3916-3923.

Campanac C, Pineau L, Payard A, Baziard-Mouysset G, Roques C. 2002. Interactions between biocide cationic agents and bacterial biofilms. Antimicrobial Agents and Chemotherapy. 46:1469-1474.

Carneiro VA, dos Santos HS, Arruda FVS, Bandeira PN, Albuquerque M, Pereira MO, Henriques M, Cavada BS, Teixeira EH. 2011. Casbane diterpene as a promising natural antimicrobial agent against biofilm-associated infections. Molecules. 16:190-201.

Ceri H, Olson ME, Stremick C, Read RR, Morck D, Buret A. 1999. The Calgary Biofilm Device: new technology for rapid determination of antibiotic susceptibilities of bacterial biofilms. Journal of Clinical Microbiology. 37:1771-1776.

Chaieb K, Kouidhi B, Jrah H, Mahdouani K, Bakhrouf A. 2011. Antibacterial activity of thymoquinone, an active principle of *Nigella sativa* and its potency to prevent bacterial biofilm formation. Bmc Complementary and Alternative Medicine. 11:6.

Chang CW, Kao CH, Liu YF. 2009. Heterogeneity in chlorine susceptibility for *Legionella pneumophila* released from *Acanthamoeba* and *Hartmannella*. Journal of Applied Microbiology. 106:97-105.

Chavant P, Gaillard-Martine B, Hebraud M. 2004. Antimicrobial effects of sanitizers against planktonic and sessile *Listeria monocytogenes* cells according to the growth phase. Fems Microbiology Letters. 236:241-248.

Ciofu O, Riis B, Pressler T, Poulsen HE, Hoiby N. 2005. Occurrence of hypermutable *Pseudomonas aeruginosa* in cystic fibrosis patients is associated with the oxidative stress caused by chronic lung inflammation. Antimicrobial Agents and Chemotherapy. 49:2276-2282.

Coenye T. 2010. Response of sessile cells to stress: from changes in gene expression to phenotypic adaptation. Fems Immunology and Medical Microbiology. 59:239-252.

Conibear TCR, Collins SL, Webb JS. 2009. Role of mutation in *Pseudomonas aeruginosa* biofilm development. Plos One. 4:-.

Cooper IR, White J, Mahenthiralingam E, Hanlon GW. 2008. Long-term persistence of a single *Legionella pneumophila* strain possessing the mip gene in a municipal shower despite repeated cycles of chlorination. Journal of Hospital Infection. 70:154-159.

Costerton J, Lewandowski Z, Caldwell D, Korber D, Lappin-Scott H. 1995. Microbial biofilms. Annual Review of Microbiology. 49:711-745.

Coulon C, Collignon A, McDonnell G, Thomas V. 2010. Resistance of *Acanthamoeba* cysts to disinfection treatments used in health care settings. Journal of Clinical Microbiology. 48:2689-2697.

Cvitkovitch DG, Liu YH, Ellen RP. 2003. Quorum sensing and biofilm formation in streptococcal infections. Journal of Clinical Investigation. 112:1626-1632.

Davies DG, Chakrabarty AM, Geesey GG. 1993. Exopolysaccharide production in biofilms - substratum activation of alginate gene-expression by *Pseudomonas aeruginosa*. Applied and Environmental Microbiology. 59:1181-1186.

Davies DG, Marques CNH. 2009. A fatty acid messenger is responsible for inducing dispersion in microbial biofilms. Journal of Bacteriology. 191:1393-1403.

Davies DG, Parsek MR, Pearson JP, Iglewski BH, Costerton JW, Greenberg EP. 1998. The involvement of cell-to-cell signals in the development of a bacterial biofilm. Science. 280:295-298.

Davison WM, Pitts B, Stewart PS. 2010. Spatial and temporal patterns of biocide action against *Staphylococcus epidermidis* biofilms. Antimicrobial Agents and Chemotherapy. 54:2920-2927.

De Beer D, Srinivasan R, Stewart PS. 1994. Direct measurement of chlorine penetration into biofilms during disinfection. Applied and Environmental Microbiology. 60:4339-4344.

DeQueiroz GA, Day DF. 2007. Antimicrobial activity and effectiveness of a combination of sodium hypochlorite and hydrogen peroxide in killing and removing *Pseudomonas aeruginosa* biofilms from surfaces. Journal of Applied Microbiology. 103:794-802.

Deva AK, Vickery K, Zou J, West RH, Selby W, Benn RA, Harris JP, Cossart YE. 1998. Detection of persistent vegetative bacteria and amplified viral nucleic acid from in-use testing of gastrointestinal endoscopes. Journal of Hospital Infection. 39:149-157.

Donlan RM. 2009. Preventing biofilms of clinically relevant organisms using bacteriophage. Trends in Microbiology. 17:66-72.

Driffield K, Miller K, Bostock JM, O'Neill AJ, Chopra I. 2008. Increased mutability of *Pseudomonas aeruginosa* in biofilms. Journal of Antimicrobial Chemotherapy. 61:1053-1056.

Dusane DH, Nancharaiah YV, Zinjarde SS, Venugopalan VP. 2010. Rhamnolipid mediated disruption of marine *Bacillus pumilus* biofilms. Colloids and Surfaces B-Biointerfaces. 81:242-248.

Dynes JJ, Lawrence JR, Korber DR, Swerhone GDW, Leppard GG, Hitchcock AP. 2009. Morphological and biochemical changes in *Pseudomonas fluorescens* biofilms induced by sub-inhibitory exposure to antimicrobial agents. Canadian Journal of Microbiology. 55:163-178.

Elhanafi D, Dutta V, Kathariou S. 2010. Genetic characterization of plasmid associated benzalkonium chloride resistance determinants in a *Listeria monocytogenes* strain from the 1998-1999 Outbreak. Applied and Environmental Microbiology. 76:8231-8238.

Fallon RJ, Rowbotham TJ. 1990. Microbiological investigations into an outbreak of Pontiac fever due to *Legionella micdadei* associated with use of a whirlpool. Journal of Clinical Pathology. 43:479-483.

Fischetti VA. 2008. Bacteriophage lysins as effective antibacterials. Current Opinion in Microbiology. 11:393-400.

Flemming HC, Wingender J. 2010. The biofilm matrix. Nature Reviews Microbiology. 8:623-633.

Frank JF, Koffi RA. 1990. Surface adherent growth of *Listeria monocytogenes* is associated with increased resistance to surfactant sanitizers and heat. Journal of Food Protection. 53:550-554.

Fux CA, Costerton JW, Stewart PS, Stoodley P. 2005. Survival strategies of infectious biofilms. Trends in Microbiology. 13:34-40.

Ganeshnarayan K, Shah SM, Libera MR, Santostefano A, Kaplan JB. 2009. Poly-N-acetylglucosamine matrix polysaccharide impedes fluid convection and transport of the cationic surfactant cetylpyridinium chloride through bacterial biofilms. Applied and Environmental Microbiology. 75:1308-1314.

Gillings MR, Duan XJ, Hardwick SA, Holley MP, Stokes HW. 2009. Gene cassettes encoding resistance to quaternary ammonium compounds: a role in the origin of clinical class 1 integrons? Isme Journal. 3:209-215.

Gillis RJ, White KG, Choi KH, Wagner VE, Schweizer HP, Iglewski BH. 2005. Molecular basis of azithromycin-resistant *Pseudomonas aeruginosa* biofilms. Antimicrobial Agents and Chemotherapy. 49:3858-3867.

Grobe KJ, Zahller J, Stewart PS. 2002. Role of dose concentration in biocide efficacy against *Pseudomonas aeruginosa* biofilms. Journal of Industrial Microbiology & Biotechnology. 29:10-15.

Guérin-Méchin L, Dubois-Brissonnet F, Heyd B, Leveau JY. 1999. Specific variations of fatty acid composition of *Pseudomonas aeruginosa* ATCC 15442 induced by quaternary ammonium compounds and relation with resistance to bactericidal activity. Journal of Applied Microbiology. 87:735-742.

Guiot E, Georges P, Brun A, Fontaine-Aupart MP, Bellon-Fontaine MN, Briandet R. 2002. Heterogeneity of diffusion inside microbial biofilms determined by fluorescence correlation spectroscopy under two-photon excitation. Photochemistry and Photobiology. 75:570-578.

Habimana O, Heir E, Langsrud S, Asli AW, Moretro T. 2010. Enhanced surface colonization by *Escherichia coli* O157:H7 in biofilms formed by an *Acinetobacter calcoaceticus* isolate from meat processing environments. Applied and Environmental Microbiology. 76:4557-4559.

Habimana O, Steenkeste K, Fontaine-Aupart MP, Bellon-Fontaine MN, Kulakauskas S, Briandet R. 2011. Diffusion of nanoparticles in biofilms is altered by bacterial cell wall hydrophobicity. Applied and Environmental Microbiology. 77:367-368.

Hancock V, Dahl M, Klemm P. 2010. Abolition of biofilm formation in urinary tract *Escherichia coli* and *Klebsiella* isolates by metal interference through competition for Fur. Applied and Environmental Microbiology. 76:3836-3841.

Hannan S, Ready D, Jasni AS, Rogers M, Pratten J, Roberts AP. 2010. Transfer of antibiotic resistance by transformation with eDNA within oral biofilms. Fems Immunology and Medical Microbiology. 59:345-349.

Harrison JJ, Ceri H, Roper NJ, Badry EA, Sproule KM, Turner RJ. 2005. Persister cells mediate tolerance to metal oxyanions in *Escherichia coli*. Microbiology-Sgm. 151:3181-3195.

Harrison JJ, Turner RJ, Joo DA, Stan MA, Chan CS, Allan ND, Vrionis HA, Olson ME, Ceri H. 2008. Copper and quaternary ammonium cations exert synergistic bactericidal and antibiofilm activity against *Pseudomonas aeruginosa*. Antimicrobial Agents and Chemotherapy. 52:2870-2881.

Hassett DJ, Ma JF, Elkins JG, McDermott TR, Ochsner UA, West SEH, Huang CT, Fredericks J, Burnett S, Stewart PS, et al. 1999. Quorum sensing in *Pseudomonas aeruginosa* controls expression of catalase and superoxide dismutase genes and mediates biofilm susceptibility to hydrogen peroxide. Molecular Microbiology. 34:1082-1093.

Hausner M, Wuertz S. 1999. High rates of conjugation in bacterial biofilms as determined by quantitative in situ analysis. Applied and Environmental Microbiology. 65:3710-3713.

Hendry ER, Worthington T, Conway BR, Lambert PA. 2009. Antimicrobial efficacy of eucalyptus oil and 1,8-cineole alone and in combination with chlorhexidine digluconate against microorganisms grown in planktonic and biofilm cultures. Journal of Antimicrobial Chemotherapy. 64:1219-1225.

Hoiby N, Bjarnsholt T, Givskov M, Molin S, Ciofu O. 2010. Antibiotic resistance of bacterial biofilms. International journal of antimicrobial agents. 35:322-332.

Hope CK, Wilson M. 2004. Analysis of the effects of chlorhexidine on oral biofilm vitality and structure based on viability profiling and an indicator of membrane integrity. Antimicrobial Agents and Chemotherapy. 48:1461-1468.

Howard K, Inglis TJ. 2005. Disinfection of *Burkholderia pseudomallei* in potable water. Water Research. 39:1085-1092.

Huber B, Riedel K, Hentzer M, Heydorn A, Gotschlich A, Givskov M, Molin S, Eberl L. 2001. The cep quorum-sensing system of *Burkholderia cepacia* H111 controls biofilm formation and swarming motility. Microbiology-Sgm. 147:2517-2528.

Hwang MG, Katayama H, Ohgaki S. 2006. Effect of intracellular resuscitation of *Legionella pneumophila* in *Acanthamoeba polyphaga* cells on the antimicrobial properties of silver and copper. Environmental Science & Technology. 40:7434-7439.

Jabbouri S, Sadovskaya I. 2010. Characteristics of the biofilm matrix and its role as a possible target for the detection and eradication of *Staphylococcus epidermidis* associated with medical implant infections. Fems Immunology and Medical Microbiology. 59:280-291.

Jang A, Szabo J, Hosni AA, Coughlin M, Bishop PL. 2006. Measurement of chlorine dioxide penetration in dairy process pipe biofilms during disinfection. Applied Microbiology and Biotechnology. 72:368-376.

Joelsson A, Kan B, Zhu J. 2007. Quorum sensing enhances the stress response in *Vibrio cholerae*. Applied and Environmental Microbiology. 73:3742-3746.

Jones MV, Herd TM, Christie HJ. 1989. Resistance of *Pseudomonas aeruginosa* to amphoteric and quaternary ammonium biocides. Microbios. 58:49-61.

Kamgang JO, Briandet R, Herry JM, Brisset JL, Naitali M. 2007. Destruction of planktonic, adherent and biofilm cells of *Staphylococcus epidermidis* using a gliding discharge in humid air. Journal of Applied Microbiology. 103:621-628.

Karpanen TJ, Worthington T, Hendry ER, Conway BR, Lambert PA. 2008. Antimicrobial efficacy of chlorhexidine digluconate alone and in combination with eucalyptus oil, tea tree oil and thymol against planktonic and biofilm cultures of *Staphylococcus epidermidis*. Journal of Antimicrobial Chemotherapy. 62:1031-1036.

Kelly BG, Vespermann A, Bolton DJ. 2009. Horizontal gene transfer of virulence determinants in selected bacterial foodborne pathogens. Food and Chemical Toxicology. 47:969-977.

Khan R, Zakir M, Khanam Z, Shakil S, Khan AU. 2010. Novel compound from *Trachyspermum ammi* (Ajowan caraway) seeds with antibiofilm and antiadherence activities against *Streptococcus mutans*: a potential chemotherapeutic agent against dental caries. Journal of Applied Microbiology. 109:2151-2159.

Kilvington S, Price J. 1990. Survival of *Legionella pneumophila* within cysts of *Acanthamoeba polyphaga* following chlorine exposure. Journal of Applied Bacteriology. 68:519-525.

King CH, Shotts EB, Jr., Wooley RE, Porter KG. 1988. Survival of coliforms and bacterial pathogens within protozoa during chlorination. Applied and Environmental Microbiology. 54:3023-3033.

Kirisits MJ, Prost L, Starkey M, Parsek MR. 2005. Characterization of colony morphology variants isolated from *Pseudomonas aeruginosa* biofilms. Applied and Environmental Microbiology. 71:4809-4821.

Knowles JR, Roller S, Murray DB, Naidu AS. 2005. Antimicrobial action of carvacrol at different stages of dual-species biofilm development by *Staphylococccus aureus* and *Salmonella enterica* serovar Typhimurium. Applied and Environmental Microbiology. 71:797-803.

Kolodkin-Gal I, Romero D, Cao SG, Clardy J, Kolter R, Losick R. 2010. D-amino acids trigger biofilm disassembly. Science. 328:627-629.

Krolasik J, Zakowska Z, Krepska M, Klimek L. 2010. Resistance of bacterial biofilms formed on stainless steel surface to disinfecting agent. Polish Journal of Microbiology. 59:281-287.

Kvist M, Hancock V, Klemm P. 2008. Inactivation of efflux pumps abolishes bacterial biofilm formation. Applied and Environmental Microbiology. 74:7376-7382.

Labbate M, Queek SY, Koh KS, Rice SA, Givskov M, Kjelleberg S. 2004. Quorum sensing-controlled biofilm development in *Serratia liquefaciens* MG1. Journal of Bacteriology. 186:692-698.

Lambert RJW, Johnston MD. 2001. The effect of interfering substances on the disinfection process: a mathematical model. Journal of Applied Microbiology. 91:548-555.

Langsrud S, Sidhu MS, Heir E, Holck AL. 2003. Bacterial disinfectant resistance - a challenge for the food industry. International Biodeterioration and Biodegradation. 51:283-290.

Leriche V, Briandet R, Carpentier B. 2003. Ecology of mixed biofilms subjected daily to a chlorinated alkaline solution: spatial distribution of bacterial species suggests a protective effect of one species to another. Environmental Microbiology. 5:64-71.

Lewis K. 2001. Riddle of biofilm resistance. Antimicrobial Agents and Chemotherapy. 45:999-1007.

Lewis K. 2005. Persister cells and the riddle of biofilm survival. Biochemistry-Moscow. 70:267-+.

Lewis K, Ausubel FM. 2006. Prospects for plant-derived antibacterials. Nature Biotechnology. 24:1504-1507.

Lisle JT, Broadaway SC, Prescott AM, Pyle BH, Fricker C, McFeters GA. 1998. Effects of starvation on physiological activity and chlorine disinfection resistance in *Escherichia coli* O157 : H7. Applied and Environmental Microbiology. 64:4658-4662.

Lu TK, Collins JJ. 2007. Dispersing biofilms with engineered enzymatic bacteriophage. Proceedings of the National Academy of Sciences of the United States of America. 104:11197-11202.

Lumjiaktase P, Diggle SP, Loprasert S, Tungpradabkul S, Daykin M, Camara M, Williams P, Kunakorn M. 2006. Quorum sensing regulates dpsA and the oxidative stress response in *Burkholderia pseudomallei*. Microbiology-Sgm. 152:3651-3659.

Luppens SBI, Kara D, Bandounas L, Jonker MJ, Wittink FRA, Bruning O, Breit TM, ten Cate JM, Crielaard W. 2008. Effect of *Veillonella parvula* on the antimicrobial resistance and gene expression of *Streptococcus mutans* grown in a dual-species biofilm. Oral Microbiology and Immunology. 23:183-189.

Lyautey E, Lacoste B, Ten-Hage L, Rols JL, Garabetian F. 2005. Analysis of bacterial diversity in river biofilms using 16S rDNA PCR-DGGE: methodological settings and fingerprints interpretation. Water Research. 39:380-388.

Ma LM, Conover M, Lu HP, Parsek MR, Bayles K, Wozniak DJ. 2009. Assembly and development of the *Pseudomonas aeruginosa* biofilm matrix. Plos Pathogens. 5:-.

Maeda S, Ito M, Ando T, Ishimoto Y, Fujisawa Y, Takahashi H, Matsuda A, Sawamura A, Kato S. 2006. Horizontal transfer of nonconjugative plasmids in a colony biofilm of *Escherichia coli*. Fems Microbiology Letters. 255:115-120.

Mai-Prochnow A, Lucas-Elio P, Egan S, Thomas T, Webb JS, Sanchez-Amat A, Kjelleberg S. 2008. Hydrogen peroxide linked to lysine oxidase activity facilitates biofilm differentiation and dispersal in several gram-negative bacteria. Journal of Bacteriology. 190:5493-5501.

Mangalappalli-Illathu AK, Korber DR. 2006. Adaptive resistance and differential protein expression of *Salmonella enterica* serovar Enteritidis biofilms exposed to benzalkonium chloride. Antimicrobial Agents and Chemotherapy. 50:3588-3596.

Mangalappalli-Illathu AK, Vidovic S, Korber DR. 2008. Differential adaptive response and survival of *Salmonella enterica* serovar Enteritidis planktonic and biofilm cells exposed to benzalkonium chloride. Antimicrobial Agents and Chemotherapy. 52:3669-3680.

Martin DJH, Denyer SP, McDonnell G, Maillard JY. 2008. Resistance and cross-resistance to oxidising agents of bacterial isolates from endoscope washer disinfectors. Journal of Hospital Infection. 69:377-383.

Maukonen J, Matto J, Wirtanen G, Raaska L, Mattila-Sandholm T, Saarela M. 2003. Methodologies for the characterization of microbes in industrial environments: a review. Journal of Industrial Microbiology & Biotechnology. 30:327-356.

McDonnell G, Russell AD. 1999. Antiseptics and disinfectants: activity, action, and resistance. Clinical Microbiology Reviews. 12:147-179.

Mechin L, Dubois-Brissonnet F, Heyd B, Leveau JY. 1999. Adaptation of *Pseudomonas aeruginosa* ATCC 15442 to didecyldimethylammonium bromide induces changes in membrane fatty acid composition and in resistance of cells. Journal of Applied Microbiology. 86:859-866.

Meyer B, Cookson B. 2010. Does microbial resistance or adaptation to biocides create a hazard in infection prevention and control? Journal of Hospital Infection. 76:200-205.

Meylheuc T, Renault M, Bellon-Fontaine MN. 2006. Adsorption of a biosurfactant on surfaces to enhance the disinfection of surfaces contaminated with *Listeria monocytogenes*. International Journal of Food Microbiology. 109:71-78.

Mitchell BA, Brown MH, Skurray RA. 1998. QacA multidrug efflux pump from *Staphylococcus aureus*: Comparative analysis of resistance to diamidines, biguanidines, and guanylhydrazones. Antimicrobial Agents and Chemotherapy. 42:475-477.

Nazer A, Kobilinsky A, Tholozan JL, Dubois-Brissonnet F. 2005. Combinations of food antimicrobials at low levels to inhibit the growth of *Salmonella* sv.Typhimurium: a synergistic effect ? Food Microbiology. 22:391-398.

Nett JE, Guite KM, Ringeisen A, Holoyda KA, Andes DR. 2008. Reduced biocide susceptibility in *Candida albicans* biofilms. Antimicrobial Agents and Chemotherapy. 52:3411-3413.

Nguyen KT, Piastro K, Gray TA, Derbyshire KM. 2010. Mycobacterial biofilms facilitate horizontal DNA transfer between strains of *Mycobacterium smegmatis*. Journal of Bacteriology. 192:5134-5142.

Ni NT, Li MY, Wang JF, Wang BH. 2009. Inhibitors and Antagonists of Bacterial Quorum Sensing. Medicinal Research Reviews. 29:65-124.

Nostro A, Roccaro AS, Bisignano G, Marino A, Cannatelli MA, Pizzimenti FC, Cioni PL, Procopio F, Blanco AR. 2007. Effects of oregano, carvacrol and thymol on *Staphylococcus aureus* and *Staphylococcus epidermidis* biofilms. Journal of Medical Microbiology. 56:519-523.

Ntsama-Essomba C, Bouttier S, Ramaldes M, Dubois-Brissonnet F, Fourniat J. 1997. Resistance of *Escherichia coli* growing as biofilms to disinfectants. Veterinary Research. 28:353-363.

Obaidat MM, Frank JF. 2009. Inactivation of *Escherichia coli* O157:H7 on the intact and damaged portions of lettuce and spinach leaves by using allyl isothiocyanate, carvacrol, and cinnamaldehyde in vapor phase. Journal of Food Protection. 72:2046-2055.

Orgaz B, Neufeld RJ, SanJose C. 2007. Single-step biofilm removal with delayed release encapsulated Pronase mixed with soluble enzymes. Enzyme and Microbial Technology. 40:1045-1051.

Oulahal-Lagsir O, Martial-Gros A, Bonneau M, Blum LJ. 2003. "*Escherichia coli*-milk" biofilm removal from stainless steel surfaces: synergism between ultrasonic waves and enzymes. Biofouling. 19:159-168.

Parkar SG, Flint SH, Brooks JD. 2004. Evaluation of the effect of cleaning regimes on biofilms of thermophilic bacilli on stainless steel. Journal of Applied Microbiology. 96:110-116.

Parsek MR, Greenberg EP. 2000. Acyl-homoserine lactone quorum sensing in Gram-negative bacteria: a signaling mechanism involved in associations with higher organisms. Proceedings of the National Academy of Sciences of the United States of America. 97:8789-8793.

Pham TK, Roy S, Noirel J, Douglas I, Wright PC, Stafford GP. 2010. A quantitative proteomic analysis of biofilm adaptation by the periodontal pathogen *Tannerella forsythia*. Proteomics. 10:3130-3141.

Pontes MH, Babst M, Lochhead R, Oakeson K, Smith K, Dale C. 2008. Quorum sensing primes the oxidative stress response in the insect endosymbiont, *Sodalis glossinidius*. Plos One. 3:-.

Poole K. 2005. Efflux-mediated antimicrobial resistance. Journal of Antimicrobial Chemotherapy. 56:20-51.

Prigent-Combaret C, Brombacher E, Vidal O, Ambert A, Lejeune P, Landini P, Dorel C. 2001. Complex regulatory network controls initial adhesion and biofilm formation in *Escherichia coli* via regulation of the csgD gene. Journal of Bacteriology. 183:7213-7223.

Prigent-Combaret C, Prensier G, Le Thi TT, Vidal O, Lejeune P, Dorel C. 2000. Developmental pathway for biofilm formation in curli-producing *Escherichia coli* strains: role of flagella, curli and colanic acid. Environmental Microbiology. 2:450-464.

Prigent-Combaret C, Vidal O, Dorel C, Lejeune P. 1999. Abiotic surface sensing and biofilm-dependent regulation of gene expression in *Escherichia coli*. Journal of Bacteriology. 181:5993-6002.

Rand JL, Hofmann R, Alam MZB, Chauret C, Cantwell R, Andrews RC, Gaynon GA. 2007. A field study evaluation for mitigating biofouling with chlorine dioxide or chlorine integrated with UV disinfection. Water Research. 41:1939-1948.

Ren D, Bedzyk LA, Thomas SM, Ye RW, Wood TK. 2004. Gene expression in *Escherichia coli* biofilms. Applied Microbiology and Biotechnology. 64:515-524.

Rivardo F, Martinotti MG, Turner RJ, Ceri H. 2010. The activity of silver against *Escherichia coli* biofilm is increased by a lipopeptide biosurfactant. Canadian Journal of Microbiology. 56:272-278.

Roberts ME, Stewart PS. 2005. Modelling protection from antimicrobial agents in biofilms through the formation of persister cells. Microbiology-Sgm. 151:75-80.

Romling U, Amikam D. 2006. Cyclic di-GMP as a second messenger. Current Opinion in Microbiology. 9:218-228.

Russell AD. 1999. Bacterial resistance to disinfectants: present knowledge and future problems. Journal of Hospital Infection. 43:S57-S68.

Russell AD. 2003. Similarities and differences in the responses of microorganisms to biocides. Journal of Antimicrobial Chemotherapy. 52:750-763.

Sabev HA, Robson GD, Handley PS. 2006. Influence of starvation, surface attachment and biofilm growth on the biocide susceptibility of the biodeteriogenic yeast *Aureobasidium pullulans*. Journal of Applied Microbiology. 101:319-330.

Saby S, Leroy P, Block JC. 1999. *Escherichia coli* resistance to chlorine and glutathione synthesis in response to oxygenation and starvation. Applied and Environmental Microbiology. 65:5600-5603.

Sandt C, Barbeau J, Gagnon MA, Lafleur M. 2007. Role of the ammonium group in the diffusion of quaternary ammonium compounds in *Streptococcus mutans* biofilms. Journal of Antimicrobial Chemotherapy. 60:1281-1287.

Sauer K. 2003. The genomics and proteomics of biofilm formation. Genome Biology. 4:-.

Sauer K, Camper AK. 2001. Characterization of phenotypic changes in *Pseudomonas putida* in response to surface-associated growth. Journal of Bacteriology. 183:6579-6589.

Sauer K, Camper AK, Ehrlich GD, Costerton JW, Davies DG. 2002. *Pseudomonas aeruginosa* displays multiple phenotypes during development as a biofilm. Journal of Bacteriology. 184:1140-1154.

Schuster FL. 1979. Small amebas and amoeboflagellates. New York, USA: Academic Press.

Shah D, Zhang ZG, Khodursky A, Kaldalu N, Kurg K, Lewis K. 2006. Persisters: a distinct physiological state of *E. coli*. BMC Microbiology. 6:-.

Sharma M, Ryu JH, Beuchat LR. 2005. Inactivation of *Escherichia coli* O157 : H7 in biofilm on stainless steel by treatment with an alkaline cleaner and a bacteriophage. Journal of Applied Microbiology. 99:449-459.

Shemesh M, Kolter R, Losick R. 2010. The biocide chlorine dioxide stimulates biofilm formation in *Bacillus subtilis* by activation of the histidine kinase KinC. Journal of Bacteriology. 192:6352-6356.

Shemesh M, Tam A, Steinberg D. 2007. Differential gene expression profiling of *Streptococcus mutans* cultured under biofilm and planktonic conditions. Microbiology-Sgm. 153:1307-1317.

Shen Y, Stojicic S, Qian W, Olsen I, Haapasalo M. 2010. The synergistic antimicrobial effect by mechanical agitation and two chlorhexidine preparations on biofilm bacteria. Journal of Endodontics. 36:100-104.

Shu M, Browngardt CM, Chen YYM, Burne RA. 2003. Role of urease enzymes in stability of a 10-species oral biofilm consortium cultivated in a constant-depth film fermenter. Infection and Immunity. 71:7188-7192.

Sillankorva S, Neubauer P, Azeredo J. 2008. *Pseudomonas fluorescens* biofilms subjected to phage phiIBB-PF7A. BMC Biotechnology. 8:12.

Simoes LC, Simoes M, Vieira MJ. 2008. Intergeneric coaggregation among drinking water bacteria: evidence of a role for *Acinetobacter calcoaceticus* as a bridging bacterium. Applied and Environmental Microbiology. 74:1259-1263.

Simoes LC, Simoes M, Vieira MJ. 2010. Influence of the diversity of bacterial isolates from drinking water on resistance of biofilms to disinfection. Applied and Environmental Microbiology. 76:6673-6679.

Simoes M, Simoes LC, Vieira MJ. 2009. Species association increases biofilm resistance to chemical and mechanical treatments. Water Research. 43:229-237.

Sintim HO, Al Smith J, Wang JX, Nakayama S, Yan L. 2010. Paradigm shift in discovering next-generation anti-infective agents: targeting quorum sensing, c-di-GMP signaling and biofilm formation in bacteria with small molecules. Future Medicinal Chemistry. 2:1005-1035.

Smith K, Gemmell CG, Hunter IS. 2008. The association between biocide tolerance and the presence or absence of qac genes among hospital-acquired and community-acquired MRSA isolates. Journal of Antimicrobial Chemotherapy. 61:78-84.

Smith K, Hunter IS. 2008. Efficacy of common hospital biocides with biofilms of multi-drug resistant clinical isolates. Journal of Medical Microbiology. 57:966-973.

Stewart MH, Olson BH. 1992. Impact of growth conditions on resistance of *Klebsiella pneumoniae* to chloramines. Applied and Environmental Microbiology. 58:2649-2653.

Stewart PS. 2002. Mechanisms of antibiotic resistance in bacterial biofilms. International Journal of Medical Microbiology. 292:107-113.

Stewart PS, Costerton JW. 2001. Antibiotic resistance of bacteria in biofilms. Lancet. 358:135-138.

Stewart PS, Franklin MJ. 2008. Physiological heterogeneity in biofilms. Nature Reviews Microbiology. 6:199-210.

Stewart PS, Rayner J, Roe F, Rees WM. 2001. Biofilm penetration and disinfection efficacy of alkaline hypochlorite and chlorosulfamates. Journal of Applied Microbiology. 91:525-532.

Stewart PS, Roe F, Rayner J, Elkins JG, Lewandowski Z, Ochsner UA, Hassett DJ. 2000. Effect of catalase on hydrogen peroxide penetration into *Pseudomonas aeruginosa* biofilms. Applied and Environmental Microbiology. 66:836-838.

Stocki SL, Annett CB, Sibley CD, McLaws M, Checkley SL, Singh N, Surette MG, White AP. 2007. Persistence of *Salmonella* on egg conveyor belts is dependent on the belt type but not on the rdar morphotype. Poultry Science. 86:2375-2383.

Stoodley P, Hall-Stoodley L, Lappin-Scott HM. 2001. Detachment, surface migration, and other dynamic behavior in bacterial biofilms revealed by digital time-lapse imaging. Methods Enzymol. 337:306-318.

Takenaka S, Trivedi HM, Corbin A, Pitts B, Stewart PS. 2008. Direct visualization of spatial and temporal patterns of antimicrobial action within model oral biofilms. Applied and Environmental Microbiology. 74:1869-1875.

Taylor RH, Falkinham JO, Norton CD, LeChevallier MW. 2000. Chlorine, chloramine, chlorine dioxide, and ozone susceptibility of *Mycobacterium avium*. Applied and Environmental Microbiology. 66:1702-1705.

Thom S, Warhurst D, Drasar BS. 1992. Association of *Vibrio cholerae* with fresh water amoebae. Journal of Medical Microbiology. 36:303-306.

Thomas V, McDonnell G, Denyer SP, Maillard JY. 2010. Free-living amoebae and their intracellular pathogenic microorganisms: risks for water quality. Fems Microbiology Reviews. 34:231-259.

Thurnheer T, Gmur R, Shapiro S, Guggenheim B. 2003. Mass transport of macromolecules within an in vitro model of supragingival plaque. Applied and Environmental Microbiology. 69:1702-1709.

Top EM, Springael D. 2003. The role of mobile genetic elements in bacterial adaptation to xenobiotic organic compounds. Current Opinion in Biotechnology. 14:262-269.

Tremoulet F, Duche O, Namane A, Martinie B, Labadie JC, Consortiu ELG. 2002. Comparison of protein patterns of *Listeria monocytogenes* grown in biofilm or in planktonic mode by proteomic analysis. Fems Microbiology Letters. 210:25-31.

Tsuneda S, Aikawa H, Hayashi H, Yuasa A, Hirata A. 2003. Extracellular polymeric substances responsible for bacterial adhesion onto solid surface. Fems Microbiology Letters. 223:287-292.

Van der Veen S, Abee T. 2010. Mixed species biofilms of *Listeria monocytogenes* and *Lactobacillus plantarum* show enhanced resistance to benzalkonium chloride and peracetic acid. International Journal of Food Microbiology. 144:421-431.

Vestby LK, Moretro T, Langsrud S, Heir E, Nesse LL. 2009. Biofilm forming abilities of *Salmonella* are correlated with persistence in fish meal- and feed factories. BMC Veterinary Research. 5:-.

Vidal O, Longin R, Prigent-Combaret C, Dorel C, Hooreman M, Lejeune P. 1998. Isolation of an *Escherichia coli* K-12 mutant strain able to form biofilms on inert surfaces: involvement of a new ompR allele that increases curli expression. Journal of Bacteriology. 180:2442-2449.

Vilain S, Cosette P, Zimmerlin I, Dupont JP, Junter GA, Jouenne T. 2004. Biofilm proteome: homogeneity or versatility? Journal of Proteome Research. 3:132-136.

Villagra NA, Hidalgo AA, Santiviago CA, Saavedra CP, Mora GC. 2008. SmvA, and not AcrB, is the major efflux pump for acriflavine and related compounds in *Salmonella enterica* serovar Typhimurium. Journal of Antimicrobial Chemotherapy. 62:1273-1276.

von Canstein H, Kelly S, Li Y, Wagner-Dobler I. 2002. Species diversity improves the efficiency of mercury-reducing biofilms under changing environmental conditions. Applied and Environmental Microbiology. 68:2829-2837.

Waters CA, Lu WY, Rabinowitz JD, Bassler BL. 2008. Quorum sensing controls biofilm formation in *Vibrio cholerae* through modulation of cyclic Di-GMT levels and repression of vpsT. Journal of Bacteriology. 190:2527-2536.

Weese JS, Rousseau J. 2006. Survival of *Salmonella* Copenhagen in food bowls following contamination with experimentally inoculated raw meat: effects of time, cleaning, and disinfection. Canadian Veterinary Journal. 47:887-889.

Werner E, Roe F, Bugnicourt A, Franklin MJ, Heydorn A, Molin S, Pitts B, Stewart PS. 2004. Stratified growth in *Pseudomonas aeruginosa* biofilms. Applied and Environmental Microbiology. 70:6188-6196.

Whiteley M, Bangera MG, Bumgarner RE, Parsek MR, Teitzel GM, Lory S, Greenberg EP. 2001. Gene expression in *Pseudomonas aeruginosa* biofilms. Nature. 413:860-864.

Wong HS, Townsend KM, Fenwick SG, Trengove RD, O'Handley RM. 2010. Comparative susceptibility of planktonic and 3-day-old *Salmonella* Typhimurium biofilms to disinfectants. Journal of Applied Microbiology. 108:2222-2228.

Xavier JB, Picioreanu C, Rani SA, van Loosdrecht MCM, Stewart PS. 2005. Biofilm-control strategies based on enzymic disruption of the extracellular polymeric substance matrix - a modelling study. Microbiology-Sgm. 151:3817-3832.

Xu KD, Franklin MJ, Park CH, McFeters GA, Stewart PS. 2001. Gene expression and protein levels of the stationary phase sigma factor, RpoS, in continuously-fed *Pseudomonas aeruginosa* biofilms. Fems Microbiology Letters. 199:67-71.

Xu KD, Stewart PS, Xia F, Huang CT, McFeters GA. 1998. Spatial physiological heterogeneity in *Pseudomonas aeruginosa* biofilm is determined by oxygen availability. Applied and Environmental Microbiology. 64:4035-4039.

Zijnge V, van Leeuwen MBM, Degener JE, Abbas F, Thurnheer T, Gmur R, Harmsen HJM. 2010. Oral biofilm architecture on natural teeth. Plos One. 5:-.

Zogaj X, Nimtz M, Rohde M, Bokranz W, Romling U. 2001. The multicellular morphotypes of *Salmonella* Typhimurium and *Escherichia coli* produce cellulose as the second component of the extracellular matrix. Molecular Microbiology. 39:1452-1463.

PRESENTATION DES RESULTATS

CHAPITRE I.

DIVERSITE ARCHITECTURALE DES BIOFILMS BACTERIENS

A. Introduction

Un biofilm, plus qu'un simple agrégat cellulaire, constitue une communauté organisée et structurée capable de fonctions spécifiques. Ces propriétés fonctionnelles, comme la capacité de métaboliser certains composés toxiques ou la résistance aux biocides, sont intimement liées à l'organisation tridimensionnelle de l'édifice biologique. Les informations structurales sont par conséquent primordiales dans la compréhension de ces mécanismes. Dans cette optique, ce premier chapitre a consisté en l'étude de la diversité architecturale des biofilms formés par une large gamme de souches bactériennes dans des conditions standardisées. Pour cela, une méthode d'investigation structurale à haut-débit a été développée. Cette étude a notamment permis d'identifier des souches produisant des biofilms intéressants d'un point de vue structural pour l'étude des mécanismes impliqués dans la résistance des biofilms aux désinfectants dans le chapitre 2.

Les techniques utilisées actuellement pour étudier les biofilms sont globalement soit des méthodes haut-débit (telles que la méthode de coloration au cristal violet en microplaque) qui procurent uniquement une quantification globale de la biomasse fixée, soit des méthodes structurales basées sur la microscopie (notamment la microscopie confocale laser à balayage) qui impliquent généralement l'utilisation de dispositifs non compatibles avec l'observation d'un grand nombre de souches de part la lourdeur des manipulations comme les chambres à flux (flow-cell). Dans le cadre de notre étude, une méthode permettant de tester un grand nombre de souches tout en pouvant obtenir des informations structurales sur les biofilms formés était requise. Une nouvelle approche haut-débit basée sur l'utilisation d'une microplaque 96 puits compatible avec l'imagerie confocale haute résolution a donc été développée et appliquée dans l'étude des biofilms formés par 60 souches bactériennes pathogènes opportunistes **(article 3 : «** *The biofilm architecture of sixty opportunistic pathogens deciphered using a high throughput CLSM method* **»)**. Les résultats obtenus ont confirmé l'existence d'une grande diversité architecturale des biofilms formés entre les espèces testées et même parfois à l'intérieur d'une même espèce comme pour *S. aureus* ou *P. aeruginosa*. Différents motifs structuraux ont été identifiés allant de structures en champignons pour *P. aeruginosa* à des biofilms plats et compacts pour *E. faecalis* en passant par des structures globalement moins denses et plus irrégulières pour *L. monocytogenes* et *E. coli*. L'espèce *S. enterica* n'a quant à elle montré qu'une faible aptitude à former des biofilms dans ces conditions expérimentales. Différents paramètres structuraux tels que le biovolume,

la rugosité, la hauteur maximale ou le pourcentage de recouvrement ont été extraits depuis les séries d'images confocales et ont permis une comparaison des biofilms formés par les 60 souches d'après plusieurs descripteurs numériques dans une analyse statistique globale.

De manière inattendue, en utilisant ce système avec l'espèce *Bacillus subtilis*, nous avons pu observer que certaines souches étaient capables de former des structures importantes avec une architecture spécifique non-décrite dans la littérature, notamment dans le cas d'une souche isolée d'un dispositif médical (souche $ND_{medical}$). La deuxième partie de ce chapitre s'est donc focalisée sur l'étude des biofilms immergés de *B. subtilis*. En effet, si cette espèce constitue un modèle pour l'étude moléculaire des voies de régulation de la formation de communautés bactériennes (Lemon *et al.*, 2008), la plupart des données ont été acquises en étudiant des modèles multicellulaires de type « pellicules » se développant à l'interface air-milieu, des macrocolonies sur gélose nutritive ou des communautés unicouche issues du développement et du mouvement coordonné d'une population bactérienne sur gélose molle (swarming). Très peu d'études se sont focalisées sur des modèles immergés associés aux surfaces (Hamon *et al.*, 2004, Hamon & Lazazzera, 2001, Stanley & Lazazzera, 2005, Stanley *et al.*, 2003). De plus, les études sont essentiellement réalisées sur des souches modèles (les souches 168 et NCIB 3610) qui ne reflètent pas forcément la diversité phénotypique présente sur le terrain.

En collaboration avec nos collègues généticiens de l'INRA de l'intitut Micalis Grignon (Dominique Le Coq et Stéphane Aymerich, équipe RG2B, Grignon), nous avons ensuite testé, dans notre modèle immergé, l'effet de quelques mutations décrites pour affecter le développement de pellicules ou de macrocolonies (gènes codant des régulateurs, des gènes de mobilité ou impliqués dans la synhèse de la matrice, Figure 1) afin de mieux comprendre les déterminants génétiques gouvernant la formation des biofilms immergés associés aux surfaces. Pour cela des mutants dérivés de la souche 168 et exprimant la GFP (green fluorescent protein) ont été construits. Ces résultats nous ont permis d'identifier 4 régulateurs (YmcA, YlbF, DegU et AbrB) jouant également un rôle clef dans le développement des biofilms immergés. Certaines mutations n'empêchant pas la formation du biofilm mais altérant sa structure tridimensionnelle ont également pu être identifiées. Nous avons pu observer que le flagelle ne jouait pas de rôle essentiel dans l'étape d'adhésion initiale au support mais que la mobilité semblait être impliquée dans le développement et la structuration des biofilms immergés. L'ensemble de ces résultats sont présentés dans l'**article 4** : « *The*

spatial architecture of Bacillus subtilis biofilms deciphered using a surface-associated model and in situ imaging ».

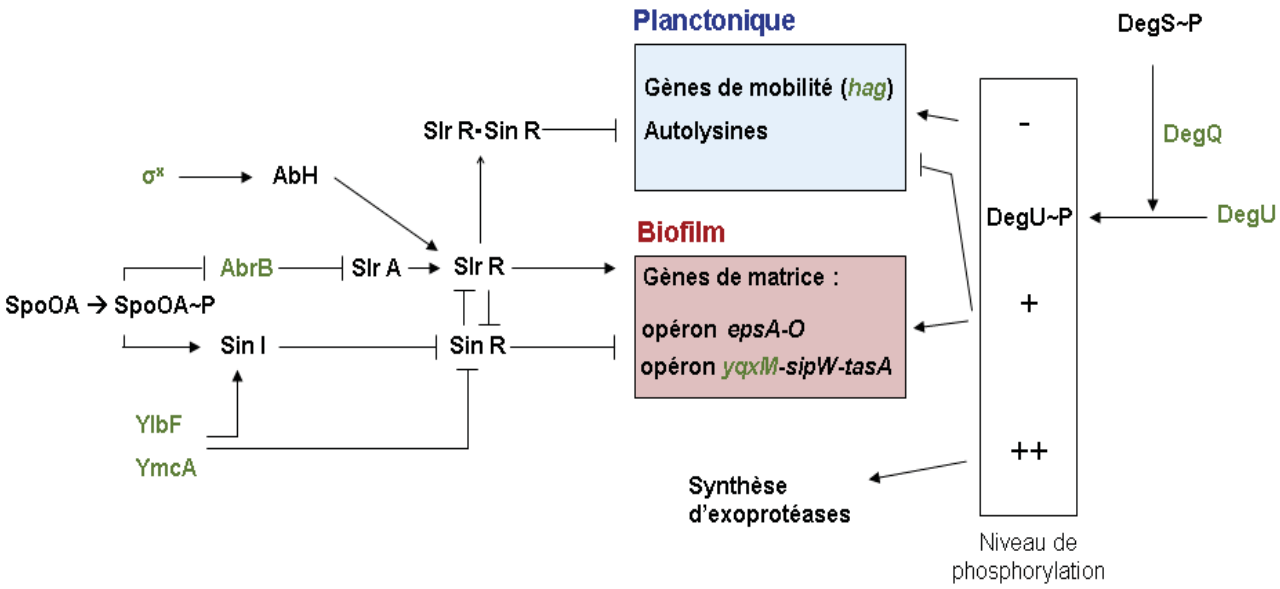

Figure 1. Schéma simplifié du réseau de régulation génétique complexe gouvernant les modes de vie exclusifs « planctonique » ou « biofilm » d'une cellule chez *B. subtilis* (d'après (Branda *et al.*, 2004, Hamon *et al.*, 2004, Kobayashi, 2007, Kobayashi, 2008, Murray *et al.*, 2009, Chai *et al.*, 2010a) . Chez une cellule en biofilm, les gènes de mobilité et les gènes codant les autolysines sont réprimés alors que les gènes impliqués dans la synthèse de la matrice sont exprimés. Les cibles génétiques testées dans l'article 4 sont indiqués en vert.

B. Article 3 :

"The biofilm architecture of sixty opportunistic pathogens deciphered using a high throughput CLSM method."

Bridier A., F. Dubois-Brissonnet, A. Boubetra, V. Thomas and R. Briandet.

Journal of Microbiological Methods, 2010, 82 :64-70.

Journal of Microbiological Methods 82 (2010) 64–70

Contents lists available at ScienceDirect

Journal of Microbiological Methods

journal homepage: www.elsevier.com/locate/jmicmeth

The biofilm architecture of sixty opportunistic pathogens deciphered using a high throughput CLSM method

A. Bridier [a], F. Dubois-Brissonnet [b], A. Boubetra [c], V. Thomas [d], R. Briandet [a,*]

[a] INRA, UMR 1319 Micalis, 25 Ave. de la République, F-91300 Massy, France
[b] AgroParisTech, UMR 1319 Micalis, 1 Ave. des Olympiades, F-91300 Massy, France
[c] ISHA, 25 Ave. de la République, F-91300 Massy, France
[d] STERIS SA, CEA, Route du Panorama, F- 92265 Fontenay-aux-Roses, France

ARTICLE INFO

Article history:
Received 15 March 2010
Received in revised form 19 April 2010
Accepted 19 April 2010
Available online 28 April 2010

Keywords:
Biofilm structure
CLSM
High throughput method

ABSTRACT

This study proposes a high throughput method based on Confocal Laser Scanning Microscopy (CLSM) combined with the use of 96-wells microtiter plates compatible with high resolution imaging for the study of biofilm formation and structure. As an illustration, the three-dimensional structures of biofilms formed by 60 opportunistic pathogens were thus observed and quantified. The results revealed the diversity of biofilm architectures. Specific spatial arrangement such as the mushroom-like structures already described for *Pseudomonas aeruginosa* was observed. Other features, such as hollow voids in microcolonies of *Salmonella enterica* strain Agona, were identified for the first time. The combined use of microplates and confocal imaging proved to be a good alternative to the other high throughput methods commonly used as it enables the direct, *in situ*, qualitative and quantitative characterization of biofilm architecture. This high content method should lead to a clearer understanding of the structure–function relationships implicated in biofilms traits.

1. Introduction

Biofilms are surface-attached microbial communities embedded in a self-produced extracellular polymeric matrix (Donlan and Costerton, 2002) and are now recognized as the prevailing microbial lifestyle in natural environments (Costerton, 1995; Watnick and Kolter, 2000). In these highly structured and organized communities, bacteria display coordinated behavior and are able to perform specific functions (Spoering and Gilmore, 2006). They can therefore play positive roles; e.g. in bioremediation because of their high microbial biomass and ability to immobilize recalcitrant compounds (Singh et al., 2006). Moreover, different studies have demonstrated the inhibition of pathogens such as *Listeria monocytogenes* by natural, indigenous biofilms (Carpentier and Chassaing, 2004; Zhao et al., 2004; Habimana et al., 2009). However, because of their high resistance to antimicrobial and cleaning treatments (Mah and O'Toole, 2001; Hogan and Kolter, 2002), biofilms also contribute markedly to the persistence of pathogens on medical devices or industrial equipment, leading to critical problems in terms of public health and a potentially major economic impact (Potera, 1999; Costerton et al., 1999; Brooks and Flint, 2008; Hall-Stoodley and Stoodley, 2009). The functional properties of biofilms are intimately related to their spatial architecture. Their resistance to antimicrobial agents due to diffusion and/or reaction delays (Lewis, 2001; Campanac et al., 2002) is a telling example of the importance of the matrix shape and the three-dimensional organization of cells. Moreover, microorganisms within biofilms respond to heterogeneous local environmental conditions because of the chemical gradients that are generated by the three-dimensional structure of these communities (Wimpenny et al., 2000; Stewart, 2003). Thus, the structural heterogeneity of biofilms leads to different gene expression patterns and specific physiological activities for the cells within the structure (Rani et al., 2007; Stewart and Franklin, 2008), resulting in the emergence of novel and global community functions. Structural data are therefore of prime importance to better understand the complex behavioral and survival strategies of biofilms and ultimately to improve the control of these biological structures.

Confocal laser scanning microscopy (CLSM) is one of the tools most widely used at present to study biofilm structure because it enables the direct *in situ* and non-destructive investigation of native multicellular structures using specific fluorescent markers. The recent development of dedicated image analysis software (Heydorn et al., 2000; Xavier et al., 2003; Beyenal et al., 2004; Daims et al., 2006) provides an opportunity to obtain detailed quantitative structural parameters on biofilms directly from confocal image stacks. Thereby, in addition to qualitative information on biofilm structure, detailed characterization with numerical data is possible and enables the performance of statistical analysis. However, the devices commonly used for the confocal study of biofilms, such as flow-cells, capillary tubes or glass coverslides, may be relatively expensive and/or involve fastidious biofilm growth protocols which are not compatible with large-scale screening. On the other hand,

* Corresponding author. Tel.: +331 69 53 64 77.
E-mail address: romain.briandet@jouy.inra.fr (R. Briandet).

0167-7012/$ – see front matter © 2010 Elsevier B.V. All rights reserved.
doi:10.1016/j.mimet.2010.04.006

many high throughput microtiter plate-based assays have been developed to quantify the formation of biofilms in a large number of strains. One of the most widely used consists in biofilm quantification by measuring the optical density of adhered cells in a 96-well microtiter plate after staining with crystal violet and rinsing (Christensen et al., 1985). Various adaptations of this test have been developed and optimized in order to enhance its accuracy and specificity (Stepanovic et al., 2000; Djordjevic et al., 2002; Burton et al., 2007; Peeters et al., 2008).

Nevertheless, although these assays are rapid, economical and thus adapted to the screening of biofilm formation in a large number of strains, they only supply a global quantification and not a detailed structural characterization of biofilms. An additional screening system, the Calgary Biofilm Device (Ceri et al., 1999), initially developed to evaluate biofilm susceptibility to antibiotics, can also give access to biofilm structural information. This system is based on the use of a microtiter plate with a removable lid that hold 96 pegs substratum allowing microscopic observations of biofilm structure (Harrison et al., 2006). However, prior microscopic observation, it is needed to remove the pegs from the growth media, to manually break the pegs one by one, and to transfer them in air on microscopic coverslips. This ex-situ preparation is time consuming and can alter the native biofilm spatial organization. Hence, we propose here a high throughput method based on a 96-well microplate that is optically compatible with high resolution CLSM observations in order to characterize biofilm architecture. This method allowed us to obtain qualitative and quantitative characterizations of the spatial biofilm structure of 60 opportunistic pathogenic strains belonging to six different bacterial species.

2. Materials and methods

2.1. Bacterial strains and culture conditions

All the strains used during this study are listed in Table 1. They consisted of 60 strains belonging to three Gram-positive species (*Enterococcus faecalis*, *Listeria monocytogenes* and *Staphylococcus aureus*) and three Gram-negative species (*Escherichia coli*, *Pseudomonas aeruginosa* and *Salmonella enterica*) which are recognized as potential human pathogens.

Bacterial stock cultures were kept at −80 °C in Tryptone Soy Broth (TSB, BioMérieux, France) containing 20% (vol/vol) glycerol. Prior to each experiment, frozen cells were subcultured twice in TSB at 30 °C.

2.2. Biofilm formation and fluorescent labeling

250 µl of the final overnight subculture adjusted to an $OD_{600\ nm}$ of 0.01 (approximately 10^6 CFU/ml) were added to the wells of a polystyrene 96-well microtiter plate (Greiner Bio-one, France) with a µclear® base (Polystyrene, thickness of 190 ± 5 µm) which allowed for high resolution imaging. After 1 h of adhesion at 30 °C, the wells were rinsed with 150 mM NaCl in order to eliminate any non-adherent bacteria before being refilled with 250 µl TSB. The plate was then incubated for 24 h at 30 °C. After the development of biofilms, the wells were rinsed with 150 mM NaCl and refilled with TSB containing 5 µM Syto9 (1:1000 dilution from a Syto9 stock solution at 5 mM in DMSO; Invitrogen, France), a cell permeant green fluorescent nucleic acid marker. The plate was then incubated in the dark at 30 °C for 20 min to enable the fluorescent labeling of the bacteria.

2.3. Confocal Laser Scanning Microscopy (CLSM) image acquisition

Prior to image acquisition, the plate was mounted on the motorized stage of a Leica SP2 AOBS Confocal laser scanning microscope (LEICA Microsystems, France) at the MIMA2 microscopy platform (http://voxel.jouy.inra.fr/mima2). All biofilms were scanned at 400 Hz using a 40× with a 0.8 N.A. (Leica HCX Apo) water immersion objective lens with a 488 nm argon laser set at 25% intensity. Emitted fluorescence was recorded within the range 500–600 nm in order to visualize Syto9 fluorescence. Three stacks of horizontal plane images (512×512 pixels

Table 1
The sixty strains used during this study.

Species	Code*	Origin/reference	Strain no.
Salmonella enterica	S24 (ser. St Paul)	Food (ISHA)	1
	I26 (ser. Agona)	Food (ISHA)	2
	S2 (ser. Brandenburg)	Food (ISHA)	3
	S19 (ser. Duby)	Food (ISHA)	4
	S59 (ser. Dublin)	Food (ISHA)	5
	S38 (ser. Enteritidis)	Food (ISHA)	6
	S12 (ser. Hadar)	Food (ISHA)	7
	S55 (ser. Indiana)	Food (ISHA)	8
	ATCC 13311 (ser. Typhimurium)	Human faeces	9
	S34 (ser. Typhimurium)	Food (ISHA)	10
Listeria monocytogenes	EGDe	Murray et al. (1926)	11
	CIP 104794	Guinea pig	12
	CIP 103573	Food	13
	CIP 103575	Food	14
	CIP 78 39	Food	15
	370P-Lm	Food (UBHM)	16
	Lm 162	Food (aerial collection, Illkirch)	17
	Lm 481	Food (aerial collection, Illkirch)	18
	LO28	Michel and Cossart (1992)	19
	BUG1641	Bierne et al. (2001)	20
Escherichia coli	PHL 565 (MG1655)	Jubelin et al. (2005)	21
	163P-Ec	Clinical (UBHM)	22
	186P-Ec	Clinical (UBHM)	23
	RS218	Clinical	24
	ATCC 8739	Human faeces	25
	ESC.1.13	Food (ISHA)	26
	ESC.1.16	Food (ISHA)	27
	ESC.1.24	Food (ISHA)	28
	ESC.1.30	Food (ISHA)	29
	ESC.1.33	Food (ISHA)	30
Pseudomonas aeruginosa	ATCC 15442	Animal room water bottle	31
	PSE.1.2	Food (ISHA)	32
	ATCC 10145	Unknown	33
	ATCC 14210	Clinical	34
	ATCC 49189	Clinical	35
	ATCC 9027	Clinical	36
	ATCC 15692	Clinical	37
	ATCC 9721	Unknown	38
	ATCC 14207	Faeces	39
	ATCC 51447	Unknown	40
Staphylococcus aureus	ATCC 6538	Clinical	41
	CIP 57.10	Milk from ewes with mastitis	42
	ATCC 9144	Unknown	43
	ATCC 29213	Clinical	44
	ATCC 27217	Sea water	45
	ATCC 25923	Clinical	46
	ATCC 29247	Unknown	47
	ATCC 8096	Clinical	48
	ATCC 43300	Clinical	49
	STA.1.5	Superficial water (ISHA)	50
Enterococcus faecalis	ATCC 19433	Unknown	51
	ATCC 51188	Clinical	52
	ATCC 33012	Unknown	53
	ATCC 49477	Clinical	54
	ATCC 33186	Unknown	55
	ATCC 27959	Bovine mastitis	56
	ATCC 700802	Clinical	57
	ATCC 29212	Clinical	58
	ATCC 29302	Unknown	59
	ATCC 51299	Clinical	60

Culture collections. ATCC: American Type Culture Collection; CIP: Collection de l'Institut Pasteur; UBHM: Unité Bioadhésion et Hygiène des Matériaux; ISHA: Institut Scientifique d'Hygiène et d'Analyses.

corresponding to 119×119 μm) with a z-step of 1 μm were acquired for each biofilm at different areas in the well. Two independent experiments were performed for each strain.

2.4. Image analysis

Three-dimensional projections of biofilms structure were reconstructed using the Easy 3D function of the IMARIS 7.0 software (Bitplane, Switzerland). Quantitative structural parameters of the biofilms, such as biovolume, substratum coverage and roughness, were calculated using PHLIP (Xavier et al., 2003), a freely available Matlab-based image analysis toolbox (http://phlip.sourceforge.net/phlip-ml).

The biovolume represented the overall volume of cells (μm^3) in the observation field (here 14,209 μm^2). Substratum coverage (%) reflected the efficiency of substratum colonization by bacteria. Roughness provided a measure of variations in biofilm thickness and was an indicator of the superficial biofilm interface heterogeneity. The maximum thickness (μm) of biofilms was also determined directly from the confocal stack images.

2.5. Statistical analysis

All statistical analyses (Principal Component Analysis (PCA), one-way ANOVA) were performed using Statgraphics v6.0 software (Manugistics, Rockville, USA). Significance was defined as a *P* value associated with a Fisher test value lower than 0.05.

3. Results

3.1. Three-dimensional structure of biofilms

Representative 24 h-biofilm structures observed using CLSM for the 60 strains under study are presented in Fig. 1. The images corresponded

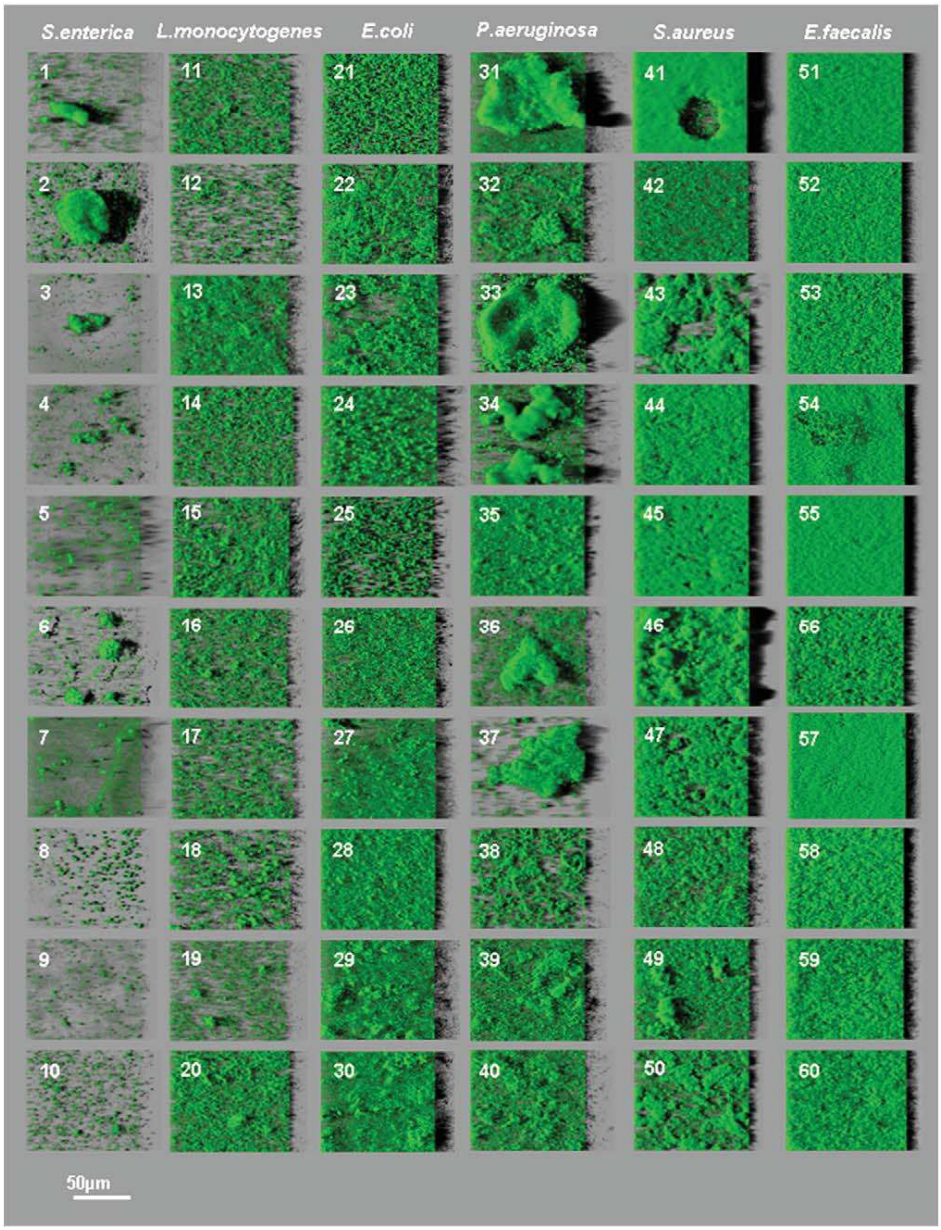

Fig. 1. 3D projections of biofilm structure obtained from confocal z-stacks using IMARIS software. These images present an aerial view of biofilm structures obtained with the 60 strains, with the shadow projection on the right.

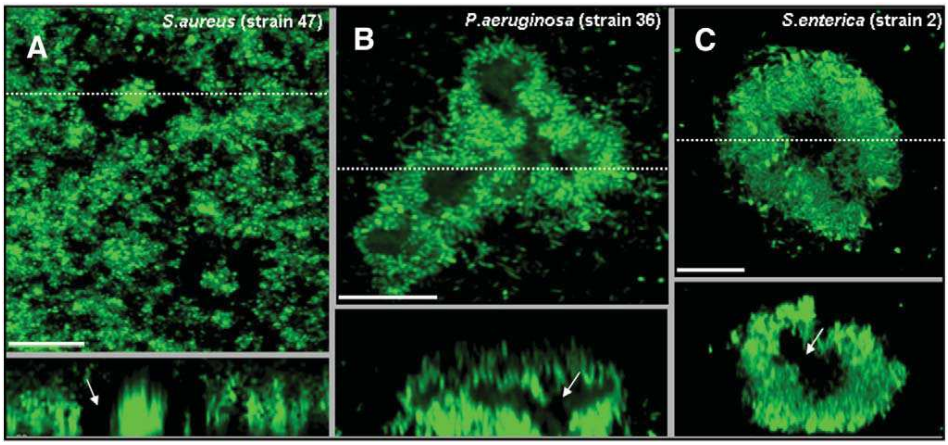

Fig. 2. Section views of hollow void structures formed by (A) *S. aureus* ATCC 29247 (strain 47), (B) *P. aeruginosa* ATCC 9027 (strain 36) and (C) *S. enterica* ser. Agona (strain 2). Dotted lines indicate vertical sections. White bars correspond to 20 µm.

to three-dimensional reconstructions obtained from confocal stack images by the IMARIS software, including virtual shadow projections on the right. We found a marked variability in three-dimensional biofilm architecture between the species. The results showed that *S. enterica* strains formed only a few, small scattered cell clusters, while *L. monocytogenes* and *E. coli* strains produced rough biofilms containing several small aggregates and of variable thickness. Most *P. aeruginosa* strains produced mushroom-shaped structures of various sizes. *S. aureus* strains displayed a high degree of variability in terms of biofilm structure. Approximately half of the strains formed flat and compact structures, while others developed biofilms with a patchy coverage and confluent growth areas where the bacteria formed clumps. All *E. faecalis* strains displayed a marked and homogeneous ability to form biofilms under these experimental conditions, and produced flat and compact structures that covered the entire surface available.

Using section views at higher magnification (Fig. 2), we identified specific free-of-cells areas within some of the three-dimensional structures. Many *S. aureus* biofilms formed with different strains repeatedly included holes of different sizes that contained highly fluorescent cell aggregates in the centre, as shown in Fig. 2A for strain no. 47. We also noted the presence of hollow voids within the microcolonies formed by different *P. aeruginosa* strains (Fig. 2B) and identified a similar phenomenon with the *S. enterica* strain serovar Agona (strain no. 2, Fig. 2C).

3.2. Quantification of structural parameters

Biovolume, maximum thickness, substratum coverage and roughness parameters were extracted from confocal stack images in order to quantify biofilm structures with numerical data that would allow statistical analysis. The results obtained were grouped by species using a box and whisker plot representation (Fig. 3). Four significantly different groups were highlighted in terms of biovolume ($P<0.05$) with respect to the six species (Fig. 3A). It should be noted that the same groups were formed when using substratum coverage values (data not shown). *S. enterica* strains, which demonstrated low biovolumes, constituted the first group. The second group was characterized by species with moderate mean biovolumes, such as *L. monocytogenes*, *E. coli* and *P. aeruginosa*. The third group was represented by *S. aureus* which displayed the highest intra-specific variability in terms of biovolume ($P<0.05$), in accordance with its high structural variability. The last group comprised *E. faecalis* strains displaying comparable abilities to form biofilms with high biovolumes under these experimental conditions. According to maximum thickness values (Fig. 3B), *P. aeruginosa* strains formed biofilms with the highest maximum thickness ($P<0.05$). Moreover, *P. aeruginosa* and *L. monocytogenes* biofilms also demonstrated significantly higher mean roughness values than the other species ($P<0.05$). Note that within-strain biovolume variation between wells was evaluated for two strains with different biofilm architecture, *P. aeruginosa* strain 31 and *S. aureus* strain 41. Considering 10 wells for each strain (and 3 z-stacks per well), we found that standard error represents 6% and 8% of the mean biovolume value for *S. aureus* strain and *P. aeruginosa* strain 31 respectively. Three-dimensional reconstructions from the 30 z-stacks are given for *S. aureus* strain 41 as example in Fig. S1.

3.3. Multivariate analysis of the structural parameters of biofilms

The four structural parameters (biovolume, substratum coverage, roughness and maximum thickness) were then analyzed using the data compression step of principal component analysis (PCA, Fig. 4). This analysis removed redundancy from the original dataset in order to obtain a small number of linear combinations of the four variables, which accounted for most of the variability in the data. Two components were extracted and together accounted for 82% of the variability of the original dataset. The first principal component PC1 (53% of total variation) was positively correlated with biovolume and substratum coverage and negatively correlated with roughness. The second principal component PC2 (29% of total variation) was mainly positively correlated with maximum thickness. The PCA results revealed the presence of two groups of strains with specific biofilm structural parameters. The first group (Group 1) was exclusively composed of Gram-positive strains, including all *E. faecalis* strains and half of the *S. aureus* strains. It was characterized by strains producing biofilms with high biovolumes and high substratum coverage. The second group (Group 2) represented more than 70% of the isolates and was mainly characterized by strains producing biofilms with a low or moderate biovolume and high roughness, and also grouped strains with variable maximum thickness.

4. Discussion

The development of high throughput methods is necessary to respond to current needs in the field of biofilm research, including comparisons of the biofilm forming abilities of different strains, the testing of new anti-biofilm compounds or to gain an understanding of the genetic regulation processes governing biofilm formation and development. Different microtiter-based tests are available to quantify biofilm but there is no high throughput method which allows the crucial assessment of their native architecture. In this context, we

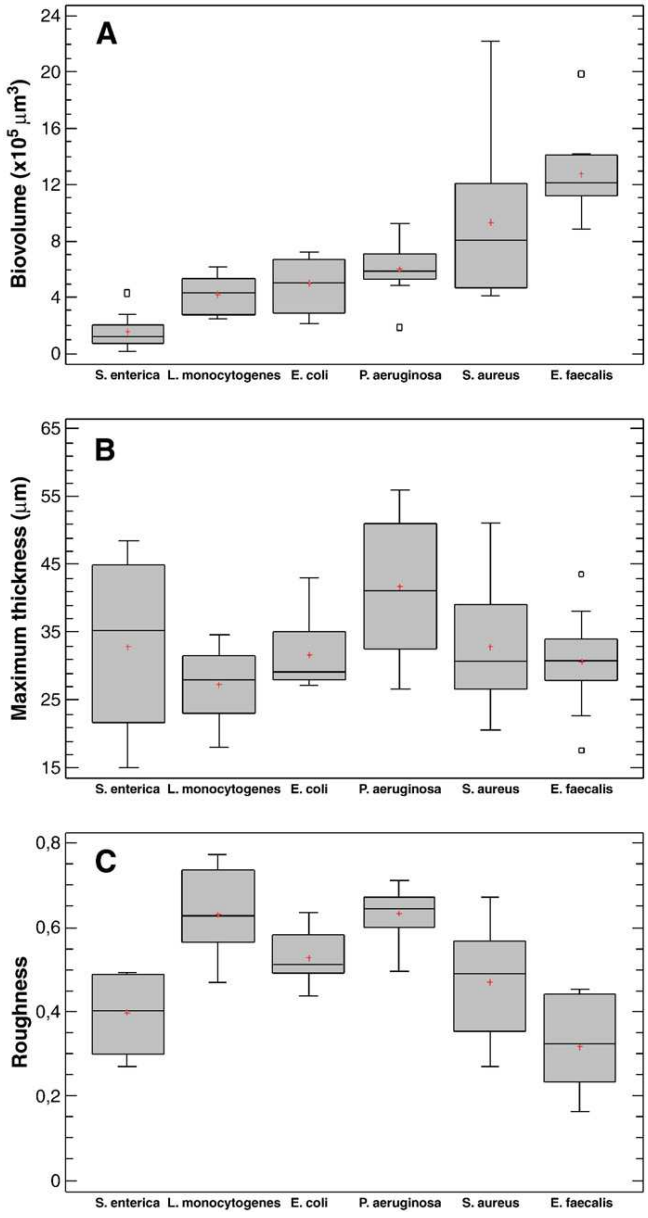

Fig. 3. Box-and-whisker diagrams depicting the distribution of biovolume (A), maximum thickness (B) and roughness (C) values observed for the 60 strains classified by species (10 strains/species). Boxes range from the 25th to 75th percentile and are intersected by the median line. Whiskers extend below and above the box range, from the lowest to the highest values, respectively. Averages are indicated by a cross symbol (+). Outliers are indicated as individual data points (□).

propose a high throughput approach based on CLSM combined with 96-well microplate compatible with high resolution imaging. As an illustration, this method was used to characterize the biofilm architecture of 60 potential human pathogens. In our acquisition conditions (1.6 s for one image acquisition images, 3 images series per well and a z-step of 1 µm) and considering biofilms of 30 µm depth in average, it is possible theoretically to scan a 96-wells microtiter plate in less than 4 h, to which an extra 2 h is necessary for manual manipulations. Associated extraction of structural parameters such as biovolume, roughness and thickness can take less than 1 h using the PHLIP batch automatic thresholding function. Overall, the full processing (acquisition and image treatment) of a 96-wells microtiter plate takes less than a working day. Acquisition time can also be dropped off by reducing image resolution or increasing scanning frequency if applicable. Furthermore, the recent availability of commercial software dedicated to automated high content screening enables the programming of the confocal microscope to scan automatically the 96-wells microplate. Acquisition could thus be done without operator that will dramatically improve the flow of the technique. Results obtained revealed marked variability in the formation and structure of biofilms, not only between different species but also within some species such as *S. aureus*. The three-dimensional structures which were identified may play a key role in the settlement, antimicrobial tolerance and persistence of these different pathogens. Specific architectural patterns previously described in the literature were identified for the different species and demonstrated the suitability of the method for structural investigations on biofilms. Moreover, conditions that promote biofilm formation in microtiter plate (media, temperature, and time incubation) can be optimized for microscopic observations as already described for *Candida albicans* (Krom et al., 2009). In line with the observations of Rieu et al. (2008) on stainless steel, we found that *L. monocytogenes*, under static conditions and after incubation for 24 h, formed thin structures covering most of the surface available. Chavant et al. (2002) showed the formation of similar structures on stainless steel and polytetrafluoroethylene (PTFE) using scanning electronic microscopy (SEM), although different incubation times and temperatures were employed. *E. coli* produced rough biofilms with clusters and irregular coverage under our conditions, as previously described in continuous flow systems (Reisner et al., 2003; May and Okabe, 2008). SEM observations of *E. faecalis* biofilm formation on dentinal root surfaces by Estrela et al. (2009) depicted the development of compact and relatively smooth structures which were in agreement with our findings. Moreover, confocal observations of *E. faecalis* biofilm by Guiton et al. (2009) revealed the formation of thick, flat structures on plastic coverslides after a 72 h incubation period under static conditions. As for *S. aureus*, the presence in biofilms of free-of-cells areas of various sizes but potentially containing cell aggregates, was reminiscent of the structure described by Yarwood et al. (2004) in a flow-cell system used to model *agr* expression in *S. aureus* biofilms. We also found that most of the *P. aeruginosa* strains produced the well-known mushroom-shaped structures previously described in other devices such as flow-cells (Klausen et al., 2003) or glass capillary tubes (Klayman et al., 2008). Moreover, the presence of hollow voids within mushroom-like structures with *P. aeruginosa* had been reported during recent studies (Webb et al., 2003, 2004; Rice et al., 2009). These authors showed that the creation of a hollow center within microcolonies involved cell death mediated by a filamentous prophage (Pf4) constituted a normal component of *P. aeruginosa* biofilm development which enhanced its virulence. Other studies have revealed similar structures within microcolonies formed by Gram-negative bacteria (Mai-Prochnow et al., 2004, 2008) and oral bacteria (Auschill et al., 2001; Hope et al., 2002), showing it may be a widespread process in the life cycle of biofilms. This phenomenon had never previously been described for *S. enterica* and may similarly contribute to the danger associated with this pathogen. It is interesting to note that the *S. enterica* strain displaying the largest structures with a hollow center (strain 2) was the Agona strain. Indeed, Vestby et al. (2009) demonstrated in other biofilm models, such as the air-liquid pellicle interface or microtiter plates using crystal violet, that *S. enterica* serovar Agona strains were better biofilm producers than *S. enterica* serovar Typhimurium strains, which was in agreement with our present observations. They also showed that this enhanced capacity for biofilm formation was correlated with a greater persistence of this serovar in manufacturing environments. The fact that we found hollow structures with only one of the ten *S. enterica* strains tested increases the importance of testing a large number of samples in order to obtain a representative view of the different phenotypes present in natural, industrial and medical environments. It therefore underlines the relevance of a high throughput method for the study of biofilm structure. One of the advantages of this technique

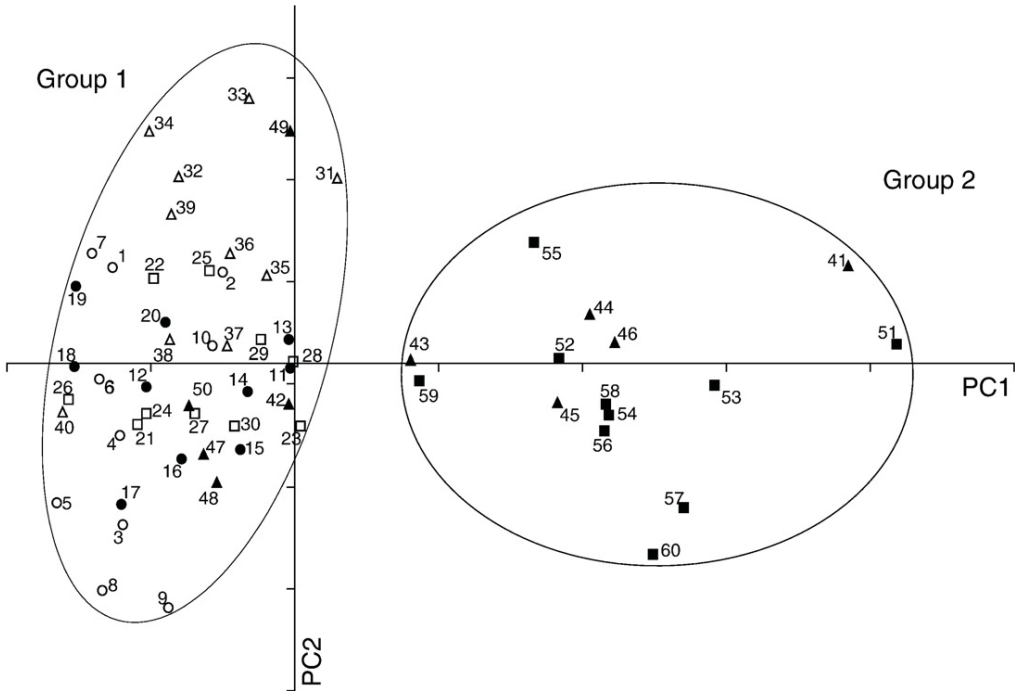

Fig. 4. Principal component analysis of combined structural parameters obtained for the 60 strains after confocal data processing by the PHLIP tool. Only the first principal component PC1 (accounting for 53% of the total variation) and the second principal component PC2 (accounting for 29% of the total variation) are shown. *E. faecalis* (■), *L. monocytogenes* (●), *S. aureus* (▲), *E. coli* (□), *S. enterica* (○) and *P. aeruginosa* (△).

is the simplicity of the biofilm growth protocol and the possibility to obtain multiple biofilms available for structural and behavioral studies. As well as generating qualitative information, the use of CLSM and dedicated image analysis software also provides numerous structural descriptors of the biofilm that enable the characterization of its architecture, whereas traditional microtiter assays only supply global quantitative data. For example, although *P. aeruginosa* strains generally produced low biovolume biofilms compared to *S. aureus* or *E. faecalis*, they formed rough biofilms containing structures with a greater maximum thickness that are known to be involved in the virulence and antimicrobial resistance of pathogens (Hentzer et al., 2001; Pamp et al., 2008). Thus the generation of structural data can enable a clearer understanding of biofilm traits. Furthermore, multivariate analysis can be performed in a large number of strains on the basis of these structural features in order to cluster individuals and identify singular phenotypes. Thus large-scale structure–function analyses of biofilms will be facilitated by combining these results with other data obtained on factors such as virulence or antimicrobial resistance. The combination of other fluorescent markers to dye specific components of matrix as polysaccharides or proteins, or to discriminate viable and non-viable bacteria can also be used to deepen the understanding of biofilm structure–function relationships.

In conclusion, the method presented here can rapidly supply *in situ* qualitative and quantitative structural data on a large number of biofilms. It could therefore be used to screen genetic mutant banks, antimicrobial compounds and anti-biofilm surface coatings, or to determine influence of different growth conditions. The materialization of fully automated systems (microtiter plate scanning and image treatment) will radically amplify the flow of available biofilm structural data that will participate to decipher biofilms traits.

Acknowledgments

This study received support from the “MEDICEN-Region Paris, Ile-de-France” Competitiveness Cluster. We would like to thank the Essonne Département for its financial support of the confocal microscopy facility (ASTRE no. A02137) and Victoria Hawken for English revision of the text.

Appendix A. Supplementary data

Supplementary data associated with this article can be found, in the online version, at doi:10.1016/j.mimet.2010.04.006.

References

Auschill, T.M., Arweiler, N.B., Netuschil, L., Brecx, M., Reich, E., Sculean, A., Artweiler, N.B., 2001. Spatial distribution of vital and dead microorganims in dental biofilms. Arch. Oral Biol. 46, 471–476.
Beyenal, H., Donovan, C., Lewandowski, Z., Harkin, G., 2004. Three-dimensional biofilm structure quantification. J. Microbiol. Meth. 59, 495–513.
Bierne, H., Gouin, E., Roux, P., Caroni, P., Yin, H.L., Cossart, P., 2001. A role for cofilin and LIM kinase in *Listeria*-induced phagocytosis. J. Cell Biol. 155, 101–112.
Brooks, J.D., Flint, S.H., 2008. Biofilms in the food industry: problems and potential solutions. Int. J. Food Sci. Technol. 43, 2163–2176.
Burton, E., Yakandawala, N., LoVreti, K., Madhyastha, M.S., 2007. A microplate spectrofluorometric assay for bacterial biofilms. J. Ind. Microbiol. Biotechnol. 34, 1–4.
Campanac, C., Pineau, L., Payard, A., Baziard-Mouysset, G., Roques, C., 2002. Interactions between biocide cationic agents and bacterial biofilms. Antimicrob. Agents Chemother. 46, 1469–1474.
Carpentier, B., Chassaing, D., 2004. Interactions in biofilms between *Listeria monocytogenes* and resident microorganisms from food industry premises. Int. J. Food Microbiol. 97, 111–122.
Ceri, H., Olson, M.E., Stremick, C., Read, R.R., Morck, D.W., Buret, A.G., 1999. The Calgary Biofilm Device: new technology for rapid determination of antibiotic susceptibilities in bacterial biofilms. J. Clin. Microbiol. 37, 1771–1776.
Chavant, P., Martinie, B., Meylheuc, T., Bellon-Fontaine, M.N., Hebraud, M., 2002. *Listeria monocytogenes* LO28: surface physicochemical properties and ability to form biofilms at different temperatures and growth phases. Appl. Environ. Microbiol. 68, 728–737.
Christensen, G.D., Simpson, W.A., Younger, J.J., Baddour, L.M., Barrett, F.F., Melton, D.M., Beachey, E.H., 1985. Adherence of coagulase-negative staphylococci to plastic tissue culture plates, a quantitative model for the adherence of staphylococci to medical devices. J. Clin. Microbiol. 22, 996–1006.
Costerton, J.W., 1995. Overview of microbial biofilms. J. Ind. Microbiol. 15, 137–140.
Costerton, J.W., Stewart, P.S., Greenberg, E.P., 1999. Bacterial biofilms, a common cause of persistent infections. Science 284, 1318–1322.
Daims, H., Lucker, S., Wagner, M., 2006. *daime*, a novel image analysis program for microbial ecology and biofilm research. Environ. Microbiol. 8, 200–213.

Djordjevic, D., Wiedmann, M., McLandsborough, L.A., 2002. Microtiter plate assay for assessement of *Listeria monocytogenes* formation. Appl. Environ. Microbiol. 68, 2950–2958.
Donlan, R.M., Costerton, J.W., 2002. Biofilms, survival mechanisms of clinically relevant microorganisms. Clin. Microbiol. Rev. 15, 167–193.
Estrela, C., Sydney, G.B., Fugueiredo, J.A.P., Estrela, C.R.A., 2009. A model system to study antimicrobial strategies in endodontic biofilms. J. Appl. Oral Sci. 17, 87–91.
Guiton, P.S., Hung, C.S., Kline, K.A., Roth, R., Kau, A.L., Hayes, E., Heuser, J., Dodson, K.W., Caparon, M.G., Hultgren, S.J., 2009. Contribution of autolysine and sortase A during *Enterococcus faecalis* DNA-dependent biofilm development. Infect. Immun. 77, 3626–3638.
Habimana, O., Meyrand, M., Meylheuc, T., Kulakauskas, S., Briandet, R., 2009. Genetic features of resident biofilm determine attachment of *Listeria monocytogenes*. Appl. Environ. Microbiol. 75, 7814–7821.
Hall-stoodley, L., Stoodley, P., 2009. Evolving concepts in biofilm infections. Cell. Microbiol. 11, 1034–1043.
Harrison, J.J., Ceri, H., Yerly, J., Stremick, C.A., Hu, Y., Martinuzzi, R., Turner, R.J., 2006. The use of microscopy and three-dimensional visualization to evaluate the structure of microbial biofilms cultivated in the Calgary Biofilm Device. Biol. Proced. 8, 194–215.
Hentzer, M., Teitzel, G.M., Balzer, G.J., Heydorn, A., Molin, S., Givskov, M., Parsek, M.R., 2001. Alginate overproduction affects *Pseudomonas aeruginosa* biofilm structure and function. J. Bacteriol. 18, 5395–5401.
Heydorn, A., Nielsen, A.T., Hentzer, M., Sternberg, C., Givskov, M., Ersboll, B.K., Molin, S., 2000. Quantification of biofilm structures by the novel computer program COMSTAT. Microbiology 146, 2395–2407.
Hogan, D., Kolter, R., 2002. Why are bacteria refractory to antimicrobials? Curr. Opin. Microbiol. 5, 472–477.
Hope, C.K., Clements, D., Wilson, M., 2002. Determining the spatial distribution of viable and non viable bacteria in hydrated microcosm dental plaques by viability profiling. J. Appl. Microbiol. 93, 448–455.
Jubelin, G., Vianney, A., Beloin, C., Ghigo, J.M., Lazzaroni, J.C., Lejeune, P., Dorel, C., 2005. CpxR/OmpR interplay regulates curli expression gene expression in response to osmolarity in *Escherichia coli*. J. Bacteriol. 187, 2038–2049.
Klausen, M., Aaes-Jorgensen, A., Molin, S., Tolker-Nielsen, T., 2003. Involvement of bacterial migration in the development of complec multicelular structures in *Pseudomonas aeruginosa* biofilms. Mol. Microbiol. 50, 61–68.
Klayman, B.J., Klaper, I., Stewart, P.S., Camper, A.K., 2008. Measurement of accumulation and displacement at the single cell cluster level in *Pseudomonas aeruginosa* biofilms. Environ. Microbiol. 10, 234–2354.
Krom, B.P., Cohen, J.B., McElhaney-Feser, G., Busscher, H.J., Van der Mei, H.C., Cihlar, R.L., 2009. Conditions for optimal *Candida* biofilm development in microtiter plates. Methods Mol. Biol. 499, 55–62.
Lewis, K., 2001. Riddle of biofilm resistance. Antimicrob. Agents Chemother. 45, 999–1007.
Mah, T.-F.C., O'Toole, G.A., 2001. Mechanisms of biofilm resistance to antimicrobial agents. Trends Microbiol. 9, 34–39.
Mai-Prochnow, A., Evans, F., Dalisay-Saludes, D., Stelzer, S., Egan, S., James, S., Webb, J.S., Kjelleberg, S., 2004. Biofilm development and cell death in the marine bacterium *Pseudoalteromonas tunicata*. Appl. Environ. Microbiol. 70, 3232–3238.
Mai-Prochnow, A., Lucas-Elio, P., Egan, S., Thomas, T., Webb, J.S., Sanchez-Amat, A., Kjelleberg, S., 2008. Hydrogen peroxide linked to lysine oxidase activity facilitates biofilm differenciation and dispersal in several gram-negative bacteria. J. Bacteriol. 190, 5493–5501.
May, T., Okabe, S., 2008. *Escherichia coli* harboring a natural IncF conjugative F plasmid develops complex mature biofilms by stimulating synthesis of colanic acid and curli. J. Bacteriol. 190, 7479–7490.
Michel, E., Cossart, P., 1992. Physical map of the *Listeria monocytogenes* chromosome. J. Bacteriol. 174, 7098–7103.
Murray, E.G.D., Webb, R.A., Swann, R.B.K., 1926. A disease of rabbits characterized by a large mononuclear leucocytosis. J. Pathol. Biol. 29, 407–439.
Pamp, S.J., Gjermansen, M., Johansen, H.K., Tolker-Nielsen, T., 2008. Tolerance to the antimicrobial peptide colistin in *Pseudomonas aeruginosa* biofilms is linked to metabolically active cells, and depends on the pmr and mexAB-oprM genes. Mol. Microbiol. 68, 223–240.
Peeters, E., Nelis, H.J., Coenye, T., 2008. Comparison of multiple methods for quantification of microbial biofilms grown in microtiter plates. J. Microbiol. Meth. 72, 157–165.
Potera, C., 1999. Forging a link between *biofilms* and disease. Science 283, 1837–1839.
Rani, S.A., Pitts, B., Beyenal, H., Veluchamy, R.A., Lewandowski, Z., Buckingham-Meyer, K., Stewart, P.S., 2007. Spatial patterns of DNA replication, protein synthesis and oxygen concentration within bacterial biofilms reveal diverse physiological states. J. Bacteriol. 189, 4223–4233.
Reisner, A., Haagensen, J.A.J., Schembri, M.A., Zechner, E.L., Molin, S., 2003. Development and maturation of *Escherichia coli* K-12 biofilms. Mol. Microbiol. 48, 933–946.
Rice, S.A., Tan, C.H., Mikkelsen, P.J., Kung, V., Woo, J., Tay, M., Hauser, A., McDougald, D., Webb, S.A., Kjelleberg, S., 2009. The biofilm life cycle and virulence of *Pseudomonas aeruginosa* are dependent on a filamentous prophage. ISME J. 3, 271–282.
Rieu, A., Briandet, R., Habimana, O., Garmyn, D., Guzzo, J., Piveteau, P., 2008. *Listeria monocytogenes* EGD-e biofilms: no mushrooms but a network of knitted chains. Appl. Environ. Microbiol. 74, 4491–4497.
Singh, R., Debarati, P., Rakesh, K.J., 2006. Biofilms, implications in bioremediation. Trends Microbiol. 14, 389–397.
Spoering, A.L., Gilmore, M.S., 2006. Quorum sensing and DNA release in bacterial biofilms. Curr. Opin. Microbiol. 9, 133–137.
Stepanovic, S., Vukovic, D., Dakic, I., Savic, B., Svabic-Vlahovic, M., 2000. A modified microtiter-plate method test for quantification of staphylococcal biofilm formation. J. Microbiol. Meth. 40, 175–179.
Stewart, P.S., 2003. Diffusion in biofilms. J. Bacteriol. 185, 1485–1491.
Stewart, P.S., Franklin, M.J., 2008. Physiological heterogeneity in biofilms. Nat. Rev. Microbiol. 6, 199–210.
Vestby, L.K., Moretro, T., Langsrud, S., Heir, E., Nesse, L.L., 2009. Biofilm forming abilities of *Salmonella* are correlated with persistence in fish meal- and feed factories. BMC Vet. Res. 5, 20.
Watnick, P., Kolter, R., 2000. Biofilm, city of microbes. J. Bacteriol. 182, 2675–2679.
Webb, J.S., Thompson, L.S., James, S., Charlton, T., Tolker-Nielsen, T., Koch, B., Givskov, M., Kjelleberg, S., 2003. Cell death in *Pseudomonas aeruginosa* biofilm development. J. Bacteriol. 185, 4585–4592.
Webb, J.S., Lau, M., Kjelleberg, S., 2004. Bacteriophage and phenotypic variation in *Pseudomonas aeruginosa* biofilm development. J. Bacteriol. 186, 8066–8073.
Wimpenny, J., Manz, W., Szewzyk, U., 2000. Heterogeneity in biofilms. FEMS Microbiol. Rev. 24, 661–671.
Xavier, J.B., White, D.C., Almeida, J.S., 2003. Automated biofilm morphology quantification from confocal laser scanning microscopy imaging. Water Sci. Technol. 47, 31–37.
Yarwood, J.M., Bartels, D.J., Volper, E.M., Greenberg, E.P., 2004. Quorum sensing in *Staphylococcus aureus* biofilms. J. Bacteriol. 186, 1838–1850.
Zhao, T., Doyle, M.P., Zhao, P., 2004. Control of *Listeria monocytogenes* in a biofilm by competitive-exclusion microorganisms. Appl. Environ. Microbiol. 70, 3996–4003.

C. Article 4 :

"The spatial architecture of *Bacillus subtilis* biofilm deciphered using a surface-associated model and *in situ* imaging"

Bridier A., D. Le Coq, F. Dubois-Brissonnet, V. Thomas, S. Aymerich and R. Briandet.

PLoS ONE, 2011, 6:e16177. doi:10.1371/journal.pone.0016177

OPEN ACCESS Freely available online

PLoS one

The Spatial Architecture of *Bacillus subtilis* Biofilms Deciphered Using a Surface-Associated Model and *In Situ* Imaging

Arnaud Bridier[1,2], Dominique Le Coq[1], Florence Dubois-Brissonnet[2], Vincent Thomas[3], Stéphane Aymerich[1], Romain Briandet[1]*

1 INRA, UMR 1319 MICALIS, Jouy-en-Josas, France, **2** AgroParisTech, UMR 1319 MICALIS, Jouy-en-Josas, France, **3** Steris, Fontenay aux Roses, France

Abstract

The formation of multicellular communities known as biofilms is the part of bacterial life cycle in which bacteria display cooperative behaviour and differentiated phenotypes leading to specific functions. *Bacillus subtilis* is a Gram-positive bacterium that has served for a decade as a model to study the molecular pathways that control biofilm formation. Most of the data on *B. subtilis* biofilms have come from studies on the formation of pellicles at the air-liquid interface, or on the complex macrocolonies that develop on semi-solid nutritive agar. Here, using confocal laser scanning microcopy, we show that *B. subtilis* strains of different origins are capable of forming biofilms on immersed surfaces with dramatically protruding "beanstalk-like" structures with certain strains. Indeed, these structures can reach a height of more than 300 μm with one undomesticated strain from a medical environment. Using 14 GFP-labeled mutants previously described as affecting pellicle or complex colony formation, we have identified four genes whose inactivation significantly impeded immersed biofilm development, and one mutation triggering hyperbiofilm formation. We also identified mutations causing the three-dimensional architecture of the biofilm to be altered. Taken together, our results reveal that *B. subtilis* is able to form specific biofilm features on immersed surfaces, and that the development of these multicellular surface-associated communities involves regulation pathways that are common to those governing the formation of pellicle and/or complex colonies, and also some specific mechanisms. Finally, we propose the submerged surface-associated biofilm as another relevant model for the study of *B. subtilis* multicellular communities.

Citation: Bridier A, Le Coq D, Dubois-Brissonnet F, Thomas V, Aymerich S, et al. (2011) The Spatial Architecture of *Bacillus subtilis* Biofilms Deciphered Using a Surface-Associated Model and *In Situ* Imaging. PLoS ONE 6(1): e16177. doi:10.1371/journal.pone.0016177

Editor: Adam Driks, Loyola University Medical Center, United States of America

Received July 30, 2010; **Accepted** December 14, 2010; **Published** January 18, 2011

Funding: This study received support from a public grant "MEDICEN-Region Paris, Ile-de-France" in the framework of the "Global deconta" program (http://www.medicen.org/). This national scientific program was coordinated by V. Thomas, employed by Steris SA. V. Thomas participated in the design of the study, but not in data collection and analysis, decision to publish, or preparation of the manuscript. The "Essonne Département" is also acknowledged for its financial support of the confocal microscopy facility (public grant ASTRE n°A02137). The "Essonnes Département" had no role in study design, data collection and analysis, decision to publish, or preparation of the manuscript.

Competing Interests: The authors have read the journal's policy and have the following conflicts. V. Thomas, co-author of the paper, is employed by a commercial company, Steris SA (STERIS SA, 18, route du Panorama 92265 Fontenay-aux-Roses FRANCE +33-146548557 (phone), +33-146549843 (fax)). However, this does not alter the authors' adherence to all the Plos ONE policies on sharing data and materials.

* E-mail: romain.briandet@jouy.inra.fr

Introduction

Bacteria can grow within multicellular, matrix-enclosed communities known as biofilms [1,2,3]. It is now largely accepted that biofilms constitute the predominant microbial lifestyle in natural and engineered ecosystems, enabling bacteria to develop coordinated architectural and survival strategies [4]. The involvement of biofilms in a large number of ecological and biotechnological processes [5], as well as in human infections [6,7,8], highlights the importance of gaining a clearer understanding of the formation, development and maintenance of these biological structures, so that their control can be improved.

Bacillus subtilis is a Gram-positive, motile, spore-forming bacterium which has served as a model for the molecular study of biofilm formation during the past ten years [9]. Complex mechanisms involved in biofilm formation and development have been elucidated using this bacterium. During biofilm development, motile single cells differentiate into aligned bundles of sessile attached cells [10,11]. This transition is accompanied by the production of an exopolymeric matrix resulting from the expression of two operons: (i) the 15-gene *epsA-O* operon which encodes the proteins required for polysaccharide synthesis and acts as an inhibitor of motility (EpsE) [12], and (ii) the *yqxM-sipW-tasA* operon which encodes a major protein component of the matrix (TasA) and its transport machinery [13,14]. Romero *et al.* [15] recently reported that TasA forms amyloid fibers that bind cells together and are essential in the formation of robust cohesive biofilms. Previous studies had shown that four pairs of global regulators: Spo0A/AbrB, SinI/SinR, SlrR/SlrA and DegS/DegU, play a key role in the formation and development of complex multicellular communities through the direct or indirect control of both of these operons and of motility-involved genes [14,16,17,18,19,20,21,22]. A phosphorylated form of the major early sporulation transcription factor Spo0A represses AbrB which negatively regulates biofilm formation [17,18]. The intermediate level of Spo0A-P also stimulates the transcription of SinI [23,24], which binds to and inactivates SinR, a major regulator of biofilm formation that directly represses the *epsO-A* and *yqxM-sipW-tasA*

operons [14,19]. In addition to SinI, two other proteins, YlbF and YmcA, have been identified as antagonizing SinR activity when conditions are favorable for biofilm formation [19]. Recent studies also reported that SinR activity is negatively controlled by SlrR, the transcription of which is in turn repressed by SinR as a downstream consequence of Spo0A phosphorylation. SinR is inhibited successively by SinI and SlrR, resulting in a de-repression of SinR direct targets (*slrR*, *eps*, and *yqxM*) and a repression of SlrR targets (*lytABC*, *lytF* – thus triggering chaining and also *hag* and possibly other σD-dependent motility genes) through formation of the SinR-SlrR complex [16,25,26,20]. The transcription factor DegU also coordinates the multicellular behavior of *B. subtilis* by regulating motility, poly-γ-glutamic acid and protease production and the expression of other swarming- and biofilm-involved genes *via* a gradient in its phosphorylation level [21,22,27,28,29].

Interestingly, the vast majority of these genetic pathways, and other data on *B. subtilis* biofilms, were identified by studying the development of pellicle at the air-liquid interface or of complex macrocolonies on agar, but only very few studies have focused on surface-associated immersed biofilm models [17,18,28,30]. Because some steps of biofilm formation (such as adhesion to the support) are specific to immersed surface-associated models, biofilm development under these conditions may involve regulation pathways than differ from those identified in pellicle and macrocolony models, leading to particular architectural features which govern specific functions.

In this context, we first of all characterized the structure of biofilms formed by different strains of *B. subtilis* on immersed surfaces using a microplate-based model combined with confocal laser scanning microscopy (CLSM). Then, using GFP-labeled strains, we studied the effects of mutations known to affect pellicle and complex colonies in our surface-associated biofilm model.

Materials and Methods

Strains and culture conditions

The *B. subtilis* strains used during this study are described in Table 1. The different strains were chosen in order to represent the diversity of *B.subtilis* strains and were thus selected from a variety of origins (collections and non-domesticated). The ATCC strains belonged to different subspecies: ATCC 6633 *B.subtilis* subsp spizizenii, ATCC 9372 *B.subtilis* subsp niger, ATCC 6051 *B.subtilis* subsp subtilis. Non-domesticated strains (ND_{food} and $ND_{medical}$) had recently been isolated from foods (dessert cream) and medical environments (endoscope washer-disinfector) and typed as *B. subtilis* using biochemical identification methods and 16S rDNA sequencing. The GFP-carrying reference strain, GM2812, was obtained by transforming strain BSB168 (a *trp*+ derivative of the reference strain 168 Marburg [31]) for spectinomycin resistance with the pDR146 plasmid (a kind gift from D. Rudner, Harvard Medical School). This placed in the *amyE* locus the *gfp (mut2)* gene controlled by the IPTG-regulated $P_{hyperspank}$ promoter. GM2812 derivatives mutated in various genes were then obtained by transformation with chromosomal DNA extracted from strains carrying the corresponding different alleles of interest marked with a suitable antibiotic resistance cassette. The extraction of chromosomal DNA, and the transformation of *B. subtilis*, were performed according to standard procedures, and the transformants were selected on LB plates supplemented with the relevant antibiotic at the following concentrations: spectinomycin, 100 μg ml^{-1}; chloramphenicol, 4 μg ml^{-1}; erythromycin, 0.5 μg ml^{-1}; neomycin and kanamycin, 8μg ml^{-1}. Before each experiment, the cells were subcultured in Tryptone Soya Broth (TSB, BioMérieux, France), supplemented with antibiotics when necessary.

The formation of surface-associated submerged biofilms

The formation of surface-associated biofilms was performed in microtiter plates, as previously described with slight modifications [32]. Briefly, 250 μl of an overnight culture in TSB adjusted to an OD_{600nm} of 0.02 were added to the wells of the polystyrene 96-well microtiter plate with a μclear® base (Greiner Bio-one, France) which enables high resolution fluorescence imaging. The microtiter plate was kept at 30°C for 1:30 to enable bacteria attachment to the bottom of the wells. After this adhesion step, the wells were rinsed with TSB to eliminate non-adherent bacteria and then refilled with 250 μl sterile TSB. The microtiter plate was then incubated for 48h at 30°C to allow biofilm development before structural analysis under the confocal laser scanning microscope (CLSM). Initial adhesion was also observed by transferring the microtiter plate under the CLSM directly after the 1:30 adhesion step. In the case of GFP-carrying strains, isopropyl β-D-thiogalactopyranoside (IPTG) was added to the medium at a final concentration of 200μM to induce GFP expression.

Macrocolony formation

To analyze colony architecture, 5 μl of an overnight culture in TSB were inoculated on 1.5% Tryptone Soya Agar (TSA, BioMérieux, France). When appropriate, the medium was supplemented with 200μM IPTG to allow GFP expression. The plates were then incubated at 30°C for 72h. Digital images of the colonies on the plates were taken using an Olympus C-5060 digital camera. The 3D architecture of macrocolonies of auto-fluorescent mutants was also observed by CLSM, as described in the section on *Confocal Laser Scanning Microscopy*.

Pellicle experiments

After an overnight culture in TSB at 30°C, 10 μl of the bacterial suspension were used to inoculate 2 ml of TSB in 24-well plates (TPP, Switzerland). Each plate was then incubated at 30°C, and pellicle formation was recorded at 48h. Digital images of the pellicles in the wells of the plates were taken using an Olympus C-5060 digital camera.

Swarming and swimming experiments

For swarming, 9 cm agar plates containing 20 ml TSB fortified with 0.8% agar were prepared and dried for 30 min with their lids open under a laminar flow hood. 10 μl of an overnight culture were then inoculated at the center of the swarming plates, dried for 15 min under the laminar flow hood and incubated at 30°C for 24h. For swimming, 9 cm agar plates containing 20 ml TSB fortified with 0.25% agar were prepared and dried for 30 min with their lids open under a laminar flow hood. 5 μl of an overnight culture were then inoculated at the center of the plate, dried for 15 min and incubated at 30°C for 24h. Digital images of the swarming and swimming plates were collected using an Olympus C-5060 digital camera. Each experiment was repeated three times.

Confocal Laser Scanning Microscopy

Adhered cells, 48h-immersed biofilms and macrocolonies were observed using a Leica SP2 AOBS inverted confocal laser scanning microscope (CLSM, LEICA Microsystems, France) at the MIMA2 microscopy platform (http://voxel.jouy.inra.fr/mima2). For observations of adhered cells and immersed biofilms, the medium in the wells of the microplate was gently replaced with fresh TSB medium after the adhesion step or biofilm development to eliminate any free floating bacteria. Strains not carrying GFP constructions were tagged fluorescently in green with Syto9 (1:1000 dilution in TSB from a Syto9 stock solution at 5mM in

Table 1. *Bacillus subtilis* strains used in this study.

Strain	Relevant genotype or description[a]	Origin or construction[b]
168	*trpC2*	Bacillus Genetic Stock Center
ATCC 6633		American Type Culture Collection
ATCC 9372		American Type Culture Collection
ATCC 6051		American Type Culture Collection
PG01		CTSCCV
$ND_{medical}$		Non-domesticated, isolated from endoscope washer-disinfectors [35]
ND_{food}		Non-domesticated, isolated from dairy product (ISHA)
BSB168	*trp+* derivative of 168	[31]
GM2812	*amyE*::P_{hyp}-*gfp (spec)*	pDR146 (D. Rudner)→BSB168
GM2815	*amyE*::P_{hyp}-*gfp (spec)*, *ΔdegQ*::*cat*	BG4138 [51]→GM2812
GM2817	*amyE*::P_{hyp}-*gfp (spec)*, *degU*::*neo*	GM719 [52]→GM2812
GM2821	*amyE*::P_{hyp}-*gfp (spec)*, *degU32-kan*	QB4371 [53]→GM2812
GM2828	*amyE*::P_{hyp}-*gfp (spec)*, *yvfV*::*pMUTIN2 (ery)*	BSFA1123→GM2812
GM2830	*amyE*::P_{hyp}-*gfp (spec)*, *yvfW*::*pMUTIN2 (ery)*	BSFA1124→GM2812
GM2832	*amyE*::P_{hyp}-*gfp (spec)*, *gtaC*::*pBS640 (cat)*	L16601gtaC [54]→GM2812
GM2812ylbF1	*amyE*::P_{hyp}-*gfp (spec)*, *ylbF*::*pMUTIN4 (ery)*	BSFA3233 [40]→GM2812
GM2812ymcA1	*amyE*::P_{hyp}-*gfp (spec)*, *ymcA*::*pMUTIN4 (ery)*	BSFA2603 [40]→GM2812
GM2850	*amyE*::P_{hyp}-*gfp (spec)*, *yxaB*::*pKN3 (ery)*	MM1701 [44]→GM2812
GM2851	*amyE*::P_{hyp}-*gfp (spec)*, *ΔabrB*::*cat*	MM1717 [44]→GM2812
GM2853	*amyE*::P_{hyp}-*gfp (spec)*, *ΔabrB*::*cat*, *yxaB*::*pKN3 (ery)*	MM1707 [44] àGM2812
GM2855	*amyE*::P_{hyp}-*gfp (spec)*, *sigX*::*pMUTIN2 (ery)*	BSFA94→GM2812
GM2857	*amyE*::P_{hyp}-*gfp (spec)*, *yqxM*::*pMUTIN3 (ery)*	BSFA4767 [40]→GM2812
GM2888	*amyE*::P_{hyp}-*gfp (spec)*, *Δhag*::*cat*	OMG954 [55]→GM2812

[a]*spec*, *cat*, *neo*, *kan* and *ery* stand for spectinomycin, chloramphenicol, neomycin, kanamycin and erythromycin resistance markers, respectively.
[b]CTSCCV, centre technique de la salaison, de la charcuterie et des conserves de viandes; ISHA, Institut Scientifique d'Hygiène et d'Analyse; BSFA strains were constructed during the "*Bacillus subtilis* functional analysis programme" [56].
doi:10.1371/journal.pone.0016177.t001

DMSO; Invitrogen, France), a nucleic acid marker. After 20 min of incubation in the dark at 30°C to enable fluorescent labeling of the bacteria, the plate was then mounted on the motorized stage of the confocal microscope. The microtiter plates were scanned using a 63×/1.2 N.A. water immersion objective lens. Fluorescent reporters excitation was performed at 488 nm with an argon laser, and the emitted fluorescence was recorded within the range 500–600 nm in order to collect Syto9 or GFP fluorescence (maximum emission of fluorescence at respectively 498 and 507 nm). To quantify the number of attached cells on the bottom of microplate wells, a total of nine images were acquired for each strain in three different wells. To generate images of the biofilms, a minimum of six Z- image series with a 1 µm step were acquired for each strain in three different wells. Furthermore, some images were acquired using a 10×/0.3 N.A. dry objective which enables a broader field of observations. Macrocolonies of GFP-carrying mutant strains were also observed using CLSM by transferring the colony from the agar plate to a glass slide which was then mounted upside-down on the stage of an inverted CLSM. The centers of macrocolonies were scanned using a 10×/0.3 N.A. dry objective and some Z-series images with a 1 µm step horizontal plane were also acquired.

Analysis of CLSM images

Easy 3D blend projections of immersed biofilms or the structure of macrocolonies were reconstructed from Z-series images using IMARIS v7.0 software (Bitplane, Switzerland). The biovolumes of immersed biofilms were calculated using PHLIP [33], a freely available Matlab-based image analysis toolbox (http://phlip.sourceforge.net/phlip-ml). The biovolume represented the overall volume of a biofilm (in μm^3) and could be used to estimate its total biomass. It was defined as the number of foreground pixels in an image stack multiplied by the voxel volume, which is the product of the squared pixel size and the scanning step size [34].

Statistical analysis

One-way ANOVA were performed using Statgraphics v6.0 software (Manugistics, Rockville, USA). Significance was defined as a P value associated with a Fisher test value lower than 0.05.

Results

Different B. subtilis strains all form submerged surface-associated biofilms with structural heterogeneity

To characterize the ability of *B. subtilis* to adhere and form multicellular communities on surfaces, the three-dimensional structure of 48h biofilms formed by seven strains of different origins on the bottom surface of wells in a microtiter plate compatible with high resolution fluorescence imaging was analyzed using CLSM. Preliminary experiments demonstrated that biofilms reached their maximum biovolume within 24h to 48h, depending on strains considered (data not shown). Representative biofilm structures observed for the seven strains are presented in Fig. 1. The images correspond to three-dimensional

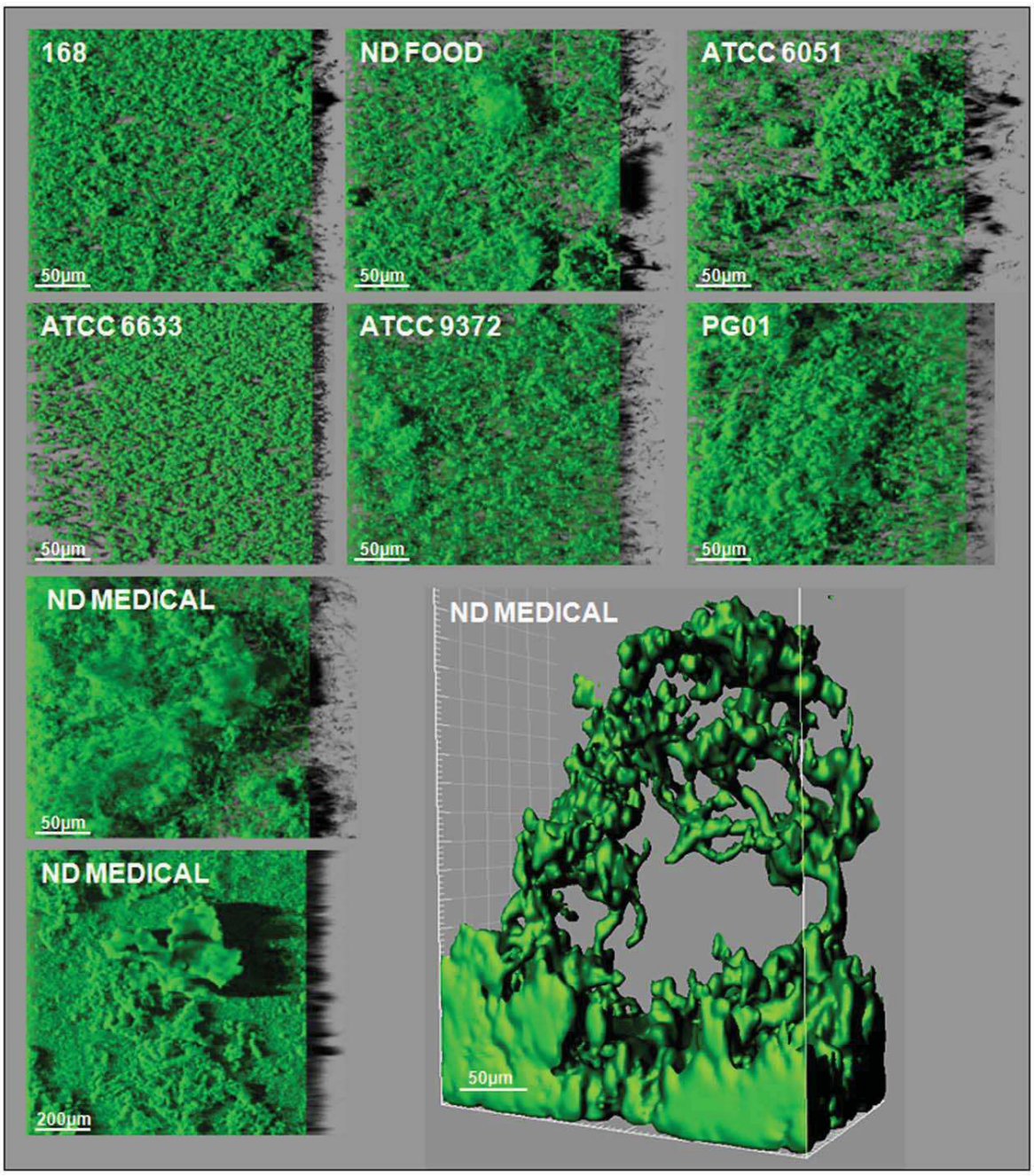

Figure 1. Three-dimensional biofilm structures obtained with the seven *B.subtilis* strains. These images present a representative, aerial, 3D view of the 48h-biofilm structures obtained with the seven *B. subtilis* strains using a microplate system, obtained from confocal image series using IMARIS software (including the shadow projection on the right). One iso-surface representation of a particular "beanstalk-like" structure is also shown for *B. subtilis* $ND_{medical}$.
doi:10.1371/journal.pone.0016177.g001

blend reconstructions obtained from confocal images series with the dedicated IMARIS software, including virtual shadow projections on the right-hand side to represent biofilm sections. The associated biovolumes calculated from the series of images are presented in Fig. 2A. The results first of all showed the ability of all *B. subtilis* strains to form biofilms on the bottom of the microtiter plate wells. They also revealed a marked structural heterogeneity in the biofilms produced that depended on the strain considered. The non-domesticated strains, ND_{food} and $ND_{medical}$, displayed the strongest biofilm-forming capacities under these growth conditions, and particularly the $ND_{medical}$ strain which demonstrated a biovolume that was statistically significantly higher than that of all the other strains ($P<0.05$) (Fig. 2A). The biofilms obtained with this strain displayed dramatic, protuberant "beanstalk-like" structures that could reach a height of more than 300 µm, as shown at the bottom of Fig. 1. These structures appeared to consist of intertwined bundles of cells rising from the mat of cells on the bottom of the well and then congregating.

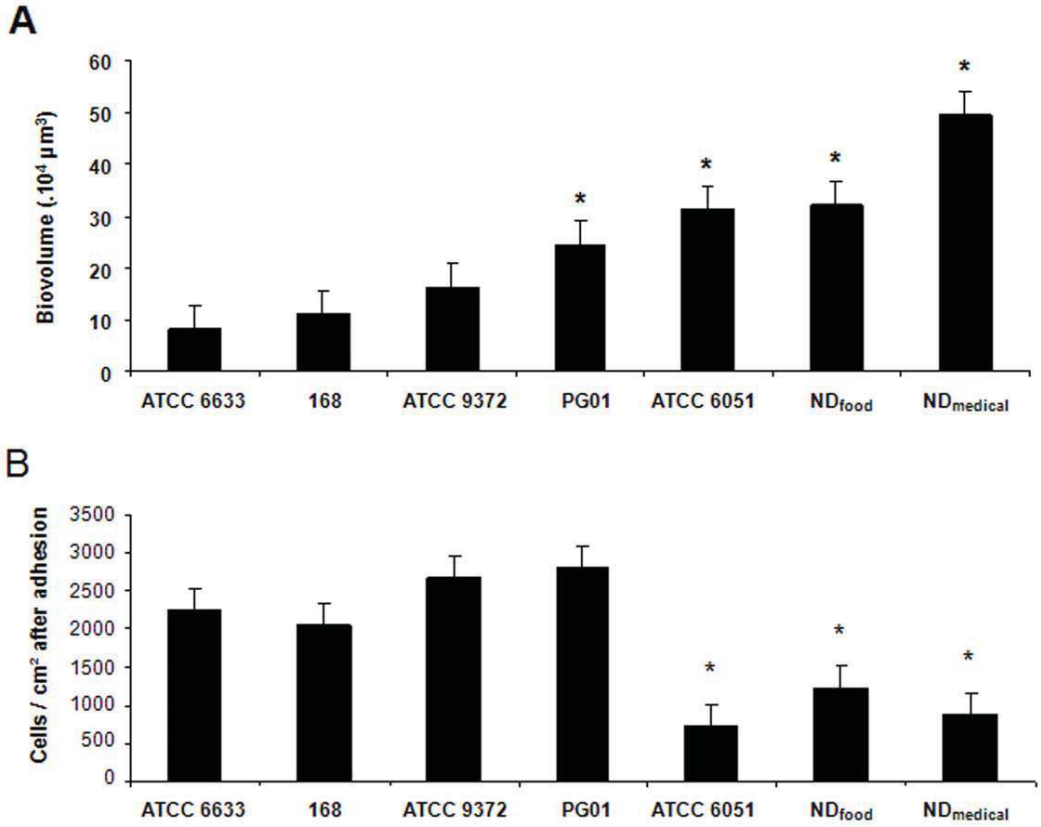

Figure 2. Biofilm biovolumes and the initial adhesion levels of the seven *B.subtilis* strains. (A) The biovolumes (μm^3) in ascending order of the 48h-biofilms obtained with the seven *B. subtilis* strains in microtiter plates from confocal image series using the PHLIP tool. (B) Number of cells adhering per cm^2 after 1h30 of adhesion in the microtiter plate. The error bars indicate the standard error and the statistically significant difference observed with strain 168 ($P<0.05$) is indicated by a star (*).
doi:10.1371/journal.pone.0016177.g002

While the other strains also produced clusters of various sizes, the structures they formed were much smaller than those displayed by $ND_{medical}$. Interestingly, the three strains producing the biofilms with the highest biovolumes (ATCC 6051, ND_{food} and $ND_{medical}$) showed a significantly smaller number of cells adhering to the bottom of the wells after 1h30 of adhesion when compared to the other strains (Fig. 2B).

The ability of the seven strains to form macrocolonies and pellicles, to swarm and to swim was also evaluated and the results are presented in Fig. 3. These showed that only undomesticated strains, ND_{food} and $ND_{medical}$, along with strain ATCC 6051, displayed a clear ability to swarm on agar, while the other four strains did not swarm at all. Interestingly, these three strains displayed the best swimming abilities and were the only strains to produce a pellicle at the air-liquid interface in the microtiter plate after 48h of incubation. The two undomesticated strains also formed markedly wrinkled colonies on the solid medium when compared to the other strains.

Immersed biofilms and other B. subtilis multicellular models are under similar but not identical genetic controls

Our initial results demonstrated the ability of *B. subtilis* to form immersed surface-associated communities with biovolumes and macro-structures that differed as a function of the strain considered. We then investigated whether mutations known to affect biofilm formation in macrocolony or pellicle models would also affect it in our immersed surface-associated model. Thus volume and structure of the biofilms formed by different GFP-labeled mutants derived from strain 168 (see Table 1) were analyzed using CLSM (Fig. 4 and 5). We first checked whether GFP expression affected the biofilm forming ability of strain 168 by comparing the biovolume and structure of the 48h-biofilms of both wild-type and GFP-labeled strains. No significant differences were found between the biovolume values (data not shown). Moreover, as shown in Fig. 1 and Fig. 5, GFP expression did not appear to affect the three-dimensional structure of the biofilm.

The biovolumes of 48h-biofilms of *B. subtilis* mutants normalized to a wild-type biovolume are presented in Fig. 4. The results showed that six of the 14 mutations tested significantly affected the biofilm biovolume in the microtiter plate. Null mutations in the *ymcA* or *ylbF*, and *degU* KO or *degU32* alleles provoked a significant reduction in the immersed biofilm biovolume ($P<0.05$). The corresponding mutants did not form immersed biofilms in TSB in microtiter plates, despite the presence of few adhered cells and small aggregates, thus showing that these regulators are required for the formation of surface-associated *B. subtilis* communities under these conditions. By contrast, we observed that an *abrB* KO mutation strongly enhanced biofilm formation in our model. It should be noted that the *abrB* and *yxaB/abrB* mutants displayed 3.3-fold and 1.9-fold increases in biofilm biovolume, respectively, when compared to the wild-type strain ($P<0.05$) (Fig. 4). Although the biofilm biovolumes of *hag*, *yqxM* and *yxaB* KO mutants did not

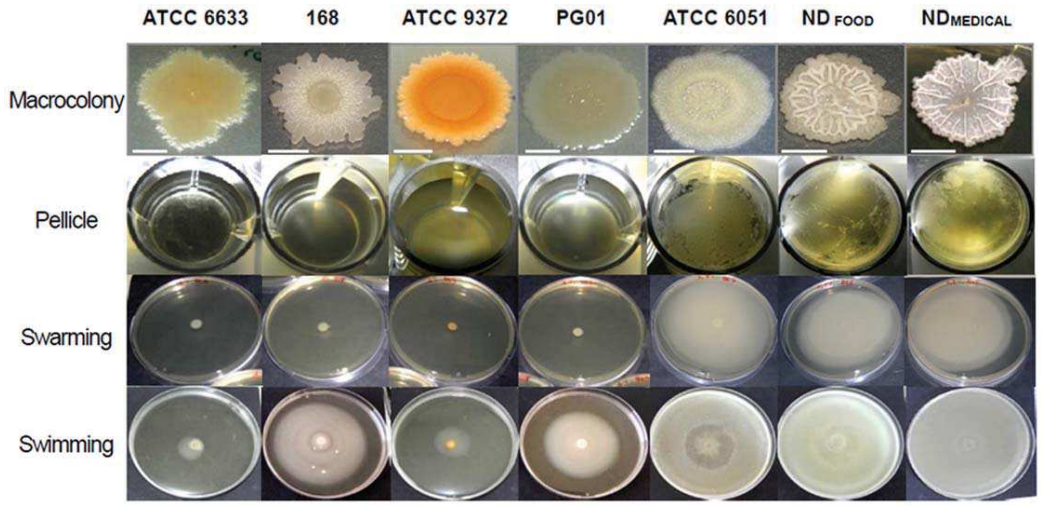

Figure 3. Macrocolony, pellicle, swarming and swimming phenotypes of the seven *B.subtilis* strains. Macrocolonies grown on TSA medium (1.5% agar) for 72h at 30°C after a central spot of 5 µl of an overnight bacterial culture in TSB. The scale bar is 5mm. Pellicles formed in 24-well microplates after 48h incubation at 30°C in TSB. Swarming plates (9 cm diameter) after 24h incubation at 30°C on TSA semi-solid medium (0.8% agar). Swimming plates (9 cm diameter) after 24h incubation at 30°C on TSA semi-solid medium (0.25% agar).
doi:10.1371/journal.pone.0016177.g003

differ significantly from those of the wild-type, these mutations led to three-dimensional structural alterations of the immersed biofilms, as shown in Fig. 5. Deletion of the *hag* gene that codes for flagellin, a major component of the flagellum, did not impede the formation of a surface-associated biofilm under our conditions, but led to a more heterogeneous structure with a larger number of cellular aggregates. We found that the *yqxM* and *yxaB* mutants formed relatively independent clusters and did not cover the entire substratum available, unlike the wild-type strain. Moreover, in terms of initial adhesion, we found that only the *yqxM* mutation provoked a significant decrease in the number of adhered cells (31% reduction, $P<0.05$) compared to the wild-type (data not shown).

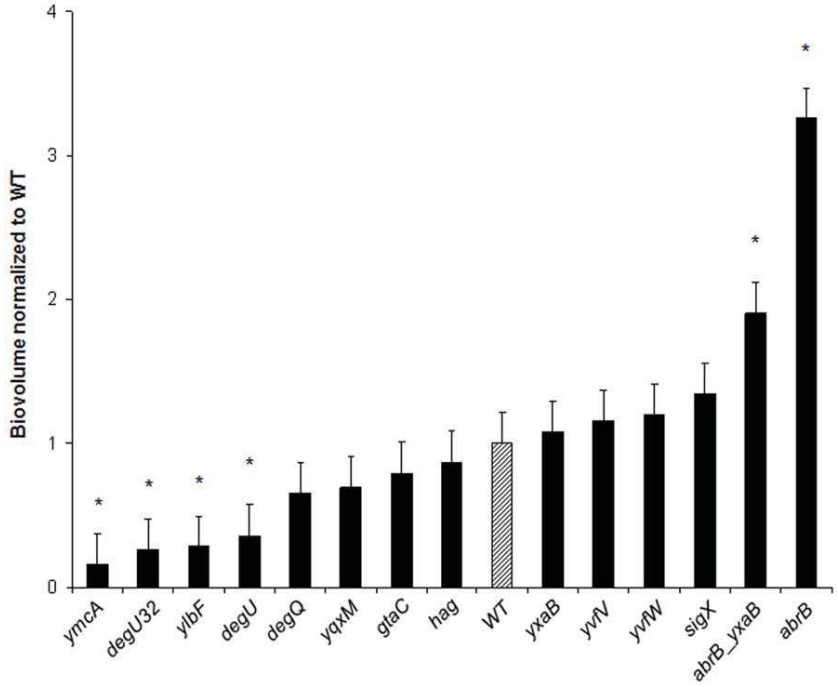

Figure 4. Biofilm biovolumes of the 14 *B.subtilis* mutant strains. Effects of mutations on the biofilm biovolumes of the 48h-biofilms obtained with the 14 mutants and wild-type strain (GM2812) (GFP-carrying strains). Biovolumes were normalized to wild-type (GM2812) and classified in ascending order. The error bars indicate the standard error and the statistically significant difference in biovolume obtained with the wild-type ($P<0.05$) is indicated by a star (*).
doi:10.1371/journal.pone.0016177.g004

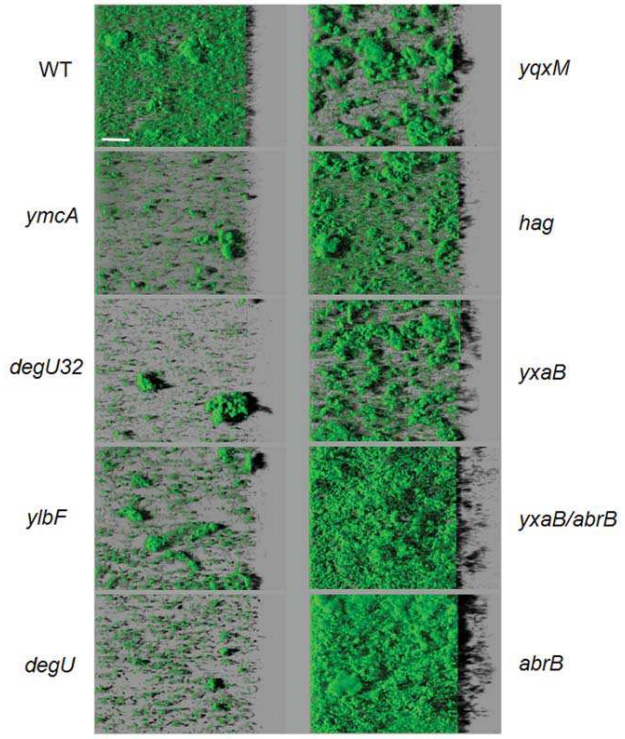

Figure 5. Effect of mutations on the three-dimensional structure of biofilms. Effects of mutations on immersed biofilm structures of the biofilms obtained with different GFP-carrying mutant strains and the corresponding reference wild-type (WT) strain from the confocal image series using the IMARIS software. Images depict an aerial view of 48h-biofilms in the microplate system. The scale bar is 50μm.
doi:10.1371/journal.pone.0016177.g005

By comparison with the wild-type strain, both *ymcA* and *ylbF* mutants produced similar flat and mucoid colonies on agar, as shown for the *ymcA* mutant in Fig. 6. *degU* KO, and to a lesser extent *degU32*, induced the formation of wrinkles in the center of the colony and altered the swimming ability of the strains (Fig. 6 and data not shown). We found that both single *abrB* and double *yxaB/abrB* (not shown) mutants produced macrocolonies with a rough morphology and small wrinkles in the center, as well as altering swimming ability when compared to the wild-type strain, as shown in Fig. 6 for the *abrB* mutant. Interestingly, the *hag* mutation, which completely inhibited motility, also provoked the formation of wrinkles in the center of colonies, as observed for the *degU* mutants. While we did not find a marked impact of the *yxaB* mutation on macrocolony morphology when compared to the wild-type strain (data not shown), the *yqxM* mutation led to a flat and featureless colony with no horizontal outgrowths on the agar (Fig. 6).

Discussion

Although the genetic pathways and mechanisms governing the formation of *B. subtilis* biofilms in air-liquid interface pellicle or colony models have been the subject of intensive study, little is known about biofilm development on solid surfaces. Indeed, since Hamon and Lazazzera [17] demonstrated the ability of *B subtilis* to form structures on abiotic surfaces, only a few studies have focused on immersed surface-associated models in order to study *B. subtilis* biofilm development [17,18,28,30].

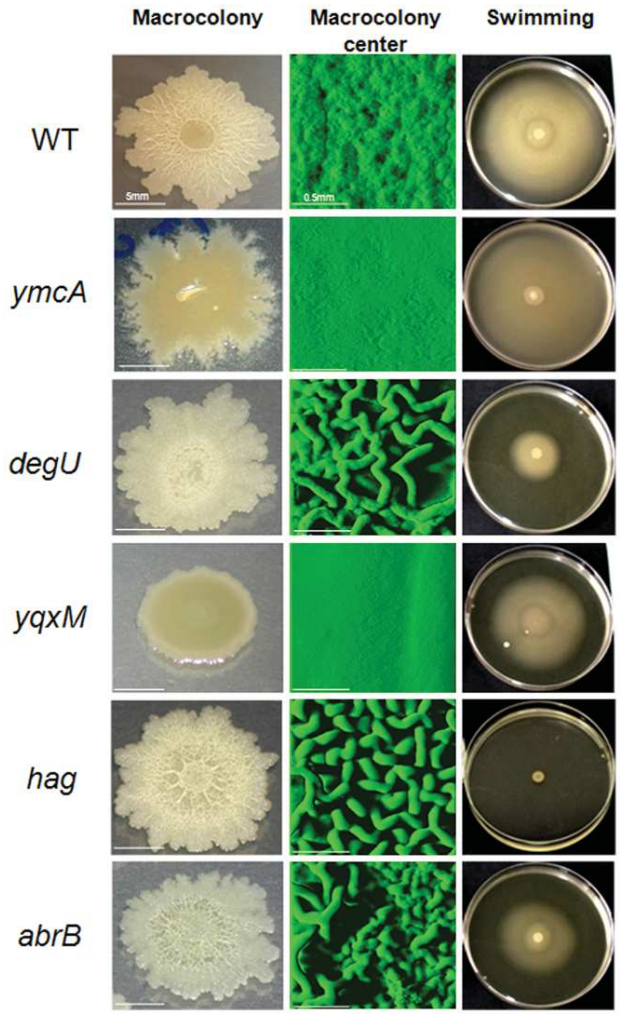

Figure 6. Effects of *ymcA*, *ylbF*, *degU*, *yqxM*, *hag* and *abrB* mutations on macrocolony and swimming phenotypes. Macrocolonies grown on TSA medium (1.5% agar) for 72h at 30°C. The left-hand column depicts macrocolony morphologies. The scale bar is 5mm. The middle column depicts aerial views of the centers of macrocolonies from confocal image series using IMARIS software. The scale bar is 0.5mm. The right-hand column shows the swimming plate (9 cm diameter, TSB+0.25% agar) after 24h of incubation at 30°C.
doi:10.1371/journal.pone.0016177.g006

For this reason, we first studied the submerged biofilm architecture of seven *B. subtilis* strains of various origins using a microplate model. We found that not only were all the strains considered able to form a biofilm on the polystyrene bottom of microplate wells, but also that some of these strains developed "beanstalk-like" rising structures with an exceptional surface to volume ratio. This was particularly striking for the non-domesticated strain $ND_{medical}$ that developed remarkable structures reaching more than 300μm in height. Indeed, we had previously showed that under similar growth conditions, *Pseudomonas aeruginosa* or *Staphylococcus aureus* strains, despite being known as excellent biofilm producers, did not form a biofilm more than 60 μm thick [32]. The $ND_{medical}$ strain was isolated from endoscope washer-disinfectors because of its high resistance to oxidizing biocide treatment [35]. The authors suggested that compared to sensitive strains, this resistance is due to the high level of matrix production, as visualized by scanning electronic

microscopy. It is therefore possible that the development of tall structures in our microtiter plate model using this strain was also related in part to a greater production of exopolymeric matrix. Interestingly, the three strains producing immersed biofilms with the highest biovolumes (ATCC 6051, ND_{food} and $ND_{medical}$) were the only strains which displayed an ability to swarm and form an air-liquid pellicle after 48h of incubation. These observations were consistent with the existence of core mechanisms determinant for the development of multicellular communities, whatever the experimental model used. In addition, we found that these three strains exhibited the best swimming abilities. Previous studies on other species such as *Bacillus cereus*, *Escherichia coli*, *Listeria monocytogenes* or *Pseudomonas aeruginosa* [36,37,38,39] had shown that motility could contribute to biofilm development through the recruitment of cells from the planktonic phase or through architectural structuring of the biological edifice. After 1h30 of adhesion, we found that the ATCC 6051, ND_{food} and $ND_{medical}$ strains displayed a significantly smaller number of cells adhering to the bottom of the plate when compared with other strains displaying weaker swimming abilities. One explanation could be that, under our static conditions, bacteria could reach the bottom of the well by sedimentation so that the most motile cells were not necessarily advantaged in adhesion, as previously shown by Houry *et al.* [37] with *B. cereus*. These authors showed that the deletion of flagellum led to an increase in the bacteria bound to a glass surface in a flow-cell, and suggested that bacteria devoid of flagellum could have access to the substratum by sedimentation and then adhere better because the flagellum did not hinder contacts between the bacterial cell wall and the glass surface. Moreover, high motility could prevent the cells from staying for a sufficient time close to the substrate to initiate irreversible adhesion.

The experimental findings of our study suggested that development of the dramatic protruding structures appeared to be intimately related to the growth conditions applied here. Indeed, the $ND_{medical}$ biofilms that formed in flow-cells under dynamic conditions were flat, compact and did not display "beanstalk-like" rising structures (data not shown), probably because of the shear forces induced by the flow. Moreover, other static systems such as immersed coupons did not seem to cause the development of such structures (data not shown). One hypothesis is that under our conditions, the small volume of TSB in the microtiter plate ensured a higher surface to volume ratio, and thus sufficient oxygenation of the medium for growth of the *B. subtilis* immersed biofilm. We also observed that repeated drastic rinsing, such as that performed during the widely employed crystal violet biofilm assay, led to a dislocation of these rising structures (data not shown). These complementary observations showed that our microtiter plate system and experimental conditions i.e. soft rinsing, might be appropriate to study the surface-associated community architecture of *B. subtilis* by providing beneficial conditions for the formation and preservation of immersed biofilms. This model could therefore be appropriate for the study of *B. subtilis* biofilms alongside pellicle and colony models, because it reflects other environmental conditions that may be encountered in natural, industrial or medical settings. Furthermore, this type of model associated with CLSM provides an opportunity to decipher the dynamic structure and reactivity of multicellular communities in a non-invasive manner, enabling a clearer understanding of structure/function relationships.

In order to better understand the mechanisms governing biofilm formation on immersed surfaces, different mutations known to affect biofilm formation in pellicle and macrocolony models were then introduced into a 168 derivative strain harboring a GFP-expression cassette. On the one hand, we found that *ymcA*, *ylbF* and *degU* KO and *degU32* alleles impeded biofilm formation in microtiter plate, indicating that these genes are required for *B. subtilis* biofilm formation and development on immersed surfaces. YmcA and YlbF are reported as regulators that are required for the formation of a macrocolony with complex surface features, or the formation of a pellicle at the air-liquid interface, because of their action on SinR activity that causes the derepression of matrix biosynthesis operons [19,40]. It is therefore not surprising to observe that these regulators also affect the immersed surface-associated biofilm model because of their involvement in the central pathway for biofilm formation. The DegU transcription factor also coordinates the multicellular behavior of *B. subtilis* through the regulation of motility, poly-γ-glutamic acid [41] and protease production *via* a gradient in its phosphorylation level [22,27,28,29]. The *degU32* mutation leads to a stabilization of the phosphorylated form of DegU [42]. In this context, a high level of DegU-P promotes the production of alkaline protease, levansucrase and other degradative exoenzymes, and inhibits motility and the production of flagella [43]. Thus the overproduction of proteases and other enzymes in the *degU32* mutant could impede matrix formation and structuring that is required for biofilm development, as shown by our observations in the microtiter plates. Conversely, previous studies had shown that an absence of the phosphorylated form of DegU led to non-activation of the genes required for mature colony or pellicle development [11,22,29]. Therefore, the gradual activation of DegU throughout its phosphorylation appears to be essential to the regulation of genes involved in the formation of immersed multicellular communities, as has been shown in other biofilm models.

On the other hand, we found that an *abrB* deletion enhanced biofilm biovolume when compared to the wild-type strain. This observation was consistent with the fact that AbrB was described as acting as a repressor of biofilm formation in previous studies [17,18]. he suppression of AbrB could therefore provoke the over-expression of biofilm genes and lead to the increase in biofilm biovolume observed here. However, these authors found that a single *abrB* mutant produced a biofilm identical to that of the wild-type, even though they used a surface-associated immersed biofilm model. This difference could be explained by the different biofilm growth conditions and experimental protocols used during both studies. Indeed, Kobayashi [11] previously reported that an *abrB* mutant formed an air-liquid pellicle with an excessive architecture by comparison with the wild-type strain but only under certain medium conditions, thus underlining the dependence of the phenotype on the growth conditions used. We observed that the double *yxaB/abrB* mutant also displayed a higher biovolume than the wild-type, although this was smaller than that seen with the *abrB* single mutant ($P<0.05$). The *yxaB* single mutant produced a biofilm with a biovolume similar to that of the wild-type but with an altered three-dimensional structure. These results are consistent with the fact that *yxaB* is negatively regulated by AbrB and with the exopolysaccharide synthase function it may encode [44]. Indeed, the specific structure of the *yxaB* mutant biofilm may have been due to decreased exopolysaccharide synthesis.

Although the *yqxM* mutant formed a flat macrocolony without complex architecture, we did not find any quantitative difference between the immersed biofilm formed by this mutant and that of the wild-type, as previously observed by Hamon *et al.* [18]. Nevertheless, the *yqxM* mutant formed independent clusters and did not produce a mat of cells that entirely covered the surface, as observed for the wild-type. Furthermore, *yqxM* was the only mutant displaying a significantly smaller number of adhered cells after 1h30 of contact with the surface when compared to the wild-type strain. YqxM is the product of the first gene of the *yqxM-sipW-*

tasA operon and appears to be involved in the proper localization of TasA to the matrix and its anchoring to the cell wall [13,45,46]. Romero *et al.* [15] recently reported that TasA forms amyloid fibers that are involved in the formation of a robust pellicle. Previous studies had shown that amyloid fibers (e.g. curli) can contribute to the attachment of bacteria to a surface or host cells and then participate in the three-dimensional structure of biofilms [47,48,49]. It is therefore possible that the specific structure of the *yqxM* mutant surface-associated biofilm may result from a weaker adhesion of the cells to the bottom of the well because of abnormal or absent TasA presentation to the cell envelope.

Interestingly, while flagella are required for the normal progression of pellicle formation [11], the flagellum deletion in the *hag* mutant did not lead to a reduction in initial cell adhesion and did not impact the biovolume of the immersed biofilm when compared to the wild-type strain. Nevertheless, the loss of flagella led to the formation of a more heterogeneous biofilm on the surface, with more clusters than the wild-type, suggesting that it plays a role in the architecture of communities. These results highlight the role of flagellum in the architectural development of submerged biofilms but not in initial adhesion to the substrate. The morphology of the center of the macrocolony suggested that motility also plays a role in macrocolony architecture. Indeed, while the wild-type strain produced a macrocolony with flat center, we observed that *hag* and *degU* null mutants, and with less pronounced phenotypes, *degU32*, single *abrB* and double *yxaB/abrB* mutants, produced a 72h-macrocolony with wrinkles in the center. Kobayashi [11] showed that a *degU* null mutant had few flagella and an *abrB* mutant containing a smaller number of flagella than that observed for the wild-type. Similarly, Amati *et al.* [43] showed that expression of the *hag* gene was also markedly reduced in a *degU32* mutant. Furthermore, our results confirmed that all these mutations caused changes to swimming abilities when compared to the wild-type strain. Interestingly, Watnick *et al.* [50] made similar observations for *Vibrio cholerae*, showing that flagellar mutants displayed rugose colonies. The authors presented evidence to suggest that the absence of flagellum results in increased EPS production in colonies, leading to the rough morphologies observed. Kobayashi [11] also suggested that flagellum proteins may play a regulatory role rather than a direct role (such as on adhesion or cell-cell interaction) in pellicle formation by *B. subtilis*.

To conclude, the surface-associated submerged model proposed here produced a diversity of *B. subtilis* biofilm architectures and the existence of remarkable protruding '"beanstalk-like" structures with some strains. As in pellicle or macrocolony models, YmcA, YlbF, DegU and AbrB regulators play a key role in the development of these immersed structures, probably because of their implication in central biofilm regulation pathways such as matrix biosynthesis. Conversely, we found that some mutations known to affect macrocolony organization or pellicle development did not markedly impede biofilm formation on a surface. The possible coexistence of an immersed biofilm on the bottom of a plate and a pellicle at the air-liquid interface in the same well raises the question of the spatial and temporal relationships between the two communities, a point that will be investigated in future studies.

Acknowledgments

We would like to thank Drs. David Rudner (Harvard Medical School, USA) for plasmid pDR146, Etienne Dervyn (INRA, Jouy-en-Josas, France) for BSFA strains and chromosomal DNA, Carlos São José (University of Lisbon, Portugal) for strain L16601gtaC, Michal Obuchowski (Medical University of Gdansk, Poland) for strains MM1701, MM1707 and MM1717, Tarek Msadek (Institut Pasteur, Paris, France) for strain QB4371, Simone Séror (Université Paris-Sud, Orsay, France) for strain OMG954, Pascal Garry (CTSCCV, Maison-alfort, France) for strain PG01, Abdelkader Boubetra (ISHA, Massy, France) for strain ND_{food} and Jean-Yves Maillard (University of Cardiff, UK) for strain $ND_{medical}$ and Victoria Hawken for English revision.

Author Contributions

Conceived and designed the experiments: AB RB SA DL VT FD-B. Performed the experiments: AB RB DL. Analyzed the data: AB RB. Contributed reagents/materials/analysis tools: AB RB DL. Wrote the manuscript: AB RB DL SA.

References

1. Costerton JW (1995) Overview of microbial biofilms. J Ind Microbiol 15: 137–140.
2. Kolter R, Greenberg EP (2006) The superficial life of microbes. Nature 441: 300–302.
3. Watnick P, Kolter R (2000) Biofilm, city of microbes. J Bacteriol 182: 2675–2679.
4. Costerton JW (2007) The biofilm primer. Springer series on biofilms. pp 5–6.
5. Singh R, Debarati P, Rakesh KJ (2006) Biofilms, implications in bioremediation. Trends Microbiol 14: 389–397.
6. Costerton JW, Stewart PS, Greenberg EP (1999) Bacterial biofilms, a common cause of persistent infections. Science 284: 1318–1322.
7. Hall-stoodley L, Stoodley P (2009) Evolving concepts in biofilm infections. Cell Microbiol 11: 1034–1043.
8. Potera C (1999) Forging a link between biofilms and disease. Science 283: 1837–1839.
9. Lemon KP, Earl AM, Vlamakis HC, Aguilar C, Kolter R (2008) Biofilm development with an emphasis on *Bacillus subtilis*. Curr Top Microbiol Immunol 322: 1–16.
10. Branda SS, Gonzalez-Pastor JE, Ben-Yehuda S, Losick R, Kolter R (2001) Fruiting body formation by *Bacillus subtilis*. Proc Natl Acad Sci USA 98: 11621–11626.
11. Kobayashi K (2007) *Bacillus subtilis* pellicle formation proceeds through genetically defined morphological changes. J Bacteriol 189: 4920–4931.
12. Blair KM, Turner L, Winkelman JT, Berg HC, Kearns DB (2008) A molecular clutch disables flagella in the *Bacillus subtilis* biofilm. Science 320: 1636–1638.
13. Branda SS, Chu F, Kearns DB, Losick R, Kolter R (2006) A major protein component of the *Bacillus subtilis* biofilm matrix. Mol Microbiol 59: 1229–1238.
14. Chu F, Kearns DB, Branda SS, Kolter R, Losick R (2006) Targets of the master regulator of biofilm formation in *Bacillus subtilis*. Mol Microbiol 59: 1216–1228.
15. Romero D, Aguilar C, Losick R, Kolter R (2010) Amyloid fibers provide structural integrity to *Bacillus subtilis* biofilms. Proc Natl Acad Sci USA 107: 2230–2234.
16. Chai Y, Kolter R, Losick R (2009) Paralogous antirepressors acting on the master regulator for biofilm formation in *Bacillus subtilis*. Mol Microbiol 74: 876–887.
17. Hamon MA, Lazazzera BA (2001) The sporulation transcription factor Spo0A is required for biofilm development in *Bacillus subtilis*. Mol Microbiol 42: 1199–1209.
18. Hamon MA, Stanley NR, Britton RA, Grossman AD, Lazazzera BA (2004) Identification of AbrB-regulated genes involved in biofilm formation by *Bacillus subtilis*. Mol Microbiol 52: 847–860.
19. Kearns DB, Chu F, Branda SS, Kolter R, Losick R (2005) A master regulator for biofilm formation by *Bacillus subtilis*. Mol Microbiol 55: 739–749.
20. Kobayashi K (2008) SlrR/SlrA controls the initiation of biofilm formation in *Bacillus subtilis*. Mol Microbiol 69: 1399–1410.
21. Murray EJ, Kiley TB, Stanley-Wall NR (2009) A pivotal role for the response regulator DegU in controlling multicellular behaviour. Microbiology 155: 1–8.
22. Verhamme DT, Murray EJ, Stanley-Wall NR (2009) DegU and Spo0A jointly control transcription of two loci required for complex colony development by *Bacillus subtilis*. J Bacteriol 191: 100–108.
23. Chai Y, Chu F, Kolter R, Losick R (2008) Bistability and biofilm formation in *Bacillus subtilis*. Mol Microbiol 67: 254–263.
24. Fujita M, Gonzalez-Pastor JE, Losick R (2005) High- and low-threshold genes in the Spo0A regulon of *Bacillus subtilis*. J Bacteriol 187: 1357–1368.
25. Chai Y, Norman T, Kolter R, Losick R (2010) An epigenetic switch governing daughter cell separation in *Bacillus subtilis*. Genes Dev 24: 754–765.
26. Chu F, Kearns DB, McLoon A, Chai Y, Kolter R, et al. (2008) A novel regulatory protein governing biofilm biofilm formation in *Bacillus subtilis*. Mol Microbiol 68: 1117–1127.

27. Kobayashi K (2007) Gradual activation of the global response regulator DegU controls serial expression of genes for flagellum formation and biofilm formation in *Bacillus subtilis*. Mol Microbiol 66: 395–409.
28. Stanley NR, Lazazzera BA (2005) Defining the genetic differences between wild and domestic strains of *Bacillus subtilis* that affect poly-gamma-DL-glutamic acid production and biofilm formation. Mol Microbiol 57: 1143–1158.
29. Verhamme DT, Kiley TB, Stanley-Wall NR (2007) DegU co-ordinates multicellular behaviour exhibited by *Bacillus subtilis*. Mol Microbiol 65: 554–568.
30. Stanley NR, Britton RA, Grossman AD, Lazazzera BA (2003) Identification of catabolite repression as a physiological regulator of biofilm formation by *Bacillus subtilis* by use of DNA microarrays. J Bacteriol 185: 1951–1957.
31. Jules M, Le Chat L, Aymerich S, Le Coq D (2009) The *Bacillus subtilis* ywjI (glpX) gene encodes a Class II Fructose-1, 6-Bisphosphatase, functionally equivalent to the Class III Fbp enzyme. J Bacteriol 191: 3168–3171.
32. Bridier A, Dubois-Brissonnet F, Boubetra A, Thomas V, Briandet R (2010) The biofilm architecture of sixty opportunistics pathogens deciphered using a high throughput CLSM method. J Microbiol Methods 82: 64–70.
33. Xavier JB, White DC, Almeida JS (2003) Automated biofilm morphology quantification from confocal laser scanning microscopy imaging. Wat Sci Tech 47: 31–37.
34. Kuehn M, Hausner M, Bungartz HJ, Wagner M, Wilderer PA, et al. (1998) Automated confocal laser scanning microscopy and semiautomated image processing for analysis of biofilms. Appl Environ Microbiol 64: 4115–4127.
35. Martin DJH, Denyer SP, McDonnell G, Maillard JY (2008) Resistance and cross-resistance to oxidising agents of bacterial isolates from endoscope washer disinfectors. J Hosp Infect 69: 377–383.
36. Barken KB, Pamp SJ, Yang L, Gjermansen M, Bertrand JJ, et al. (2008) Roles of type IV pili, flagellum-mediated motility and extracellular DNA in the formation of mature multicellular structures in *Pseudomonas aeruginosa* biofilms. Environ Microbiol 10: 2331–2343.
37. Houry A, Briandet R, Aymerich S, Gohar M (2010) Motility and flagellum involvement in *Bacillus cereus* biofilm formation. Microbiol 156: 1009–1018.
38. Lemon KP, Higgins DE, Kolter R (2007) Flagellar is critical for *Listeria monocytogenes* biofilm formation. J Bacteriol 189: 4418–4424.
39. Wood TK, Gonzalez Barrios AF, Herzberg M, Lee J (2006) Motility influences biofilms architecture in *Escherichia coli*. Appl Microbiol Biotechnol 72: 361–367.
40. Branda SS, Gonzalez-Pastor JE, Dervyn E, Ehrlich D, Losick R, et al. (2004) Genes involved in formation of structured multicellular communities by *Bacillus subtilis*. J Bacteriol 186: 3970–3979.
41. Ohsawa T, Tsukahara K, Ogura M (2009) *Bacillus subtilis* response regulator DegU is a direct activator of pgsB transcription involved in gamma-poly-glutamic acid synthesis. Biosci Biotechnol Biochem 73: 2096–2102.
42. Dahl MK, Msadek T, Kunst F, Rapaport G (1992) The phosphorylation state of the DegU response regulator acts as a molecular switch allowing either degradative enzyme synthesis or expression of genetic competence in *Bacillus subtilis*. J Biol Chem 267: 14509–14514.
43. Amati G, Bisicchia P, Galizzi A (2004) DegU-P represses expression of the motility fla-che operon in *Bacillus subtilis*. J Bacteriol 186: 6003–6014.
44. Nagorska K, Hinc K, Strauch MA, Obuchowski M (2008) Influence of the σ^B stress factor and yxaB, the gene for a putative exopolysaccharide synthase under σ^B control, on biofilm formation. J Bacteriol 190: 3546–3556.
45. Kolodkin-Gal I, Romero D, Cao S, Clardy J, Kolter R, et al. (2010) D-amino acids trigger biofilm disassembly. Science 328: 627–629.
46. Stöver AG, Driks A (1999) Control of synthesis and secretion of the *Bacillus subtilis* protein YqxM. J Bacteriol 181: 7065–7069.
47. Jonas K, Tomenius H, Kader A, Normak S, Römling U, et al. (2007) Roles of curli, cellulose and BapA in Salmonella biofilm morphology studied by atomic force microscopy. BMC Microbiol 7: 70.
48. Prigent-Combaret C, Prensier G, Le Thi TT, Vidal O, Lejeune P, et al. (2000) Developmental pathway for biofilm formation in curli-producing *Escherichia coli* strains: role of flagella, curli and colanic acid. Environ Microbiol 2: 450–464.
49. Ryu JH, Beuchat LR (2005) Biofilm formation by *Escherichia coli* 0157:H7 on stainless steel: Effect of exopolysaccharide and Curli production on its resistance to chlorine. Appl Environ Microbiol 71: 247–254.
50. Watnick PI, Lauriano CM, Klose KE, Croal L, Kolter R (2001) The absence of a flagellum leads to altered colony morphology, biofilm development and virulence in *Vibrio Cholerae* 0139. Mol Microbiol 39: 223–235.
51. Yang M, Shimotsu H, Ferrari E, Henner DJ (1987) Characterization and mapping of the *Bacillus subtilis* prtR gene. J Bacteriol 169: 434–437.
52. Crutz AM, Steinmetz M (1992) Transcription of the *Bacillus subtilis* sacX and sacY genes, encoding regulators of sucrose metabolism, is both inducible by sucrose and controlled by the DegS-DegU signalling system. J Bacteriol 174: 6087–6095.
53. Kiel JAKW, Ten Berge AM, Borger P, Venema G (1995) A general method for the consecutive integration of single copies of a heterologous gene at multiple locations in the *Bacillus subtilis* chromosome by replacement recombination. Appl Env Microbiol 61: 4244–4250.
54. Baptista C, Santos MA, São-José C (2008) Phage SPP1 reversible adsorption to *Bacillus subtilis* cell wall teichoic acids accelerates virus recognition of membrane receptor YueB. J Bacteriol 190: 4989–4996.
55. Hamze K, Julkowska D, Autret S, Hinc K, Nagorska K, et al. (2009) Identification of genes required for different stages of dendritic swarming in *Bacillus subtilis*, with a novel role for phrC. Microbiol 155: 398–412.
56. Kobayashi K, Ehrlich SD, Albertini A, Amati G, Andersen KK, et al. (2003) Essential *Bacillus subtilis* genes. Proc Natl Acad Sci USA 100: 4678–4683.

D. Résultats complémentaires :

L'initiation des biofilms immergés de *B. subtilis* se fait selon une dynamique biphasique

Afin de mieux comprendre l'implantation des biofilms de *B. subtilis* dans notre modèle immergé, des acquisitions 4D (xyzt) en microscopie confocale laser ont été réalisées. Pour cela, deux souches parmi les sept étudiées dans l'article précédent (**Article 4**) ont été sélectionnées du fait de leur phénotype architectural de biofilm différent : la souche de collection 168 et la souche de terrain $ND_{medical}$. Nous avons pu observer, après quelques heures de développement, que l'on assistait à un retour coordonné très brusque des cellules à la vie planctonique puis dans un deuxième temps à une reprise du développement du biofilm immergé illustrant un développement « biphasique » original.

Matériels et méthodes

Souches bactériennes et conditions de culture

Pour permettre le suivi de croissance du biofilm en microscopie confocale de manière non-invasive, la souche $ND_{medical}$ a été rendue autofluorescente. Il s'est avéré que cette souche « non domestiquée » était en fait transformable par les protocoles classiquement utilisés. De ce fait, comme décrit dans l'**article 4** pour la souche 168, la souche a été transformée avec le plasmide pDR146 portant une cassette de résistance à la spectinomycine et dans lequel est inséré au niveau du locus *amyE,* le gène *gfp* (*mut2*) sous contrôle du promoteur $P_{hyperspank}$ inductible à l'IPTG. Avant chaque expérience, les souches sont pré-cultivées en Tryptone Soya Broth (TSB, Biomérieux, France) supplémenté par 100 µg/ml de spectinomycine et 200 µM d'IPTG pour induire l'expression de la GFP.

Dynamique structurale des biofilms

Les dynamiques de formation de biofilm pour les deux souches GFP de *B. subtilis* (168 et $ND_{medical}$) ont été observées par microscopie confocale. Expérimentalement, une culture de 18h à 30 °C est ajustée à une DO_{600nm} de 0.02 puis 250 µl de cette suspension sont inoculés dans un puits de la microplaque. Le milieu est supplémenté par 200 µM d'IPTG pour induire

l'expression de la GFP. Après 1h30 d'adhésion, le puits est rincé et 250 µl de TSB contenant 200 µM IPTG sont ajoutés. La microplaque est ensuite transférée sur la platine du microscope confocal et l'acquisition est lancée après réglage du microscope. Le logiciel du microscope est paramétré pour prendre une série d'image xyz (avec un pas en z de 1 µm) toutes les 15 minutes pendant 15h. Les biofilms sont scannés en utilisant un objectif ×63 à immersion à huile et la fluorescence de la GFP est collectée de 500 à 600 nm après excitation à 488 nm (laser Argon).

Des images (xy) ont également été réalisées pour les deux souches (non GFP) après marquage fluorescent au FM4-64 (Invitrogen), un marqueur lipophile de membrane et avec la lectine FL-1171 (Vector Laboratories) qui reconnaît les oligomères de N-acetylglucosamine (préférentiellement les trimères et tétramères) avec des longueurs d'ondes d'excitation/émission de 633/640-740nm pour le FM4-64 et de 488/500-600nm pour la lectine.

Traitements des séries d'images confocales

La structure tridimensionnelle des biofilms est recomposée pour chaque temps d'acquisition en traitant les séries d'images xyz acquises par CLSM avec le logiciel IMARIS (Bitplane).

Résultats

Le développement des biofilms formés par les souches 168 et $ND_{medical}$ a été suivi en temps réel par CLSM. La figure 2 présente pour chaque souche une série représentative d'images illustrant la structure du biofilm à différents temps et les films correspondants sont disponibles sur le CD associé au manuscrit (dossier *Chapitre I/ Résultats complémentaires*). Chaque image correspond à une reconstruction tridimensionnelle du biofilm en vue aérienne après traitement par le logiciel IMARIS et incluant une projection virtuelle de l'ombre sur la droite qui matérialise la section. Une attention particulière doit être porté au fait que cette section représente les cellules adhérées mais également les cellules en suspension du fait que l'on se trouve dans un système statique. Les vidéos fournies sur le CD joint au manuscrit permettent d'avoir une meilleure visualisation des deux populations.

Souche 168

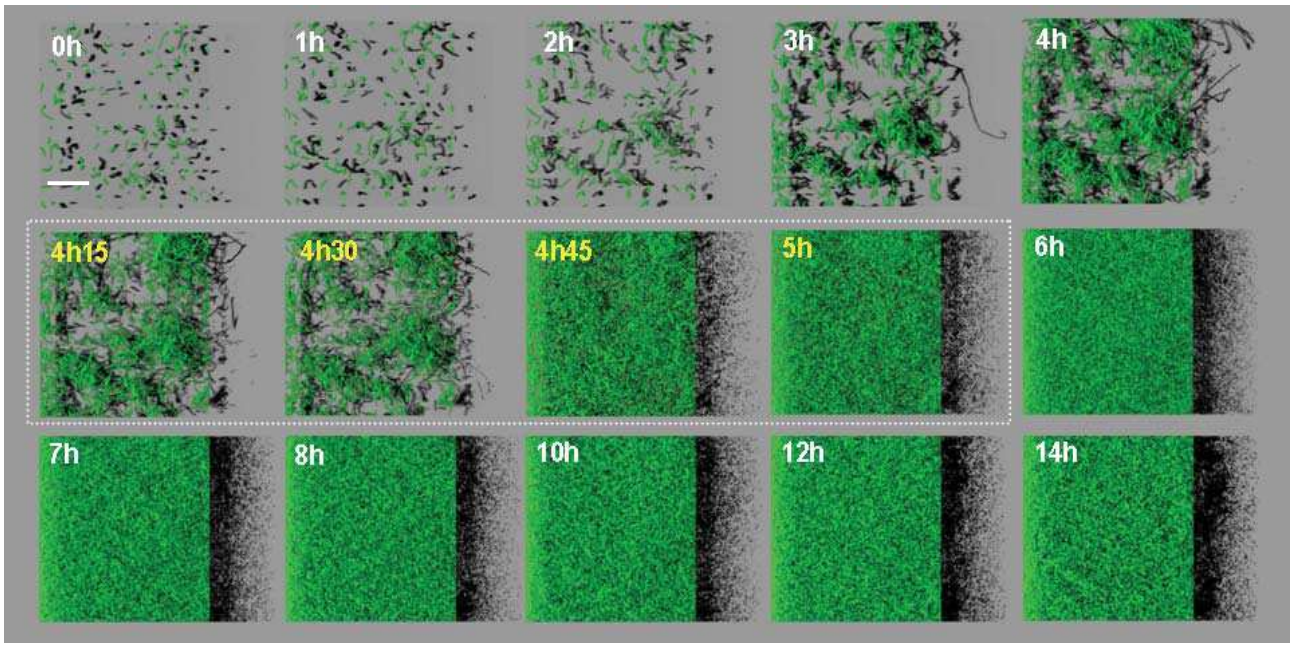

Souche $ND_{medical}$

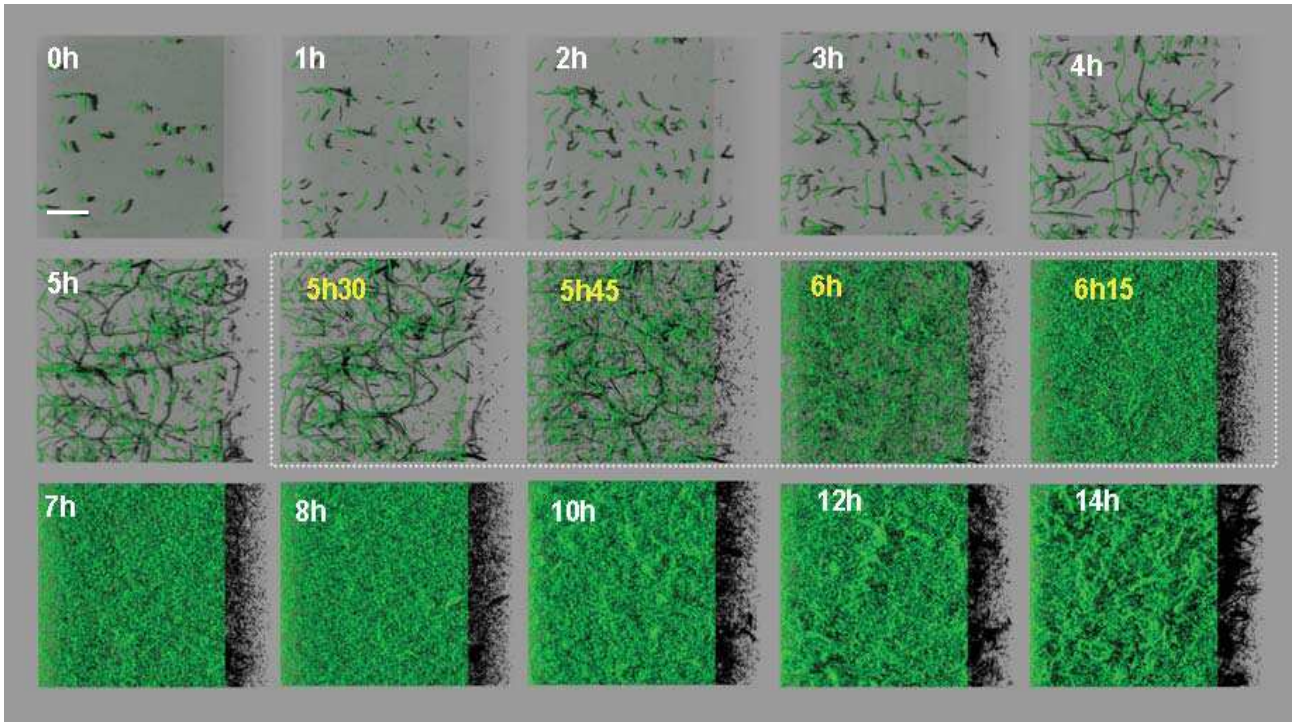

Figure 2. Dynamique structurelle des biofilms des souches de *B. subtilis* 168 et $ND_{medical}$. La barre d'échelle correspond à 50 µm.

Les observations ont montré un schéma de développement en deux étapes pour les deux souches. Durant les premières heures de développement, les cellules s'allongent pour former de longs filaments pouvant atteindre plusieurs dizaines de micromètres. Des observations faites 4h après adhésion et en utilisant des marqueurs membranaires et de polysaccharides ont démontré que ces filaments étaient en réalité des chaînettes de cellules compartimentées et connectées à certains endroits par des amas polysaccharidiques (Figure 3). Après un court développement du biofilm associé à la surface (4 à 5h selon la souche considérée dans les expériences présentées ici et dans une fenêtre de 3 à 6h pour l'ensemble des dynamiques réalisées), une grande quantité de cellules planctoniques apparaissent brusquement dans le champ d'observation et semblent provenir du découpage des chaînettes et de la remobilisation des cellules. Cette transition s'opère très brutalement, en 15 à 30 minutes pour les deux souches (séquences d'images encadrées dans la figure 2, vidéos sur le CD associé), suggérant une réponse rapide et coordonnée des bactéries à leur environnement. Quelques heures après ce phénomène, des structures fixées réapparaissent clairement pour la souche $ND_{medical}$ illustrant la reprise du développement du biofilm immergé et pouvant résulter de la multiplication des quelques cellules restées adhérées à la surface et/ou du recrutement de cellules planctoniques. Pour la souche 168, les cellules en suspension ne permettent pas de voir clairement la reprise du développement du biofilm associé à a surface.

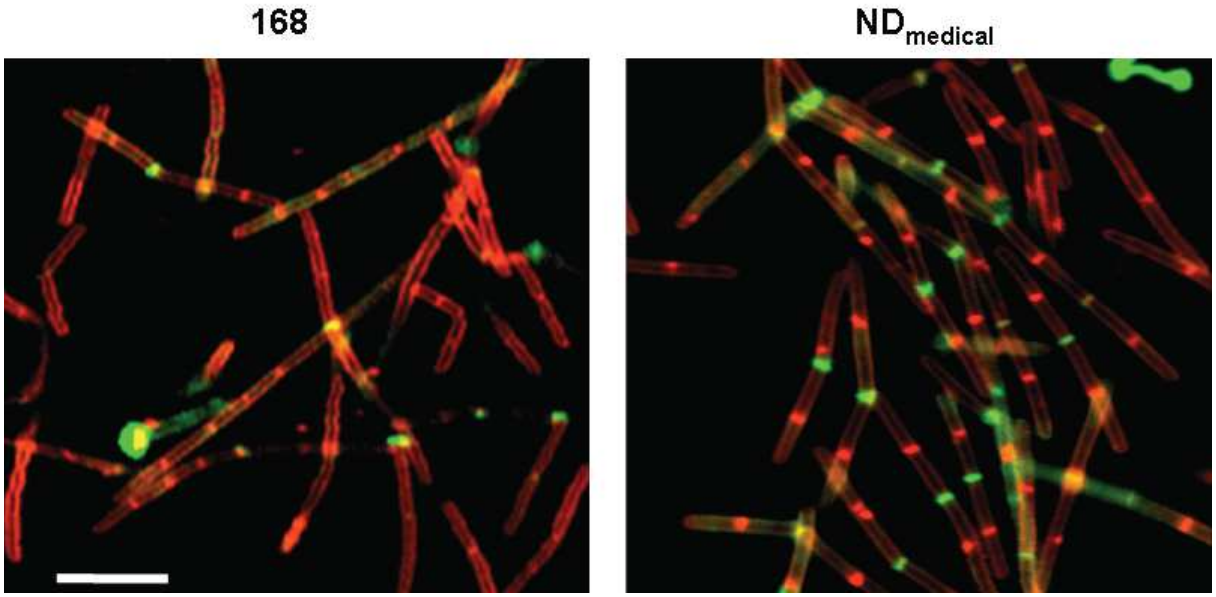

Figure 3. Morphologies des cellules en biofilm 4h après adhésion. Les membranes apparaissent en rouge (FM4-64) et les polysaccharides en vert (lectine FL-1171).

CHAPITRE II.

RELATIONS STRUCTURE/FONCTION DANS LA RESISTANCE DES BIOFILMS A LA DESINFECTION

A. Introduction

Le deuxième chapitre de ce travail repose sur l'étude de la résistance des biofilms bactériens à la désinfection. Son objectif principal est une meilleure compréhension des mécanismes susceptibles de limiter l'efficacité des désinfectants dans ces structures notamment par des approches innovantes d'imagerie 4D (xyzt) non-invasive.

De nombreuses études rapportent la grande résistance des cellules en biofilms aux traitements de désinfection en comparaison de leurs homologues planctoniques (Campanac *et al.*, 2002, Smith & Hunter, 2008, Nett et al., 2008). Comme décrit dans la synthèse bibliographique, les mécanismes explicatifs avancés tels que les problèmes de diffusion/réaction des molécules dans la structure ou les modifications de l'état physiologique des cellules se trouvant dans des microenvironnements particuliers sont directement ou indirectement liées à l'organisation tridimensionnelle de l'édifice. Les biofilms étant des structures complexes, la résistance des cellules dans ces structures est donc souvent très hétérogène. Cette hétérogénéité souligne l'importance de s'intéresser à la réactivité locale des désinfectants au sein de ces structures afin de mieux comprendre les mécanismes de résistance impliqués.

Actuellement, la plupart des méthodes pour mesurer l'action d'antimicrobiens dans les biofilms sont destructives et ne prennent pas en compte l'hétérogénéité spatiale de la résistance présente au sein de ces structures. Par les techniques classiques de dénombrement, l'ensemble de l'échantillon est sacrifié à chaque mesure pour quantifier le nombre de bactéries tuées par le traitement et les informations structurales sont perdues. De plus, ces techniques ne sont pas compatibles avec le suivi dans le temps d'un échantillon donné durant le traitement et ne permettent donc pas d'obtenir des informations sur la dynamique réelle de l'inactivation des cellules dans la structure. Dans ce contexte, afin d'aller plus loin dans la compréhension des mécanismes de résistance des biofilms aux traitements désinfectants, nous nous sommes intéressés à une méthode d'investigation non-invasive en temps réel reposant sur la microscopie confocale laser à balayage. Cette technique est basée sur le suivi de la perte de fluorescence des bactéries au sein du biofilm due à la fuite d'un fluorophore hors des cellules après la perméabilisation de la membrane bactérienne par l'agent antimicrobien (Figure 4). Elle a été récemment utilisée par l'équipe de P. S. Stewart du centre de Bio-ingénierie des biofilms du Montana pour étudier les dynamiques d'action de molécules antimicrobiennes dans des biofilms formés par des souches à Gram positif (Takenaka *et al.*,

2008, Davison *et al.*, 2010). Nous avons étendu ici la technique à des souches à Gram négatif en adaptant notamment le marquage fluorescent. Après avoir optimisé les conditions d'acquisition pour notre modèle microplaque développé précédemment, cette technique a été appliquée au suivi spatiotemporel de l'action de désinfectants au sein de biofilms bactériens dans le but de mieux comprendre les limitations rencontrées par ces molécules dans ces structures biologiques.

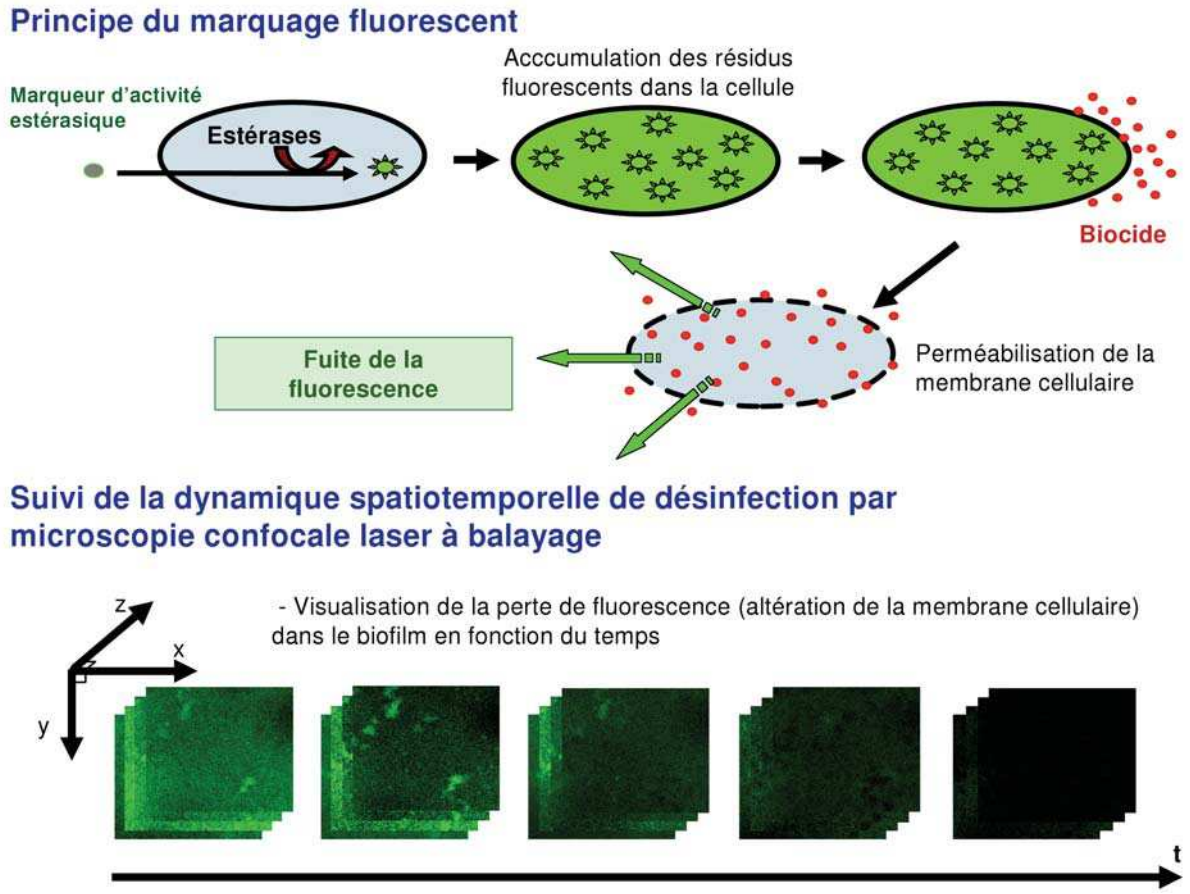

Figure 4. Principe expérimental du marquage fluorescent et de la technique confocale de visualisation en temps réel de l'action de biocides au sein des biofilms.

Dans un premier temps, nous nous sommes intéressés à l'espèce *P. aeruginosa*. Dans la première partie de l'étude, nous avons pu observer que certaines des souches testées pouvaient former des biofilms importants avec des structures tridimensionnelles spécifiques dans notre système en microplaque. De plus, cette espèce est bien connue pour être à l'origine d'un grand nombre d'infections (Hassett *et al.*, 2009, Hassett *et al.*, 2010) et constitue un modèle pour l'étude des biofilms. L'objectif du premier article de ce chapitre (**article 5 :**

"Dynamics of the action of biocides in Pseudomonas aeruginosa biofilms.") était donc de mieux comprendre les mécanismes impliqués dans la résistance des biofilms de *P. aeruginosa* à deux désinfectants couramment utilisés dans les domaines médicaux et industriels et aux modes d'action différents : l'acide péracétique, un agent oxydant, et le chlorure de benzalkonium, un ammonium quaternaire. Nous nous sommes d'abord focalisé sur les biofilms de la souche ATCC 15442 qui formait des structures en champignons importantes dans notre système microplaque (souche 31 dans l'**article 3**) et qui est également une des souches de référence utilisées dans les normes de d'évaluation de l'activité bactéricide des désinfectants (Anonyme, 1997). Les résultats ont montré une plus grande résistance des biofilms aux deux désinfectants en comparaison des cellules planctoniques notamment pour le chlorure de benzalkonium. La perte de résistance aux deux biocides observée après la remise en suspension et le lavage des cellules suggère que la résistance des biofilms ne semble pas liée à une adaptation physiologique ou génétique des cellules mais plus à la limitation de l'activité du désinfectant du fait de la structure tridimensionnelle du biofilm et de la présence d'une matrice extracellulaire. L'utilisation de la technique de visualisation en temps réel par microscopie confocale a montré que si l'acide péracétique entrainait une perte de fluorescence homogène dans les biofilms formés par la souche ATCC 15442, le chlorure de benzalkonium provoquait quant à lui une perte de fluorescence hétérogène et progressive dans la structure illustrant un problème de pénétration du désinfectant dans le biofilm (les vidéos S1 et S2 correspondantes sont disponibles sur le CD associé au manuscrit dans le dossier *Chapitre II/ Article 5_Dynamics of the action of biocides in Pseudomonas aeruginosa biofilms*). L'extension des observations pour le chlorure de benzalkonium aux biofilms formés par trois souches cliniques fournies par l'hopîtal universitaire de Lausanne (Laus 3, Laus 16 et Laus 21) a confirmé l'existence de phénomènes similaires suggérant que la pénétration limitée du chlorure de benzalkonium pourrait être un des mécanismes majeurs expliquant la résistance des biofilms de *P. aeruginosa* à ce désinfectant (vidéos S3, S4 et S5 sur le CD). L'ajustement de modèles de destruction aux courbes de fluorescence obtenues pour les biofilms des quatre souches a permis d'extraire des paramètres cinétiques d'inactivation (shoulder et k_{max}) et de rapprocher ces données avec celles obtenues lors des tests biochimiques de la composition de la matrice extracellulaire (teneurs en sucres et en protéines). Ces résultats ont montré une corrélation entre la nature de la matrice et les paramètres d'inactivation (Fig. 5) soulignant ainsi l'importance des interactions entre les constituants de la matrice extracellulaire et le chlorure de benzalkonium dans les phénomènes de limitation de pénétration observés.

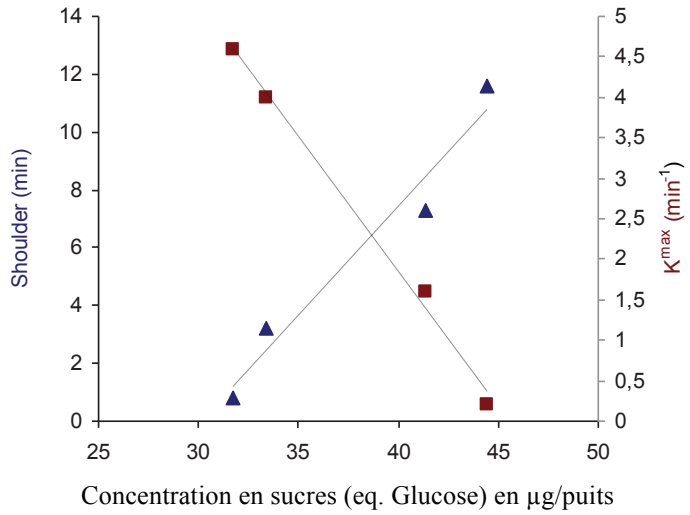

Figure 5. Corrélation entre la concentration en sucres de la matrice extracellulaire des 4 souches de *P. aeruginosa* (ATCC 15442, Laus 3, Laus 16 et Laus 21) et les paramètres cinétiques d'inactivation *Shoulder* (▲) et k_{max} (■) extraits des courbes de décroissance d'intensité de fluorescence au centre des agrégats cellulaires.

La deuxième partie de ce chapitre s'est focalisée sur le cas de la souche de *B. subtilis* $ND_{medical}$. Cette souche a été isolée d'un laveur-désinfecteur d'endoscopes dans lequel elle a été soumise régulièrement à des concentrations élevées d'agents désinfectants (Martin *et al.*, 2008). Lors de la première partie de l'étude, elle a démontré une grande aptitude à former des biofilms immergés dans notre système (**article 4**). De plus, les cellules en suspension ont par ailleurs montré une résistance importante aux traitements oxydants qui pourrait être liée à une production de matrice importante (**article 7** en annexe, (Martin et al., 2008). Ces propriétés semblent témoigner de l'adaptation de cette souche à son environnement et en fait donc un modèle d'étude concret d'intérêt. La résistance du biofilm formé par cette souche à l'acide péracétique, un désinfectant couramment utilisé dans les traitements de décontamination des endoscopes, a donc été évaluée. Les résultats ont montré une résistance marquée du biofilm à la concentration et au temps d'utilisation du désinfectant dans le milieu médical confirmant la capacité de persistance de la souche malgré les traitements de décontamination. D'après les observations réalisées en microscopie confocale en temps réel (vidéo disponible sur le CD dans le dossier *Chapitre II/ Article 6_Are resident Bacillus subtilis biofilms of concern in hospital acquired infections*) et en microscopie électronique à balayage, cette grande résistance du biofilm pourait en effet être liée au moins en partie à une production importante de substances extracellulaires. Les tests de désinfection sur cellules du biofilm re-suspendues donnant des résultats similaires aux homologues planctoniques semblent confirmer cette hypothèse. Nous avons ensuite constaté que dans un biofilm mixte avec *S. aureus*, un

pathogène souvent incriminé dans des infections nosocomiales, les structures formées par la souche $ND_{medical}$ pouvaient protéger le pathogène vis-à-vis du traitement à l'acide péracétique, ce qui souligne l'importance des interactions multi-espèces dans la résistance des flores pathogènes à la désinfection. L'ensemble de ces résultats sont présentés dans l'**article 6** en cours de préparation « *Are resident Bacillus subtilis biofims of concern in hospital aquired infections ?»*.

B. Article 5 :

"Dynamics of the action of biocides in *Pseudomonas aeruginosa* biofilms."

Bridier A., F. Dubois-Brissonnet, G. Greub, V. Thomas and R. Briandet.

Antimicrobial Agents and Chemotherapy, 2011, 55 : 2648-2654

ANTIMICROBIAL AGENTS AND CHEMOTHERAPY, June 2011, p. 2648–2654 Vol. 55, No. 6
0066-4804/11/$12.00 doi:10.1128/AAC.01760-10

Dynamics of the Action of Biocides in *Pseudomonas aeruginosa* Biofilms▽†

A. Bridier,[1,2] F. Dubois-Brissonnet,[2] G. Greub,[3] V. Thomas,[4] and R. Briandet[1]*

INRA, UMR 1319 MICALIS, F-78350 Jouy-en-Josas, France[1]; AgroParisTech, UMR 1319 MICALIS, F-91300 Massy, France[2]; Institute of Microbiology, University Hospital of Lausanne, 1011 Lausanne, Switzerland[3]; and STERIS S.A., Fontenay-aux-Roses, France[4]

Received 16 December 2010/Returned for modification 11 January 2011/Accepted 9 March 2011

The biocidal activity of peracetic acid (PAA) and benzalkonium chloride (BAC) on *Pseudomonas aeruginosa* biofilms was investigated by using a recently developed confocal laser scanning microscopy (CLSM) method that enables the direct and real-time visualization of cell inactivation within the structure. This technique is based on monitoring the loss of fluorescence that corresponds to the leakage of a fluorophore out of cells due to membrane permeabilization by the biocides. Although this approach has previously been used with success with various Gram-positive species, it is not directly applicable to the visualization of Gram-negative strains such as *P. aeruginosa*, particularly because of limitations regarding fluorescence staining. After adapting the staining procedure to *P. aeruginosa*, the action of PAA and BAC on the biofilm formed by strain ATCC 15442 was investigated. The results revealed specific inactivation patterns as a function of the mode of action of the biocides. While PAA treatment triggered a uniform loss of fluorescence in the structure, the action of BAC was first localized at the periphery of cell clusters and then gradually spread throughout the biofilm. Visualization of the action of BAC in biofilms formed by three clinical isolates then confirmed the presence of a delay in penetration, showing that diffusion-reaction limitations could provide a major explanation for the resistance of *P. aeruginosa* biofilms to this biocide. Biochemical analysis suggested a key role for extracellular matrix characteristics in these processes.

The control of microbial surface contamination is a major concern in terms of public health. *Pseudomonas aeruginosa* is a Gram-negative bacterium that is well known to be involved in a large number of human infections (14, 30). Numerous outbreaks have been linked directly to its presence on medical equipment (11, 15, 16, 25). The persistence of this bacterium in the environment can be attributed to its ability to form biofilms that increase its resistance to disinfection treatments. Numerous studies have indeed reported the high resistance of *P. aeruginosa* biofilms (compared to their planktonic counterparts) to numerous biocides, including chlorine, quaternary ammonium compounds, and aldehydes (5, 10, 13, 26). Although the precise mechanisms underlying this resistance remain unclear, it appears to be a multifactorial process that is primarily related to the physiological and structural characteristics of the biofilm. It is now generally accepted that biofilms constitute heterogeneous structures that group subpopulations with distinct physiological states and resistance phenotypes (28).

Data on biocide reactivity within these heterogeneous structures could provide a clearer understanding of the mechanisms involved in biofilm resistance and ultimately facilitate the development of new and more efficient treatments. Recently, a noninvasive technique based on confocal laser scanning microscopy (CLSM) was developed and used to investigate spatial and temporal patterns of antimicrobial action in biofilms formed by Gram-positive strains (8, 29). This method enables the direct visualization of the patterns of loss of fluorescence in biofilms due to the leakage of unbound fluorophores (fluorescent calcein) out of cells after the bacterial membrane has been altered by antimicrobial agents. However, this method is not directly applicable to the study of *P. aeruginosa* because of limitations with respect to fluorescent staining. The principal limitation encountered with the fluorogenic esterase substrate is linked to active dye extrusion out of the cells by efflux pumps, resulting in weak fluorescent labeling (18). During the present study, we adapted the staining procedure to the time-lapse CLSM study of biofilms formed by the Gram-negative strain *P. aeruginosa*. The spatiotemporal action of peracetic acid and benzalkonium chloride was then visualized in the biofilms formed by the reference strain used for the testing of disinfectants (ATCC 15442). The observations were also extended to three *P. aeruginosa* clinical isolates for benzalkonium chloride, with characterization of the exopolymeric matrix and correlation to the kinetic profiles of inactivation obtained for the four strains, in order to shed light on the obstacles encountered by biocides in biofilms.

MATERIALS AND METHODS

Bacterial strains and growth conditions. The results presented here were obtained using *Pseudomonas aeruginosa* ATCC 15442, the reference strain used for the testing disinfectants under the NF EN 1040 (1), and three *P. aeruginosa* clinical isolates provided by the Institute of Microbiology at Lausanne University Hospital (named Laus 3, Laus 16, and Laus 21). Bacterial stock cultures were kept at −20°C in tryptone soy broth (TSB; bioMérieux, France) containing 20% (vol/vol) glycerol. Prior to each experiment, frozen cells were subcultured twice in TSB at 30°C. The final overnight culture was used as an inoculum for the growth of biofilms.

* Corresponding author. Mailing address: UMR1319 MICALIS, 25 Ave. de la République, 91300 Massy, France. Phone: 33 (0) 1 69 53 64 77. Fax: 33 (0) 1 69 93 51 44. E-mail: romain.briandet@jouy.inra.fr.

† Supplemental material for this article may be found at http://aac.asm.org/.

▽ Published ahead of print on 21 March 2011.

Antibacterial agents. An oxidizing agent and a quaternary ammonium compound were chosen, and both are widely used in medical environments: peracetic acid (PAA; molecular weight [MW], 76.05; 32% [by weight] in dilute acetic acid [Sigma-Aldrich, France]) and benzalkonium chloride C14 (BAC; MW, 368.04; puriss., anhydrous, ≥99.0% [Fluka, France]). The disinfectants were diluted in sterile deionized water to the desired concentrations on the day of the experiment.

Determination of concentrations for biofilm and planktonic cell eradication. The biocide concentrations required to eradicate a biofilm of *P. aeruginosa* ATCC 15442 were evaluated by using an minimal biofilm eradication concentration (MBEC) assay (6) for PAA and BAC. This system consists in a standard, 96-well microtiter plate which has a lid with 96 pegs on which the biofilm can grow. Experimentally, the overnight culture was adjusted to an optical density at 600 nm (OD_{600}) of 0.01 (~10^6 CFU/ml) in TSB, and 150 μl of this culture was transferred into the wells of the microtiter plate before the lid with pegs was replaced (this level of inoculation would enable ~10^8 CFU/peg after biofilm development). The system was then incubated at 30°C for 24 h to allow biofilm development on the pegs. After incubation, the lid was removed, and biofilms on the pegs were rinsed in 150 mM NaCl. The biofilms were then transferred to microtiter plates containing increasing concentrations of PAA or BAC (200 μl per well) for exposure to a biocide for 5 min at 20°C. After being rinsed in 150 mM NaCl, the biofilms on the pegs were then transferred to a neutralizing solution (3 g of L-α-phosphatidyl choline, 30 g of Tween 80, 5 g of sodium thiosulfate, 1 g of L-histidine, and 30 g of saponin $liter^{-1}$) in order to halt the action of the biocide (5 min at 20°C). Finally, the lid was transferred to a microtiter plate containing 200 μl per well of TSB and was then incubated at 30°C for 24 h. After incubation, the MBEC corresponding to the concentration at which regrowth was not observed was determined for each biocide. In parallel, the biofilm population on pegs before the disinfectant challenge was determined by obtaining viable plate counts on tryptic soy agar (TSA; bioMérieux, France). After the biofilms were rinsed in 150 mM NaCl, the pegs were snapped off the lid and transferred to 150 mM NaCl before sonication for 10 min and vortexing for 30 s. The cells recovered were then enumerated on TSA after serial 10-fold dilutions, drop plating, and incubation at 30°C for 24 h.

Eradication concentrations were also evaluated for planktonic cells using a similar protocol in microtiter plates so that biofilm and planktonic susceptibilities to both biocides could be compared. Experimentally, 20 μl of an adjusted overnight culture (to obtain a final concentration of 10^8 CFU/well in a microtiter plate) was transferred to the wells of a 96-well microtiter plate containing 180 μl of increasing concentrations of the biocides and then left at 20°C for 5 min. After exposure to the biocide, 200 μl was transferred to a 24-well microtiter plate containing 1.8 ml of neutralizing agent to stop the action of the biocide, and the plate was then left at 20°C for 5 min. A total of 2 ml of the neutralized suspension was then transferred to 18 ml of TSB and incubated at 30°C for 24 h. After incubation, biocide concentrations leading to the complete eradication of planktonic cells were determined, as previously described for biofilms. Each of these experiments was performed in triplicate.

Biofilm formation for CLSM analysis. Biofilms were grown in a polystyrene 96-well microtiter plates (Greiner Bio-One, France) with a μClear base (polystyrene; 190 ± 5 μm thick), which enabled high-resolution imaging as previously described (4). Briefly, 250 μl of the final overnight subculture adjusted in TSB to an OD_{600} of 0.01 (10^6 CFU ml^{-1}) was added to the wells of the microtiter plate. After 1 h of adhesion at 30°C, the wells were rinsed to eliminate any nonadherent bacteria before being refilled with 250 μl of TSB. The plate was then incubated for 24 h at 30°C to allow for biofilm development.

Fluorescent labeling. The biofilms were stained with Chemchrome V6 (AES Chemunex, Ivry-sur-Seine, France). Chemchrome V6 is an esterase marker that can penetrate passively into a cell where it is cleaved by cytoplasmic esterases, leading to the intracellular release of fluorescent residues (green fluorescence). Experimentally, the biofilms were rinsed in 150 mM NaCl in order to eliminate any used medium and planktonic cells, and then the wells were refilled with 100 μl of solution containing Chemchrome V6 (1:100 of commercial solution diluted in Chemsol B16 buffer [AES Chemunex, Ivry-sur-Seine, France]). The microtiter plate was then incubated in the dark at 20°C for 1 h in order to reach fluorescence equilibrium.

Time-lapse CLSM analysis. After fluorescent labeling of the biofilms, the microtiter plates were rinsed to eliminate any excess Chemchrome V6 and then refilled with 100 μl of Chemsol B16 buffer. The microtiter plate was then mounted on the stage of a Leica SP2 AOBS confocal laser scanning microscope (Leica Microsystems, France) at the MIMA2 microscopy platform (http://voxel.jouy.inra.fr/mima2). The CLSM control software was set to take a series of time-lapse image scans (512 × 512 pixels corresponding to 140 by 140 μm) at intervals of 15 s. The biofilms were scanned at 800 Hz using a 63× objective lens with a 1.4 numerical aperture and a 488-nm argon laser set at 10% of its maximum intensity. These settings had been shown to avoid photobleaching of the sample during preliminary scans performed using distilled water instead of biocides, and they were conserved for all of the time lapse experiments. Emitted fluorescence was recorded within a range of 500 to 600 nm in order to capture V6 Chemchrome green fluorescence. After the launch of the time series images, 100 μl of PAA at 0.1 or 0.7% and BAC at 1%, respectively (in order to obtain final concentrations of 0.05 or 0.35% for PAA and 0.5% for BAC in the well), were gently added to the well just after completion of the first scan. The biofilms were then scanned every 15 s for 25 min, and all loss of fluorescence within the structure was recorded.

Image analysis. The intensity of green fluorescence was quantified by using the LCS Lite confocal software (Leica Microsystems). The fluorescence intensity was captured at the different time points (every 15 s) from three different square areas (areas 1, 2, and 3) of 100 μm^2 in the cell clusters. Intensity values were normalized by dividing the fluorescence intensity recorded at the different measurement time points by the initial fluorescence intensity values obtained at the same location.

Application of bacterial destruction models to fluorescence intensity curves. GinaFiT, a freeware add-in for Microsoft Excel developed by Geeraerd et al. (12), was used to model inactivation kinetics. This tool can test nine different types of microbial survival models, and the choice of the best fit depends on five statistical measures (i.e., the sum of squared errors, the mean sum of squared errors and its root, R^2, and adjusted R^2). During the present study, the "shoulder + log-linear + tail", "log-linear + tail", or "log-linear" inactivation models were fit to the fluorescence intensity curves obtained from the CLSM image series during biocide treatment. Two inactivation kinetic parameters were then extracted from this fitting: Sl, the shoulder length (min) that corresponded to the length of the lag phase, and k_{max}, the inactivation rate (min^{-1}).

Resistance of cells recovered from biofilms or planktonic suspensions. The susceptibilities to PAA and BAC of *P. aeruginosa* ATCC 15442 biofilm cells immediately after biofilm disruption, and of planktonic cells, were evaluated and compared. Experimentally, 24-h-old biofilms were rinsed with distilled water, and attached cells were recovered from the microtiter plate by scraping the bottoms of the wells with tips and aspirating and expelling the suspension at least 10 times. The cells recovered were vortex mixed using glass beads before being washed in 150 mM NaCl after centrifugation (7,000 rpm, 10 min, 20°C) and adjusted to 10^8 CFU ml^{-1} in 150 mM NaCl for the disinfection step. Planktonic cells were harvested from a 24-h-old culture in TSB at 30°C by centrifugation (7,000 rpm, 10 min, 20°C), washed in 150 mM NaCl, and then also adjusted to 10^8 CFU/ml. Biocide susceptibility was then tested according to the protocol of the European standard NF EN 1040 (1). Each experiment was performed in triplicate.

Determination of the sugar and protein contents of the biofilm matrix. The protein and sugar levels of the biofilm matrix were determined for the four strains of *P. aeruginosa*. After development, the biofilms were rinsed in distilled water and recovered from the microtiter plate by scraping the bottoms of the wells with tips and aspirating and expelling the suspension at least 10 times. The biofilm suspension thus recovered was then vortexed for 30 s, sonicated for 5 min to disperse aggregates, vortex mixed again for 30 s, and then centrifuged at 10,000 rpm for 10 min. The supernatants were then filtered at 0.45-μm-pore-size to remove any remaining bacteria, and the solutions were kept at −20°C until biochemical assays were performed. Protein levels were determined by using the Bradford assay (3) with bovine serum albumin as the standard. Sugar levels were evaluated by using the phenol-sulfuric assay procedure with glucose as the standard (9). Each experiment was performed in triplicate on three separate biofilm extractions.

RESULTS

Resistance of biofilms and planktonic cells to biocides. The PAA and BAC concentrations required to completely eradicate *P. aeruginosa* ATCC 15442 biofilm cells in 5 min were determined by using an MBEC assay. A density of 7.98 ± 0.52 log (CFU/peg) was attained by *P. aeruginosa* ATCC 15442 after 24 h of development. The cell suspension density was adjusted to the same population level in order to determine planktonic cell resistance so that the eradication concentrations could be compared in both states (biofilm and planktonic). The eradication concentrations for planktonic and bio-

TABLE 1. Biocide concentrations required to eradicate planktonic bacteria and biofilms of *P. aeruginosa* ATCC 15442 after 5 min of contact[a]

Biocide	Expt	Concn (%)	
		$C_{planktonic}$	$C_{biofilm}$
PAA	1	0.01	0.15
	2	0.01	0.15
	3	0.01	0.20
BAC	1	0.05	5
	2	0.05	5
	3	0.05	5

[a] The biocide concentrations required to eradicate planktonic bacteria ($C_{planktonic}$) and biofilms ($C_{biofilm}$) of *P. aeruginosa* ATCC 15442 after 5 min of contact are presented. The results of three independent experiments are presented for both biocides.

film cells are presented in Table 1 (the three replicates are shown). The results demonstrated a higher resistance of biofilms to biocide treatments compared to planktonic cells. The PAA concentrations required to totally eradicate biofilm cells were 15- to 20-fold higher than those necessary to kill the same amount of planktonic cells. With BAC, total eradication of the biofilm was attained using a biocide concentration that was 100-fold higher than that used for planktonic cells.

Visualization and modeling of biocide action in *P. aeruginosa* biofilms. The action of PAA and BAC in *P. aeruginosa* ATCC 15442 biofilms was visualized by using time-lapse CLSM. During control experiments (treatment with distilled water), we observed a loss of fluorescence of less than 4% ± 3% of initial fluorescence, after 25 min of treatment. Illustrative experiments showing the spatial and temporal patterns of fluorescence loss in cell clusters treated with 0.5% BAC and 0.05% PAA are presented (Fig. 1 and 2; see also Videos S1 and S2 in the supplemental material). These images represent horizontal sections of the biofilms 0, 5, 10, 15, 20, and 25 min after addition of the biocide. The fluorescence intensity curves presented in Fig. 2 correspond to the intensity recorded at the different areas (areas 1, 2, and 3) indicated in Fig. 1 during biocide treatments. GInaFIT inactivation models were applied to these experimental data. The "shoulder + log-linear + tail" inactivation model was applied to the fluorescence intensity curves for areas 1 and 2 (R^2 of 0.983 and 0.992, respectively), and the "log-linear + tail" inactivation model was applied to the curve for area 3 ($R^2 = 0.992$) under BAC treatment. The "log-linear" model was applied to the curves for the three areas under PAA treatment ($R^2 > 0.971$). Different patterns of fluorescence loss were observed as a function of the biocide used (Fig. 1 and 2). PAA treatments caused a homogeneous loss of fluorescence within the cell clusters. Indeed, the application of 0.05% PAA caused a simultaneous reduction in fluorescence in all layers of the cell cluster as from the beginning of treatment (Sl = 0 min) (Fig. 2A). The inactivation rates ranged from 0.06 to 0.09 min^{-1}. Treatment with 0.35% PAA led to an immediate and uniform loss of fluorescence in the cell cluster. The mean inactivation rate in the center of cluster was thus very high (mean $k_{max} = 14.9\ min^{-1}$), as shown in Table 2.

We found that the application of BAC led to a nonhomogeneous loss of fluorescence within the structure. Cells at the cluster periphery (area 3 in the white square) started to be inactivated immediately after application of the biocide (Sl = 0 min), whereas cells located in the intermediate area (area 2 in the gray square) and in the center of the cluster (area 1 in the black square) were steadily inactivated during treatment (Sl of 7.6 and 12.0 min, respectively) (Fig. 2B). Inactivation rate k_{max} values were between 0.37 min^{-1} in the intermediate region and 0.51 min^{-1} at the periphery of the cluster. It should be noted that few cells remained fluorescent throughout the structure after 25 min of treatment (Fig. 1 and Video S1 in the supplemental material).

These results showed that, depending on the biocides used, the spatiotemporal patterns of biofilm inactivation differed. We then investigated the action of BAC (the biocide with which we had observed a nonuniform activity pattern in the structure of *P. aeruginosa* ATCC 15442 biofilm) in different biofilm structures formed by the clinical *P. aeruginosa* isolates Laus 3, Laus 16, and Laus 21. The results of illustrative exper-

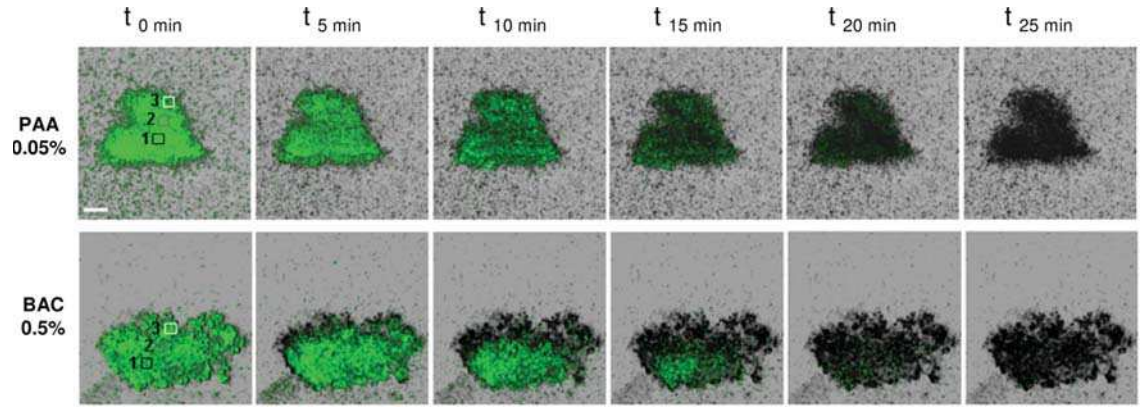

FIG. 1. Visualization of Chemchrome V6 fluorescence loss (cell membrane permeabilization) in *P. aeruginosa* ATCC 15442 biofilms during treatments with PAA and BAC biocides after 0, 5, 10, 15, 20, and 25 min of application. Each image corresponds to the superimposition of green fluorescence images on grayscale images of the initial fluorescent at the same location. Images were recorded ~5 μm above the bottom of the well. Three squares are indicated to represent area 1 (black square in the center of the cluster), area 2 (gray square in the intermediate region), and area 3 (white square at the periphery). Scale bar, 20 μm.

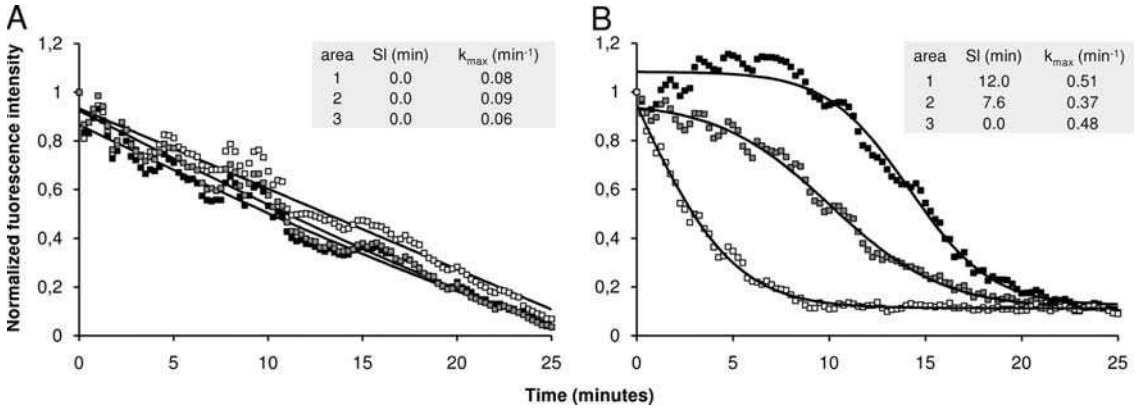

FIG. 2. Quantification of fluorescence intensity during biocide treatments. The values shown represent the loss of fluorescence at three different areas: 1 (■), 2 (▨), and 3 (□) in the biofilm cluster under treatment with 0.05% PAA (A) and 0.5% BAC (B). Two inactivation parameters, Sl (shoulder length) and k_{max} (inactivation rate), were obtained after fitting GInaFIT inactivation models (solid lines) to experimental data and are represented for each area.

iments are presented in Fig. 3, and videos are also available (see Videos S3, S4, and S5 in the supplemental material). The mean inactivation parameters, Sl and k_{max}, at the center of cell clusters were also determined by fitting GInaFIT inactivation models to experimental data and are shown in Table 2 for the different strains. The results revealed a variety of spatial and temporal inactivation patterns, depending on the strain. BAC activity was first localized at the periphery of the cluster of Laus 3 and Laus 21 strains and then gradually migrated toward the inner layers, as previously observed with *P. aeruginosa* ATCC 15442. However, the inactivation parameters differed between strains. With Laus 3, antimicrobial activity migrated rapidly to the center of the cluster (mean Sl of 3.2 min), and the mean inactivation rate k_{max} of 4.0 min^{-1} was relatively high compared to that obtained with strain ATCC 15442 (mean k_{max} = 1.6 min^{-1}). Antimicrobial activity more slowly attained the center of Laus 21 cell clusters, there being a noticeable delay of 11.6 min after biocide application, and the inactivation rate was very low (mean k_{max} = 0.2 min^{-1}). A different pattern of fluorescence loss was observed with the Laus 16 strain. Treatment with BAC led to a stretching of the biofilm and a uniform loss of fluorescence from all parts of the biofilm, from the start of treatment (mean Sl of 0.8 min^{-1}). After approximately 8 min of treatment, the loss of fluorescence became more rapid at the periphery of the cluster and then steadily reached the center of the cell cluster (Fig. 3 and see Video S5 in the supplemental material). The mean k_{max} value was similar to that obtained with Laus 3 (Table 2).

Involvement of the biofilm matrix in resistance to biocides. In order to determine the role of the matrix in biofilm resistance to biocides, the susceptibilities of *P. aeruginosa* ATCC 15442 cells recovered from a biofilm immediately after washing or from a planktonic suspension were compared. Log reductions of 2.7 ± 0.2 and 2.8 ± 0.3 were obtained for planktonic and biofilm cells, respectively, when they were exposed for 5 min to 5 ppm of PAA. Exposure to 5 ppm of BAC for 5 min led to log reductions of 3.8 ± 0.2 and 3.9 ± 0.1 for planktonic and recovered biofilm cells, respectively. These cells did not therefore display any significant differences in terms of their resistance to PAA and BAC ($P > 0.05$), suggesting a major role for the three-dimensional structure and exopolymeric matrix in the resistance of *P. aeruginosa* biofilms to these biocides.

The sugar and protein contents of the biofilm exopolymeric matrix of *P. aeruginosa* ATCC 15442 and the three clinical isolates Laus 3, Laus 16, and Laus 21 were then determined by using biochemical assays. The results presented in Fig. 4 show that the biofilm of the Laus 21 clinical isolate was clearly characterized by a higher protein content (88 μg/well) than in the three other strains (ranging from 52 to 55 μg/well) ($P < 0.05$). We also found that the biofilms of strains ATCC 15442 and Laus 21 displayed higher sugar contents than the Laus 3 and Laus 16 strains ($P < 0.05$).

TABLE 2. Inactivation parameters for biocides in the internal areas of cell clusters of the four *P. aeruginosa* strains[a]

Strain	Biocide	$C_{biocide}$ (%)	No. of expts	Mean ± SEM		
				Sl (min)	k_{max} (min^{-1})	R^2
ATCC 15442	PAA	0.05	4	0.3 ± 0.6	0.4 ± 0.5	0.973 ± 0.028
	PAA	0.35	2	0.0 ± 0.0	14.9 ± 1.1	0.983 ± 0.015
	BAC	0.5	4	7.3 ± 3.7	1.6 ± 0.9	0.990 ± 0.004
Laus 3	BAC	0.5	3	3.2 ± 1.7	4.0 ± 4.3	0.961 ± 0.005
Laus 16	BAC	0.5	3	0.8 ± 1.3	4.6 ± 4.0	0.981 ± 0.014
Laus 21	BAC	0.5	3	11.6 ± 4.3	0.2 ± 0.1	0.970 ± 0.004

[a] Sl (shoulder length) and k_{max} (inactivation rate) values were obtained after fitting GInaFIT inactivation models to experimental fluorescence intensity data. $C_{biocide}$, biocide concentration.

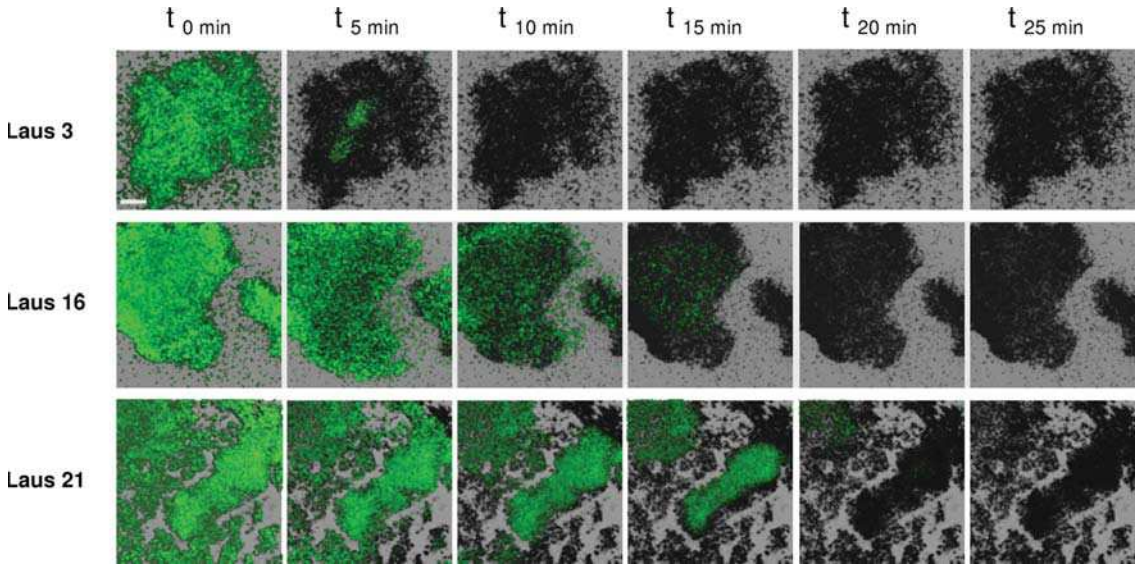

FIG. 3. Visualization of Chemchrome V6 fluorescence loss (cell membrane permeabilization) in *P. aeruginosa* clinical isolate biofilms during BAC treatments after 0, 5, 10, 15, 20, and 25 min of application. Each image corresponds to the superimposition of green fluorescence images on grayscale images of the initial fluorescence at the same location. Scale bar, 20 μm.

DISCUSSION

Biofilms are well known to display a high degree of resistance to antibiotic and biocide treatments (17, 21, 32). In agreement with previous studies (5, 10, 13, 26), we confirm here that *P. aeruginosa* biofilm cells displayed resistance to PAA (an oxidizing agent) and more markedly BAC (a quaternary ammonium compounds) that was greater than that of their planktonic counterparts. It is now generally recognized that biofilms are heterogeneous structures (23, 28) and that the appearance of specific biofilm functions such as resistance to antimicrobial agents is intimately related to the inherent three-dimensional organization of cells and exopolymeric matrix and results from multifactorial processes. The development of tools for the *in situ* investigation of antimicrobial activity within biofilms at a single cell level while taking account of local heterogeneity is thus essential to gain an understanding of the limitations of these treatments to develop new and more efficient strategies. A time-lapse CLSM method was recently developed and used to investigate the spatial and temporal patterns of antimicrobial activity in a biofilm formed by *Staphylococcus epidermidis* alone and a mixed biofilm of *Streptococcus oralis*, *Streptococcus gordonii*, and *Actinomyces naeslundii* (8, 29). During these studies, the bacteria were stained first by incubating the cells with calcein-AM. This fluorogenic esterase substrate penetrates passively into cells, where it is cleaved by cytoplasmic esterases, causing the release of fluorescent residues and thus triggering cell fluorescence. The inactivation of cells in the biofilm was then visualized by monitoring the fluorescence loss that corresponded to the leakage of fluorophores outside the cells once the biocide had permeabilized the membrane. Although this technique had been shown to be well suited to the study of some Gram-positive species, it is not directly applicable to studying other species, mainly because of limitations to fluorescent labeling. Indeed, one of the first requirements of this technique is that fluorescent residues must remain trapped in the cells if the membrane is not compromised. However, in Gram-negative strains, and particularly *Pseudomonas* sp., intense efflux pump activity can lead to the release of fluorescent residues from the cells, so that a stable and intense level of intracellular fluorescence cannot be achieved (18).

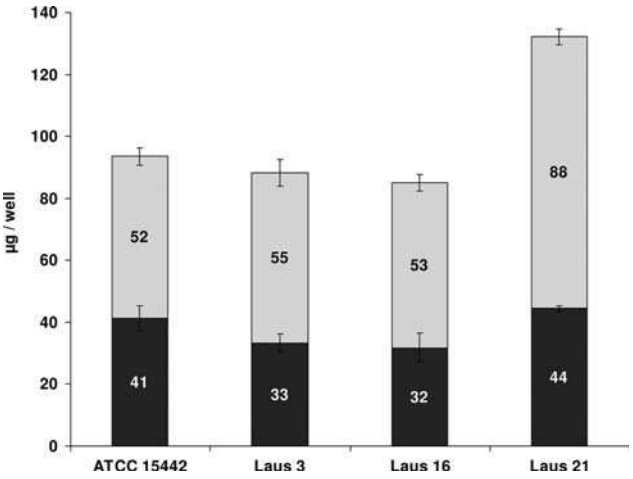

FIG. 4. Sugar (black bars) and protein (gray bars) levels in the biofilm of the four *P. aeruginosa* strains. Values (μg/well) correspond to the mean of three independent experiments and are shown inside the bars. Error bars represent the standard deviations.

During the present study, we used the Chemchrome V6 esterase marker/Chemsol B16 staining buffer kit, which can block efflux pump activity and thus maintain fluorophores inside the cells (18). This staining proved to be stable for several hours with *P. aeruginosa* and was successful with other Gram-negative species such as *Salmonella enterica*. In addition, the levels of biofilm inactivation achieved by CLSM agreed well

with those obtained using the plate count method (data not shown).

Using time-lapse CLSM combined with Chemchrome V6/Chemsol B16 staining, the action of PAA and BAC in *P. aeruginosa* biofilms was thus investigated. Different patterns of fluorescence loss were observed as a function of the biocides used, thus illustrating the specificity of action and limitations of each compound. PAA caused a uniform and linear loss of fluorescence in cell clusters of *P. aeruginosa* ATCC 15442, suggesting that the greater resistance of the biofilm compared to planktonic cells observed here could not be due to limitations affecting penetration of the biocide into the biofilm, as previously reported in the case of *P. aeruginosa* with other oxidizing agents such as chlorine or hydrogen peroxide (7, 27, 31). Nevertheless, even though PAA was able to diffuse inside the clusters, the biocidal compounds may partly have been consumed through quenching reactions with exopolymeric substances, leading to the greater biofilm resistance observed. In line with this, we observed that disruption of the biofilm and the washing of cells enabled the recovery of the same susceptibility as that observed for planktonic cells; this finding was consistent with the fact that biofilm resistance appeared mainly to be due to the presence of the exopolymeric matrix. The efficacy of oxidizing agents is indeed well known to be profoundly affected by the presence of organic materials such as the constituents of the biofilm matrix (polysaccharides, proteins, and nucleic acids) (2, 19, 22). In addition, the presence of protective enzymes such as catalases in the extracellular matrix has also been reported to be involved in the resistance of *P. aeruginosa* biofilms to oxidizing agents (27).

In contrast, BAC treatment caused a nonuniform loss of fluorescence in *P. aeruginosa* ATCC 15442 biofilms. Cells in peripheral layers were inactivated first, and then the action of the biocide spread steadily into the cluster structure. This gradual inactivation of the structure, together with the fact that disruption of the three-dimensional biofilm structure and elimination of the matrix led to a recovery of biocide efficiency, suggests that BAC encountered obstacles to penetration within the cluster, probably caused by interactions with biofilm components. In a recent study, Davison et al. (8) estimated that the time required for diffusive access in the absence of a reaction or sorption was 24 s for quaternary ammonium compounds (MW, 357) in a cell cluster with a diameter of ~150 μm. Under our experimental conditions, the cell cluster diameters were smaller (80 to 120 μm), and the mean time before fluorescence decreased within the clusters (Sl) under treatment with 0.5% BAC (MW, 368.02) was more than 7 min for *P. aeruginosa* ATCC 15442 (Table 2). The involvement of hydrophobic and/or charge interactions in barriers to the penetration of quaternary ammonium compounds has indeed already been proposed with respect to the biofilms formed by different strains, including *P. aeruginosa* (5, 8, 24). Another explanation for the resistance of an ATCC 15442 biofilm to BAC is that few cells remained alive at different areas in the cluster, despite the apparent penetration of the biocide after 25 min of treatment (Fig. 1 and see the videos in the supplemental material). These cells may have been located in areas difficult for the biocides to attain; for example, the cells may have been located in areas protected by a large quantity of matrix and other cells. In addition, it cannot be excluded that these few cells expressed highly resistant phenotypes throughout physiological adaptations, e.g., persisters (20), or throughout genetic mutations.

Interestingly, visualization of the action of BAC in biofilms formed by clinical *P. aeruginosa* isolates also revealed patterns of inactivation that confirmed the existence of transport limitations and suggested that the restricted penetration of BAC into biofilms might be one of the key processes explaining the resistance of *P. aeruginosa* biofilms to this biocide. The characterization and comparison of the sugar and protein contents in the biofilms of the four *P. aeruginosa* strains supported the idea that the exopolymeric matrix plays a key role in these transport limitations. We observed that the biofilm of the Laus 21 clinical isolate, in which a high delay of BAC penetration was recorded, was characterized by a larger quantity of matrix than that of other strains, mainly due to a high protein content. Moreover, biofilms of Laus 3 and Laus 16 were characterized by the lowest sugar levels, which were associated with a more rapid penetration of BAC into biofilms compared to the ATCC 15442 and Laus 21 biofilms (see the kinetic inactivation parameters in Table 2). It should also be noted that the speed of penetration did not seem to be directly related to the size of cell clusters (Fig. 3). The diversity of the composition and density of biofilm matrix are thus more likely to explain the differences in BAC inactivation dynamics between the strains analyzed.

In conclusion, we adapted the time-lapse CLSM visualization and modeling of biocide action to biofilms formed by the Gram-negative pathogen *P. aeruginosa*. The dynamics of biocidal action thus recorded made it possible to identify mechanisms involved in biofilm resistance, such as spatial diffusion and/or reaction limitations. These local molecular processes need to be taken into account in the development of innovative and efficient strategies for biofilm control.

ACKNOWLEDGMENTS

This study received support from the MEDICEN-Region Paris, Ile-de-France Competitiveness Cluster. We thank the Essonne Département for its financial support of the confocal microscopy facility (ASTRE no. A02137).

Victoria Hawken is acknowledged for her English revision of the manuscript.

REFERENCES

1. **Anonymous.** 1997. Chemical disinfectants and antiseptics: basic bactericidal activity–test method and requirements (phase 1), NF EN 1040 ed. AFNOR, La Plaine Saint-Denis, France.
2. **Bessems, E.** 1998. The effect of practical conditions on the efficacy of disinfectants. Int. Biodeterior. Biodegrad. **41:**177–183.
3. **Bradford, M. M.** 1976. A rapid and sensitive method for quantitation of microgram quantities of protein utilizing the principle of protein-dye-binding. Anal. Biochem. **72:**248–254.
4. **Bridier, A., F. Dubois-Brissonnet, A. Boubetra, V. Thomas, and R. Briandet.** 2010. The biofilm architecture of sixty opportunistic pathogens deciphered using a high throughput CLSM method. J. Microbiol. Methods **82:**64–70.
5. **Campanac, C., L. Pineau, A. Payard, G. Baziard-Mouysset, and C. Roques.** 2002. Interactions between biocide cationic agents and bacterial biofilms. Antimicrob. Agents Chemother. **46:**1469–1474.
6. **Ceri, H., et al.** 1999. The Calgary Biofilm Device: new technology for rapid determination of antibiotic susceptibilities of bacterial biofilms. J. Clin. Microbiol. **37:**1771–1776.
7. **Chen, X., and P. S. Stewart.** 1996. Chlorine penetration into artificial biofilm is limited by a reaction-diffusion interaction. Environ. Sci. Technol. **30:**2078–2083.
8. **Davison, W. M., B. Pitts, and P. S. Stewart.** 2010. Spatial and temporal patterns of biocide action against *Staphylococcus epidermidis* biofilms. Antimicrob. Agents Chemother. **54:**2920–2927.
9. **Dubois, M., K. A. Gilles, J. K. Hamilton, P. A. Rebers, and F. Smith.** 1956.

Colorimetric method for determination of sugars and related substances. Anal. Chem. **28:**350–356.
10. **Dubois-Brissonnet, F., C. Ntsama, M. Bouix, J. Y. Leveau, and J. Fourniat.** 1995. Activité bactéricide de six désinfectants sur des biofilms de *Pseudomonas aeruginosa* obtenus en conditions statiques, p. 295–304. *In* M. N. Bellon-Fontaine and J. Fourniat (ed.), Adhesion des microorganismes aux surfaces. Technique et Documentation, Lavoisier, France.
11. **Engelhart, S., et al.** 2002. *Pseudomonas aeruginosa* outbreak in a haematology-oncology unit associated with contaminated surface cleaning equipment. J. Hosp. Infect. **52:**93–98.
12. **Geeraerd, A. H., V. P. Valdramidis, and J. F. Van Impe.** 2005. GInaFiT, a freeware tool to assess non-log-linear microbial survivor curves. Int. J. Food Microbiol. **102:**95–105.
13. **Grobe, K. J., J. Zahller, and P. S. Stewart.** 2002. Role of dose concentration in biocide efficacy against *Pseudomonas aeruginosa* biofilms. J. Indus. Microbiol. Biotechnol. **29:**10–15.
14. **Hall-Stoodley, L., and P. Stoodley.** 2009. Evolving concepts in biofilm infections. Cell. Microbiol. **11:**1034–1043.
15. **Hota, S., et al.** 2009. Outbreak of multidrug-resistant *Pseudomonas aeruginosa* colonization and infection secondary to imperfect intensive care unit room design. Infect. Cont. Hosp. Epidemiol. **30:**25–33.
16. **Iversen, B. G., et al.** 2007. An outbreak of *Pseudomonas aeruginosa* infection caused by contaminated mouth swabs. Clin. Infect. Dis. **44:**794–801.
17. **Izano, E. A., S. M. Shah, and J. B. Kaplan.** 2009. Intercellular adhesion and biocide resistance in nontypeable *Haemophilus influenzae* biofilms. Microb. Pathog. **46:**207–213.
18. **Joux, F., and P. Lebaron.** 2000. Use of fluorescent probes to assess physiological functions of bacteria at single cells level. Microbes Infect. **2:**1523–1535.
19. **Lambert, R. J. W., and M. D. Johnston.** 2001. The effect of interfering substances on the disinfection process: a mathematical model. J. Appl. Microbiol. **91:**548–555.
20. **Lewis, K.** 2008. Multidrug tolerance of biofilms and persister cells, p. 322. *In* T. Romeo (ed.), Bacterial biofilms. Springer-Verlag, Berlin, Germany.
21. **Mah, T. F., et al.** 2003. A genetic basis for *Pseudomonas aeruginosa* biofilm antibiotic resistance. Nature **426:**306–310.
22. **McDonnell, G., and A. D. Russell.** 1999. Antiseptics and disinfectants: activity, action, and resistance. Clin. Microbiol. Rev. **12:**147–179.
23. **Rani, S. A., et al.** 2007. Spatial patterns of DNA replication, protein synthesis, and oxygen concentration within bacterial biofilms reveal diverse physiological states. J. Bacteriol. **189:**4223–4233.
24. **Sandt, C., J. Barbeau, M. A. Gagnon, and M. Lafleur.** 2007. Role of the ammonium group in the diffusion of quaternary ammonium compounds in *Streptococcus mutans* biofilms. J. Antimicrob. Chemother. **60:**1281–1287.
25. **Schelenz, S., and G. French.** 2000. An outbreak of multidrug-resistant *Pseudomonas aeruginosa* infection associated with contamination of bronchoscopes and a endoscope washer-disinfector. J. Hosp. Infect. **46:**23–30.
26. **Smith, K., and I. S. Hunter.** 2008. Efficacy of common hospital biocides with biofilms of multidrug-resistant clinical isolates. J. Med. Microbiol. **57:**966–973.
27. **Stewart, P. S., et al.** 2000. Effect of catalase on hydrogen peroxide penetration into *Pseudomonas aeruginosa* biofilms. Appl. Environ. Microbiol. **66:**836–838.
28. **Stewart, P. S., and M. J. Franklin.** 2008. Physiological heterogeneity in biofilms. Nat. Rev. Microbiol. **6:**199–210.
29. **Takenaka, S., H. M. Trivedi, A. Corbin, B. Pitts, and P. S. Stewart.** 2008. Direct visualization of spatial and temporal patterns of antimicrobial action within model oral biofilms. App. Environ. Microbiol. **74:**1869–1875.
30. **Wagner, V. E., and B. H. Iglewski.** 2008. *Pseudomonas aeruginosa* biofilms in CF infection. Clinic. Rev. Allerg. Immunol. **35:**124–134.
31. **Xu, X., P. S. Stewart, and X. Chen.** 1996. Transport limitations of chlorine disinfection of *Pseudomonas aeruginosa* entrapped in alginate beads. Biotechnol. Bioeng. **49:**93–100.
32. **Xu, K. D., G. A. McFeters, and P. S. Stewart.** 2000. Biofilm resistance to antimicrobial agents. Microbiology **146:**547–549.

C. Article 6 :

"Are resident *Bacillus subtilis* biofilms of concern in hospital acquired infections?"

Bridier A., F. Dubois-Brissonnet, D. Le Coq, T. Meylheuc, V. Thomas, S. Aymerich and R. Briandet.

En cours de préparation.

ARE RESIDENT *BACILLUS SUBTILIS* BIOFIMS OF CONCERN IN HOSPITAL AQUIRED INFECTIONS?

A. Bridier[1,2], F. Dubois-Brissonnet[2], D. Le Coq[1], T. Meylheuc[1], V. Thomas[3], S. Aymerich[1], R. Briandet[1]

[1]INRA, UMR 1319 MICALIS, F-78350 Jouy-en-Josas, France ; [2]AgroParisTech, UMR 1319 MICALIS, F-78350 Jouy-en-Josas, France, [3]Steris, Fontenay aux Roses, France.

ABSTRACT

The development of a biofilm constitutes a survival strategy by providing bacteria in a protective environment safe from stresses such as biocide action. The presence of biofilms of microbial pathogens on medical devices and environmental surfaces leads to nosocomizl infections and important health-care problems. In this study, the resistance of the biofilm formed by a *B. subtilis* strain recently isolated from endoscope washer-disinfectors (hereafter called $ND_{medical}$) was evaluated with respect to peracetic acid (PAA), a commonly used biocide in endoscope decontamination. The results showed that this isolate demonstrate the ability to make very large amount of biofilm accompanied by hyper-resistance to the concentration of the biocide normally used in hospitals (3500 ppm). Some evidence strongly suggests that the enhanced resistance of the $ND_{medical}$ strain was related to the specific three-dimensional structure of the biofilm and the large amount of the extracellular matrix. When grown in mixed biofilm with *Staphylococcus aureus*, the $ND_{medical}$ strain demonstrated the ability to protect the pathogen from PAA action, thus enabling its persistence in the environment. Finally, this work points out the ability of bacteria to adapt to an extremely hostile environment, and the importance of considering a multi-organism ecosystem instead of single species model.

INTRODUCTION

In response to environmental conditions, bacteria have developed different strategies to adapt and survive. The formation of multicellular communities known as biofilms is one such strategy, which is mostly associated with increased bacterial resistance to environmental stress accompanying antimicrobial treatments (Cloete, 2003; Høiby *et al.,* 2010). It has indeed been shown that non-lethal concentrations of antibiotics or disinfectants can stimulate biofilm formation (Hoffman *et al.,* 2005; Shemesh *et al.,* 2010) which constitutes a defensive response to the toxic effects of the biocides. Mechanisms involved in the resistance of biofilms remain unclear but appear to result from multifactorial processes related to the architecture of the edifice and the phenotypic features of the cells. The presence of a protective extracellular matrix via the expression of specific genes in the biofilm, the metabolic state of cells due to microenvironmental conditions have all been identified as playing a role in biofilm resistance to antimicrobial agents (Donlan and Costerton, 2002). In the clinical settings, biofilms promote infection through, for example, the persistence of bacteria on medical devices and thus can act as reservoir for pathogens (Potera, 1999; Francolini and Donelli, 2010). Of all medical devices used, flexible endoscopes are among the most frequently associated with outbreaks of infectious organisms (Spach *et al.,* 1993; Kressel and Kidd, 2001; Srinivasan *et al.,* 2003; Rutala and Weber, 2004, DiazGranados *et al.,* 2009). Indeed, some studies have reported the presence of persistent bacteria on endoscopes despite cleaning and disinfection procedures (Deva *et al.,* 1998; Machado *et al.,* 2006). Interestingly, a viable strain of *B. subtilis* was recently isolated from an endoscope washer-disinfector after high level disinfection with chlorine dioxide (Martin *et al.,* 2008), which had developed resistance against this and other oxidising agents using a standard suspension test. Recently, we showed that this stable isolate was able to produce a thick immersed biofilm with specific protruding structures (Bridier *et al.,* 2011). In this work, we have now investigated the resistance of this strain in biofilm to peracetic acid (PAA), an oxidizing agent commonly used in endoscope disinfection. In addition, we examined the ability of the $ND_{medical}$ strain in a mixed biofilm to protect *Staphylococcus aureus*, a pathogen responsible of a large number of nosocomial infections (Perl and Golub, 1998), from biocide action.

MATERIALS AND METHODS

Bacterial strains and growth conditions

The bacterial strains used in this study are listed in Table 1. The GFP-carrying *Bacillus subtilis* $ND_{medical}$ strain was obtained by transforming *B. subtilis* $ND_{medical}$ to spectinomycin resistance with the pDR146 plasmid (a kind gift from D. Rudner, Harvard Medical School). This placed in the *amyE* locus the *gfp (mut2)* gene controlled by the IPTG-regulated $P_{hyperspank}$ promoter. Transformation was performed according to standard procedures and the transformants were selected on LB plates supplemented with spectinomycin at 100 µg/ml. Before each experiment, bacteria were subcultured twice in Tryptone Soya Broth (TSB, BioMérieux, France), supplemented with isopropyl β-D-thiogalactopyranoside (*IPTG*) at a final concentration of 200 µM to induce GFP production and/or with antibiotics when necessary at the following concentrations: spectinomycin, 100 µg/ml; erythromycin, 3 µg/ml.

Strain	Relevant genotype or description[a]	Reference or construction
Bacillus subtilis		
168	*trpC2*	Bacillus Genetic Stock Center
$ND_{medical}$	Freshly isolated from endoscope washer-disinfectors	Martin et al (2008)
$ND_{medical}$ GFP	*amyE*::P_{hyp}-*gfp* (*spec*^{R})	pDR146 → $ND_{medical}$
Staphylococcus aureus		
AH478	Strain RN4220 carrying pAH9-mCherry (*ery*^{R})	Malone et al (2009)

[a] *spec* and *ery* stand for spectinomycin and erythromycin resistance markers respectively

Biofilm formation

Biofilms were formed in polystyrene 96-well microtiter plates with a µclear® base (Greiner Bio-one, France), which enables high-resolution fluorescence imaging with slight modifications as previously described (Bridier *et al.,* 2010). For single species biofilms, 250 µl of an overnight culture in TSB adjusted to an OD_{600nm} of 0.02 were added to the wells of the microtiter plate. For mixed species biofilm, overnight cultures in TSB of *S. aureus* AH478 mcherry and the *B. subtilis* GFP strains were adjusted to an OD_{600nm} of 0.02 in TSB and mixed at a ratio of 1:2. IPTG was added to the medium to a final concentration of 200 µM to

induce GFP production in the *B. subtilis* strains. The microtiter plate was then kept at 30°C for 90 min to enable bacteria to attach to the bottom of the wells. After this adhesion step, the wells were rinsed with TSB to eliminate non-adherent bacteria and then refilled with 250 µl sterile TSB. The microtiter plate was then incubated for 24h at 30°C to allow biofilm development.

Disinfectant treatment

After development, biofilms in the microtiter plates were rinsed and the wells refilled with 100 µl of TSB. Then, 100µl of peracetic acid (PAA) (32 wt. % in dilute acetic acid (Sigma-Aldrich, France)) at 7000 ppm were then added in the wells to obtain a final concentration of 3500 ppm. After 5 min of contact, biocide solutions were gently removed and wells were refilled by a quenching solution (3 g/L L-α-phosphatidyl cholin, 30 g/L Tween 80, 5 g/L sodium thiosulfate, 1 g/L L-histidine, 30 g/L saponine) and left for 5 min to stop biocide action. The bottom of the wells was then scraped with tips and the suspension aspirated and expelled many times to detach and recover survivor cells from biofilms. The suspensions were then serially diluted in 150 mM NaCl and plated on Tryptone Soya Agar (TSA, Biomérieux, France) before being incubated at 30°C for 24-48h.

To determine the sensitivity of *B. subtilis* $ND_{medical}$ cells to PAA following disruption of the biofilm, biofilms were rinsed with TSB and cells were recovered by scraping the bottom of the wells with tips and aspirating and expelling many times the suspension. The recovered cells were mixed with 150mM NaCl containing glass beads and suspension vortexed for 30 s to separate cells and extracellular matrix. The suspension was then washed after centrifugation (7000 rpm, 10 min, 20 °C) and adjusted to 10^8 CFU/ml in 150mM NaCl. In parallel, planktonic bacteria were harvested from a 24h culture in TSB at 30° C by centrifugation (7000 rpm, 10 min, 20° C) followed vortexing with glass beads for 30 s and then washed in 150 mM NaCl before also adjusting to 10^8 CFU/mL. Biocide susceptibility was then tested according to the standard European NF EN 1040 procedure (Anonymous, 1997). Survivors were counted after incubation by comparing the number of colonies with those obtained when biocide was replaced by distilled water. Each experiment was done in triplicate.

Detection of spores

In order to check the presence of spores in the biofilm after 24h of development, cells were recovered from the microtiter plates as described above and resuspended in 150 mM NaCL and boiled at 100°C for 10 min. Bacterial numbers (cfu/ml) were checked before and after the heat treatment.

Confocal laser scanning microscopy and fluorescent labelling

Time lapse CLSM analysis of PAA action was performed in *B. subtilis* biofilms. This technique permits the direct visualization of cell inactivation patterns in biofilm structures during biocide action. The methods is based on the monitoring of fluorescence loss caused by the leak of an unbound fluorophore outside the cells after disruption of the bacterial membrane by antimicrobial agents. Experimentally, 24h biofilms in a microtiter plate were rinsed with TSB in order to eliminate medium and planktonic cells. The wells were then refilled with 100µl of TSB containing Chemchrome V6 (1:100 of commercial solution (AES Chemunex, France)). Chemchrome V6 is an esterasic marker which enter cells passively where it is cleaved by cytoplasmic esterases leading to the intracellular release of fluorescent residues (green fluorescence). Microtiter plates were incubated in the dark at 20°C for 1h in order to reach fluorescence equilibrium. Biofilms were then rinsed to eliminate excess Chemchrome V6 and refilled with 100 µl of TSB. The microtiter platee were then mounted on the motorized stage of a Leica TCS SP2 AOBS Confocal laser scanning microscope (LEICA Microsystems, France) at the MIMA2 microscopy platform (http://voxel.jouy.inra.fr/mima2). The CLSM control software was set to take a series of time-lapse xyzt scans (256 × 256 pixels) at intervals of 15 s at five different depths in the biofilm. Biofilms were scanned at 400 Hz using a 63× oil objective with a 1.4 numerical aperture with a 488 nm argon laser set at 10% of its maximal intensity. These settings, which were shown to avoid photobleaching of the sample, by preliminary scans performed using distilled water instead of biocides, were used in all time-lapse experiments. Emitted V6 Chemchrome green fluorescence was recorded within the range 500–600 nm. After the starting of the xyzt scan serie, 100 µl of PAA at 7000 ppm were gently added to the wells just after the completion of the first scan. Biofilms were then scanned every 15 s at five different depths over 10 min, and fluorescence loss within the structure recorded. Three experiments were performed for each strain.

A series of images xyz with a z-step of 1 µm were also performed to obtain the three-dimensional structure of the biofilms. Both single and mixed biofilms were scanned using an excitation wavelength of 458 nm (argon laser, 25% intensity) and 543 nm (helium-neon laser, 50% intensity), with emission wavelengths from 480 to 530 nm and from 580 to 700 nm in order to collect GFP and mCherry fluorescence respectively.

Images of 24h-biofilms stained with thioflavin T (10µM), were also collected to observe amyloid fibres. Biofilms were scanned using an excitation wavelength of 458nm (argon laser, 80% intensity) and an emission wavelength from 475 to 530 nm.

Image analysis

Three-dimensional projections of biofilm structures were reconstructed using the Easy 3D function of the IMARIS 7.0 software (Bitplane, Switzerland) directly from xyz images series.

Quantification of green fluorescence intensity from time-lapse (xyzt) CLSM image series was performed using confocal software LCS Lite (Leica Microsystems, France). For each experiment, fluorescence intensity was measured each 15 s during biocide treatment. Intensity values were normalized by dividing the fluorescence intensity recorded by the initial fluorescence intensity value at the same location. Fluorescence intensity curves shown are the mean of three experiments, each experiment constituting the average of five horizontal sections along the depth of the biofilm.

Application of bacterial destruction models on fluorescence intensity curves

GinaFiT, a freeware Add-inn for Microsoft® Excel developed by Geeraerd et al. (2005) was used to model inactivation kinetics. This tool enables testing of nine different types of microbial survival models, and the choice of the best fit depends on five statistical measures (i.e., sum of squared errors, mean sum of squared errors and its root, R^2, and adjusted R^2). During this study, the "log-linear + tail" inactivation model was fitted on fluorescence intensity curves obtained from CLSM image series during biocide treatment. The inactivation rate k_{max} (min^{-1}) was extracted from the fitting.

Congo Red and Calcofluor indicator plate tests

The ability of both *B. subtilis* strains to bind Congo Red and calcofluor white was tested using indicator plates. Experimentally, 5 µl of an overnight culture in TSB were inoculated on TS agar (1.5%) containing 40 µg/ml Congo Red (Sigma-Aldrich, France), or 20 µg/ml calcofluor white (Sigma-Aldrich, France). Plates were then incubated for 72 h at 30° C. Macrocolonies were observed using UV excitation of Calcofluor indicator plates.

Scanning Electronic Microscopy (SEM) observations of biofilms

For SEM observations, *B. subtilis* biofilms were prepared by immerging aluminium coupons in the wells of a 24-well polystyrene plate containing bacterial suspensions adjusted to an OD_{600nm} of 0.02. After 90 min of adhesion, coupons are rinsed and wells were refilled with 1 ml of TSB. The plate was then incubated at 30° C for 24h. After development, biofilms were rinsed with 150mM NaCl and attached bacterial cells were fixed in a solution containing 2.5% glutaraldehyde, 0.1 M sodium cacodylate (pH 7.4), 0.075% ruthenium red and 0.015% Alcian blue for 20 h. Samples were then washed three times for 10 min with a solution containing 0.1 M sodium cacodylate, 0.075% ruthenium red and 0.015% Alcian blue before being transferred into 50% ethanol. Samples were progressively dehydrated by passage through a graded series of ethanol solutions from 50% to 100%. Finally, the samples were critical point dehydrated (Emitech K850, UK) using carbon dioxide as the transition fluid and coated with gold-palladium in an automatic sputter coater (Polaron SC7640, UK). Scanning electron microscopy Quanta 650 FEG-SEM (FEI, Japan) was used to observe the samples.

Statistical analysis

One-way ANOVA was performed using Statgraphics v6.0 software (Manugistics, Rockville, USA). Significance was defined as a *P* value associated with a Fisher test value lower than 0.05.

RESULTS

B. subtilis $ND_{medical}$ biofilms exhibit a marked resistance to PAA

A non-domesticated *B. subtilis* strain ($ND_{medical}$) recently isolated from an endoscope washer-disinfector and the *B. subtilis* collection strain 168 were compared for their ability to form a biofilm and to resist PAA treatment. First, the architecture of biofilms formed by both *B. subtilis* GFP strains was observed after 24 h of development as presented in Fig. 1. The images correspond to three-dimensional reconstructions obtained from confocal stack images by the IMARIS software, including virtual shadow projections on the right. We found that the non-domesticated *B. subtilis* $ND_{medical}$ strain clearly developed a thicker biofilm with protruding structures in comparison to strain 168 in these experimental conditions.

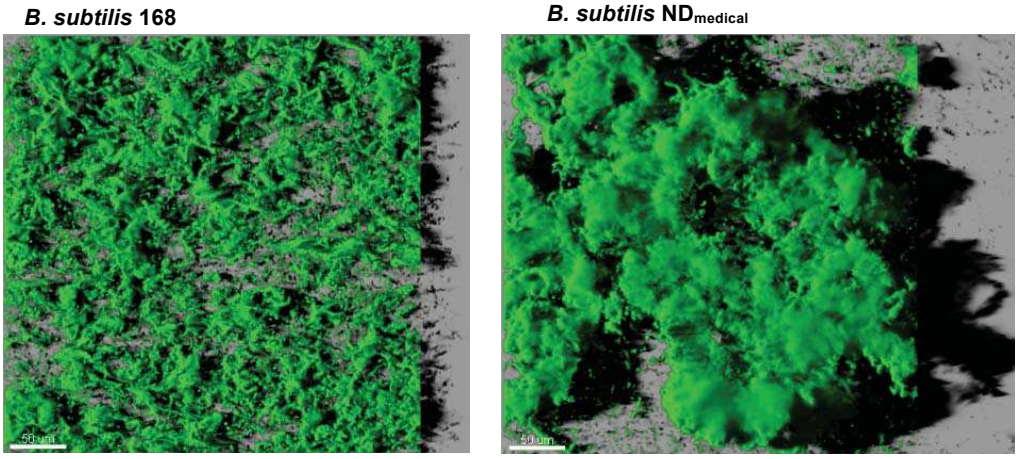

Figure 1. Three-dimensional projection of *B. subtilis* biofilms obtained from xyz confocal images series using IMARIS software. Images present an aerial view of biofilm structure with the virtual shadow projection on the right. Scale bar correspond to 50 μm.

The resistance of biofilms formed by both strains exposed to 3500 ppm of PAA for 5 min was next investigated. These conditions represent the *in-use* PAA concentration and the time of exposiure that are commonly used in the disinfection treatment of endoscopes in hospitals. The results showed substantial resistance of the *B. subtilis* $ND_{medical}$ strain which exhibited only 3.8 Logs of reduction while no survivor were detected on plates for strain 168 corresponding to a reduction greater than 5.6 Logs (Fig. 2). We confirmed that $ND_{medical}$ biofilm did not contain any spores at 24h of development showing that the resistance observed was displayed by vegetative cells.

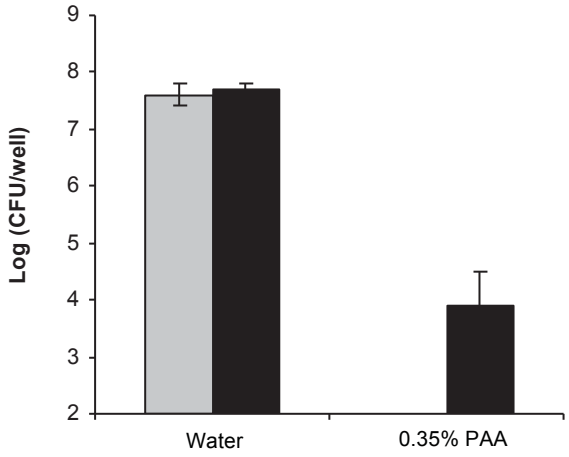

Figure 2. Log (cfu/well) after 5 min of treatment with water or 0.35% Peracetic acid (PAA) for *B. subtilis* 168 (grey bars) and $ND_{medical}$ (black bars) biofilms. Data shown are the mean of three experiments and error bars show the standard deviation.

The resistance of the $ND_{medical}$ biofilm was investigated further by time-lapse CLSM microscopy allowing us to visualize biocide action in real-time within the biofilm structures of both *B. subtilis* strains. Figure 3A presents the dynamics of fluorescence loss (membrane permeabilisation) within the biofilms during treatment with 500 ppm of PAA. This concentration was chosen in order to enable the visualization of biofilm damage in approximately 10 min. Note that when biofilms were treated with distilled water as a control, we observed a loss of fluorescence of less than 1% (n=4) of the initial fluorescence after 10 min of treatment. The GinaFIT "Log linear + tail" inactivation model (Geeraerd *et al.*, 2005) was applied to these experimental data to extract the inactivation rate k_{max} and this revealed satisfactory adjustment (R^2 >0.982). The results confirmed the greater resistance of the biofilm of strain $ND_{medical}$ compared to the laboratory strain 168. Thus, while PAA treatment resulted in an immediate and uniform loss of fluorescence of cells in the biofilm of strain 168, the loss of fluorescence in the $ND_{medical}$ biofilm was slow and heterogeneous during disinfection treatment. The extracted k_{max} inactivation rates showed a large and significant difference between strain 168 and $ND_{medical}$ (inset in Fig. 1, P<0.05) with values of 14.0 and 0.4 respectively. Spatial patterns of fluorescence loss in biofilms treated with 500 ppm PAA are presented in Figure 3B and videos are available in supplementary material (videos S1 and S2). A homogeneous and sharp loss of fluorescence was seen in the whole biofilm structure of strain 168 following the application of biocide. Conversely, PAA application led to a non-homogenous loss of fluorescence within the biofilm structure of the $ND_{medical}$ strain. Indeed, with this strain, we observed that spreading of PAA was difficult in some areas and these remained fluorescent even after 10 min treatment illustrating the high resistance and associated low inactivation rate k_{max} displayed by this strain.

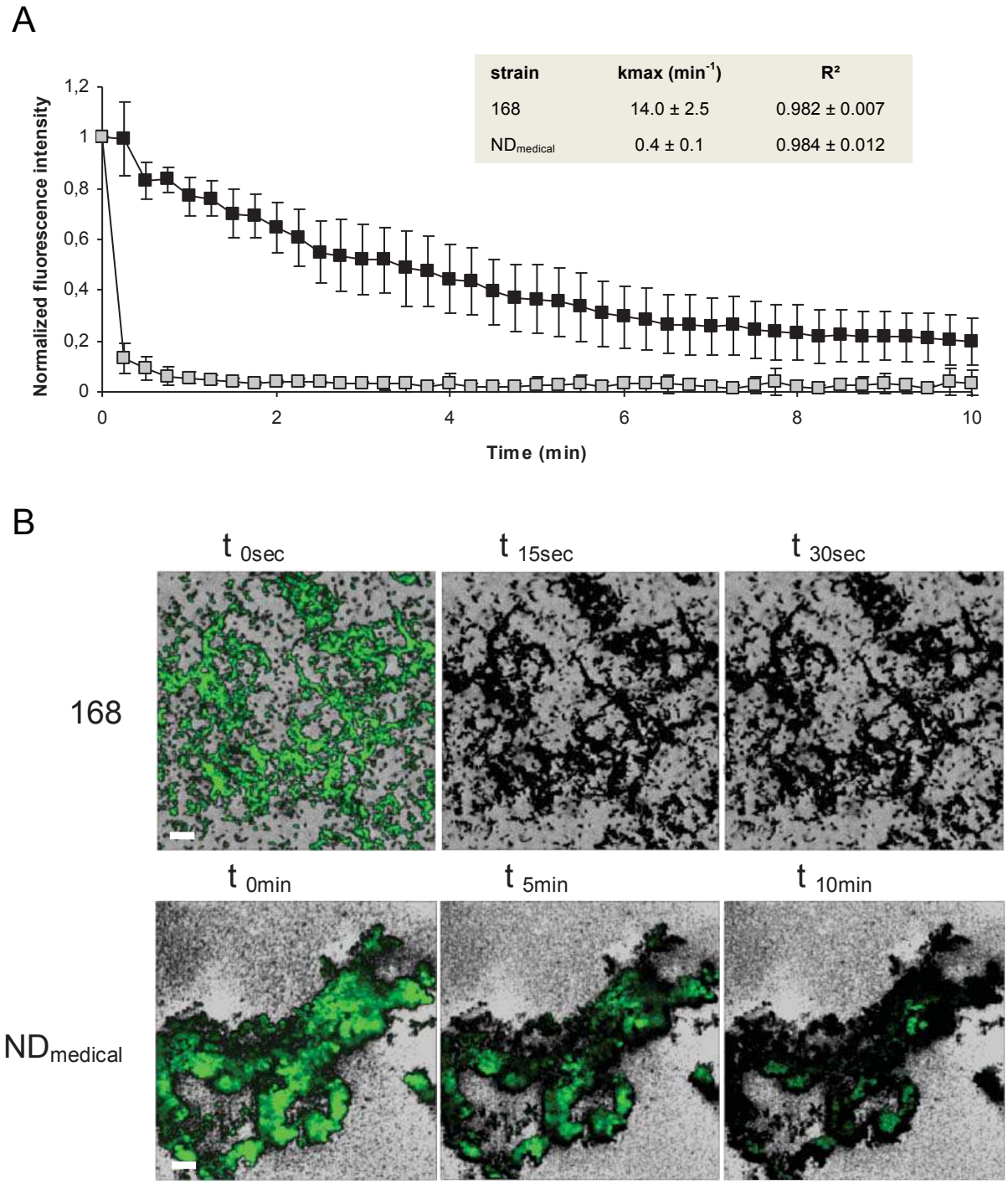

Figure 3. (A) Quantification of Chemchrome V6 fluorescence intensity in *B. subtilis* 168 (grey squares) and $ND_{medical}$ (black squares) biofilms during PAA treatment at 500 ppm. Values shown correspond to the average fluorescence at five depths in the biofilm with standard deviation for a representative experiment. Inactivation rate k_{max} was obtained after fitting the GinaFIT "Log linear + tail" inactivation model to experimental data. The mean of the three experiments ± standard deviation are presented in the inset. (B) Visualization of Chemchrome V6 fluorescence loss (membrane permeabilisation) in *B. subtilis* 168 and $ND_{medical}$ biofilms at 0, 15 and 30 s and 0, 5 and 10 min respectively during PAA treatment (0.05%). Each image corresponds to the superimposition of the green fluorescence image of a representative experiment on a grey scale image of the initial fluorescence at the same location. Scale bar correspond to 20 μm.

PAA resistance of the $ND_{medical}$ strain is dependent upon the 3D structure of the biofilm

The resistance to PAA (5 ppm) of cells following removal and washing from the biofilm of strain $ND_{medical}$ was investigated and compared to the resistance of th corresponding planktonic cells. Reductions of 2.9 ± 0.3 and 2.8 ± 0.1 Logs (cfu/ml) were obtained for planktonic cells and detached cells respectively i.e. no significant difference (P>0.05). The disruption of the biofilm and at least partial elimination of extracellular substances thus led to the disappearence of the PAA resistance suggesting an important role for the three-dimensional structure of the biofilm and therefore presumably the extracellular matrix in the resistance of $ND_{medical}$ biofilm.

In order to visualize the extracellular material produced in biofilms of both *B. subtilis* 168 and The $ND_{medical}$ strain, SEM observations were performed. In both cases, the extracellular material detected appeared to be composed of tangled thread-like strands forming a complex network. However, this was clearly much denser in the biofilm of the $ND_{medical}$ strain as shown in Fig. 4. It should be note here that SEM observations required several dehydration steps during sample preparation and therefore the electron micrographs cannot be considered faithful representations of fully hydrated biofilms. However, these results indicated that presence of larger amount of extracellular substances in $ND_{medical}$ strain biofilm could explain its high resistance to PAA.

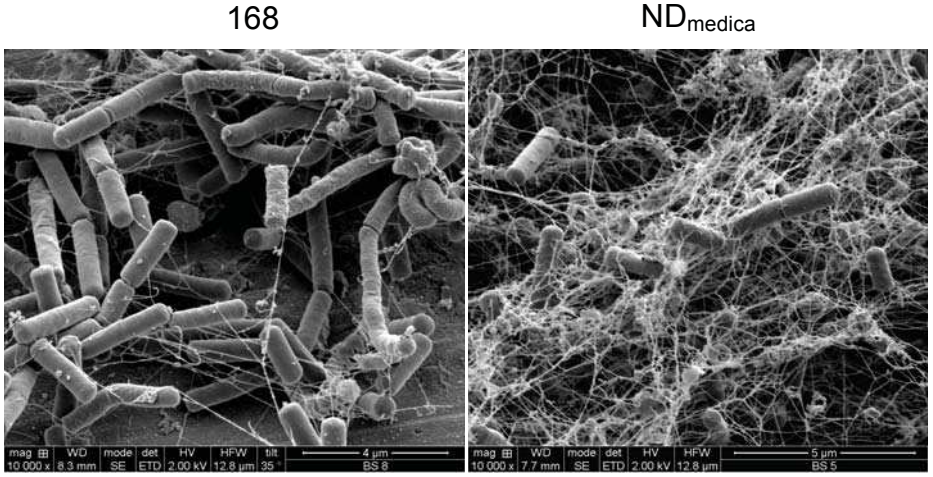

Figure 4. SEM images of 24h-biofilms of *B. subtilis* 168 and $ND_{medical}$ strains

Since cellulose (Hamon and lazazzera, 2001) and amyloid protein fibers (TasA) (Romero *et al.,* 2010) have been demonstrated to be components of the *B. subtilis* biofilm matrix, a method firstly used to investigate the ability of *Escherichia coli* or *Salmonella enterica* to produce cellulose and curli amyloid fibre (Zogaj *et al.,* 2003), was applied in order to

compare both *B. subtilis* strains. This method is based on the ability of cellulose to bind calcofluor and the ability of amyloid fibres to bind congo red on indicator plates. Macrocolonies of both *B. subtilis* strains grown for 72h on the appropriate indicator plates are presented in Fig. 5 A. First, we observed that $ND_{medical}$ produced highly wrinkled macrocolonies in comparison of strain 168. While no difference was observed between colonies of both strains for their ability to bind calcofluor and thus to produce cellulose, the $ND_{medical}$ strain stained red more intensively on Congo Red indicator plates suggesting a higher amount of amyloid fibres. The presence of amyloid fibres in strain $ND_{medical}$ 24 h-biofilms in microtiter plates was confirmed after thioflavin T staining and observation under CLSM (Fig. 5 B) Romero *et al.,* 2010).

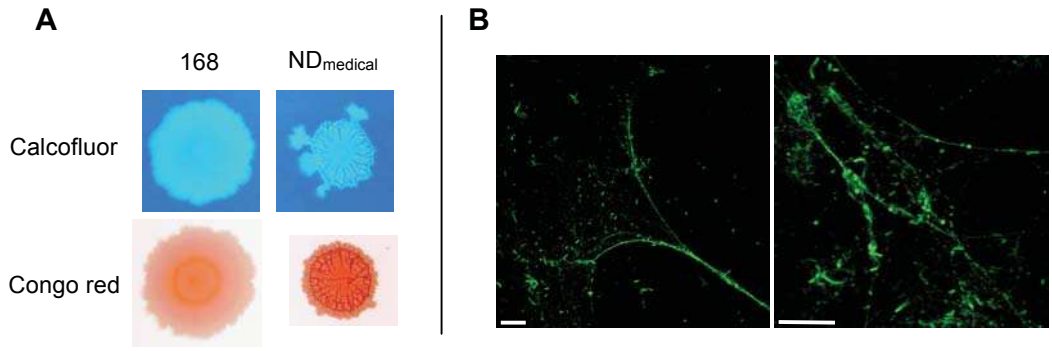

Figure 5. (A) Dye binding properties of *B. subtilis* 168 and $ND_{medical}$ macrocolonies grown for 72h on Calcofluor or Congo red indicator plates. (B) Confocal image of amyloid fibers in $ND_{medical}$ 24h-biofilm revealed by thioflavin T staining. Scale bars correspond to 20 μm.

The $ND_{medical}$ strain affords protection to *S. aureus* against PAA in a mixed biofilm

The previous results showed that the $ND_{medical}$ biofilm exhibited marked resistance to PAA treatment and suggested that the extracellular matrix probably plays an important role in this resistance. We next investigated whether the $ND_{medical}$ biofilm can provide protection in a mixed biofilm to *S. aureus*, a pathogenic strain present in medical environments and often incriminated in nosocomial infections.

As shown on Fig. 6 A, *S. aureus* alone produced flat and regular biofilm with a thickness of 20-30 µm. When this single species biofilm was exposed to 3500 ppm of PAA for 5 min, the small numbers of survivors on plates corresponded to a more than 7.3 Logs of reduction

compared to distilled water control (Tab. 2). However, when growing in a mixed biofilm with *B. subtilis* $ND_{medical}$, the same PAA treatment produced a 5.9 Logs reduction of *S. aureus* suggesting that pathogenic strain acquired benefit from strain association. Note that *B. subtilis* $ND_{medical}$ resistance to PAA was similar in both single and mixed biofilms with 3.8 and 3.4 Logs reduction respectively. In contrast, mixed biofilm composed of the lab strain *B. subtilis* 168 and *S. aureus* AH478 did gain a higher resistance to PAA compared to the single species biofilms.

		Log (CFU/well)	
	Strain	water	0,35% PAA
Single species biofilm	*B. subtilis* 168	7.6 ± 0.2	-
	B. subtilis NDmedical	7.7 ± 0.1	3.9 ± 0.6
	S.aureus AH478	9.3 ± 0.1	-
Mixed species biofilm	*B. subtilis* 168	7.5 ± 0.5	-
	S.aureus RN4220	8.2 ± 0.4	-
	B. subtilis NDmedical	7.3 ± 0.3	3.9 ± 0.3
	S.aureus RN4220	8.4 ± 0.1	2.5 ± 0.5

Table 2. Log (cfu/well) after 5 min treatment by water or 0.35% PAA for single and mixed species biofilms. Data shown are the mean of three experiments ± standard deviation. Samples from which no survivors were recovered are represented by (-). Minimum detection of < 2 Logs cfu/well.

Confocal observations showed that, in the presence of *S. aureus* AH478, *B. subtilis* $ND_{medical}$ was able to develop three-dimensional structures similar to those observed in the single species biofilm of this strain (Fig. 6 B). The *S. aureus* cells largely covered the surface of the bottom of the wells not occupied by the *B. subtilis* strain although some cells were trapped in the protruding structures formed by the $ND_{medical}$ strain as shown by confocal section in figure 7 B.

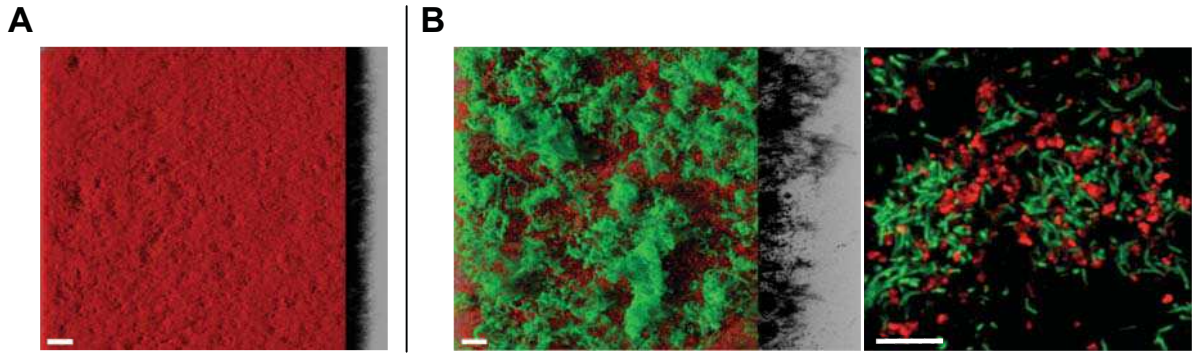

Figure 6. (A) 3D reconstruction of *S.aureus* AH478 mCherry biofilms. (B) 3D reconstruction and section at higher magnification of a mixed species biofilm of *B. subtilis* $ND_{medical}$ GFP (green) / *S. aureus* AH478 mcherry (red). Scale bars correspond to 20 μm.

DISCUSSION

In a previous study, Martin et al. (2008) isolated a stable strain of *B. subtilis* (called $ND_{medical}$ in this study) from an endoscope washer-disinfector and showed that this strain developed a high resistance against various oxidising agents using a standard suspension test. On the basis of SEM observations, they suggested that this resistance could be due to a higher production of matrix in comparison with sensitive strains. Recently, we showed that this stable isolate produces a very thick biofilm with specific protruding and elevated structures in comparison to other *B. subtilis* strains (Bridier *et al.,* 2011), and was confirmed by our present observations. As biofilm formation is frequently associated with increased resistance to sanitizing treatments and antibiotic therapies (Pan *et al.,* 2006; Cooper and Hanlon, 2010; Ito *et al.,* 2009), the enhanced biofilm-forming ability of strain $ND_{medical}$ can thus represent a strategy to survive despite the regular exposure to biocide treatments. In line with this, Shemesh et al (2010) showed that sublethal doses of chlorine actually stimulated biofilm formation by *B. subtilis* reflecting an apparent defensive response against biocide action. In addition, it has been shown in *P. aeruginosa* that hyper-biofilm forming variants appear due to self-generated diversity that occurred in the biofilm, was correlated with higher resistance of the whole community to hydrogen peroxide (Boles *et al.,* 2004). Our present results showed a very high resistance of the $ND_{medical}$ biofilm to PAA, an oxidizing agent commonly used in endoscope disinfection, highlighting that biofilm formation can indeed enable this strain to persist despite drastic disinfection treatments applied during endoscope decontamination. Some evidence appears to suggest that this high resistance could be mainly

related to an increased production of extracellular matrix in agreement with the previous observations made by Martin et al. (2008) with planktonic cells. First, the disruption of the three-dimensional biofilm structure and washing of cells led to the restoration of a PAA sensitivity similar to that observed for planktonic cells. In addition, SEM observations clearly showed that the $ND_{medical}$ strain produced a denser and more abundant biofilm matrix when compared with strain 168, which was much more sensitive to PAA. This abundant matrix could play a protective role through the interaction with and the quenching of PAA that reduces penetration into the biofilm. Previous studies reported that penetration limitations encountered by chlorine, another oxidising agent, in biofilms of different species can explain at least partly the reduced activity of PAA probably resulting from interactions with biofilm constituents (De Beer *et al.,* 1994; Grobe *et al.,* 2002; Jang *et al.,* 2006). Kinetic profiles and spatial patterns of fluorescence loss (cell membrane permeabilization) obtained using CLSM time lapse visualization of PAA action in the $ND_{medical}$ biofilm (Fig. 3, video S2 in supplementary material) were consistent with these observations. In particular, the progressive action of PAA in the heterogeneous structure with cells in some internal areas remaining fluorescent even after 10 min of treatment. The *Bacillus subtilis* biofilm matrix has been shown to be composed predominantly of exopolysaccharides resulting from the expression of the 15-gene *epsA-O* operon (Branda *et al.,* 2004; Kearns *et al.,* 2005; Blair *et al.,* 2008) and the TasA protein (forming amyloid fibres) resulting from the expression of the *yqxM-tasA-sipW* operon (Branda *et al.,* 2006; Romero *et al.,* 2010). We confirmed that the $ND_{medical}$ 24 h-biofilm contained amyloid fibres after thioflavine staining and CLSM observations (Fig. 5 B). Moreover, since we found that $ND_{medical}$ macrocolonies bound the amyloid-specific Congo Red dye more intensively than strain 168, it is tempting to speculate that this strain produced more TasA protein. Amyloids are filamentous protein structures formed by the assembly of monomers into intermolecularly hydrogen bonded cross β-sheets (Fowler *et al.,* 2007). Prions are the most studied amyloid proteins due to their implication in neurodegenerative diseases (Chiti *et al.,* 2006) and demonstrated a high resistance to standard decontamination treatment including protease, radiation and chemical treatments (Fichet *et al.,* 2004, Giles *et al.,* 2009). Curli constitutes another kind of amyloid fiber which is present on the membrane surface of bacterial species such as *Escherichia coli* or *Salmonella enterica,* which have been identified as playing a role in cell aggregation, adhesion to surface and biofilm formation (Römling *et al*., 1998; Chapman *et al*., 2002). Interestingly, Ryu and Beuchat (2005) reported that a curli hyper-producing mutant of *E. coli* 0157:H7 demonstrated

a higher resistance to chlorine than the wild-type strain, showing that curli afford effective protection to bacteria. In our case, a higher production of amyloid fibres of TasA in the $ND_{medical}$ biofilm may thus constitute an efficient protection against PAA. However, additional experiments are needed to better characterize the exopolymeric matrix composition of $ND_{medical}$ biofilm and to explain precisely the origin of the resistance observed.

We also investigated, whether *S. aureus* can be protected from disinfection in a mixed biofilm with *B. subtilis* $ND_{medical}$ strain. *S. aureus* is a bacterial pathogen commonly found in hospitals and responsible for a large number of infections (Perl and Golub, 1998; Gardam, 2000). Moreover, numerous studies have in particular reported the presence of *S. aureus* on endoscopes even after disinfection procedures (Lee *et al.,* 1998; Machado *et al.,* 2006). Results demonstrated that more than 7.3 Logs of reduction (no survivor was enumerated) were obtained for *S. aureus* single species biofilm after PAA treatment at 3500 ppm whereas we found only 5.9 Logs of reduction when growing in mixed biofilm with $ND_{medical}$ strain (Tab. 2). These results showed a protective effect of the presence of *B. subtilis* $ND_{medical}$ strain to *S. aureus* against PAA activity. Confocal images revealed that some *S. aureus* cells were entrapped in the protruding structures formed by the $ND_{medical}$ strain and thus probably benefited from the protective matrix of the *B. subtilis* strain. Different works already reported that species associations in mixed biofilms can result in a higher resistance to disinfection compared to single species biofilms (Burmølle *et al.,* 2006; Kara *et al.,* 2006; Simões *et al.,* 2009; Simões *et al.,* 2010) and that some species can protect another throughout interspecies spatial associations. Leriche et al (2003) reported for instance that *S. sciuri* was protected in a mixed biofilm against a chlorinated solution by microcolonies formed by *Kocuria* sp., a more resistant strain. As it is clear that microbial communities present in medical or industrial areas are complex multispecies associations rather than controlled single species model, these findings highlight the importance to challenge biocides on representative biofilm models of the environment considered.

In conclusion, this work points out that the selection pressure maintained in healthcare environments by regular disinfection treatments can lead to the emergence of strains with hyper-resistance phenotypes. This is related to the great ability of bacteria to adapt to their environments developing efficient survival strategies such as biofilm development. Particular attention should thus be placed on the choice of strains which are representative of the reality of medical areas in disinfectant testing. In addition, the necessity to consider the resident

microbial ecosystem (including non-pathogenic but hyper resistant strains as *B. subtilis* $ND_{medical}$) instead of pathogen alone is emphasized since the persistence of a strain can be related not directly to its intrinsic resistance but also from the interactions with other species present in the environment. Future works will focuses on the understanding of the adaptation mechanisms leading to an increased resistance of bacteria to biocides in these environments. Genome of strain $ND_{medical}$ in now in sequencing to this end.

ACKNOWLEDGEMENTS

This study received support from the "MEDICEN-Region Paris, Ile-de-France" Competitiveness Cluster. The Essonne Department is acknowledged for its financial support of the confocal microscopy facility (ASTRE n°A02137). We would like to thank Drs. J.-Y Maillard for *B. subtilis* $ND_{medical}$ strain , C.L. Malone for *S. aureus* AH478 mCherry strain and D. Rudner for plasmid pDR146.

REFERENCES

Anonymous. 1997. Chemical disinfectants and antiseptics - basic bactericidal activity – test method and requirements (phase 1). Ed. AFNOR.1997.NF EN 1040.

Blair KM, Turner L, Winkelman JT, Berg HC and Kearns DB. 2008. A molecular clutch disables flagella in the Bacillus subtilis biofilm. *Science*. 320: 1636–1638.

Boles BR, Thoendel, M and Singh PK. 2008. Self-generated diversity produces "insurance effects" in biofilm communities. *Proc. Natl. Acad. Sci.* 101: 16630-16635.

Branda SS, Gonzalez-Pastor JE, Dervyn E, Ehrlich D, Losick R, et al. 2004. Genes involved in formation of structured multicellular communities by Bacillus subtilis. *J. Bacteriol*. 186: 3970–3979.

Branda SS, Chu F, Kearns DB, Losick R and Kolter R. 2006. A major protein component of the Bacillus subtilis biofilm matrix. *Mol. Microbiol*. 59: 1229–1238.

Bridier A., Dubois-Brissonnet F, Boubetra A, Thomas V and Briandet R. 2010. The biofilm architecture of sixty opportunistics pathogens deciphered using a high throughput CLSM method. *J. Microbiol. Methods* 82: 64-70.

Bridier A, Le Coq D, Dubois-Brissonnet F, Thomas V, Aymerich S, et al. 2011. The Spatial Architecture of Bacillus subtilis Biofilms Deciphered Using a Surface-Associated Model and in situ Imaging. *PLoS ONE*. 6(1): e16177. doi:10.1371/journal.pone.0016177.

Burmølle M, Webb JS, Rao D, Hansen LH, Sørensen SJ, Kjelleberg S. 2006. Enhanced biofilm formation and increased resistance to antimicrobial agents and bacterial invasion are caused by synergistic interactions in multispecies biofilms. *Appl. Environ. Microbiol*. 2006. 72: 3916-23.

Chapman MR, Robinson LS, Pinkner JS, Roth R, Heuser J, Hammar M, Normark S and Hultgren SJ. 2002. Role of Escherichia coli curli operons in directing amyloid fiber formation. *Science*. 295: 851-5.

Chiti Z, Knutsen OM, Betmouni S and Greene JR. 2006. An integrated, temporal study of the behavioural, electrophysiological and neuropathological consequences of murine prion disease. *Neurobiol. Dis*. 22 : 363-373.

Cloete ET. 2003. Resistance mechanisms of bacteria to antimicrobial compounds. *Int. Biodeterior. Biodegrad*. 51: 277-282.

Cooper IR and Hanlon GW. 2010. *Resistance of* Legionella pneumophila *serotype 1 biofilms to chlorine-based disinfection*. *J. Hosp. Infect*. 74:152-159.

De Beer D, Srinivasan R and Stewart PS. 1994. Direct Measurement of Chlorine Penetration into Biofilms during Disinfection. *App. Environ. Microbiol*. 60: 4339-434.

Deva AK, Vickery K, Zou j, West RH, Selby W *et al*. 1998. Detection of persistent vegetative bacteria and amplified viral nucleic acid from in-use testing of gastrointestinal endoscopes. *J. Hosp. Infect*. 39: 149-157.

DiazGranados CA, Jones MY, Kongphet-Tran T, White N, Shapiro M, *et al*. 2009. Outbreak of Pseudomonas aeruginosa infection associated with contamination of a flexible bronchoscope. *Infect. Control. Hosp. Epidemiol*.30: 550-555.

Donlan RM and Costerton JW. 2002. Biofilms: survival mechanisms of clinically relevant microorganisms. *Clin. Microbiol. Rev*. 15: 167-192

Fichet G, Comoy E, Duval C, Antloga K, Dehen C, Charbonnier A, McDonnell G, Brown P, Lasmézas CI and Deslys JP. 2004. Novel methods for disinfection of prion-contaminated medical devices. *Lancet*. 364: 521-526.

Fowler DM, Koulov AV, Balch WE and Kelly JW. *2007*. Functional *amyloid* - from bacteria to humans. *Trends Biochem. Sci*. 32: 217-224.

Francolini I and Donelli G. 2010. Prevention and control of biofilm-based medical-device-related infections. *FEMS Immunol. Med. Microbiol*.59:227-238.

Gardam MA. 2000. Is methicillin-resistant Staphylococcus aureus an emerging community pathogen? A review of the literature. *Can. J. Infect. Dis*. 11: 202-11.

Geeraerd, AH, Valdramidis VP and Van Impe JF. 2005. GInaFiT, a freeware tool to assess non-log-linear microbial survivor curves. *Int. J. Food Microbiol*. 102:95-105.

Giles K, Glidden DV, Beckwith R, Seoanes R, Peretz D, et al. 2008. Resistance of Bovine Spongiform Encephalopathy (BSE) Prions to Inactivation. *PLoS Pathog*. 4(11): e1000206. doi:10.1371/journal.ppat.1000206.

Grobe KJ, Zahller J and Stewart PS. Role of dose concentration against biocide efficacy in *Pseudomonas aeruginosa* biofilms. *J. Ind. Microbiol. Biotechnol*. 29: 10-15

Hamon MA and Lazazzera BA. 2001. The sporulation transcription factor Spo0A is required for biofilm development in Bacillus subtilis. *Mol Microbiol* 42: 1199–1209.

Hoffman LR , D'Argenio DA , MacCoss MJ , Zhang Z, Jones RA and Miller SI. 2005. Aminoglycoside antibiotics induce bacterial biofilm formation. *Nature Let*. 436: 1171-1175

Høiby N, Bjarnsholt T, Givskov M, Molin S and Ciofu O. 2010. Antibiotic resistance of bacterial biofilms. *Int. J. Antimicrob. Agents*. 35: 322-332.

Ito A, Taniuchi A, May T, Kawata K and Okabe S. 2009. Increased Antibiotic Resistance of Escherichia coli in Mature Biofilms. *App. Environ. Microbiol*. 75: 4093-4100.

Jang A, Szabo J, Hosni AA, Coughlin M and Bishop PL. 2006. Measurement of chlorine dioxide penetration in dairy process pipe biofilms during disinfection. *App. Environ. Microbiol*. 72:368-376.

Kara D, Luppens SB and Cate JM. 2003. Differences between single- and dual-species biofilms of Streptococcus mutans and Veillonella parvula in growth, acidogenicity and susceptibility to chlorhexidine. *Eur. J. Oral Sci*. 114: 58-63.

Kearns DB, Chu F, Branda SS, Kolter R and Losick R. 2005. A master regulator for biofilm formation by Bacillus subtilis. *Mol. Microbiol*. 55: 739–749.

Kressel AB and Kidd F. 2001. Pseudo-outbreak of Mycobacterium chelonae and *Methylobacterium mesophilicum* caused by contamination of an automated endoscopy washer. *Infect. Control. Hosp. Epidemiol*. 22 :414-418.

Lee RM, Kozarek RA, Sumida SE and Raltz SL. 1998. Risk of contamination of sterile biopsy forceps in disinfected endoscopes. *Gastrointest. Endosc*. 47: 377-381.

Leriche V, Briandet R and Carpentier B. 2003. Ecology of mixed biofilms subjected daily to a chlorinated alkaline solution: spatial distribution of bacterial species suggests a protective effect of one species to another. *Environ. Microbiol*. 5: 64-71.

Machado AP, Pimenta AT, Contijo PP, Geocze S, Fischman O. 2006. Microbiologic profile of flexible endoscope disinfection in two Brazilian hospitals. *Arq. Gastroenterol*. 43: 255-258.

Malone CL, Boles BR, Lauderdale KJ, Thoendel M, Kavanaugh JS, Horswill AR. 2009. Fluorescent reporters for *S. aureus*. *J. Microbiol. Methods*. 77: 251-260.

Martin DJH, Denyer SP, McDonnell G and Maillard JY. 2008. Resistance and cross-resistance to oxidising agents of bacterial isolates from endoscope washer disinfectors. J. Hosp. Infect. 69: 377-383.

Pan Y, Breidt Jr. F and Kathariou S. 2006. Resistance of *Listeria monocytogenes* Biofilms to Sanitizing Agents in a Simulated Food Processing Environment. *App. Environ. Microbiol. 72:*7711-7717

Perl TM and Golub JE. 1998. New approaches to reduce *Staphylococcus aureus* nosocomial infection rates: treating S. aureus nasal carriage. *Ann. Pharmacother*. 32:S7-16.

Potera C 1999. Forging a link between biofilms and disease. *Science*. 283: 1837–1839.

Romero D, Aguilar C, Losick R and Kolter R. 2010. Amyloid fibers provide structural integrity to Bacillus subtilis biofilms. *Proc Natl Acad Sci USA* 107: 2230–2234.

Römling U, Bian Z, Hammar M, Sierralta WD, Normark S. 1998. Curli fibers are highly conserved between *Salmonella typhimurium* and *Escherichia coli* with respect to operon structure and regulation. *J. Bacteriol*. 180: 722-731.

Rutala WA and Weber DJ. 2004. Reprocessing endoscopes: United States perspective. *J. Hosp. Infect*. 56:S27-39

Ryu JH and Beuchat LR. 2005. Biofilm formation by *Escherichia coli* O157:H7 on stainless steel: effect of exopolysaccharide and Curli production on its resistance to chlorine. *Appl. Environ. Microbiol*. 71: 247-54.

Shemesh M, Kolter R and Losick R. 2010. The biocide chlorine dioxide stimulates biofilm formation in *Bacillus subtilis* by activation of the histidine kinase KinC. *J. Bacteriol*. 192: 6352–6356.

Simões M, Simões LC, Vieira MJ. 2009. Species association increases biofilm resistance to chemical and mechanical treatments. *Water Res*. 43: 229-237.

Simões LC, Simões M, Vieira MJ. 2010. Influence of the diversity of bacterial isolates from drinking water on resistance of biofilms to disinfection. Appl. Environ. Microbiol. 76: 6673-6679.

Spach DH, Silverstein FE and Stamm WE. 1993. Transmission of infection by gastrointestinal endoscopy and bronchoscopy. *Ann. Intern. Med*. 118 : 117-128.

Srinivasan A, Wolfenden LL, Song X, Mackie K, Hartsell TL, *et al*. 2003. An outbreak of Pseudomonas aeruginosa infections associated with flexible bronchoscopes. *N. Engl. J. Med*. 348: 221-227.

Zogaj X, Nimtz M, Rohde M, Bokranz W and Romling U. 2001. The multicellular morphotypes of *Salmonella typhimurium* and *Escherichia coli* produce cellulose as the second component of the extracellular matrix. *Mol Microbiol* 39: 1452–1463.

CONCLUSION GENERALE ET PERSPECTIVES

La qualité microbiologique des surfaces est une problématique récurrente dans les secteurs industriels et de santé. Des traitements de nettoyage/désinfection sont régulièrement appliqués pour assurer l'hygiène des surfaces dans ces environnements mais ils ont parfois une efficacité limitée, ce qui peut engendrer des problèmes particulièrement importants sur le plan de la santé publique. Ceci peut s'expliquer par le fait que les normes d'évaluation de l'efficacité bactéricide des désinfectants sont basées sur des protocoles qui ne reflètent pas la réalité du terrain. En effet, ces tests sont réalisés sur des espèces/souches de référence qui ne sont pas forcément représentatives de la diversité et la résistance bactérienne rencontrées dans les environnements industriels ou médicaux (**article 7** en annexe) et sont basés sur l'utilisation des cellules en suspension ou déposées et séchées, occultant l'état « biofilm ». Or, quels que soient les matériaux utilisés pour les équipements industriels ou médicaux, les bactéries présentes dans l'environnement peuvent, en milieu humide, adhérer aux surfaces et former des biofilms. La formation de ces structures engendre une résistance accrue des cellules incluses vis-à-vis des traitements de désinfection. Un apport de connaissances scientifiques sur ces édifices biologiques tridimensionnels et notamment sur les mécanismes impliqués dans leur résistance est donc primordial afin d'optimiser les traitements de désinfection. Pour répondre à cette problématique, du fait du lien intime existant entre l'architecture du biofilm et sa résistance, nous nous sommes appuyés dans ce travail de thèse sur des techniques d'imagerie non invasive permettant une analyse *in situ* de la structure, de la dynamique et de la réactivité de ces communautés bactériennes.

Dans une première étape, une méthode structurale haut-débit basée sur l'utilisation d'une microplaque 96 puits combinée à la microscopie confocale laser à balayage a été développée afin d'étudier la diversité architecturale des biofilms bactériens formés par une large palette de souches. Nous avons ainsi pu identifier des souches produisant des biofilms importants et avec des motifs structuraux spécifiques comme *P. aeruginosa* formant des structures en champignon ou *E. faecalis* formant des biofilms plats et homogènes. Ce système nous a permis de mettre en évidence la capacité de *B. subtilis* à former des structures particulières sur une surface immergée notamment pour une souche isolée d'un dispositif médical (souche $ND_{medical}$). Cette souche pouvait atteindre dans notre système des hauteurs de plus de 300 µm avec une architecture spécifique non décrite dans la littérature. Afin de mieux comprendre la mise en place de ces structures, la souche $ND_{medical}$ a été rendue autofluorescente par une construction GFP pour permettre le suivi du développement du biofilm en temps réel par microscopie confocal laser à balayage. De façon assez inattendue,

nous avons pu constater que cette souche de terrain était transformable par les procédés classiquement utilisés avec la souche de laboratoire 168. En effet, la souche *B. subtilis* 168 a été obtenue à partir de la souche parentale « marburg » (NCIB3610 ou ATCC6051) après « domestication » au laboratoire, ce qui la rendue naturellement compétente facilitant ainsi les manipulations génétiques (Anagnostopoulos & Spizizen, 1961, Zeigler *et al.*, 2008). Cependant, cette domestication a entraîné la perte de certains déterminants génétiques nécessaires à la formation de biofilm robustes (McLoon *et al.*, 2011). Le caractère transformable de la souche $ND_{medical}$ est donc intéressant dans le sens où les souches présentant un phénotype biofilm fort et actuellement utilisées pour étudier les communautés multicellulaires de *B. subtilis* (souches qualifiées de « sauvage » comme la souche NCIB3610) ne présentent pas cette compétence naturelle. Elles sont classiquement modifiées génétiquement par transduction, un procédé plus lourd à mettre en œuvre que la transformation (Nijland *et al.*, 2010a). La souche atypique $ND_{medical}$ pourrait donc constituer une nouvelle souche modèle pour l'étude des biofilms de *B. subtilis* de part sa capacité à former des biofilms importants et sa compétence naturelle.

Le suivi dans le temps de la formation des biofilms de la souche $ND_{medical}$ GFP par microscopie confocale a révélé un développement en deux étapes. Cette dynamique fait intervenir une transition brutale de l'état « chaînettes adhérées » à l'état « cellules planctoniques libres » quelques heures après l'adhésion, suivie d'une reprise du développement du biofilm immergé au bout de quelques heures. Ce phénomène a également été observé pour la souche de référence 168 montrant que cette dynamique n'est pas spécifique à la souche atypique $ND_{medical}$ et qu'elle pourrait potentiellement s'appliquer plus largement à l'espèce. Cette disruption brutale et coordonnée du biofilm précoce suggère le déclenchement d'un système de signalisation intercellulaire de type quorum-sensing en réponse à l'augmentation de la densité cellulaire dans le fond du puits. La construction de souches portant des fusions transcriptionnelles GFP sous contrôle des gènes de mobilité (*hag)*, des autolysines (*lyt*), de la synthèse d'EPS (*epsA-O*, *yqxM-sipW-TasA*), ou de régulateurs (*slrR*, *sinR)* associée au suivi de la dynamique structurelle des biofilms par microscopie confocale laser à balayage pourrait permettre de mieux identifier les mécanismes de régulation génétique impliqués dans ce phénomène. Ces différents gènes jouent en effet un rôle dans le développement du biofilm et la transition entre l'état « chaînette » et l'état « cellules libres mobiles » (Chai *et al.*, 2010b, Kobayashi, 2008).

De plus, une meilleure compréhension de la nature du signal moléculaire et des processus responsables du détachement des cellules pourrait permettre d'identifier des cibles intéressantes pour des applications thérapeutiques ou de décontamination alternatives, une voie de recherche en plein essor (Kaplan, 2010). En effet, différentes molécules signal entrainant la dispersion du biofilm tels que l'acide gras cis-2-décanoïque (Davies & Marques, 2009) ou l'oxyde nitrique (Barraud *et al.*, 2006) ont déjà été identifiés chez *P. aeruginosa* par exemple. Des processus de dispersion impliquant la production d'enzymes dégradant les composés de la matrice extracellulaire (Boles & Horswill, 2008, Karatan & Watnick, 2009, Nijland *et al.*, 2010b) ou de substances tensioactives comme les rhamnolipides (Boles *et al.*, 2005, Kaplan, 2010) ont également été mis en évidence chez différentes espèces telles que *Vibrio cholerae*, *S. aureus*, *P . aeruginosa*, *Streptococcus mutans*. Chez *B. subtilis*, il a récemment été montré qu'un mélange d'acides aminés (D-leucine, D-méthionine, D-tyrosine, et D-tryptophane), à des concentrations nanomolaires, entrainerait la déstructuration du biofilm en provoquant le détachement de fibres protéiques (TasA) ancrées aux cellules et assurant le maintien de la structure (Kolodkin-Gal *et al.*, 2010).

L'utilisation de notre système de microplaque combiné à la microscopie confocale laser à balayage, nous aura permis d'identifier des souches et des phénomènes intéressants dans l'étude des biofilms. D'un aspect méthodologique, cette approche haut-débit ouvre de nouvelles possibilités quant à la compréhension des mécanismes impliqués dans la formation et la réactivité des biofilms. En plus d'une simple quantification globale, le fait de pouvoir extraire différents descripteurs structuraux (rugosité, hauteur moyenne, pourcentage de recouvrement,…) permet de caractériser plus finement le biofilm et ouvre des possibilités d'analyse statistiques comparatives à grande échelle. Par exemple, l'application de cette méthodologie au criblage de banques de mutants génétiques donne la possibilité d'étudier le rôle de gènes candidats d'un réseau de régulation entier au travers d'une approche structurale globale. Le criblage de chimiothèques de molécules anti-biofilm peut également être envisagé permettant d'accéder à un niveau supérieur d'information sur l'activité des molécules grâce aux données structurales. Le développement d'outils d'automatisation, de l'acquisition des données par la programmation du microscope pour scanner la microplaque (comme l'application *high content screening* très récemment développée par LEICA) jusqu'au traitement des séries d'images confocales obtenues (logiciels PHLIP (Xavier *et al.*, 2003) ou ISA3D (Beyenal *et al.*, 2004)), offre des perspectives prometteuses en termes d'amplification

du débit de données acquises et devrait ainsi participer à une meilleure compréhension des relations structure/fonction au sein des biofilms.

La deuxième partie du travail a consisté en l'étude des mécanismes de résistance des bactéries en biofilm. Pour cela, une technique de visualisation en temps réel basée sur la microscopie confocale laser à balayage couplée à un marquage fluorescent spécifique a été adaptée et utilisée. Le suivi, par cette technique non-invasive, de la perte de fluorescence au sein de la structure des biofilms en fonction du temps a permis d'obtenir des informations utiles à la compréhension des phénomènes limitant l'activité des désinfectants testés. Deux modèles bactériens ont été choisis pour cette étude d'après l'analyse architecturale réalisée dans la première partie : *Pseudomonas aeruginosa* et *Bacillus subtilis*.

Concernant *Pseudomonas aeruginosa*, nous avons étudié dans un premier temps l'action de l'acide péracétique et du chlorure de benzalkonium au sein des biofilms formés par la souche ATCC 15442, une des souches de référence des normes d'évaluation de l'activité bactéricide des désinfectants et qui formait dans notre système des structures tridimensionnelles importantes. Les cinétiques d'inactivation obtenues se sont avérées très différentes selon le désinfectant utilisé illustrant le mode d'action et la réactivité spécifique de chaque molécule. Nous avons pu mettre en évidence les difficultés de pénétration du chlorure de benzalkonium au sein des structures « en champignons », ce qui pourrait expliquer la résistance des biofilms à ce désinfectant. Des phénomènes similaires ont pu être observés dans les biofilms formés par trois souches cliniques. Les paramètres cinétiques d'inactivation, extraits des courbes de fluorescence, ont pu être corrélés avec les données obtenues par la caractérisation biochimique de la matrice (teneur en protéines et en sucres) pour les quatre souches, ce qui suggère ici un rôle majeur des substances extracellulaires dans la limitation de pénétration du désinfectant.

Dans un deuxième temps, nous nous sommes intéressés à la résistance du biofilm formé par la souche *B. subtilis* $ND_{medical}$ à l'acide péracétique. Cette souche manifestait une grande capacité à former des biofilms dans notre système microplaque et le fait qu'elle ait été isolée d'un laveur-désinfecteur d'endoscope en fait un cas d'étude concret du domaine médical. Les résultats ont montré une résistance marquée du biofilm de la souche $ND_{medical}$ à la concentration et au temps d'utilisation du biocide dans le milieu médical confirmant la

capacité de persistance de cette souche malgré les traitements utilisés pour la décontamination des endoscopes. Cette hyper-résistance du biofilm apparaît être liée au moins en partie à une production importante de substances extracellulaires. En effet, les résultats des observations réalisées en microscopie confocale en temps réel ont révélé une perte de viabilité membranaire progressive des cellules au sein du biofilm avec des zones dans la structure qui restaient fluorescentes après 10 minutes de traitement. Les observations réalisées en microscopie électronique à balayage et les résultats obtenus par les tests de désinfection sur les cellules resuspendues et lavées confortent l'idée que la matrice dense du biofilm de la souche $ND_{medical}$ pourrait interférer avec l'acide péracétique et ainsi limiter son efficacité au sein de la structure.

D'un point de vue méthodologique, la technique non-invasive de visualisation de l'action de désinfectants dans les biofilms utilisée ici a démontré des potentialités intéressantes pour la compréhension des phénomènes limitant leur efficacité dans ces structures. Cependant, une des limitations de cette technique est le fait qu'elle ne soit compatible qu'avec des molécules entrainant une perméabilisation de la membrane cellulaire. De plus, la perte de fluorescence des cellules signifie qu'elles ont été rendues plus perméables par le traitement mais ne correspond pas nécessairement à une perte totale de viabilité des bactéries et réciproquement. Des développements sont nécessaires afin d'établir une corrélation plus étroite entre la perte de fluorescence observée et la perte de viabilité cellulaire et cela requiert des données expérimentales propres à chaque désinfectant et chaque modèle bactérien. Il est également nécessaire d'obtenir une meilleure compréhension des interactions spécifiques entre les désinfectants et les marqueurs de viabilité du fait de leur importance sur la cinétique d'extinction de la fluorescence.

D'un point de vue biologique, les résultats obtenus avec les différentes souches et désinfectants montrent de manière générale un rôle majeur de la matrice extracellulaire dans la résistance des biofilms. La nature de cette matrice complexe est très variable en fonction des souches, hétérogène et évolue avec l'âge du biofilm et les conditions environnementales. Cette spécificité de nature conditionne une réactivité différente selon les souches considérées et qui peut varier selon les caractéristiques physico-chimiques du désinfectant comme nous l'avons vu avec le chlorure de benzalkonium entre les différentes souches de *P. aeruginosa* ou avec l'acide péracétique entre la souche *P. aeruginosa* ATCC 15442 et la souche *B. subtilis* $ND_{medical}$. Une caractérisation plus fine de cet espace intercellulaire apparaît donc nécessaire à

une meilleure compréhension des limitations rencontrées par les désinfectants. L'utilisation de techniques telles que la FCS (Fluorescence correlation spectroscopy) permettant de mesurer la mobilité particulaire de sondes fluorescentes fonctionnalisées (par greffage de groupements hydrophobes/hydrophiles ou chargés par exemple) au sein du biofilm pourrait constituer une approche complémentaire à la méthode de visualisation en temps réel utilisé dans ce travail procurant des informations précises sur l'hétérogénéité physico-chimique locale et la dynamique de la matrice (Guiot *et al.*, 2002, Aldeek, 2010). De même, d'autres techniques d'analyse *in situ* telles que la spectroscopie infra-rouge (FTIR, fourrier transform infra-red) (Holman *et al.*, 2009), la spectroscopie Raman (Ivleva *et al.*, 2009) ou la microscopie à rayon X (STXM, scanning transmission X-ray microscopy) (Dynes *et al.*, 2009) pourraient permettre de mieux caractériser la composition biochimique de la matrice et ainsi d'identifier plus précisément la nature des interactions entre les biocides et les constituants du biofilm.

L'exemple de la souche *B. subtilis* $ND_{medical,}$ isolée d'un laveur-désinfecteur d'endoscopes, illustre bien la capacité des bactéries à s'adapter aux environnements les plus hostiles. La sélection de bactéries résistantes du fait de mutations génétiques par les traitements régulièrement appliqués dans les environnements industriels et médicaux constitue en effet une problématique majeure en termes de sécurité sanitaire. Le biofilm peut constituer lui-même un environnement favorable aux processus d'adaptation. Boles *et al*. (Boles *et al*., 2004) ont montré chez *P. aeruginosa* que le passage en biofilm engendrait une diversité génétique plus importante des bactéries en comparaison d'une culture planctonique et que cette diversité pouvait être associée à l'émergence de variants plus résistants au peroxyde d'hydrogène. Afin d'apporter des éléments nouveaux quant aux caractéristiques particulières de la souche $ND_{medical}$, nous avons entrepris la détermination de la séquence complète de son génome. Si la séquence obtenue s'avère être proche de celle des souches de collection, elle nous permettra d'identifier les déterminants génétiques responsables du phénotype très particulier de la souche atypique en termes de formation de biofilm et de résistance. Si la séquence est très différente de celles des souches de collection, elle permettra potentiellement d'identifier de nouveaux processus génétiques chez *B. subtilis*. Par ailleurs, très peu de génomes de souches de *B. subtilis* sont disponibles dans les bases de données.

Outre les phénomènes d'adaptation génétique, les différents stress subis par les bactéries dans les environnements industriels et médicaux, comme la croissance en présence de concentrations sublétales de désinfectants, peuvent également engendrer des modifications

temporaires de la physiologie des bactéries conduisant alors à une plus grande résistance. En effet, comme nous l'avons vu pour le chlorure de benzalkonium dans les biofilms de *P. aeruginosa* par exemple, les problèmes de pénétration observés pourraient résulter en des concentrations sublétales du biocide dans les strates profondes de la structure entrainant des adaptations physiologiques des cellules. Dans ce sens, il a été montré chez *S. enterica* que des cellules en biofilms cultivées en présence de chlorure de benzalkonium s'adaptaient mieux à ce désinfectant que leurs homologues planctoniques dans les même conditions (Mangalappalli-Illathu et al., 2008). Ces modifications physiologiques peuvent concerner les caractéristiques de l'enveloppe bactérienne ou la synthèse de protéines impliquées dans la réponse au stress par exemple (Mechin *et al*., 1999, Lin *et al*., 2002, Mangalappalli-Illathu & Korber, 2006). Chez *B. subtilis*, il a également été montré que des doses sublétales de dioxyde de chlore pouvaient induire la formation de biofilm résultant en une meilleure protection de la souche vis-à-vis du biocide (Shemesh *et al*., 2010). La prise en compte de ces phénomènes d'adaptation, qu'ils soient génétiques ou physiologiques, est donc primordiale dans l'évaluation de l'efficacité des désinfectants et souligne la nécessité de considérer des souches représentatives du terrain, et donc potentiellement adaptées aux stress subis dans l'environnement considéré.

Les résultats obtenus dans cette thèse ont également montré l'importance sur un plan sanitaire d'étudier les mécanismes de protection croisée entre souches pathogènes et flores résidentes adaptées, telle que la souche *B. subtilis* $ND_{medical}$ étudiée dans ce travail. En effet, nous avons pu constater que dans un biofilm mixte avec la bactérie pathogène *S. aureus*, les structures tridimensionnelles formées par la souche $ND_{medical}$ pouvaient permettre une protection du germe pathogène vis-à-vis du traitement à l'acide péracétique et ainsi potentiellement conduire à sa persistance dans l'environnement. Ces observations viennent compléter le nombre croissant de travaux scientifiques montrant l'effet synergique de l'interaction de différentes espèces au sein de biofilms mixtes dans leur résistance aux biocides (Leriche *et al.*, 2003, Simoes *et al.*, 2010, van der Veen & Abee, 2011). Les biofilms étant reconnus comme des associations multi-espèces complexes dans les environnements industriels, médicaux ou naturels, la prise en compte de ces interactions apparaît donc essentielle pour le développement de traitements de désinfection efficaces, alors que l'utilisation de modèles mono-espèce de bactéries pathogènes est encore aujourd'hui majoritairement privilégiée dans nos laboratoires. Cette prise en compte passe par une

meilleure compréhension des relations inter-espèces au sein des biofilms et dans ce sens, les outils de modélisation individus-centrés (IBM) constituent une approche intéressante (Xavier *et al.*, 2005, Picioreanu *et al.*, 2004). Les modèles individus-centrés sont des outils puissants pour simuler le comportement d'une population donnée, en décrivant les individus qui constituent cette population. Ils donnent la possibilité de tester de nombreuses hypothèses sur l'influence de différents paramètres sur la croissance d'une souche dans une communauté complexe servant ainsi de « laboratoires virtuels ». Les données fournies par ces modèles permettent d'obtenir une représentation spatiale d'une population donnée et également de simuler les nouvelles tendances des interactions entre les individus de deux à plusieurs autres populations en fonction de paramètres ajustables relatifs aux conditions environnementales et intrinsèques aux individus-bactéries modélisés (Kreft *et al.*, 2001). Ces modèles pourraient donc permettre de prédire les interactions spatiales entre un pathogène et une flore résidente lors du développement d'un biofilm mixte en fonction des conditions environnementales et ainsi, de mieux appréhender les facteurs favorisant son implantation ou sa résistance aux traitements de désinfection par exemple. Les progrès des techniques d'imagerie de fluorescence (résolution spatiale, temporelle et spectrale) et de la biologie moléculaire (construction de souches exprimant des protéines fluorescentes variées) permettent maintenant de visualiser *in situ* et à l'échelle de la cellule, le développement de structures complexes multi-espèces et ainsi de procurer les données expérimentales nécessaires à la validation de modèles solides et réalistes (Xavier *et al.*, 2004). Cette thématique fait actuellement l'objet d'un programme de recherche (ANR DISCO : Modélisation multi-échelles du COuplage bioDIversité Structure dans les biofilms) ayant pour objectif le développement de modèles informatiques et mathématiques de la dynamique des biofilms, en tenant compte de la diversité biologique (la distribution des espèces de bactéries) et la structure spatiale, projet auquel je participerai après ma thèse.

En conclusion, ce travail de thèse aura permis d'apporter des éléments explicatifs quant aux mécanismes impliqués dans la résistance des biofilms à la désinfection. Dans les conditions de notre étude, les résultats obtenus soutiennent un rôle primordial de l'architecture et de la matrice des biofilms dans ces phénomènes de résistance et soulignent ainsi l'apport des techniques d'imagerie de fluorescence non-invasive dans l'étude et la compréhension de la réactivité de ces structures biologiques complexes. Il nous semble essentiel de poursuivre le développement de ces outils et de favoriser les approches multidisciplinaires alliant la photophysique, la microbiologie et la biologie moléculaire afin de mieux comprendre les

phénomènes dynamiques gouvernant la vie microbiologique sur les surfaces et d'identifier des cibles de maîtrise des communautés microbiennes. D'un point de vue sanitaire, il apparaît urgent de prendre en compte l'état biofilm et des conditions d'étude plus proches de la réalité des environnements industriels et médicaux (interactions multi-espèces, flores microbiennes adaptées) dans le développement et la validation de traitements de désinfection efficaces.

REFERENCES BIBLIOGRAPHIQUES*

(* hors articles)

Aldeek, F., (2010) Synthèse et fonctionnalisation de nanocristaux fluorescents (Quantum dots) pour l'imagerie et la caractérisation des propriétés hydrophobes/hydrophiles de biofilms bactériens. *Thèse de Doctorat, 215 pages* Université Nancy-Henri Poincaré.

Anagnostopoulos, C. & J. Spizizen, (1961) Requirements for transformation in *Bacillus subtilis*. *Journal of Bacteriology* 81: 741-746.

Anonyme, (1997) Chemical disinfectants and antiseptics - Basic bactericidal activity - Test method and requirements (phase 1): NF EN 1040. *Ed. AFNOR*.

Barraud, N., D. J. Hassett, S. H. Hwang, S. A. Rice, S. Kjelleberg & J. S. Webb, (2006) Involvement of nitric oxide in biofilm dispersal of Pseudomonas aeruginosa. *Journal of Bacteriology* 188: 7344-7353.

Beyenal, H., C. Donovan, Z. Lewandowski & G. Harkin, (2004) Three-dimensional biofilm structure quantification. *Journal of Microbiological Methods* 59: 395-413.

Boles, B. R. & A. R. Horswill, (2008) agr-mediated dispersal of Staphylococcus aureus biofilms. *Plos Pathogens* 4: -.

Boles, B. R., M. Thoendel & P. K. Singh, (2004) Self-generated diversity produces "insurance effects" in biofilm communities. *Proceedings of the National Academy of Sciences of the United States of America* 101: 16630-16635.

Boles, B. R., M. Thoendel & P. K. Singh, (2005) Rhamnolipids mediate detachment of Pseudomonas aeruginosa from biofilms. *Molecular Microbiology* 57: 1210-1223.

Branda, S. S., J. E. Gonzalez-Pastor, E. Dervyn, S. D. Ehrlich, R. Losick & R. Kolter, (2004) Genes involved in formation of structured multicellular communities by Bacillus subtilis. *Journal of Bacteriology* 186: 3970-3979.

Brooks, J. D. & S. H. Flint, (2008) Biofilms in the food industry: problems and potential solutions. *International Journal of Food Science and Technology* 43: 2163-2176.

Burmolle, M., T. R. Thomsen, M. Fazli, I. Dige, L. Christensen, P. Homoe, M. Tvede, B. Nyvad, T. Tolker-Nielsen, M. Givskov, C. Moser, K. Kirketerp-Moller, H. K. Johansen, N. Hoiby, P. O. Jensen, S. J. Sorensen & T. Bjarnsholt, (2010) Biofilms in chronic infections - a matter of opportunity - monospecies biofilms in multispecies infections. *Fems Immunology and Medical Microbiology* 59: 324-336.

Campanac, C., L. Pineau, A. Payard, G. Baziard-Mouysset & C. Roques, (2002) Interactions between biocide cationic agents and bacterial biofilms. *Antimicrobial Agents and Chemotherapy* 46: 1469-1474.

Carpentier, B. & O. Cerf, (1993) Biofilms and Their Consequences, with Particular Reference to Hygiene in the Food-Industry. *Journal of Applied Bacteriology* 75: 499-511.

Chai, Y. R., R. Kolter & R. Losick, (2010a) Reversal of an epigenetic switch governing cell chaining in Bacillus subtilis by protein instability. *Molecular Microbiology* 78: 218-229.

Chai, Y. R., T. Norman, R. Kolter & R. Losick, (2010b) An epigenetic switch governing daughter cell separation in Bacillus subtilis. *Genes & Development* 24: 754-765.

Cloete, T. E., (2003) Resistance mechanisms of bacteria to antimicrobial compounds. *International Biodeterioration & Biodegradation* 51: 277-282.

Costerton, J. W., G. G. Geesey & K. J. Cheng, (1978) How Bacteria Stick. *Scientific American* 238: 86-&.

Davies, D. G. & C. N. H. Marques, (2009) A Fatty Acid Messenger Is Responsible for Inducing Dispersion in Microbial Biofilms. *Journal of Bacteriology* 191: 1393-1403.

Davison, W. M., B. Pitts & P. S. Stewart, (2010) Spatial and Temporal Patterns of Biocide Action against Staphylococcus epidermidis Biofilms. *Antimicrobial Agents and Chemotherapy* 54: 2920-2927.

Delmas, G., N. Jourdan Da Silva, N. Pihier, F.-X. Weill, V. Vaillant & H. De Valk, (2010) Les toxi-infections alimentaires collectives en France entre 2006 et 2008. *Bulletin Epidemiologique Hebdomadaire*: 344-348.

Dynes, J. J., J. R. Lawrence, D. R. Korber, G. D. W. Swerhone, G. G. Leppard & A. P. Hitchcock, (2009) Morphological and biochemical changes in Pseudomonas fluorescens biofilms induced by sub-inhibitory exposure to antimicrobial agents. *Canadian Journal of Microbiology* 55: 163-178.

Flemming, H. C. & J. Wingender, (2010) The biofilm matrix. *Nature Reviews Microbiology* 8: 623-633.

Guiot, E., P. Georges, A. Brun, M. P. Fontaine-Aupart, M. N. Bellon-Fontaine & R. Briandet, (2002) Heterogeneity of diffusion inside microbial biofilms determined by fluorescence correlation spectroscopy under two-photon excitation. *Photochemistry and Photobiology* 75: 570-578.

Haeghebaert, S., F. Le Querrec, V. Vaillant, E. D. Astagneau & P. Bouvet, (2001) Food poisoning in France in 1998. *Bulletin Epidemiologique Hebdomadaire*: 65-70.

Hall-Stoodley, L. & P. Stoodley, (2009) Evolving concepts in biofilm infections. *Cellular Microbiology* 11: 1034-1043.

Hamon, M. A. & B. A. Lazazzera, (2001) The sporulation transcription factor Spo0A is required for biofilm development in Bacillus subtilis. *Molecular Microbiology* 42: 1199-1209.

Hamon, M. A., N. R. Stanley, R. A. Britton, A. D. Grossman & B. A. Lazazzera, (2004) Identification of AbrB-regulated genes involved in biofilm formation by Bacillus subtilis. *Molecular Microbiology* 52: 847-860.

Hassett, D. J., T. R. Korfhagen, R. T. Irvin, M. J. Schurr, K. Sauer, G. W. Lau, M. D. Sutton, H. W. Yu & N. Hoiby, (2010) Pseudomonas aeruginosa biofilm infections in cystic fibrosis: insights into pathogenic processes and treatment strategies. *Expert Opinion on Therapeutic Targets* 14: 117-130.

Hassett, D. J., M. D. Sutton, M. J. Schurr, A. B. Herr, C. C. Caldwell & J. O. Matu, (2009) Pseudomonas aeruginosa hypoxic or anaerobic biofilm infections within cystic fibrosis airways. *Trends in Microbiology* 17: 130-138.

Holman, H. Y. N., R. Miles, Z. Hao, E. Wozei, L. M. Anderson & H. Yang, (2009) Real-Time Chemical Imaging of Bacterial Activity in Biofilms Using Open-Channel Microfluidics and Synchrotron FTIR Spectromicroscopy. *Analytical Chemistry* 81: 8564-8570.

Ivleva, N. P., M. Wagner, H. Horn, R. Niessner & C. Haisch, (2009) Towards a nondestructive chemical characterization of biofilm matrix by Raman microscopy. *Analytical and Bioanalytical Chemistry* 393: 197-206.

Jang, A., J. Szabo, A. A. Hosni, M. Coughlin & P. L. Bishop, (2006) Measurement of chlorine dioxide penetration in dairy process pipe biofilms during disinfection. *Applied Microbiology and Biotechnology* 72: 368-376.

Kaplan, J. B., (2010) Biofilm Dispersal: Mechanisms, Clinical Implications, and Potential Therapeutic Uses. *Journal of Dental Research* 89: 205-218.

Karatan, E. & P. Watnick, (2009) Signals, Regulatory Networks, and Materials That Build and Break Bacterial Biofilms. *Microbiology and Molecular Biology Reviews* 73: 310-+.

Kim, H., J. H. Ryu & L. R. Beuchat, (2007) Effectiveness of disinfectants in killing Enterobacter sakazakii in suspension, dried on the surface of stainless steel, and in a biofilm. *Applied and Environmental Microbiology* 73: 1256-1265.

Kobayashi, K., (2007) Gradual activation of the response regulator DegU controls serial expression of genes for flagellum formation and biofilm formation in Bacillus subtilis. *Molecular Microbiology* 66: 395-409.

Kobayashi, K., (2008) SlrR/SlrA controls the initiation of biofilm formation in Bacillus subtilis. *Molecular Microbiology* 69: 1399-1410.

Kolodkin-Gal, I., D. Romero, S. G. Cao, J. Clardy, R. Kolter & R. Losick, (2010) D-Amino Acids Trigger Biofilm Disassembly. *Science* 328: 627-629.

Kreft, J. U., C. Picioreanu, J. W. T. Wimpenny & M. C. M. van Loosdrecht, (2001) Individual-based modelling of biofilms. *Microbiology-Sgm* 147: 2897-2912.

Lemon, K. P., A. M. Earl, H. C. Vlamakis, C. Aguilar & R. Kolter, (2008) Biofilm development with an emphasis on Bacillus subtilis. *Bacterial Biofilms* 322: 1-16.

Leriche, V., R. Briandet & B. Carpentier, (2003) Ecology of mixed biofilms subjected daily to a chlorinated alkaline solution: spatial distribution of bacterial species suggests a protective effect of one species to another. *Environmental Microbiology* 5: 64-71.

Lin, J., S. X. Huang & Q. J. Zhang, (2002) Outer membrane proteins: key players for bacterial adaptation in host niches. *Microbes and Infection* 4: 325-331.

Mack, D., H. Rohde, L. G. Harris, A. P. Davies, M. A. Horstkotte & J. K. M. Knobloch, (2006) Biofilm formation in medical device-related infection. *International Journal of Artificial Organs* 29: 343-359.

Mangalappalli-Illathu, A. K. & D. R. Korber, (2006) Adaptive resistance and differential protein expression of Salmonella enterica serovar Enteritidis biofilms exposed to benzalkonium chloride. *Antimicrobial Agents and Chemotherapy* 50: 3588-3596.

Mangalappalli-Illathu, A. K., S. Vidovic & D. R. Korber, (2008) Differential adaptive response and survival of Salmonella enterica serovar enteritidis planktonic and biofilm cells exposed to benzalkonium chloride. *Antimicrobial Agents and Chemotherapy* 52: 3669-3680.

Martin, D. J. H., S. P. Denyer, G. McDonnell & J. Y. Maillard, (2008) Resistance and cross-resistance to oxidising agents of bacterial isolates from endoscope washer disinfectors. *Journal of Hospital Infection* 69: 377-383.

McLoon, A. L., S. B. Guttenplan, D. B. Kearns, R. Kolter & R. Losick, (2011) Tracing the domestication of a biofilm-forming bacterium. *Journal of Bacteriology*: Epub ahead of print.

Mechin, L., F. Dubois-Brissonnet, B. Heyd & J. Y. Leveau, (1999) Adaptation of Pseudomonas aeruginosa ATCC 15442 to didecyldimethylammonium bromide induces changes in membrane fatty acid composition and in resistance of cells. *Journal of Applied Microbiology* 86: 859-866.

Murray, E. J., M. A. Strauch & N. R. Stanley-Wall, (2009) sigma(X) Is Involved in Controlling Bacillus subtilis Biofilm Architecture through the AbrB Homologue Abh. *Journal of Bacteriology* 191: 6822-6832.

Nett, J. E., K. M. Guite, A. Ringeisen, K. A. Holoyda & D. R. Andes, (2008) Reduced biocide susceptibility in Candida albicans biofilms. *Antimicrobial Agents and Chemotherapy* 52: 3411-3413.

Neu, T. R., B. Manz, F. Volke, J. J. Dynes, A. P. Hitchcock & J. R. Lawrence, (2010) Advanced imaging techniques for assessment of structure, composition and function in biofilm systems. *Fems Microbiology Ecology* 72: 1-21.

Nijland, R., J. G. Burgess, J. Errington & J. W. Veening, (2010a) Transformation of Environmental Bacillus subtilis Isolates by Transiently Inducing Genetic Competence. *Plos One* 5: -.

Nijland, R., M. J. Hall & J. G. Burgess, (2010b) Dispersal of Biofilms by Secreted, Matrix Degrading, Bacterial DNase. *Plos One* 5: -.

Picioreanu, C., J. U. Kreft & M. C. M. van Loosdrecht, (2004) Particle-based multidimensional multispecies Biofilm model. *Applied and Environmental Microbiology* 70: 3024-3040.

Prakash, B., B. M. Veeregowda & G. Krishnappa, (2003) Biofilms: A survival strategy of bacteria. *Current Science* 85: 1299-1307.

Shemesh, M., R. Kolter & R. Losick, (2010) The Biocide Chlorine Dioxide Stimulates Biofilm Formation in Bacillus subtilis by Activation of the Histidine Kinase KinC. *Journal of Bacteriology* 192: 6352-6356.

Shirtliff, M. & J. Leid, (2009) The role of biofilms in device-related infections. *Springer series on biofilms* 3.

Simoes, L. C., M. Simoes & M. J. Vieira, (2010) Influence of the Diversity of Bacterial Isolates from Drinking Water on Resistance of Biofilms to Disinfection. *Applied and Environmental Microbiology* 76: 6673-6679.

Smith, K. & I. S. Hunter, (2008) Efficacy of common hospital blocides with biofilms of multi-drug resistant clinical isolates. *Journal of Medical Microbiology* 57: 966-973.

Stanley, N. R., R. A. Britton, A. D. Grossman & B. A. Lazazzera, (2003) Identification of catabolite repression as a physiological regulator of biofilm formation by Bacillus subtilis by use of DNA microarrays. *Journal of Bacteriology* 185: 1951-1957.

Stanley, N. R. & B. A. Lazazzera, (2005) Defining the genetic differences between wild and domestic strains of Bacillus subtilis that affect poly-gamma-DL-glutamic acid production and biofilm formation. *Molecular Microbiology* 57: 1143-1158.

Stewart, P. S. & M. J. Franklin, (2008) Physiological heterogeneity in biofilms. *Nature Reviews Microbiology* 6: 199-210.

Stewart, P. S., J. Rayner, F. Roe & W. M. Rees, (2001) Biofilm penetration and disinfection efficacy of alkaline hypochlorite and chlorosulfamates. *Journal of Applied Microbiology* 91: 525-532.

Takenaka, S., H. M. Trivedi, A. Corbin, B. Pitts & P. S. Stewart, (2008) Direct visualization of spatial and temporal patterns of antimicrobial action within model oral biofilms. *Applied and Environmental Microbiology* 74: 1869-1875.

van der Veen, S. & T. Abee, (2011) Mixed species biofilms of Listeria monocytogenes and Lactobacillus plantarum show enhanced resistance to benzalkonium chloride and peracetic acid. *International Journal of Food Microbiology* 144: 421-431.

Xavier, J. B., C. Picioreanu & M. C. M. van Loosdrecht, (2004) Assessment of three-dimensional biofilm models through direct comparison with confocal microscopy imaging. *Water Science and Technology* 49: 177-185.

Xavier, J. B., C. Picioreanu & M. C. M. van Loosdrecht, (2005) A framework for multidimensional modelling of activity and structure of multispecies biofilms. *Environmental Microbiology* 7: 1085-1103.

Xavier, J. B., D. C. White & J. S. Almeida, (2003) Automated biofilm morphology quantification from confocal laser scanning microscopy imaging. *Water Science and Technology* 47: 31-37.

Zeigler, D. R., Z. Pragai, S. Rodriguez, B. Chevreux, A. Muffler, T. Albert, R. Bai, M. Wyss & J. B. Perkins, (2008) The Origins of 168, W23, and Other Bacillus subtilis Legacy Strains. *Journal of Bacteriology* 190: 6983-6995.

ANNEXES

ANNEXE 1.

Article 7: " Comparative biocidal activity of peracetic acid, benzalkonium chloride and ortho- phthalaldehyde on 77 bacterial strains "

Bridier A, Briandet R, Thomas V et Dubois-Brissonnet F.

Journal of Hospital Infection, 2011, 78 : 208-213

Préambule :

L'article « *Comparative biocidal activity of peracetic acid, benzalkonium chloride and ortho- phthalaldehyde on 77 bacterial strains* » présente une étude comparative de la résistance de 77 souches bactériennes à trois désinfectants utilisés dans les milieux médicaux et industriels selon le protocole des normes réglementaires actuels. Cette première partie constituait une étape préliminaire à l'étude de la résistance des bactéries en biofilms et une volonté des partenaires du projet de confronter les souches de référence utilisées dans les normes d'évaluation de l'activité des désinfectants avec un large panel de souches afin de vérifier leur pertinence.

Journal of Hospital Infection 78 (2011) 208–213

Available online at www.sciencedirect.com

Journal of Hospital Infection

journal homepage: www.elsevierhealth.com/journals/jhin

Comparative biocidal activity of peracetic acid, benzalkonium chloride and *ortho*-phthalaldehyde on 77 bacterial strains

A. Bridier [a,b], R. Briandet [b], V. Thomas [c], F. Dubois-Brissonnet [a,*]

[a] *AgroParisTech, UMR 1319 MICALIS, Massy, France*
[b] *INRA, UMR 1319 MICALIS, Jouy-en-Josas, France*
[c] *STERIS SA, CEA, Fontenay-aux-Roses, France*

ARTICLE INFO

Article history:
Received 17 September 2010
Accepted 10 March 2011
by S.J. Dancer
Available online 8 June 2011

Keywords:
Bacterial resistance
Benzalkonium chloride
Disinfection
Minimum bactericidal concentration
Ortho-phthalaldehyde
Peracetic acid

SUMMARY

Despite numerous reports on biocide activities, it is often difficult to have a reliable and relevant overview of bacterial resistance to disinfectants because each work challenges a limited number of strains and tested methods are often different. The aim of this study was to evaluate the bactericidal activity of three different disinfectants commonly used in industrial or medical environments (peracetic acid, benzalkonium chloride and *ortho*-phthalaldehyde) against 77 bacterial strains from different origins using one standard test method (NF EN 1040). Results highlight the existence of high interspecific variability of resistance to disinfectants and, contrary to widespread belief, Gram-positive strains generally appeared more resistant than Gram-negative strains. Resistance was also variable among strains of the same species such as *Bacillus subtilis* to peracetic acid, *Pseudomonas aeruginosa* to benzalkonium chloride and *Staphylococcus aureus* to *ortho*-phthalaldehyde.

Introduction

Disinfectants are widely used to eliminate micro-organisms in industrial, food and medical environments in order to avoid or limit contamination. The evaluation and comparison of disinfectant activity against a large number of bacterial strains is expected in order to optimise disinfection processes and in the development of newer, efficient formulations. Disinfectants, unlike antibiotics, have a broad spectrum of antimicrobial activity and generally act on several targets in microbial cells.[1] Contrary to antibiotics, where resistance is defined within 'cut-off' points, resistance to disinfectants is generally described as a comparative concept: a strain is said to be resistant if it is not inactivated by a concentration that inactivates the majority of strains of that organism or often a single reference strain.[2,3] Many reviews describe the mechanisms of antimicrobial resistance in bacteria. Briefly, bacterial resistance to biocides may be intrinsic, acquired resistance or by phenotypic adaptation. Intrinsic insusceptibility is a natural, chromosomally controlled ability to resist to biocidal activity.[4] Acquired resistance is the ability of a micro-organism to acquire resistance by mutation or by procurement of transferable genetic elements (plasmids and transposons).[1] Phenotypic adaptation, which may also be considered as intrinsic, is a transient reduced susceptibility obtained when bacteria are cultivated under non-optimal environments.[3] Although a relatively large amount of information exists on bacterial resistance characteristics, many of these investigations deal with a small number of species and strains. Moreover, because of the differences between testing methods, it is often difficult to compare results and to draw precise conclusions about antimicrobial activities. The purpose of the present study was to screen and compare the antimicrobial activities of disinfectants against 77 bacterial strains of different origins (food or clinical environments, collection or recently isolated strains) belonging to 10 different species. The biocides were chosen among those commonly used in food or medical environments for their distinct modes of action: peracetic acid (oxidant), benzalkonium chloride (membrane-active compound) and *ortho*-phthalaldehyde (cross-linking agent).

Methods

Bacterial strains and growth conditions

The 77 strains used in this study are described in Table I. Tryptone soya broth (TSB, bioMérieux, Marcy l'Etoile, France) for

* Corresponding author. Address: AgroParisTech, UMR 1319 Micalis, B2HM, 25 avenue République, F-91300 Massy, France. Tel.: +33 1 69 53 64 72; fax: +33 1 69 93 51 44.
E-mail address: florence.dubois-brissonnet@jouy.inra.fr (F. Dubois-Brissonnet).

0195-6701/$ – see front matter © 2011 The Healthcare Infection Society. Published by Elsevier Ltd. All rights reserved.
doi:10.1016/j.jhin.2011.03.014

Table I
List of the 77 strains used in this study

Species	Code	Origin
Bacillus subtilis	ATCC 6633	Unknown
	PG01	Food, CTSCCV
	ATCC 9372	Unknown
	$WD_{isolate}$	Endoscope washer-disinfectors (Martin *et al.*)[14]
	BAC.4.1	Food, ISHA
	ATCC 6051	Unknown
	BGSC 168	Unknown
Escherichia coli	ATCC 10536	Unknown
	PHL644	Clinical (Vidal *et al.*)[20]
	PHL818	Clinical (Prigent-Combaret *et al.*)[27]
	PHL628	Clinical (Vidal *et al.*)[26]
	RS218	Clinical
	ATCC 8739	Human faeces
	ESC.1.13	Food, ISHA
	ESC.1.16	Food, ISHA
	ESC.1.24	Food, ISHA
	ESC.1.30	Food, ISHA
	ESC.1.33	Food, ISHA
Enterococcus faecalis	ATCC 19433	Unknown
	ATCC 51188	Clinical
	ATCC 33012	Unknown
	ATCC 49477	Clinical
	ATCC 33186	Unknown
	ATCC 27959	Bovine mastitis
	ATCC 700802	Clinical
	ATCC 29212	Clinical
	ATCC 29302	Unknown
	ATCC 51299	Clinical
Listeria monocytogenes	EGDe	(Murray *et al.*)[28]
	CIP 104794	Guinea-pig
	CIP 103573 (ser. 1/2c)	Food
	CIP 103575 (ser. 4b)	Food
	CIP 78 39	Food
	370P-Lm	Food, ISHA
	Lm 162 (ser. 1/2a)	Food, Aerial
	Lm 481 (ser. 1/2b)	Food, Aerial
	LO28	(Michel and Cossart)[29]
	BUG1641	(Bierne *et al.*)[30]
Pseudomonas aeruginosa	ATCC 15442	Animal room water bottle
	PSE.1.2	Food, ISHA
	ATCC 10145	Unknown
	ATCC 14210	Clinical
	ATCC 49189	Clinical
	ATCC 9027	Clinical
	ATCC 15692	Clinical
	ATCC 9721	Unknown
	ATCC 14207	Faeces
	ATCC 51447	Unknown
Staphylococcus aureus	ATCC 6538	Clinical
	CIP 57.10	Milk of ewes with mastitis
	ATCC 9144	Unknown
	ATCC 29213	Clinical
	ATCC 27217	Sea water
	ATCC 25923	Clinical
	ATCC 29247	Unknown
	ATCC 8096	Clinical
	ATCC 43300	Clinical
	STA.1.5	Superficial water, ISHA
Salmonella enterica	S24 (ser. St Paul)	Food, ISHA
	I26 (ser. Agona)	Food, ISHA
	S2 (ser. Brandenburg)	Food, ISHA
	S19 (ser. Duby)	Food, ISHA
	S59 (ser. Dublin)	Food, ISHA
	S38 (ser. Enteritidis)	Food, ISHA
	S12 (ser. Hadar)	Food, ISHA
	S55 (ser. Indiana)	Food, ISHA
	ATCC 13311 (ser. Typhimurium)	Human faeces
	S34 (ser. Typhimurium)	Food, ISHA
Mycobacterium chelonae	645P-Mc	Clinical
	646P-Mc	Clinical
	647P-Mc	Clinical
	648P-Mc	Clinical
	649P-Mc	Clinical
	650P-Mc	Clinical
	ATCC 35752	Tortoise
Mycobacterium avium	ATCC 15769	Tuberculous hen
Mycobacterium terrae	ATCC 15755	Clinical

CTSCCV, Centre Technique de Salaison, de la Charcuterie et des Conserves de Viandes; ATCC, American Type Culture Collection; BGSC, *Bacillus* Genetic Stock Center; CIP, the Collection de l'institut Pasteur; UBHM, Unité Bioadhésion et Hygiène des Matériaux; ISHA, Institut Scientifique d'Hygiène et d'Analyse; Aerial, the Centre de Ressources Technologiques et Institut Technique Agro-Industriel, Illkirch, France.

Gram-positive and -negative bacteria or Middlebrook 7H9 broth with ADC enrichment (7H9, Difco, le Pont de Claix, France) for mycobacteria were inoculated at 10% v/v with a standardised inoculum obtained after two subcultures in the same medium from frozen cells (−80 °C). Cultures were incubated statically at 30 °C for 18 h (Gram-positive and -negative), 7 days (*Mycobacterium chelonae*) or 15 days (*Mycobacterium avium* and *Mycobacterium terrae*).

Antibacterial agents

Three biocides commonly used in food and medical environments were selected: peracetic acid (PAA) (32 wt% in dilute acetic acid) (Sigma–Aldrich, St Louis, MO, USA), benzalkonium chloride C14 (BAC) (≥99.0%, Fluka, Buchs, Switzerland) and *ortho*-phthalaldehyde (OPA) (≥97%, Sigma–Aldrich). Disinfectants were diluted in sterile deionised water to final concentrations.

Disinfectant testing

Biocide susceptibility was tested according to European standard NF EN 1040.[5] Experimentally, the bacterial culture was harvested by centrifugation (7000 *g*, 10 min), washed twice in 150 mM NaCl before being adjusted to $1.5–5 \times 10^8$ cfu/mL. One millilitre was then added to the disinfectant solution (8 mL), mixed thoroughly, and left at 20 °C for 5 min. Following contact, 1 mL was transferred to a quenching solution (3 g/L L-α-phosphatidylcholine, 30 g/L Tween 80, 5 g/L sodium thiosulphate, 1 g/L L-histidine, 30 g/L saponine), mixed thoroughly, and left at 20 °C for 5 min to neutralise the activity of the disinfectant.

After serial dilutions, enumeration was achieved on tryptone soya agar (TSA, bioMérieux) by a drop plate method.[6] Petri plates were incubated at 30 °C for 24 h, survivors were enumerated and $\log_{10}$ reductions calculated from the initial population. The use of the drop plate method instead of the pour plate method recommended in disinfection standard NF EN 1040 was first validated with *Staphylococcus aureus* ATCC 6538 and *Pseudomonas aeruginosa* ATCC 15442.

Interspecies comparison of bacterial susceptibility

The susceptibility of one strain of each species (referred to hereafter as the model strain) to at least five concentrations of each biocide was evaluated as previously described. Each experiment was performed at least twice and up to five times from independent bacterial cultures. Minimum bactericidal concentrations

(MBCs) were defined as the minimum concentrations that gave a 5 $\log_{10}$ reduction from the initial population. To determine accurate MBCs, the Chick and Watson disinfection model was fitted on experimental results.[7] In this model, the rate of inactivation of a micro-organism is dependent upon the concentration of the disinfectant and contact time:

$$\log_{10} R = KC_t^n$$

where $\log_{10} R$ is the decimal log reduction, K and n are empirical constants, C is the biocide concentration and t is disinfection contact time.

Intraspecies comparison of bacterial susceptibility

The bactericidal activity of one relevant concentration of the three biocides was evaluated using adapted NF EN 1040 protocol on ~10 strains of each species. Each experiment was repeated twice. Biocide concentrations applied for each species were determined as the concentration that gave ~3 $\log_{10}$ reduction of the model strain in the interspecies study (exact concentrations are indicated on Figure 1). These concentrations enabled the visualisation of variability from 0 to 6 $\log_{10}$ reductions. In order to provide a normalised representation of intraspecific variability, a 'resistance coefficient (Qr)' was calculated for all strains as: Qr = $\log_{10}$ ($\log_{10}$ reduction of the model strain of the species/$\log_{10}$ reduction of the tested strain). Thus, if Qr > 0, the test strain was more resistant than the model strain, and reciprocally so.

Statistical analysis

The statistical analyses on the data (one-way analysis of variance, simple linear regression model II) were performed using the Statgraphics v6.0 software (Manugistics, Rockville, MD, USA). The *P*-values tested the statistical significance of each factor through *F*-tests. At $P < 0.05$, these factors had a statistically significant effect at the 95% confidence level.

Results

Interspecies variability of susceptibility to biocides

One strain for each species was exposed to different concentrations of PAA, BAC and OPA for 5 min. Concentrations causing 2, 3 and 5 $\log_{10}$ reductions of the initial population were determined by fitting the Watson and Chick model on experimental results (Table II). Considering all Gram-positive and -negative bacteria, we observed that PAA MBCs of model strains were all evaluated between 7 and 11 mg/L except for *Bacillus subtilis* which was more susceptible (MBC: 4.8 mg/L). Greater variability was observed between species for BAC (Table II). *S. aureus* was the most resistant with MBC at 70 mg/L, followed by *Enterococcus faecalis* (MBC: 52 mg/L). *B. subtilis* was again the most susceptible with MBC of 8.8 mg/L. Gram-positive strains were more resistant to OPA than Gram-negative strains in our experimental conditions (Table II), especially *Listeria monocytogenes* and *E. faecalis*. Results obtained for *Mycobacterium* showed the very high resistance of this organism to the different biocide treatments. BAC proved to be completely ineffective with regards to the very weak reduction (0.2 $\log_{10}$) obtained even at 24 000 mg/L.

Intraspecies variability of susceptibility to biocides

We tested ~10 strains for each species at the concentration giving ~3 $\log_{10}$ reduction of the model strain tested in the interspecies study. Qr resistance coefficient results are presented using box-and-whisker plot representation for each biocide on Figure 1. Results showed various degrees of intraspecies resistance variability depending on biocide and species. *B. subtilis* strains demonstrated the highest intraspecific variability of susceptibility to PAA, mainly due to the high resistance of the strain $WD_{isolate}$ (outlier value, $P < 0.05$) freshly isolated from an endoscope washer-disinfector, but little resistance variability with the other biocides. *E. faecalis* strains did not exhibit high intraspecific variability in their resistance to the three biocides. *L. monocytogenes* displayed relatively high variations with PAA and OPA treatments; low variability was observed for BAC (Figure 1). Similar resistance of *S. aureus* strains was observed with PAA, but strains varied widely in their response to OPA and BAC. Interestingly, for both these biocides, the model strain (ATCC 6538 used as the reference strain in disinfection standard NF EN 1040) was among the most sensitive strains. *P. aeruginosa* strains exhibited significant variability to BAC treatment with some strains showing a higher resistance than the model strain ATCC 15442, the other reference strain in NF EN 1040. We did not observe variability of *P. aeruginosa* strains to the other biocides. *E. coli* and *S. enterica* species did not demonstrate significant resistance variability to the biocides. Mycobacteria had moderate variability to PAA and OPA, and showed lower resistance than the model strain *M. chelonae*.

Discussion

Despite numerous studies on bacterial resistance to biocides, it is often difficult to compare results because of differences in test methods or in definitions of what is bacterial insusceptibility. Bacterial resistance can be characterised following the measurement of bacterial minimum inhibitory concentrations (MICs), as it is generally conducted for antibiotics and sometimes for disinfectants, or by the determination of bactericidal activity.[2,8] As disinfectants, unlike antibiotics, are intended to kill quickly the microbial population, the measurement of bactericidal activity is regarded as more accurate. The latter can be evaluated by a survivor curve (a single concentration is applied and the survivors are enumerated over time) or by the establishment of the MBC (a range of concentrations are applied during one definite time and survivors are enumerated). Depending on reports, MBCs can be defined as the concentration which leads to 3 $\log_{10}$, 5 $\log_{10}$ reductions, or to total eradication of the initial population.[5,9,10] In this study, the response of 77 different strains from different species and origins to the bactericidal activity of three biocides was evaluated in the same conditions, in order to propose a reliable and relevant overview of bacterial resistance.

Disinfectants have multiple cellular targets such as the cell wall (or the outer membrane), the cytoplasmic membrane, functional and structural proteins, DNA, RNA and other cytosolic components. The three chosen disinfectants have different modes of action: OPA is a cross-linking agent, BAC, a quaternary ammonium compound, is a membrane-active agent and peracetic acid acts as an oxidising agent.[11]

Our results confirmed that mycobacteria demonstrated a marked resistance to all the biocides. Despite the non-specific mode of action of PAA, MBC was about 350 times higher than those of all other vegetative bacteria. OPA was efficient but at very high concentrations, much higher than those obtained by Wash *et al.*[12] BAC was inefficient even at very high concentrations, in agreement with numerous studies which state that QACs alone have no mycobactericidal activity.[13] High resistance to all biocides is mostly due to the efficient barrier established by the mycobacterial waxy cell wall.[1]

Among Gram-positive and -negative bacteria, we found very close MBCs for PAA against all species and a low variability among

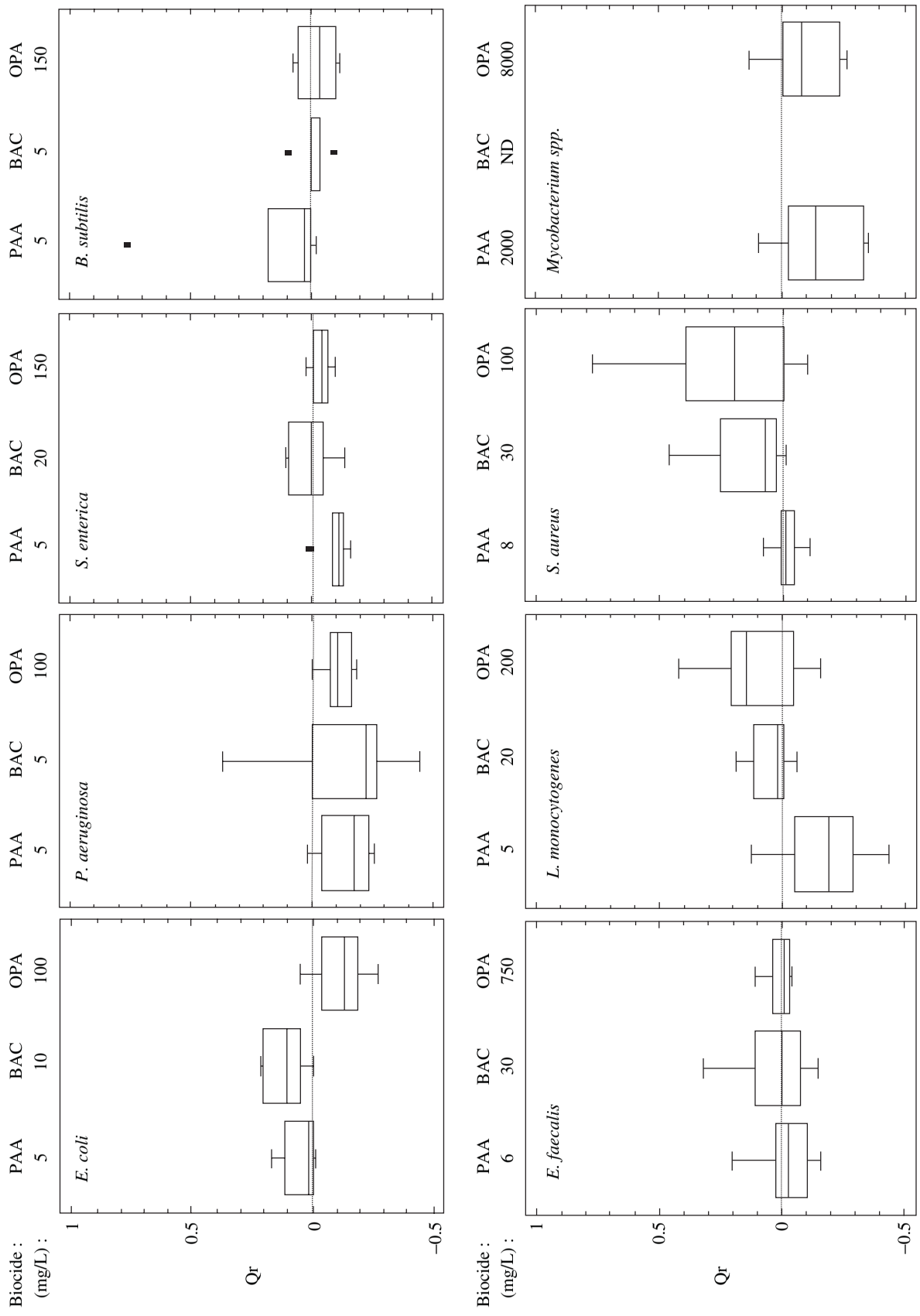

Figure 1. Box-and-whisker diagrams depicting intraspecific variability of susceptibility to peracetic acid (PAA), benzalkonium chloride (BAC) and *o*-phthalaldehyde (OPA) of the different species (~10 strains/species). Boxes range from the 25th to 75th percentile and are intersected by the median line. Whiskers extending below and above the box range from the lowest to the upper value, respectively. Outlier values are also plotted. $Qr = \log_{10}$ (reduction of model strain/$\log_{10}$ reduction of test strain).

Table II
Concentration of peracetic acid (PAA), benzalkonium chloride (BAC) and *o*-phthalaldehyde (OPA) needed to achieve 2, 3 or 5 $\log_{10}$ reductions (R) of the initial population for our model strains of the different species after 5 min of treatment

Strains	PAA (mg/L)			BAC (mg/L)			OPA (mg/L)		
	2 $\log_{10}$ R	3 $\log_{10}$ R	5 $\log_{10}$ R (MBC)	2 $\log_{10}$ R	3 $\log_{10}$ R	5 $\log_{10}$ R (MBC)	2 $\log_{10}$ R	3 $\log_{10}$ R	5 $\log_{10}$ R (MBC)
Escherichia coli PHL 628	3.4	4.8	7.4	10	15	24	75	110	180
Pseudomonas aeruginosa ATCC 15442	2.9	5.1	10.3	2	5	16	50	100	205
Salmonella enterica S24 (ser. St Paul)	4.5	5.9	8.2	13	22	42	115	135	175
Bacillus subtilis ATCC 6633	2.9	3.6	4.8	4	5	9	110	160	250
Enterococcus faecalis ATCC 19433	5.1	6.4	8.5	23	33	52	620	910	1490
Listeria monocytogenes EGDe	5.4	6.8	9.1	16	20	28	110	245	670
Staphylococcus aureus ATCC 6538	8.0	9.1	10.8	20	35	70	70	115	210
Mycobacterium chelonae 647P-Mc	1365	1920	2940	>24 000	–	–	6580	8520	11 800

MBC, minimum bacterial concentration. Values were obtained after fitting the Chick and Watson model on experimental data.[7]

strains except for *B. subtilis*. This is likely to be due to the non-specific mode of action of this highly reactive oxidising antimicrobial agent. The *B. subtilis* strain $WD_{isolate}$ was clearly an exception, demonstrating higher resistance (outlier in Figure 1; $P < 0.05$). We confirmed here the observations of Martin *et al.*[14] who isolated this strain from an endoscope washer-disinfector and described higher tolerance to oxidising agents (peracetic acid, chlorine dioxide, hydrogen peroxide). The authors proposed that this strain was surrounded by a high amount of exopolymeric substances that probably play a protective role by deactivating oxidising agents. We verified that *B. subtilis* strain $WD_{isolate}$ sample did not contain any spores at the time of testing by checking the total inactivation of the bacterial population after 10 min of boiling (data not shown).

BAC MBCs showed that *S. aureus* and *E. faecalis* were the most resistant species. The high susceptibility of *E. coli* and *P. aeruginosa* strains should also be noted. Indeed, overall Gram-negative bacteria and especially *Pseudomonas* spp. are generally considered more resistant to disinfection than Gram-positive bacteria due to the presence of the outer membrane that can limit the uptake of antibacterial agents.[4] Nevertheless, some reports demonstrated high resistance of *S. aureus* to QACs (MBC ~64 mg/L).[15,16] Resistance of Gram-positive strains may be due to the presence of plasmids encoding for QAC resistance, as it has already been demonstrated in *S. aureus* strains.[17] *E. faecalis* or *L. monocytogenes* can also encode a multidrug efflux pump that could similarly increase the resistance to BAC.[18,19] Other reports have described low resistance of *Pseudomonas* to QACs, with MBCs in the range 10–20 mg/L similar to our results.[20,21,16] In our study, *Pseudomonas* showed the highest variability to bacterial activity of BAC. The two most resistant strains to BAC were significantly less negatively charged than other more sensitive strains (data not shown). This may suggest that for *P. aeruginosa*, the electrostatic interactions between the negatively charged cell surface and the positively charged BAC play a key role in its antimicrobial efficiency.[22] One explanation for the heterogeneity in QAC MBCs against *Pseudomonas* in the literature could also be explained by its ability to adapt to biocides, notably to quaternary ammonium compounds.[23,24] Generally, the claim of 'higher' resistance of Gram-negative strains in the literature often relies on their ability to grow in the presence of biocides (MIC determination) but no direct relationship could be established between MIC and MBC values.[2] This is fundamental as, for most disinfection applications, MBC is the most important criterion to consider, and the MIC has little practical use.

OPA demonstrated high resistance of *L. monocytogenes* and *E. faecalis*, but was relatively effective against the other species, including Gram-negative strains. Whereas OPA is a cross-linking agent, it has been demonstrated to be more active than glutaraldehyde against Gram-negative bacteria because of its lipophilic aromatic component which is likely to assist in its uptake through their lipid-rich cell wall structure.[25] Results showed a high variability of *S. aureus* resistance to OPA and most of the strains demonstrated a higher resistance than the reference strain used in disinfection standards, *S. aureus* ATCC 6538. This raises an important concern over the choice of relevant strains for disinfectant evaluation.

In conclusion, we have compared the susceptibility of 77 strains from 10 different species to three different biocides and found that most of the tested Gram-positive bacteria were more resistant than Gram-negative bacteria, contrary to what is generally reported. These results highlight the importance of having standard protocols and guidelines for the testing of bacterial resistance to biocides. Our investigations are continuing to evaluate biocide resistance of bacteria grown in biofilms, as such communities generally demonstrate superior resistance to antimicrobials and have been shown to cause significant public health concerns.

Acknowledgements

The authors thank V. Thiry, J. Deschamps and B. Ouazza for technical assistance. The authors warmly thank P. Garry (CTSCCV, Maison-alfort, France) for *B. subtilis* strain PG01, J-Y. Maillard (University of Cardiff, UK) for *B. subtilis* strain $WD_{isolate}$, V. Stahl (Aerial, Illkirch, France) for *L. monocytogenes* strains Lm162 and Lm481, and A. Boubetra (ISHA, Massy, France) for all ISHA strains.

Conflict of interest statement
None declared.

Funding source
This study received support from the 'MEDICEN-Region Paris, Ile-de-France' Competitiveness Cluster.

References

1. Russell AD. Similarities and differences in the response of microorganisms to biocides. *J Antimicrob Chemother* 2003;**52**:750–763.
2. Cerf O, Carpentier B, Sanders P. Tests for determining in-use concentrations of antibiotics and disinfectants are based on entirely different concepts: "resistance" has different meanings. *Int J Food Microbiol* 2010;**136**:247–254.
3. Langsrud S, Sidhu MS, Heir E, Holck AL. Bacterial disinfectant resistance – a challenge for the food industry. *Int Biodeter Biodegrad* 2003;**51**:283–290.
4. Murtough SM, Hiom SJ, Palmer M, Russell AD. Biocide rotation in the healthcare setting: is there a case for policy implementation? *J Hosp Infect* 2001;**48**:1–6.
5. Anonymous. *Chemical disinfectants and antiseptics – Basic bactericidal activity – Test method and requirements (phase 1)*; 1997. NF EN 1040. AFNOR.
6. Chen CY, Nace GW, Irwin PL. A 6 × 6 drop plate method for simultaneous colony counting and MPN enumeration of *Campylobacter jejuni, Listeria monocytogenes*, and *Escherichia coli*. *J Microbiol Methods* 2003;**55**:475–479.
7. Chick H. An investigation of the laws of disinfection. *J Hygiene* 1908;**8**:92–157.

8. Lambert RJW, Pearson J. Susceptibility testing: accurate and reproducible minimum inhibitory concentration (MIC) and non-inhibitory concentration (NIC) values. *J Appl Microbiol* 2000;**88**:784–790.
9. Smith K, Hunter LS. Efficacy of common hospital biocides with biofilms of multi-drug resistant clinical isolates. *J Med Microbiol* 2008;**57**:966–973.
10. Liu QZ, Liu MN, Wu Q, Li C, Zhou TL, Ni YX. Sensitivities to biocides and distribution of biocide resistance genes in quaternary ammonium compound tolerant *Staphylococcus aureus* isolated in a teaching hospital. *Scand J Infect Dis* 2009;**41**:403–409.
11. McDonnell G, Russell AD. Antiseptics and disinfectants: activity, action, and resistance. *Clin Microbiol Rev* 1999;**12**:147–179.
12. Walsh SE, Maillard JY, Russell AD, Hann AC. Possible mechanisms for the relative efficacies of *ortho*-phthalaldehyde and glutaraldehyde against glutaraldehyde-resistant *Mycobacterium chelonae*. *J Appl Microbiol* 2001;**91**:80–92.
13. Russell AD. Activity of biocides against mycobacteria. *J Appl Bacteriol* 1996;**81**: S87–101.
14. Martin DJH, Denyer SP, McDonnell G, Maillard JY. Resistance and cross-resistance to oxidising agents of bacterial isolates from endoscope washer disinfectors. *J Hosp Infect* 2008;**69**:377–383.
15. Narui K, Takano M, Noguchi N, Sasatsu M. Susceptibilities of methicillin-resistant *Staphylococcus aureus* isolates to seven biocides. *Biol Pharm Bull* 2007;**30**: 585–587.
16. Ohta S, Misawa Y, Miyamoto H, *et al*. A comparative study of characteristics of current-type and conventional-type cationic bactericides. *Biol Pharm Bull* 2001;**24**:1093–1096.
17. Littlejohn TG, Paulsen IT, Gillespie MT, *et al*. Substrate specificity and energetics of antiseptic and disinfectant resistance in *Staphylococcus aureus*. *FEMS Microbiol Lett* 1992;**95**:259–266.
18. Aase B, Sundheim G, Langsrud S, Rorvik LM. Occurrence of and a possible mechanism for resistance to a quaternary ammonium compound in *Listeria monocytogenes*. *Int J Food Microbiol* 2000;**62**:57–63.
19. Lee EW, Chen J, Huda MN, Kuroda T, Mizushima T, Tsuchiya T. Functional cloning and expression of *emeA*, and characterization of EmeA, a multi-drug efflux pump from *Enterococcus faecalis*. *Biol Pharm Bull* 2003;**26**: 266–270.
20. Guérin-Méchin L, Dubois-Brissonnet F, Heyd B, Leveau JY. Specific variations of fatty acid composition of *Pseudomonas aeruginosa* ATCC 15442 induced by quaternary ammonium compounds and relation with resistance to bactericidal activity. *J Appl Microbiol* 1999;**87**:735–742.
21. Langsrud S, Sundheim G, Borgmann-Strahsen R. Intrinsic and acquired resistance to quaternary ammonium compounds in food-related *Pseudomonas* spp. *J Appl Microbiol* 2003;**95**:874–882.
22. Bruinsma GM, Rustema-Abbing M, van der Mei HC, Lakkis C, Busscher HJ. Resistance to a polyquaternium-1 lens care solution and isoelectric points of *Pseudomonas aeruginosa* strains. *J Antimicrob Chemother* 2006;**57**: 764–766.
23. Johnson JA, Forbes B, Lambert RJW. Adaptive resistance to benzalkonium chloride, amikacin, and tobramycin: the effect on susceptibility to other antimicrobials. *J Appl Microbiol* 2002;**93**:96–107.
24. Méchin L, Dubois-Brissonnet F, Heyd B, Leveau JY. Adaptation of *Pseudomonas aeruginosa* ATCC 15442 to didecyldimethylammonium bromide induces changes in membrane fatty acid composition and in resistance of cells. *J Appl Microbiol* 1999;**86**:859–866.
25. Simons C, Walsh SE, Maillard JY, Russell AD. *Ortho*-phthalaldehyde: proposed mechanism of action of a new antimicrobial agent. *Lett Appl Microbiol* 2000;**31**: 299–302.
26. Vidal O, Longin R, Prigent-Combaret C, Dorel C, Hooreman M, Lejeune P. Isolation of an *Escherichia coli* K-12 mutant strain able to form biofilms on inert surfaces: involvement of a new ompR allele that increases curli expression. *J Bacteriol* 1998;**180**:2442–2449.
27. Prigent-Combaret C, Prensier G, Le Thi TT, Vidal O, Lejeune P, Dorel C. Developmental pathway for biofilm formation in curli-producing *Escherichia coli* strains: role of flagella, curli and colanic acid. *Environmental Microbiology* 2000;**2**:450–464.
28. Murray EGD, Webb RA, Swann RBK. A disease of rabbits characterized by a large mononuclear leucocytosis. *J Pathol Biol* 1926;**29**:407–439.
29. Michel E, Cossart P. Physical map of the *Listeria monocytogenes* chromosome. *J Bacteriol* 1992;**174**:7098–7103.
30. Bierne H, Gouin E, Roux P, Caroni P, Yin HL, Cossart P. A role for cofilin and LIM kinase in *Listeria*-induced phagocytosis. *J Cell Biol* 2001;**155**:101–112.

ANNEXE 2. Valorisation scientifique

Publications scientifiques

[1] **A. BRIDIER**, F. DUBOIS-BRISSONNET, A. BOUBETRA, V. THOMAS, R. BRIANDET. The biofilm architecture of sixty opportunistic pathogens deciphered by a high throughput CLSM method. *Journal of Microbiological Methods* 82: 64–70 (2010).

[2] **A. BRIDIER**, D. LE COQ, F. DUBOIS-BRISSONNET, V. THOMAS, S. AYMERICH AND R. BRIANDET. The spatial architecture of *Bacillus subtilis* biofilms deciphered using a surface-associated model and in situ imaging. *PLoS One* 6: e16177. (2011).

[3] **A. BRIDIER**, E. TISCHENKO, F. DUBOIS-BRISSONNET, J.-M. HERRY, V. THOMAS, S. DADDI-OUBEKKA, F. WAHARTE, K. STEENKESTE, M.-P. FONTAINE-AUPART AND R. BRIANDET. Deciphering biofilms structure and reactivity by multiscale time-resolved fluorescence analysis. *Advances in Experimental Medicine and Biology* 715: 333-349 (2011) , *Review*.

[4] **A. BRIDIER**, F. DUBOIS-BRISSONNET, G. GREUB, V. THOMAS, R. BRIANDET. Dynamics of the action of biocides in *Pseudomonas aeruginosa* biofilms.*Antimicrobial Agents and Chemotherapy.* Sous presse (2011).

[5] **A. BRIDIER**, R. BRIANDET, V. THOMAS, F. DUBOIS-BRISSONNET. Comparative biocidal activity of peracetic acid, benzalkonium chloride and ortho- phthalaldehyde on 77 bacterial strains. *Journal of Hospital Infection* 78: 208-213 (2011).

[6] **A. BRIDIER**, R. BRIANDET, V. THOMAS, F. DUBOIS-BRISSONNET. Resistance of bacterial biofilms to disinfectants: a review. *Accepté dans Biofouling*. (2011), *Review*.

[7] **A. BRIDIER**, F. DUBOIS-BRISSONNET, D. LE COQ, T. MEYLHEUC, V. THOMAS, S. AYMERICH AND R. BRIANDET. Are resident *bacillus subtilis* biofims of concern in hospital aquired infections? *En cours de préparation*.

Communications orales

[8] E. TISHCHENKO, V. THOMAS, **A. BRIDIER**, F. DUBOIS-BRISSONNET, R. BRIANDET. Time and spatial dynamics of antimicrobial action in biofilms, 3eme journées thématiques du Réseau National Biofilms, 24-25 juin 2008 Dourdan.

[9] E. TISHCHENKO, V. THOMAS, F. DUBOIS-BRISSONNET, **A. BRIDIER**, K. STEENSKESTE, M.P. FONTAINE-AUPART, R. BRIANDET, Time and spatial dynamics of antimicrobial action in biofilms*,* 3rd International Conference, 6 - 8 October, 2008, Munich, Germany.

[10] **A.BRIDIER**, F. DUBOIS-BRISSONNET, E. TISHCHENKO, V. THOMAS, R. BRIANDET. Biofilms et désinfection : relation entre la structure et la résistance. Congrès SFM « Les moyens de maîtrise des contaminants microbiologiques de la chaîne alimentaire », 5 novembre 2009, Paris, France.

[11] **A.BRIDIER**, F. DUBOIS-BRISSONNET, V. THOMAS, R. BRIANDET. Biocides tolerance and architecture of opportunistic pathogens biofilms using the Calgary device, III International Conference on Environmental, Industrial and Applied Microbiology (BioMicroWorld2009), 2-4 December 2009, Lisbon, Portugal.

[12] **A. BRIDIER**, F. DUBOIS-BRISSONNET, V. THOMAS, R. BRIANDET. Confocal analysis of 60 biofilms structure using a microplate based high throughput method, III International Conference on Environmental, Industrial and Applied Microbiology (BioMicroWorld2009), 2-4 December 2009, Lisbon,

Portugal.

[13] **A. BRIDIER**, F. DUBOIS-BRISSONNET, V. THOMAS, R. BRIANDET. « *Bacillus subtilis* and the beamstalk », Colloque « Biofilm et Santé », 4eme journées thématiques du Réseau National Biofilms, 12 janvier 2010, Poitiers, France.

[14] **A. BRIDIER**, D. LE COQ, F. DUBOIS-BRISSONNET, V. THOMAS, S. AYMERICH AND R. BRIANDET. Bacillus subtilis biofilms: there is life below the pellicle! Biofilms 4 International Conference, 1-3 september 2010, Winchester, UK.

[15] S. DADDI-OUBEKKA, **A. BRIDIER**, R. BRIANET, K. STEENKESTE , M-.P. FONTAINE-AUPART. Correlative dynamic optical microscopy (TL, FRAP, FCS, FLIM) to decipher medical biofilm reactivity. 8th European Biophysics Congress, ESBA, 23-27 August 2011, Budapest, Hungary.

Posters

[16] F. DUBOIS-BRISSONNET, A. PEREIRA, S. DURIEUX, **A. BRIDIER** AND R. BRIANDET. Membrane fatty acids adaptation of Salmonella Typhimurium grown in static biofilms. Eurobiofilm 2009, 2-5 septembre, Rome, Italie.

[17] **A. BRIDIER**, F. DUBOIS-BRISSONNET, E. TISHCHENKO, V. THOMAS, R. BRIANDET, Biofilm structural diversity of 60 foodborne pathogens, Eurobiofilm 2009, 2-5 septembre, Rome., Italie.

[18] E. TISHCHENKO, V. THOMAS, F. DUBOIS-BRISSONNET, **A. BRIDIER** , M.P FONTAINE-AUPART, AND R. BRIANDET. Biofilm Inactivation Dynamics and Biofilm Spatial Structure Changes caused by Biocide Action, Eurobiofilm 2009, 2-5 septembre, Rome, Italie.

[19] **A. BRIDIER**, F. DUBOIS-BRISSONNET, V. THOMAS, R. BRIANDET. Dynamic reactivity of biocides in biofilm structures. Journées des microbiologistes de l'INRA, 5-7 mai 2010, Poitiers, France.

[20] **A.BRIDIER**, R. BRIANDET, S. BOUDJAY, V. THOMAS, F. DUBOIS-BRISSONNET. 2010. Staphylococcus aureus and Pseudomonas aeruginosa biofilm resistance to disinfectants using the Calgary biofilm device. IAFP's 6th European Symposium on Food Safety, June 9-11, 2010, Dublin, Irlande.

[21] **A.BRIDIER**, F. DUBOIS-BRISSONNET, V. THOMAS, R. BRIANDET. Dynamic reactivity of biocides in biofilm structures. 22nd International ICFMH Symposium, Food Micro 2010, 30 August - 3 September 2010, Copenhagen, Denmark.

[22] **A. BRIDIER**, F. DUBOIS-BRISSONNET, D. LE COQ, T. MEYLHEUC, V. THOMAS, S. AYMERICH AND R. BRIANDET. High biofilm resistance to peracetic acid of a *Bacillus subtilis* hospital isolate and protection of *Staphylococcus aureus* in mixed biofilm. Eurobiofilm 2011, 6-8 juillet 2011, Copenhague, Danemark.

Architecture des biofilms et résistance à la désinfection : Apport de l'imagerie de fluorescence multimodale

Résumé :

Dans les environnements naturels, industriels ou médicaux, les microorganismes sont majoritairement présents en étant associés aux surfaces dans des communautés hautement organisées appelées biofilms. Ces édifices biologiques constituent une stratégie de survie étonnement efficace témoignant d'une grande capacité de résistance à différent stress environnementaux tels que les traitements de nettoyage et de désinfection. L'impact des biofilms d'un point de vue sanitaire est donc considérable du fait qu'ils permettent la persistance et la transmission de germes pathogènes dans l'environnement. Dans ce contexte, ce travail de thèse avait pour objectif une meilleure compréhension des phénomènes limitant l'efficacité de désinfectants au sein des biofilms en s'appuyant notamment sur des techniques innovantes d'imagerie de fluorescence non-invasive. Le but final étant d'apporter des éléments utiles à l'optimisation des traitements de désinfection.

Dans une première partie, une méthode d'investigation structurale à haut-débit par microscopie confocale a été développée et utilisée pour étudier la diversité architecturale des biofilms bactériens formés par un large panel de souches. Cette étude nous a permis d'identifier des souches d'intérêt en termes de structures de biofilms formés pour la suite du travail. Nous avons notamment pu mettre en évidence la capacité de *B. subtilis* à former des structures importantes et avec une architecture spécifique dans un système immergé.

Dans une deuxième partie, les dynamiques d'action spatiotemporelles de désinfectants ont été visualisées dans les biofilms de souches de *P. aeruginosa* ou *B. subtilis* par des approches de microscopie confocale de fluorescence en temps réel. L'utilisation de cette technique nous a permis de mettre en évidence les difficultés de pénétration du chlorure de benzalkonium au sein des structures formées par différentes souches de *P. aeruginosa*. La corrélation des paramètres cinétiques d'inactivation et des données obtenues par la caractérisation biochimique de la matrice suggère un rôle majeur des substances extracellulaires dans la limitation de pénétration du désinfectant. Nous avons également pu montrer une résistance marquée du biofilm formé par une souche de *B. subtilis* isolée d'un dispositif médical à l'acide péracétique, à la concentration et au temps d'utilisation du biocide dans le milieu médical. De plus, les structures tridimensionnelles formées par cette souche étaient capables de protéger le pathogène *Staphylococcus aureus* dans un biofilm mixte vis-à-vis du même traitement soulignant l'importance des interactions multi-espèces dans la résistance des bactéries aux désinfectants et la persistance de pathogènes dans nos environnements.

Mots clés : biofilm, microscopie confocale, fluorescence, désinfection, chlorure de benzalkonium, acide peracétique, *Pseudomonas aeruginosa*, *Bacillus subtilis*

Architecture of biofilms and resistance to disinfection: Contribution of multimodal fluorescence imaging

Abstract :

In natural, industrial or medical environments, microorganisms are present mainly in being associated with surfaces in highly organized communities called biofilms. These biological structures cosntitute a surprisingly effective survival strategy showing a large ability to withstand environmental stresses such as cleaning and disinfection treatments. Therefore, biofilms have a considerable impact on public health because they allow the persistence and transmission of pathogens. In this context, this work aimed to better understand the phenomena limiting the effectiveness of disinfectants in biofilms noticeably by using innovative imaging fluorescence non-invasive techniques. The ultimate goal was to provide data which can help to optimize disinfection treatments.

In the first part, a high-throughput structural method based on confocal microscopy was developed and used to study the architectural diversity of bacterial biofilms formed by a wide range of strains. This study allowed us to identify strains of interest in terms of biofilm structure for the second part of the work. In particular, we demonstrated the ability of *B. subtilis* to form protruding structures with a specific architecture in a submerged system.

In the second part, the spatiotemporal dynamic of the action of disinfectants were visualized in the biofilms of *P. aeruginosa* or *B. subtilis* strains by a time-lapse fluorescence confocal microscopy method. Using this technique, we showed that benzalkonium chloride encountered problems of penetration in the biofilms formed by *P. aeruginosa* strains. The correlation of kinetic inactivation parameters and data obtained by the characterization biochemical matrix suggested a key role of extracellular substances in the penetration limitations of the disinfectant. We also observed a pronounced resistance of the biofilm formed by a strain of *B. subtilis* isolated from a medical device to peracetic acid at the *in-use* concentration and time of biocide in medical areas. In addition, three-dimensional structures formed by this strain afforded protection to the pathogen *Staphylococcus aureus* in mixed biofilm against the same treatment. This point highlights the importance of multi-species interactions in bacterial resistance to disinfectants and in the persistence of pathogens in our environments.

Keywords : biofilm, confocal microscopy, fluorescence, disinfection, benzalkonium chloride, peracetic acid *Pseudomonas aeruginosa*, *Bacillus subtilis*